Advances in
Molecular Toxicology

Volume 3

For information on all Elsevier publications
visit our website at elsevierdirect.com

CONTRIBUTORS

EDITOR'S PREFACE

The Editor is grateful to the Authors for outstanding contributions in this third volume in the Series. Once again emphasis is on the eclectic areas, pursuits, and technologies that are subsumed in the topic *Molecular Toxicology*. It is anticipated that the reader will delve in, be awakened, and edified at this diversity.

Patrizia Ciminiello, Carmela Dell'Aversano, Ernesto Fattorusso, and Martino Forino open this volume in Chapter 1 with review of the elaborate toxins of marine origin, specifically algal toxins. Algal blooms increasingly impact the shore life and aquatic farms, particularly of populated regions. The structural array of toxins produced by some of these algae is impressive and focus of this chapter is on relatively recent incidences in the contained to the Mediterranean Sea.

In the 1970s the U.S. EPA sharply curtailed the uses of asbestos, a known human carcinogen. The mechanism by which asbestos fibers cause lung cancer is unknown, but there is a large literature on the array of variables that collude to elicit transformation of these fibers. Reactive oxygen species and inflammation are certainly involved and there are a number of signaling pathways and extranuclear effectors as well. Tom Hei surveys this complex set of considerations in fiber carcinogenesis in Chapter 2.

The last two decades of technological improvements in mass spectrometry have made it a key technology for application to solving innumerable biochemical problems. The problem of idiosyncratic reactions to pharmaceuticals is responsible for discontinuation of many drug candidates and sometimes the withdrawal of approved agents from the market. Such drug reactions are often the result of metabolic activation through reactive intermediates. New technologies are increasingly employed to identify and characterize these reactive metabolites. Mingshe Zhu and Bo Wen elaborate in Chapter 3 the application of quadrupole-linear ion trap mass spectrometry in problems of metabolite characterization and high-throughput screening in drug development.

The causes of Parkinson's disease, despite the focus of extensive research, are still not clearly understood, particularly what are the toxins that give rise to neuronal decay. Juan Segura-Aguilar considers the molecular mechanisms of action of a number of neurotoxins that have been studied as models for therapeutic intervention and discusses the utility of a new agent of utility in preclinical approaches in Chapter 4.

Cigarette smoke contains a smorgasbord of carcinogens, one among which is 4-(methylnitrosamino)-1-(3-pyridyl)-1-butanone (NNK), a proven rodent

lung carcinogen. In humans it undergoes metabolism to yield a variety of reactive agents that can contribute to its activity as a lung carcinogen. Lisa Peterson surveys the literature on this agent in Chapter 5 with a view toward strategies for perspective chemoprevention and understanding how underlying genotype can be predisposing to carcinogenesis by NNK.

Heme is a critical iron–containing heterocycle with diverse roles from oxygen transport, serving a key residue at the active cite of redox active enzymes (e.g., the p450 enzymes) and in electron transport as well as other functions. It is also the source of the derivative bilirubin which serves an important role as an antioxidant. Andrew Smith and Tatyana Chernova discuss the basis of toxicity of a family of haloaromatics that can dramatically alter heme synthesis in Chapter 6.

Plants of the genus *Aristolochia* are found in various parts of the globe and their constituents have found their way into the human food chain and in herbal personal care products and therapies. A set of compounds derived therefrom, the aristiolochic acids, have been shown to be nephrotoxins and presumed causatives of Balkin endemic neuropathy and Chinese herb nephropathy. Arthur Grollman, John Scarborough, and Bohan Jelakovic review the molecular and clinical toxicology of these agents in Chapter 7.

Recent Developments in Mediterranean Harmful Algal Events

Patrizia Ciminiello, Carmela Dell' Aversano, Ernesto Fattorusso,* and Martino Forino

Contents

Dipartimento di Chimica delle Sostanze Naturali, Via Domenico Montesano, 49, 80131 Napoli, Italy

* Corresponding author. Tel.: +39 081 678 503; Fax: +39 081 678 552
Email address: fattoru@unina.it

1. INTRODUCTION

Marine toxins from harmful algae are listed among the most important causative agents of poisoning episodes occasionally involving seafood consumers [1–3]. Out of the thousands of species of microscopic algae lying at the base of the marine food chain there are several dozens, which produce very potent toxins (Figure 1). These toxins normally occur in small quantities and do not pose any serious problem to public health. Proliferations of harmful algae may mostly happen as massive "red tides" or blooms of cells capable of discoloring seawater. However, sometimes dilute and/or inconspicuous concentrations of harmful cells get noticed only because of the harm caused by the highly potent toxins they produce.
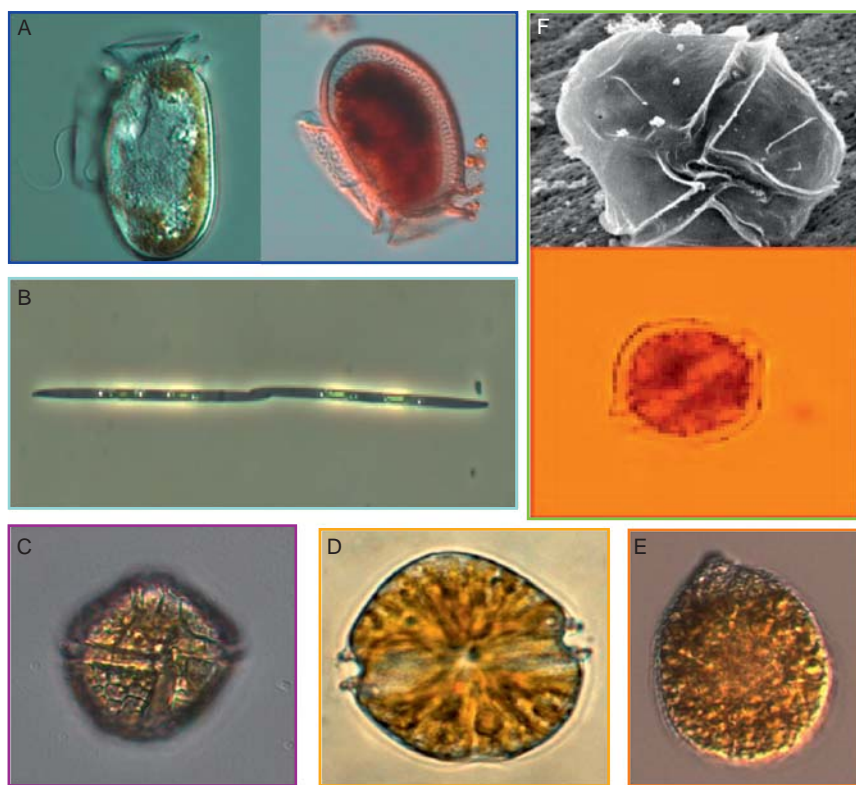

Figure 1   Most occurring harmful algae in the Mediterranean basin: (A) *Dinophysis fortii* (left); *Dinophysis acuminata* (right); (B) *Pseudonitschia pungens*; (C) *Protoceratium reticulatum*; (D) *Alexandrium ostenfeldii*; (E) *Ostreopsis ovata*; (F) *Alexandrium tamarense* (top); *Alexandrium minutum* (bottom).

Well documented is the process through which shellfish can accumulate marine biotoxins in their edible tissues from harmful algae; it is also known that other organisms, such as reef fish, crabs, and tunicates, can be affected by proliferation of toxic plankton. Therefore, harmful algal toxins can find their way through the different levels of the food chain ending up on the table of unaware consumers, thus provoking a variety of gastrointestinal and neurological illnesses. Moreover, toxins can also cause alterations of marine trophic structure through adverse effects on larvae and other life history stages of commercial fishery species [4,5].

In addition to those toxins passed along to consumers through the food chain, particular phytoplankton blooms can directly affect humans accidentally exposed to toxic algae through swimming or breathing aerosols. It is also to be underlined that other harmful algal proliferations can induce severe ecological disruption through widespread killing of sea life including marine mammals and seabirds [6,7].

The extent of harmful algal blooms has changed considerably over the last decades. If in the past only a few regions were affected in scattered locations, now virtually every coastal state is threatened by toxic outbreaks, in many cases even over large geographic areas and by more than one toxic algal species. Even though the causes for this apparent expansion are still largely unknown, the explosive growth of toxic plankton is sometimes clearly intertwined with changes in weather conditions. Important contributing causes may also be found in variations in upwelling, temperature, transparency, turbulence, or salinity of seawater, as well as in concentration of dissolved nutrients, wind, and surface illumination [8].
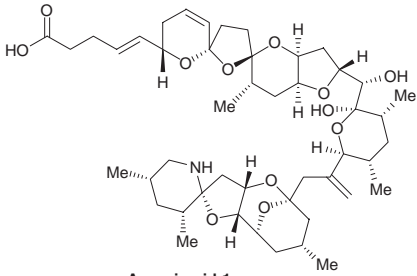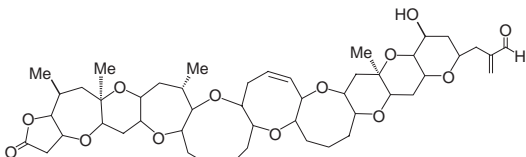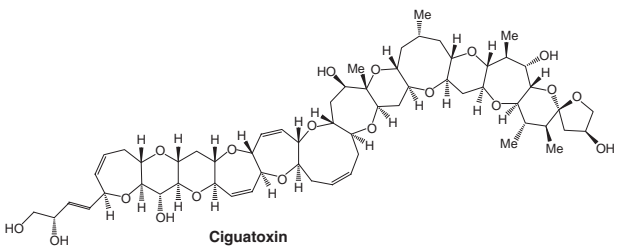
It is not clear why some micro–algal species produce toxic compounds, secondary metabolites playing no explicit role in the internal economy of the producer organisms. These toxins are probably used as a tool for competing for space, fighting predation, or as a defense against the overgrowth of other organisms [9].

A wide diversity of marine algal toxins has been discovered so far, but those of major significance can be gathered into eleven classes reported in Table 1.

Phytoplankton marine toxins rank among the most potent and extremely dangerous toxins in the world. For some of them, doses in the range of micrograms per kilogram may be lethal to humans. In fact, small quantities of contaminated seafood are able to kill a normal, healthy, adult human. Alongside these extremely potent biotoxins, there are also dozens of less potent toxins, which can be all the more accumulated to such a high level to still cause harm to humans.

Unfortunately, poisonous seafood neither looks nor tastes different from uncontaminated seafood, and cooking or other culinary treatment do not destroy toxins.

Table 1   Algal toxins

Toxins class	Azaspiracids
Main algal source	*Protoperidinium crassipes*
Toxicity	Neurotoxic
Structure of a representative	

Azaspiracid-1

Toxins class	Brevetoxins
Main algal source	*Karenia brevis*
Toxicity	Neurotoxic
Structure of a representative	

Brevetoxin-1

Toxins class	Ciguatoxins
Main algal source	*Gambierdiscus toxicus*
Toxicity	
Structure of a representative	

Ciguatoxin

Toxins class	Domoic Acid
Main algal source	*Pseudo-nitzschia* species
Toxicity	Amnesic
Structure of a representative	

Domoic acid
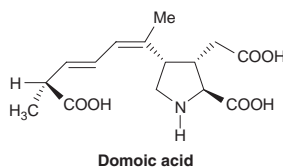
Toxins class	Gymnodimines
Main algal source	*Karenia selliformis*
Toxicity	
Structure of a representative	

Gymnodimine
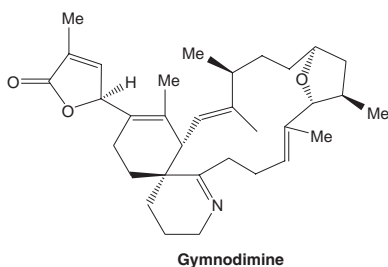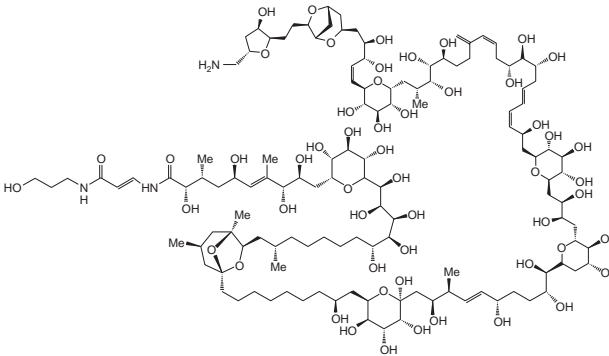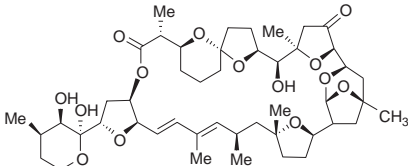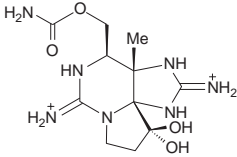
Toxins class	Okadaic acids
Main algal source	*Dinophysis* species
	Prorocentrum lima
Toxicity	Diarrhetic tumor promoter
Structure of a representative	
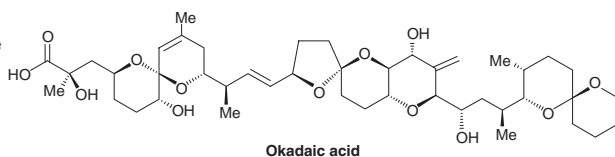
Okadaic acid

Table 1 (*continued*)

Toxins class	Palytoxins
Main algal source	*Ostreopsis* species
Toxicity	Neurotoxic tumor promoter
Structure of a representative	

Palytoxin

Toxins class	Pectenotoxins
Main algal source	*Dinophysis* species
Toxicity	Diarrhetic
Structure of a representative	

Pectenotoxin-2

Toxins class	Saxitoxins
Main algal source	*Alexandrium* species
Toxicity	Paralytic
Structure of a representative	

Saxitoxin

Toxins class	Spirolides
Main algal source	*Alexandrium ostenfeldii*
Toxicity	
Structure of a representative	

Spirolide 13-DesMeC
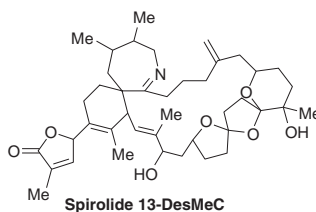
Toxins class	Yessotoxins
Main algal source	*Protoceratium reticulatum*
Toxicity	
Structure of a representative	

Yessotoxin
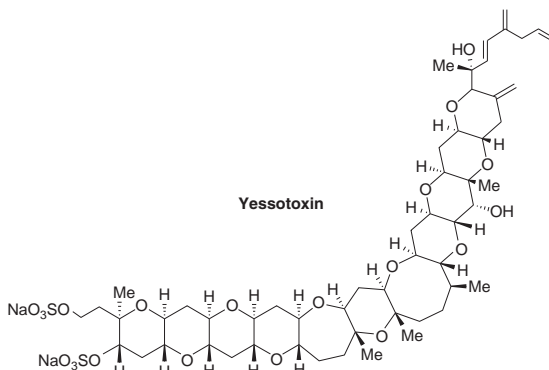
Therefore, fish and shellfish farms infested by toxic algal species need to run costly monitoring programs for checking the occurrence of toxic algae in seafood. Whenever these are present, regular tests for toxins in seafood products need to be attentively carried out. As toxicity is the only common factor among the diverse phycotoxins isolated so far, it is no wonder that live-animal toxicity assay is currently the most widely used method for toxin detection in regulatory settings. At the moment, the most common test is the mouse bioassay. This test is carried out by injecting a sample extract into intraperitoneal cavity of a 20 g mouse that is observed for a given stretch of time in order to determine symptoms and time–to–death generally correlated to the amount of toxin present [10].

2. Distribution of Algal Toxins in the Mediterranean Sea

Due to its geographical features, the Mediterranean basin is home to a large variety of living species, some of which endemic and unknown elsewhere. Survival of this biodiversity depends strongly on conservation of its necessary biotope. Unfortunately, many indicators have clearly shown a declining quality of the Mediterranean seawater and sediments, as testified by the alarming surge of harmful algal blooms over the last two decades [11]. These toxic episodes occurred basically across the whole Mediterranean basin with disquieting frequency and intensity. Figure 2, alongside the geographical location of the toxic outbreaks, details also the chemical nature of the major causative toxins, whose levels in seafood have frequently edged and sometimes exceeded guideline values.

In particular, the Northern Adriatic Sea—which shows a peculiar and complex toxin profile—has been plagued by okadaic acids (OAs), yesso-toxins (YTXs), and lately also by spirolides [12]; French, Spanish, and North African coasts have mainly been interested by the occurrence of saxitoxins [11], while relatively simpler appears the Greek toxic profile where only OA has been detected this far [13]. Very recently, a new, most alarming, threat has been impending over the Mediterranean Sea where the tropical alga *Ostreopsis* spp. is rife [14,15]. Over the past years, such an alga has been causing severe sanitary emergencies and economic losses due to its production of palytoxins [16,17] brought ashore through the marine aerosol [18].

Figure 2   Major reported toxic outbreaks in the Mediterranean basin over the past two decades.

In the ensuing paragraphs, first of all, we intend to shortly describe the chemistry and the toxicology of the main toxins that have been infesting the Mediterranean Sea up to date. Successively, we will provide insights into the latest Mediterranean toxic outbreaks, discussing their impact on human health, economy, monitoring programs, and related law provisions.

2.1. Saxitoxins

Saxitoxin and its analogues (Figure 3) are potent water-soluble neurotoxins that block voltage-gated sodium channel on excitable cells. Currently, over 29 congeners of saxitoxin are known [19]. They represent a suite of heterocyclic guanidines, whose structures vary by different combination of hydroxyl and sulfate substitutions at four sites on the molecule. Based on substitutions at R4, saxitoxins can be subdivided into four groups: the carbamoyl–, sulfocarbamoyl–, decarbamoyl–, and deoxydecarbamoyl–saxitoxins. Substitution at R4 results in substantial changes in toxicity, with the carbamoyl toxins being the most potent.

These compounds—responsible for the syndrome known as Paralytic Shellfish Poisoning (PSP)—are toxic at submicromolar concentrations and represent a severe public health risk.

A number of dinoflagellate species are known to produce saxitoxins: *Alexandrium* (formerly *Gonyaulax* or *Protogonyaulax*), *Gymnodinium* and *Pyrodinium* spp. [20]; most of these dinoflagellates have not been shown to be directly toxic to fish or shellfish. By far, most cases of human PSP intoxications are caused by the consumption of shellfish that have accumulated saxitoxins after filtration of toxic marine dinoflagellates.

PSP symptoms develop fairly rapidly, within 0.5–2 h after ingestion of shellfish, depending on the amount of toxin consumed [20]. In humans the peripheral nervous system is affected, with symptoms ranging from tingling of the tongue and lips, followed by a numbness spreading towards the extremities, to vomiting, pain, diarrhea, loss of coordination, and breathing difficulty.

R^1	R^2	R^3	R^4	Carbamoyl saxitoxins $-O{\overset{O}{\underset{}{}}}NH_2$	N-Sulfocarbamoyl saxitoxins $-O{\overset{O}{\underset{}{}}}NHSO_3^-$	Decarbamoyl saxitoxins $-OH$	Deoxydecarbamoyl saxitoxins $-H$
H	H	H		STX	GTX5, B1	dcSTX	doSTX
OH	H	H		NEO	GTX6, B2	dcNEO	
H	H	OSO_3^-		GTX2	C1	dcGTX2	doGTX2
H	OSO_3^-	H		GTX3	C2	dcGTX3	doGTX3
OH	H	OSO_3^-		GTX1	C3	dcGTX1	
OH	OSO_3^-	H		GTX4	C4	dcGTX4	
H	H	OH		11αOH-STX		11αOH-dcSTX	
H	OH	H		11βOH-STX		11βOH-dcSTX	
OH	H	OH		11αOH-NEO		11αOH-dcNEO	
OH	OH	H		11βOH-NEO		11βOH-dcNEO	

STX = saxitoxin
NEO = neosaxitoxin
GTX = gonyautoxin

Figure 3   Chemical structure of saxitoxin and its analogues.

In severe cases, ataxia, muscle weakness, and respiratory paralysis can occur. Without intervention, symptoms can turn into coma or death from suffocation. When respiratory support is provided within 12 h of exposure, recovery usually is complete, with no lasting side effects. In unusual cases, because of the weak hypotensive action of the toxins, death may occur from cardiovascular collapse despite respiratory support.

PSP is prevented by large-scale monitoring programs (assessing toxin levels in mussels, oysters, scallops, clams) and rapid closures to harvest of suspect or demonstrated toxic areas.

2.2. Okadaic acids

OA is the parent compound of a group of polyether toxins—consisting of at least eight congeners—responsible for the Diarrhetic Shellfish Poisoning (DSP) syndrome, associated with seafood consumption and characterized by an acute gastrointestinal disturbance [21]. OA, dinophysistoxin 1 [22], and dinophysistoxin 2 [23] (Figure 4) are the primary congeners involved in shellfish poisoning, with the other congeners believed either precursors or shellfish-modified products of the active toxins.

The toxins are produced both by several *Dinophysis* species including *Dinophysis acuta*, *Dinophysis fortii*, *Dinophysis acuminata*, *Dinophysis norvegica*, *Dinophysis mitra* [24], and *Dinophysis caudata* [25], and by benthic species such as *Prorocentrum lima* [26,27]. The toxins are accumulated by several bivalves, which filter the seawater containing the toxic phytoplankton and cause human poisoning after ingestion.

Oral assumption of OAs can lead to gastrointestinal distresses, often beginning within 30 min after consumption of contaminated shellfish. The main DSP symptom is represented by diarrhea, often associated with other disturbances such as nausea, vomiting, and abdominal pain [28]. No

R_1	R_2	R_3	
CH_3	H	H	Okadaic acid (OA)
CH_3	CH_3	H	Dinophysistoxin 1 (DTX1)
H	CH_3	H	Dinophysistoxin 2 (DTX2)

Figure 4 Chemical structure of okadaic acid and some of its analogues.

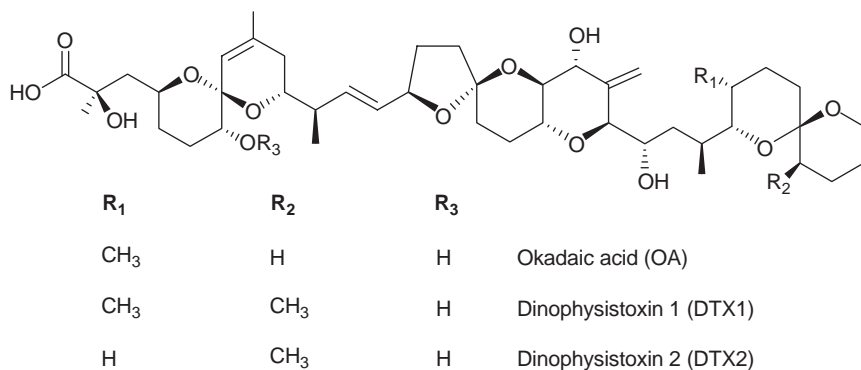human casualty has been to date reported in literature due to any case of DSP poisoning, although sometimes considerable morbidity has resulted in hospitalization. The clinical symptoms of DSP may have been often mistaken for those of bacterial gastric infections and the problem may be much more widespread than currently thought. The treatment, if necessary, is only supportive to replace fluid and electrolyte losses.

OA is a potent tumor promoter [29] and chronic exposure to it may promote tumor formation in the digestive system.

The mechanism of action underlying diarrheic as well as tumor-promoting activity is explained mainly by their potent inhibitory action against ser/thr protein phosphatases [30,31]. Inhibitory activity is specific for classes PP2A and PP1, whilst PP2B is inhibited only at high concentrations of OA and PP2C is practically insensitive.

2.3. Yessotoxins

YTXs represent a group of polycyclic ether molecules (Figure 5). The parent compound of this class of marine toxins is YTX, a disulphated polyether, first reported as a contaminant of the scallop *Patinopecten yessoensis* [32].

YTX in shellfish results from ingestion of toxic algae. The first species reported as a YTX producer is the dinoflagellate *Protoceratium reticulatum* [33]. However, more recent studies have shown that YTX is also produced by the closely related species *Lingulodinium polyedrum* [34] and *Gonyaulax spinifera* [35].

YTX represents the dominant toxin in algal cultures; there is, however, a report in which the major toxin of *P. reticulatum* cultures is homoYTX [36]. This conflicting result, which is indirectly confirmed by the toxin profiles in some contaminated shellfish [37–39], can be attributed to a genetic variability of the producer species inducing a slight modification of the genes involved in the YTX biosynthesis. Some YTX analogues present in large quantities in contaminated shellfish—45-hydroxyYTX, carboxyyessotoxin (carboxyYTX), noroxoYTX, and/or their homo–analogues—are supposed to derive from oxidative modification of the absorbed YTX or homoYTX within the mollusk [40].

YTX and its analogues were at beginning included within the DSP group because they are not distinguishable from OAs on the basis of the mouse bioassay-based standard procedure [10]. However, their toxic activities are significantly different; in fact, YTX and its analogues do not induce diarrhea, whereas their cardiotoxic effects have been demonstrated in mice after intraperitoneal (i.p.) and oral exposure to very high doses of YTX [41]. For these reasons, YTXs are not included in the list of DSP toxins anymore. YTX is highly toxic towards mice when administered after i.p. injection, while its oral toxicity is at least 10-fold lower [42].

	R¹	R²	R³	n

	R^1	R^2	R^3	n
Yessotoxin (YTX)	OSO_3H	OSO_3H		1
45-Hydroxyyessotoxin (45-hydroxyYTX)	OSO_3H	OSO_3H		1
Homoyessotoxin (homoYTX)	OSO_3H	OSO_3H		2
45-Hydroxyhomoyessotoxin (45-OHhomoYTX)	OSO_3H	OSO_3H		2
Carboxyyessotoxin (carboxyYTX)	OSO_3H	OSO_3H		1
Carboxyhomoyessotoxin(carboxyhomoYTX)	OSO_3H	OSO_3H		2
Noroxohomoyessotoxin (NoroxohomoYTX)	OSO_3H	OSO_3H		2
Noroxoyessotoxin (NoroxoYTX)	OSO_3H	OSO_3H		2

Figure 5 Chemical structure of yessotoxins from the Adriatic Sea.

Although no human intoxication caused by consumption of shellfish contaminated by YTXs has been reported, the widespread occurrence of these compounds in shellfish, sometimes at high levels, arouses an increasing interest in studying YTX toxicity. Nonetheless, no one has so far succeeded in proposing a unitary model for its mechanism of action. The chemical structure of YTX resembles that of brevetoxins, which are known to interfere with the voltage-sensitive sodium channel [43]; this finding suggested a possible interaction between YTX and cellular ion channels. Recently, however, it has been observed that YTX does not interact with sodium channels nor induces any competitive displacement of brevetoxins

from site five of sodium channels [44]. It has been proposed that YTX may interact with calcium channels inducing an uptake of calcium in human lymphocytes [45,46]. Finally, studies on immune cells point to phospho-diesterases as an intracellular target for YTX [47].

2.4. Domoic acids

Domoic acid (DA) is a water soluble excitatory tricarboxylic aminoacid (Figure 6), structurally resembling the excitatory neuro-transmitter gluta-mic acid. It has been recognized as the causative toxin of Amnesic Shellfish Poisoning (ASP) syndrome [48].

DA is produced by *Pseudo-nitzschia pungens* f. *multiseries*, a diatom widely distributed in coastal waters all around the world [49]. Several further species of *Pseudo-nitzschia* (*P. australis*, *P. pseudo-delicatissima*, *P. galaxiae*) have been found to produce DA, although some species are not always toxic and there is a considerable variability in toxicity [50–52].

Up to date, several congeners of DA have been identified, among which three geometrical isomers, isodomoic acids D, E, and F and the
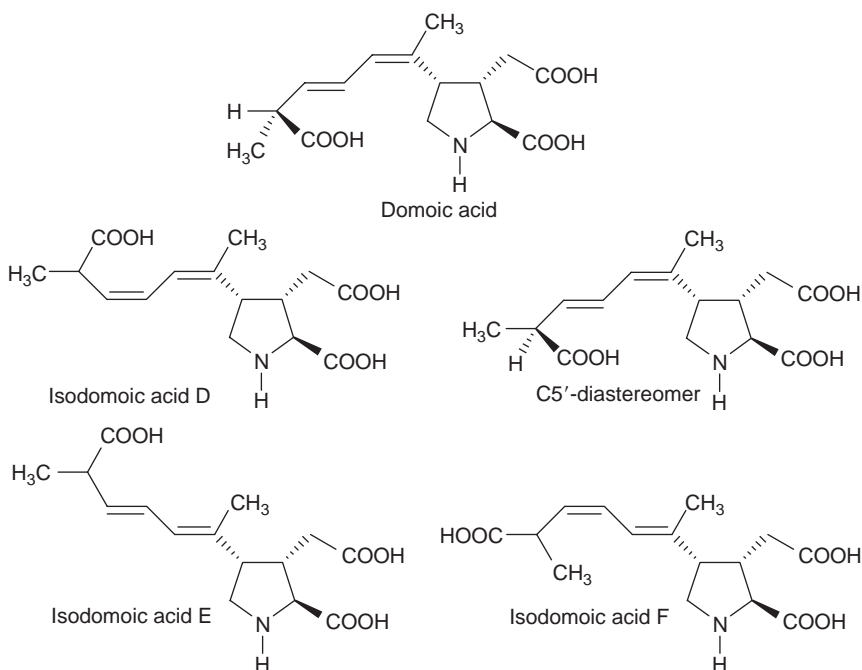

Figure 6 Chemical structure of domoic acid and its stereoisomers.

C5′-diastereomer have been found in small amounts in both the producing diatom and shellfish tissue [53] (Figure 6).

Due to their structural analogies, DA and glutamic acid share the same mechanism of action, even though DA shows a far stronger receptor affinity. More in details, DA binds predominantly to *N*-methyl-d-aspartate (NMDA) receptors in the central nervous system, thus causing depolarization of neurons. As a consequence, the permeability to calcium ions increases, thus inducing cell dysfunction and even death. This provokes lesions in those areas of the brain where glutaminergic pathways are heavily concentrated, particularly in the CA1 and CA3 regions of the hippocampus responsible for learning and memory processes [54].

The clinical symptoms of ASP include abdominal cramps, vomiting, diarrhea, incapacitating headaches, disorientation, and short-term memory loss. In the worst-case scenario patients are victims of seizures, coma, profuse respiratory secretions, unstable blood pressure, and also death [55].

2.5. Pectenotoxins

Pectenotoxins (PTXs) are lipophilic macrocyclic polyethers, whose chemical structures resemble OA in having cyclic ethers and a carboxyl group in the molecule. Unlike OA, the carboxyl moiety in many PTXs is in a form of macrocyclic lactone (Figure 7).

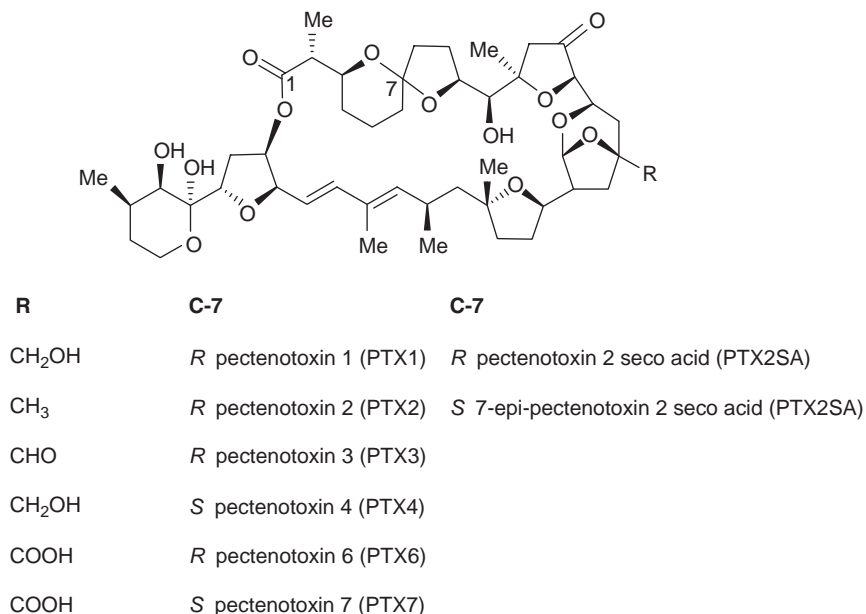| R	C-7		C-7	
CH$_2$OH	*R*	pectenotoxin 1 (PTX1)	*R*	pectenotoxin 2 seco acid (PTX2SA)
CH$_3$	*R*	pectenotoxin 2 (PTX2)	*S*	7-epi-pectenotoxin 2 seco acid (PTX2SA)
CHO	*R*	pectenotoxin 3 (PTX3)		
CH$_2$OH	*S*	pectenotoxin 4 (PTX4)		
COOH	*R*	pectenotoxin 6 (PTX6)		
COOH	*S*	pectenotoxin 7 (PTX7)		

Figure 7   Chemical structure of pectenotoxins.

A number of PTXs have been isolated or identified in a range of source organisms [56]. The PTXs in shellfish originate from dietary microalgae. This far, only the genus *Dinophysis* (e.g., *D. acuta*, *D. fortii*, *D. acuminata*, and *D. caudata*) has been implicated in contamination of shellfish with PTXs [56]. However, only PTX-2 and the *seco* acids of PTX-2 (PTX-2SA and *epi*-PTX-2SA) have been isolated from phytoplankton, while the other compounds have been detected only in shellfish samples. Therefore, it has been supposed that many of these PTXs are products of shellfish metabolism, produced after ingestion of PTX–contaminating algae [56,57].

Similarly to YTXs, also PTXs have been grouped at the beginning together with DSP toxins because of their coextractability with OAs. However, animal studies have indicated that PTXs are much less toxic than the latter ones through oral route and that they do not induce diarrhea [58]. Additionally, many DSPs have been found to be potent phosphatase inhibitors [59], but PTX-1 and PTX-6 were found to be inactive against PP-1 and PP2A [60]. Therefore, they are currently considered as a separate group.

Since PTXs often cooccur with other phycotoxins in shellfish, no toxic episodes in humans could be unequivocally related to them and therefore there is no information about their toxicity to humans.

It has been shown that PTXs are potently cytotoxic [61] and cause necrosis to hepatocytes [62]. Nothing is known of the chronic toxicology of PTXs or the potential implications to public health in the long term.

2.6. Spirolides

Spirolides constitute a group of toxins featuring a spiro-linked tricyclic ether ring system and an unusual 7-membered spiro-linked cyclic imine moiety (Figure 8).

The causative microorganism producing spirolide toxins has been unequivocally identified as the dinoflagellate *Alexandrium ostenfeldii* [63,64]. Chemical studies performed on strains of *A. ostenfeldii* from several geographical areas have individuated a considerable number of spirolide toxins differing in slight structural details [65–70].

Spirolides induce a fast lethal toxic effect when i.p. administered to both mice and rats, and are less toxic by oral administration. Spirolide toxicity on humans still remains unknown, although gastric distress and tachycardia were diagnosed in shellfish consumers in coincidence with the occurrence of spirolides in Canadian mollusks. The unique cyclic imine moiety seems to be the pharmacophore responsible for the fast–acting syndrome induced in mice when spirolides are i.p. administered (LD_{50} = 40 μg/kg) [71]. In fact, two hydrolysis derivatives of the cyclic imine functionality, namely spirolide E and spirolide F, reported by Hu *et al.* in 1996 are inactive in the mouse bioassay [66] (Figure 8).
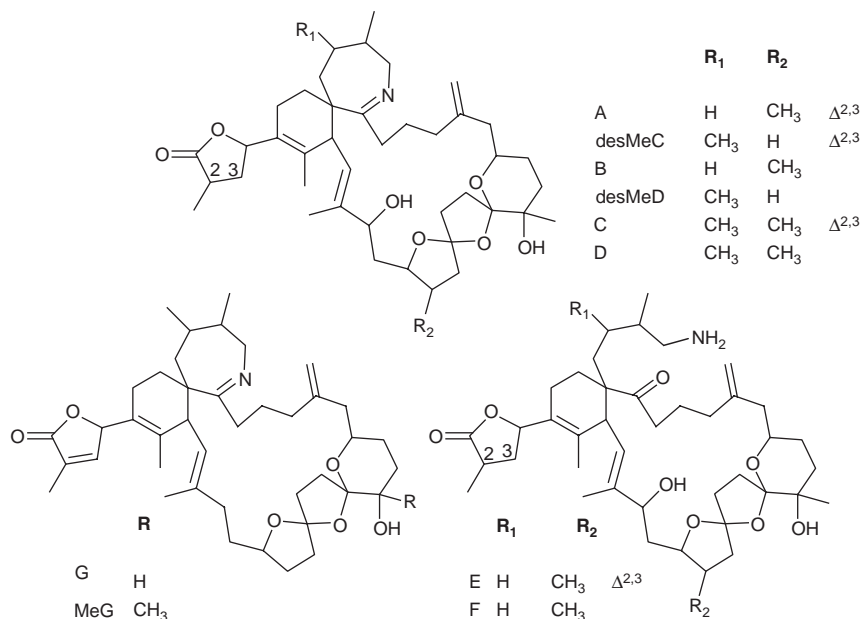
Figure 8 Chemical structure of spirolides.

2.7. Palytoxins

Palytoxin (Figure 9) is a complex polyhydroxylated water-soluble compound and one of the most potent nonprotein marine toxins known so far.

It was first isolated in 1971 by the soft coral *Palythoa toxica* [72] but its gross structure was elucidated only 10 years later by two groups independently, namely Moore's [73] and Hirata's group [74]. In 1982, Kishi and coworkers disclosed the complete stereochemistry of the natural isomer of palytoxin isolated from *Palythoa tubercolosa* [75], which was confirmed a few years later by the total synthesis of palytoxin [76].

Although palytoxin has been isolated worldwide from zoanthids belonging to the genus *Palythoa*, its origin has long been controversial. Recently, dinoflagellates belonging to the genus *Ostreopsis* have been suggested as probable biogenetic origin of palytoxin [77,78]. Support to this hypothesis is provided by identification of putative palytoxin as the causative toxin of cases of clupeotoxism occurred during *Ostreopsis siamensis* blooms [79] and, most importantly, by identification of a number of palytoxin–like compounds from various *Ostreopsis* spp., namely:

    a. ostreocin–D (from *O. siamensis*), whose complete structure (Figure 8) was assigned as 42-hydroxy-3,26-didemethyl–19,44-dideoxypalytoxin, basing on NMR data [77,80], and verified by negative-ion
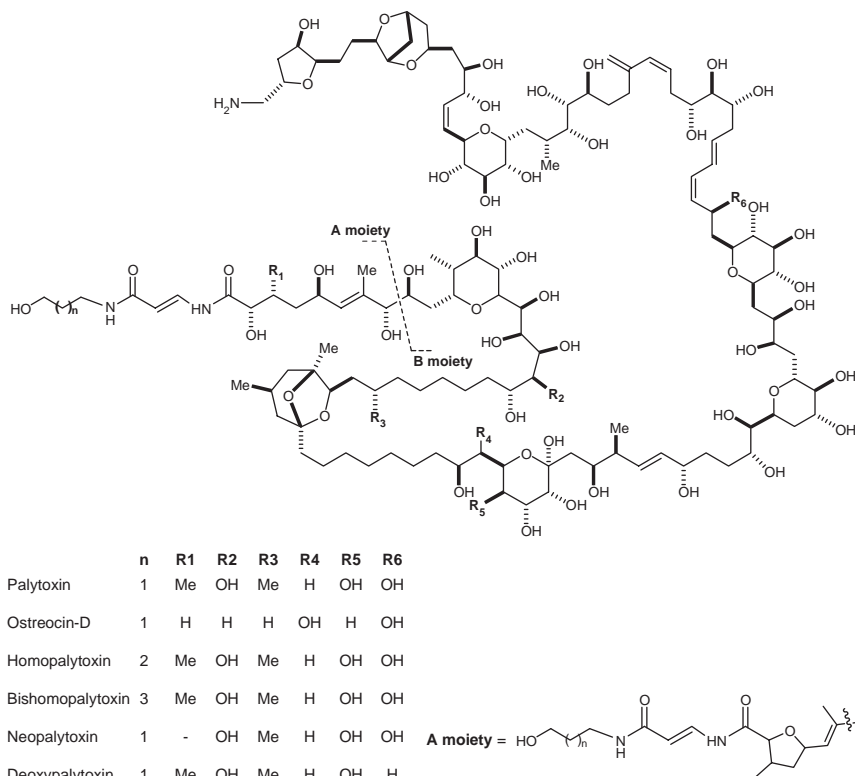
	n	R1	R2	R3	R4	R5	R6
Palytoxin	1	Me	OH	Me	H	OH	OH
Ostreocin-D	1	H	H	H	OH	H	OH
Homopalytoxin	2	Me	OH	Me	H	OH	OH
Bishomopalytoxin	3	Me	OH	Me	H	OH	OH
Neopalytoxin	1	-	OH	Me	H	OH	OH
Deoxypalytoxin	1	Me	OH	Me	H	OH	H

Figure 9 Structure of palytoxin and its analogues.

fast–atom bombardment collision-induced dissociation tandem mass spectrometry [81].

b. mascarenotoxins [82] (from *O. mascarenensis*) purified and identified as palytoxin-like compounds based on comparison of their mass spectrum profiles and fragmentation patterns with those of a reference standard of palytoxin.

c. ovatoxin–a (from *O. ovata*) [17], whose LC/MS/MS structure determination is largely described in Section 3.5.

Other analogues of palytoxin, namely homo-, bishomo-, neo-, and deoxy-palytoxin (Figure 9) were isolated from the soft coral *Palythoa tuberculosa* [83] but they have not yet proved to be produced by *Ostreopsis* spp.

Palytoxin exhibits high toxicity in mammals with intravenous LD_{50} ranging between 25 and 450 ng/kg [84]. Although no data is available on toxicity of palytoxin by oral administration, studies on rats demonstrated that toxicity by intra-gastric administration is significantly lower with an $LD_{50} > 40$ μg/kg [84,85].

Despite palytoxin high lethality to terrestrial animals, some marine animals appear not to be affected by the toxin, namely crabs [86], filefish [87], triggerfish [88], and mackerel [89]. Such animals accumulate palytoxin and enable it to enter the human food chain. Some fatal human poisonings attributed to palytoxin have been reported worldwide [90,91]. Symptoms of intoxication include vasoconstriction, hemorrhage, ataxia, muscle weakness, ventricular fibrillation, pulmonary hypertension, ischemia, and death. Palytoxin binds to the Na^+, K^+-ATPase and converts this pump into an open channel [92–95].

In the late 1980s, palytoxin was also identified as a skin tumor promoter [96,97]. In contrast to TPA (12-*O*-tetradecanoylphorbol–13-acetate), palytoxin induces neither ornithine decarboxylase in mouse skin nor HL–60 cell adhesion. Furthermore, palytoxin neither binds to protein kinase C *in vitro* nor increases ornithine decarboxilase activity in the mouse skin. On the basis of such evidence, palytoxin is classified as a non–TPA-type tumor promoter [98].

Detection and quantitation of palytoxin in biological samples can be accomplished by both analytical means and biological assays. However, it is often necessary to use a combination of methods to confirm the presence of the toxin. The simplest way to detect palytoxin is the mouse bioassay (LD_{50} = 450 ng/kg) [99]. Alternative assays take advantage of palytoxin functional properties and include *in vitro* cytotoxicity [100], delayed hemolysis [101], and antibody-based hemolysis neutralization tests [102]. All these assays are extremely sensitive but, in most regulatory situations, positive results require further confirmation by instrumental methods.

Recently, a precolumn derivatization method has been proposed for the separation and quantification of palytoxin; it takes advantage of the presence of one amino terminal group in the palytoxin molecule and uses the 6-aminoquinolyl–*N*-hydroxysuccinimidyl carbamate as derivatization reagent [103].

A new method for detection of palytoxin based on liquid chromatography with electrospray ionization and tandem mass spectrometric detection (LC-ESI-MS) has been recently developed by our group [16] and extensively described in Section 3.5.

3. Recent Insights into the Latest Mediterranean Toxic Outbreaks

3.1. Historical background

Across the Mediterranean basin, toxic outbreaks due to harmful algal blooms have been spreading with an ever increasing incidence over the past decades. Such toxic events have been particularly monitored and

studied across the Northern Adriatic Sea, where mollusk consumers have experienced recurring sanitary problems, and shellfish farmers suffered heavy economic losses. Towards the late 1980s—when for the first time in Italy some cases of gastroenteritis were related to the presence of producers of DSP toxins both in seawater and shellfish [104]—our group undertook a research line aimed at investigating the occurrence of marine biotoxins in Italian seas. Ever since, we have contributed to provide insightful details on the complex and peculiar Mediterranean toxin profile.

As mentioned above, when in the late 1980s DSP-producers, (e.g., *D. fortii*, *D. sacculus*, and *D. tripos* [105]), bloomed in the Adriatic Sea, we succeeded in isolating and unambiguously identifying OA from a bulky batch of contaminated shellfish [104]. This afforded the very first experimental evidence of the occurrence of DSP-toxins in the Mediterranean Sea. Since then, OAs have been the main Adriatic marine biotoxins through the mid 1990s [106–108].

Around 1995, in fact, discrepant results deriving from mouse bioassays and analytical HPLC-based methodologies suggested the presence in Adriatic mussels of toxins other than OAs. This assumption was also prompted by a concomitant proliferation of a new dinoflagellate, *P. reticulatum*, in the Northern Adriatic Sea. Through analyzing a huge amount of toxic mussels (about 300 kg), for the first time in Italy we could isolate YTX (Figure 5) in addition to only trace quantity of OA [109].

Successively, beside relatively large amount of 45-hydroxyYTX [110], two new analogues, homoYTX and 45-hydroxyhomoYTX [111], were also isolated from Italian mussels.

Over the following years, our continuous studies on toxic shellfish led us to isolate and fully characterize a number of new YTX analogues, namely adriatoxin (ATX), [112] carboxyYTX [113], carboxyhomoyessotoxin (carboxyhomoYTX) [114], and 42,43,44,45,46,47,55-heptanor-41-oxohomoYTX (noroxohomoYTX) [115] (Figure 5).

From 1995 on, YTXs have played a dominant role in Adriatic mussel poisoning, while OAs have slowly subsided until virtually disappearing around the turn of the new millennium.

3.2. The diverse relative harmfulness of YTXs and OAs: A problem for DSP mouse test

The presence of YTXs and OAs in shellfish has pushed scientists to set up analytical methods capable of unambiguously discerning and exactly quantifying the toxin responsible for seafood contamination. In fact, YTX and OAs pose completely different hazards to human health, on the basis of their substantially diverse toxicology. In fact, even though almost as potent as OAs when tested through the mouse bioassay, YTXs appear significantly less toxic than OAs when orally administered [116].

Consequently, on account of their diverse relative harmfulness, the EU has recently established an allowance level for YTX in shellfish which is almost 10-fold as high as that set for DSP-toxins (16 μg of OA and 100 μg of YTX in 100 g of mollusk, respectively) [117]. Such a provision required a revision of the official protocol for checking the presence of marine biotoxins in mollusks. In fact, it was necessary setting up a new official procedure for analyzing seafood capable of separating YTXs and OAs in distinct layers [117] (Figure 10). In fact, the old official scheme did not allow any separation between YTXs and OAs; therefore, the mouse bioassay alone could not lead to any confident assessment of toxin(s) involved [118]. This was successfully resolved by a new official extraction procedure capable of separating YTXs and DSP-toxins in distinct phases (Figure 10).

Lately, national institutions entitled to monitor toxicity in Adriatic shellfish have noticed that, as the hydrophilic phase (aqueous methanol) was becoming less and less toxic, the CH_2Cl_2 one was proving toxic again. This reasonably prompted a further change in the Adriatic toxin profile with a likely decrease of YTXs accompanied by a comeback of OAs, which, as mentioned above, had faded away around 2000.

In order to verify this assumption, we analyzed a batch of Adriatic toxic mussels collected in October 2004, whose only CH_2Cl_2 fraction obtained from 100 g of mussels had resulted positive to the mouse bioassay. This fraction was subsequently analyzed through LC/MS [119] and, against any expectation, no peak related to DSP-toxins was recorded, nor was any of

Mytilus galloprovincialis hepatopancreas

- Acetone extraction
- Acetone removal
- Methanol addition to afford a 60% aqueous methanol solution

Aqueous methanol solution   Dichloromethane

Yessotoxins

DSP-toxins
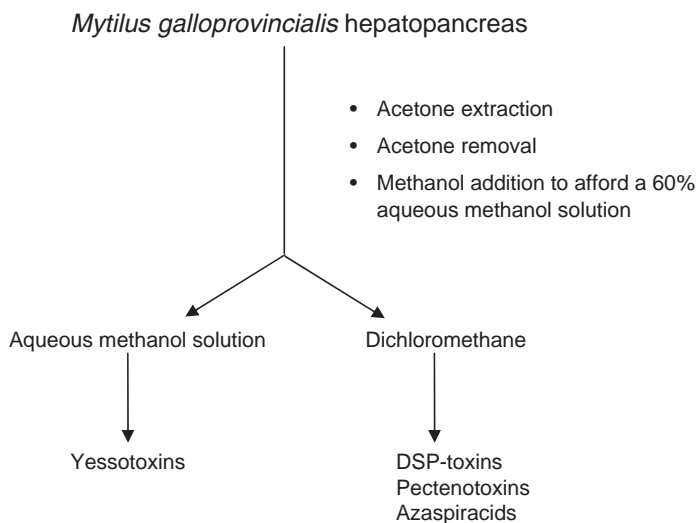Pectenotoxins
Azaspiracids

Figure 10 Extraction protocol for toxic shellfish currently in force in the European Community [117]. Such experimental procedure allows now to separate yessotoxins and DSP-toxins in different layers on the basis of their relative lipophilicity.

the other main lipophilic toxins usually coextracted in the CH_2Cl_2 phase, namely PTXs and azaspiracids.

The presence of a new toxin was assumed.

A massive extraction of Adriatic toxic mussel (about 150 kg) was carried out for isolating any contaminating toxin in sufficient amount for its NMR characterization. This was a laborious and time consuming procedure that eventually afforded two toxic fractions containing 200 and 300 μg of pure compounds, respectively.

It must be emphasized that the small quantity of pure biotoxins isolated did not correspond to its real occurrence in natural samples. In fact, a large part of each compound was unavoidably lost during the several steps of extraction and purification as well as consumed through the mouse bioassay indispensable for following up toxicity throughout the purification.

Despite the small quantity of the isolated toxins, their structural elucidation was successfully carried out by MS and 1D and 2D NMR-based techniques.

At first glance, ^{1}H NMR spectra of both compounds highlighted a YTX-like structure and more precisely a close similarity to carboxyhomoYTX previously isolated in our laboratory [114]. Interpreting COSY, TOCSY, and ROESY spectra alongside MS/MS experiments, we accomplished to classify the two toxins as 1–desulfocarboxyhomoyessotoxin and 4–desulfocarboxyhomoyessotoxin, respectively (Figure 11) [120].

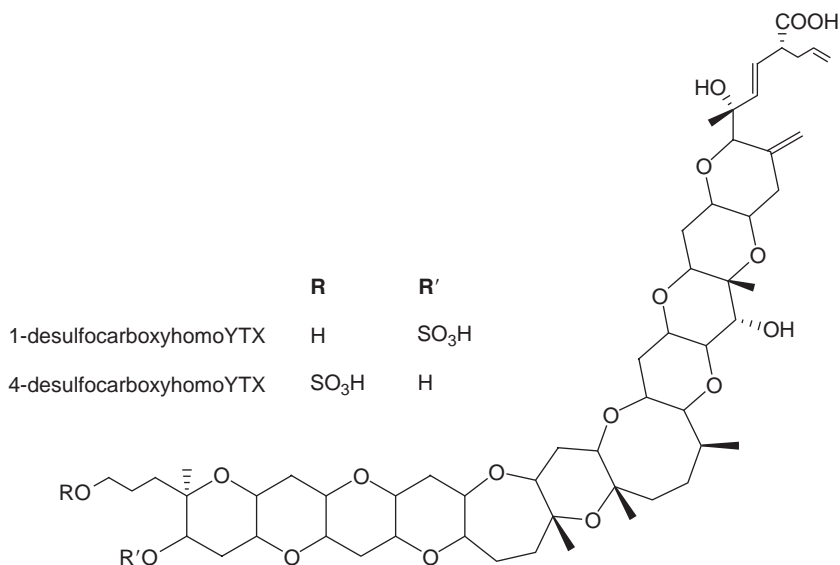|	R	R′
1-desulfocarboxyhomoYTX	H	SO$_3$H
4-desulfocarboxyhomoYTX	SO$_3$H	H

Figure 11 Chemical structure of desulfocarboxyhomoYTXs.

In spite of their small structural innovation in comparison to other YTXs and in particular to carboxyhomoYTX, the occurrence of desulfocarboxy-homoyessotoxins in the Adriatic mussels raises some issues that would be worth studying over the next future. First, it must be noted that these new two desulfoyessotoxins are unexpectedly recovered in the lipophilic layer, so that the purpose of the European new protocol fails. Hence an overhaul of the EU control procedure is urgently needed.

In addition, the toxicity of desulfocarboxyhomoyessotoxins should be carefully investigated, as the lack of a sulfate group surely decreases the hydrophilicity of desulfoyessotoxins in comparison to YTXs. As a consequence, desulfoyessotoxins could permeate living biomembranes more than YTX itself, thus resulting more toxic to humans by oral ingestion.

Finally, it would be also interesting to assess if the lack of a sulfate ester in carboxyhomodesulfoYTXs is an outcome of the mollusk metabolism.

3.3. A threat impending over the Mediterranean Sea: DA

From 2000 on, approximately in coincidence with the surge of desulfoyes-sotoxins, the diatom *Pseudo-nitzschia* spp. has started spreading in the Adria-tic Sea. Such a diatom is the producing organism of DA, the causative toxin of ASP syndrome. Even though the concentration of this toxin in Adriatic shellfish has been so far estimated always below its regulatory level, it requires an attentive monitoring because of its serious harmfulness.

Once established the presence of DA in Adriatic shellfish, we had to tackle the problem of monitoring such a molecule in a rapid, reliable, and sensitive way. In fact, reported bioassay and instrumental methods [121] for detection of DA in shellfish and phytoplankton were all flawed by a number of setbacks, as illustrated below.

The Association of Official Analytical Chemists (AOAC) mouse bioas-say for PSP toxins can be employed for detecting DAs pretty unique toxicity, which enables analysts to distinguish this biotoxin among the other most occurring hydrophilic toxic agents [122]. This method, basically consisting in boiling shellfish tissue with an equal volume of 0.1 N HCl, provides a common extract for screening both DA and PSP toxins. How-ever, unlike PSP-toxins, i.p. injection in mice of an extract containing DA induces a typical symptomatology characterized by scratching of shoulders by hind legs, sedation–akinesia, rigidity, loss of posteral control, convul-sions, and death [123]. Unfortunately, such symptoms are observed only when DA is present at a concentration >40 μg/g of edible tissue, which is twice as high as the regulatory limit for DA set at 20 μg/g of shellfish tissue. Therefore, the relative insensitivity of this assay precludes its use for any regulatory purpose.

Instrumental methods provided a far more sensitive detection of DA. In particular, liquid chromatography with UV detection (LC-UV) was

the preferred analytical technique for determination of DA in shellfish [124, 125]. For this analysis, mollusk tissue could be extracted either by the AOAC procedure [124], or by an aqueous methanol (1:1, v/v) solution [125], which used to afford a better yield and a more stable extract. The detection limit for DA provided by this method ranged between 0.1 and 1 μg DA/g tissue, depending on the sensitivity of the UV detector. However, also this method was affected by some inconveniences, such as interferences with crude extracts leading to false positives. Particularly, tryptophan and its derivatives, commonly contained in mollusks, could elute close to DA, thus making interpretation of the results not straightforward at all.

Sensitive techniques based on derivatization with 9-fluorenylmethyl-chloroformate (FMOC) followed by LC analysis with fluorescence detection were also developed for monitoring DA in marine matrices [126]. However, these methods were more difficult for the analysis of shellfish tissue because of matrix interferences with the derivatization reactions.

Even capillary electrophoresis (CE) with UV detection used to be applied for determining DA in shellfish, but in this procedure two clean-up steps were required in order to achieve reliable results [127,128].

More recently, the LC–MS technique has been employed for rapid and highly selective analysis of DA in crude extracts. Quilliam *et al.* clearly demonstrated the potential of the electrospray (ESI)–MS technique for the confirmation of DA and other seafood toxins in shellfish extracts [129]. However, as contaminated shellfish samples may contain several toxin analogues belonging to the same class, or even different classes of toxins, it would have been useful to develop multitoxin determination methods. Thus, a method allowing a combined analysis of DA and PSP toxins, normally coextracted with them, was highly desirable. This prompted our research efforts in this field, which resulted in setting up an analytic method based on hydrophilic interaction liquid chromatography–mass spectrometry (HILIC–MS) technique [130–132]. The high percentage of organic modifier in the mobile phase and the omission of ion pairing reagents, both favored in HILIC, resulted in enhanced MS detection limits. Due to their highest sensitivity and selectivity, multiple reaction monitoring (MRM) experiments were used for screening and quantitative analyses.

Our method proved suitable to combined analysis of DA and PSP toxins in a single 35 min chromatographic run with a gradient elution, whereas an isocratic elution allowed the detection of DA in 10 min [132]. The minimum detection levels for the toxin in tissue were found to be 63 and 190 ng/g in positive and negative MRM experiments, respectively, which are well below the regulatory limit of DA in tissue (20 μg/g). Consequently, as this method is able to reveal DA at concentrations lying far below its allowance level, it might be proposed as official test for regulatory purposes.

We applied this method to a number of samples of *Mytilus galloprovincialis* from the Adriatic Sea collected from 2000 to 2004. Our results

demonstrated for the first time the presence of DA as a new toxin that has entered the Adriatic *M. galloprovincialis* toxin profile [132]. Such results clearly demonstrate that there are DA producing species in the Adriatic Sea. Although concentrations of DA in the analyzed samples were far below the current regulatory level, careful monitoring of this toxin in Italian shellfish is strongly recommended.

3.4. Occurrence of Spirolides in phytoplankton and mussels from the Adriatic Sea

The spreading of DA producing species in the Adriatic Sea further compounds sanitary problems associated to shellfish contamination in that area already plagued by the presence of YTXs and DSP-toxins. To make the picture even more alarming, a new threat to human health is now impending over the Adriatic Sea: the toxic dinoflagellate *A. ostenfeldii*.

Ever since November 2003, high concentrations of *A. ostenfeldii* cells have been detected along the Northern Adriatic coasts (Italy), and in concomitance with these toxic outbreaks we started analyzing the toxin profile of Adriatic *A. ostenfeldii* cultures [133] as well as that of mussels grown in areas massively infested by this dinoflagellate.

In literature, *Alexandrium* strains are reported to produce different classes of marine biotoxins depending on its geographical provenience. In Canadian strains, high levels of spirolides have been described [64]; whilst strains from New Zealand have been proven to produce PSP-toxins [134]. Even more complex is the toxin profile of certain *A. ostenfeldii* populations detected in Scandinavia, where both spirolides and PSP-toxins have been found [135]. On the basis of these reports, we searched the occurrence of both spirolides and PSP-toxins in samples of toxic mussels and in cultures of *A. ostenfeldii* from the Adriatic Sea. Our study characterized the Adriatic *A. ostenfeldii* as an organism producing several spirolides but none of the major PSP-toxins [133].

Chemical studies performed on strains of *A. ostenfeldii* from several geographical areas have individuated a considerable number of spirolide toxins differing in slight structural details [65,67–70]. Among the isolated compounds, 13-desmethyl spirolide C represents the major component of the spirolide content of all the *A. ostenfeldii* strains analyzed this far [68].

Some preliminary studies performed on Adriatic *A. ostenfeldii* cultures in our laboratories proved that 13-desmethyl spirolide C was the main toxin produced by the dinoflagellate in accordance with what already reported in literature [133]. Alongside this major already known spirolide, our analysis highlighted the occurrence of a complex mixture of other, potentially new, spirolides. Unfortunately, the small amount of available material kept us from fully assigning the structures of these new spirolides. Therefore, large

scale culturing of *A. ostenfeldii* was carried out in order to isolate the new derivatives in amount sufficiently large for NMR investigation.

Starting from such greater quantity of *A. ostenfeldii* culture we were able to detect a much higher number of spirolides than that reported in our previous study. Some of the detected derivatives corresponded to those described by other authors on the basis of $[M + H]^+$ ions and fragmentation patterns [68–70], while some others appeared to have been never reported before. Among them, three major spirolides were identified: the recently described 13,19-didesmethyl spirolide C [70] and 13-desmethyl spirolide C [67] (Figure 8), as well as a compound at *m/z* 694.5 which appeared a potentially new spirolide. Consequently, its structural determination was achieved by employing both MS- and NMR-based experiments, which led us to define it as 27-OH-13,19-didesmethyl spirolide C [136] (Figure 12).

A number of minor spirolides were also detected by LC-MS experiments, but they were all present in too small quantity for NMR investigation. As a consequence, for these new spirolides only structural hypothesis have been provided on the basis of MS/MS analyses [136]. HRMS experiments are needed to achieve better structural hypotheses, even though conclusive structural assignments might be yielded only through NMR investigation.

Besides the analysis of Adriatic *A. ostenfeldii* cultures, we have also investigated the toxin content of shellfish samples collected along the Adriatic coastline in coincidence with the occurrence of high concentrations of *A. ostenfeldii* in seawater. Studies carried out on these toxic samples provided almost the same conclusions we afforded by investigating the Adriatic *A. ostenfeldii* cultures. In particular, LC-MS analyses clearly highlighted the occurrence of 13,19-didesmethyl spirolide C and 13-desmethyl spirolide C as major component of the spirolide content (data not published).
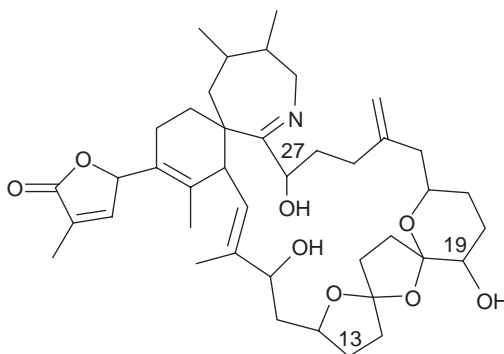

Figure 12 Chemical structure of 13,19-didesmethyl-27-hydroxy spirolide C from Adriatic *A. ostenfeldii*.

3.5. *Ostreopsis* spp. blooms and palytoxins outbreaks in the Mediterranean Sea

Dinoflagellates belonging to *Ostreopsis* genus have been blooming along the Mediterranean coastlines since the late 1990s (Figure 13). The first documented cases occurred in summers 1998, 2000, and 2001 along Northwestern Tuscanian coasts [137], when massive blooms of *O. ovata* resulted in extensive benthonic biocenosis sufferings. Concurrently, most of the emerging rocks and pebbly sea-bottom as well as seaweeds were covered by a reddish-brown jelly film teeming with *O. ovata* [138]. Human sufferings were occasionally recorded during these events and in following summers when an *Ostreopsis* population bloomed along the Apulian coasts [139].

In summer 2005, the phenomenon broke out with alarming proportion along the Ligurian coasts and caught the attention of both national and international media. Hundreds of people required medical attention after exposure to marine aerosol during recreational or working activities on the beach and promenade of Genoa (Italy). The symptoms shown by all the patients included high fever associated to serious respiratory distress such as watery rhinorrhea, dry or mildly productive cough, bronchoconstriction with mild dyspnea. and wheezes. Conjunctivitis was also observed in some

Figure 13   Map of Italy. The coastal regions where *Ostreopsis ovata* blooms and/or outbreaks occurred in the years 1998–2007 are labeled.

cases and 20 people required extended hospitalization. During the event, weather conditions were quite stable, the sea water appeared clear and barely circulating, and its temperature was around 25 °C. Some people described a metallic taste of the water. At the same time, an environmental suffering involving mostly epibenthos, both sessile (cirripeds, bivalves, gastropods) and mobile (echinoderms, cephalopods, little fishes), was observed. A careful look at the marine plankton brought to the light that an unusual proliferation of the tropical microalga *O. ovata* (1.8×10^6 cells/L) was occurring along the investigated coastal areas during the toxic outbreak. Most symptoms in humans disappeared as the population of *O. ovata* started fading away.

Our group analyzed a plankton sample collected off Genoa coasts during the toxic outbreak. The aqueous–methanol extract of the sample was proved to induce mice death within 30 min after i.p. injection. Initially, the presence in the extract of the following phycotoxins was investigated by liquid chromatography-mass spectrometry (LC-MS) [119,131,132]: (a) OA, spirolides, YTXs, saxitoxins, and DA, that are commonly found in the Mediterranean Sea [140]; (b) brevetoxins that, although never reported in the Mediterranean Sea, are usually associated with poisonings due to marine aerosols [141]. None of the above toxins was detected in the plankton sample [16].

Since some *Ostreopsis* species are regarded as producers of palytoxin-like compounds (Figure 9), the need arose to set up a new method for detection of palytoxin to investigate whether the *O. ovata* blooming during the Genoa endemic disease was producing the toxin.

Liquid chromatography with electrospray ionization–tandem mass spectrometric detection (LC-ESI-MS/MS) has great potential for rapid, sensitive, and unambiguous identification of palytoxin in contaminated material. In fact, the capability of ESI to produce multiply charged molecules under mild conditions has accessed detection of a high MW compound such as palytoxin ($C_{129}H_{223}N_3O_{54}$) by extending the mass range for m/z-limited mass spectrometers.

Figure 14 shows a full–MS spectrum in positive ion mode obtained by direct infusion of the toxin standard in a mixture of acetonitrile–water (1:1, v/v) both eluents containing 30 mM acetic acid. Basing on full-MS spectra, the following ions were selected for selected ion monitoring (SIM) experiments: m/z 1340.7 $[M + 2H]^{2+}$, 1331.7 $[M + 2H-H_2O]^{2+}$, and 906.1 $[M + 2H + K]^{3+}$. Whatever was the precursor ion used, either bi-charged or tri-charged, the fragmentation pattern of palytoxin produced in the product ion spectra contained an intense ion at m/z 327, which arises from the cleavage between the carbons 8 and 9 of the toxin molecule and the additional loss of a molecule of water [83]. Thus, the following transitions Q1 → Q3 at m/z values of 1340.7 → 327.1, 1331.7 → 327.1, and 906.1 → 327.1 were selected for MRM experiments, which permit better selectivity and better signal-to-noise ratios than SIM.
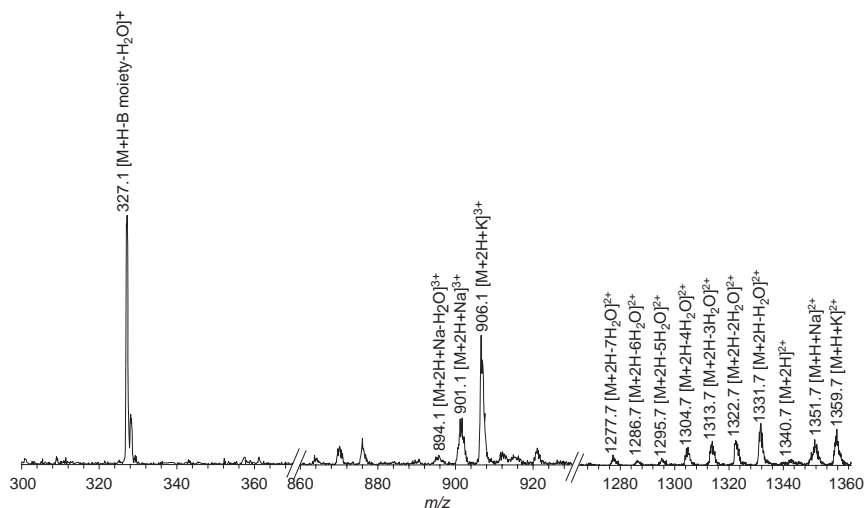
Figure 14 *Full scan* MS spectrum of palytoxin standard acquired on an ESI triple quadrupole MS instrument in positive ion mode.

The best LC conditions which allowed determination of palytoxin in a 15 min analysis are the following:

Column: 5 μm Gemini C-18, 150 × 2.00 mm, (Phenomenex, Torrance, CA, USA)

Mobile phase: A = water with 30 mM acetic acid
                         B = acetonitrile/water (95:5, v/v) with 30 mM acetic acid

Elution: Gradient = 20–100% B over 10 min and hold 4 min

Flow: 200 μl/min

Temperature: room temperature (21 °C)

Under the used conditions, limits of detection (LOD, S/N = 3) and quantitation (LOQ, S/N = 10) in MRM mode were calculated to be 25 and 84 ng/ml for matrix-free palytoxin, respectively; while they resulted to be 38 and 127 ng/ml for matrix-matched palytoxin, respectively.

Based on the newly developed method for detection of palytoxin, we analyzed the plankton extract and detected a peak in MRM chromatogram which matched perfectly in retention time, fragmentation, and ion ratios those of a reference sample injected under the same experimental conditions. This indicated that putative palytoxin was contained in the plankton extract at levels of 3.30 μg which matched with the mouse bioassay results. Due to the complex stereo-structure of palytoxin we referred to the

detected compound as putative palytoxin rather than palytoxin, as the possibility that the compound is a palytoxin isomer cannot be excluded on the basis of the obtained LC–MS results [16].

Following this event, in 2006 the presence of *O. ovata* was monitored along the Ligurian coasts (Figure 13) in order to prevent further human sufferings. Indeed, a remarkable proliferation of *O. ovata* was detected in the Mediterranean Sea from July through August 2006. Bathing was forbidden in several Italian coastal areas and, thus, the number of people suffering from the toxic outbreak was significantly limited in comparison to the 2005 event.

Four plankton samples were collected in summer 2006 along the Ligurian coasts in the area of Genoa and La Spezia and they were analyzed by the newly developed method for detection of palytoxin [16]. The obtained results paralleled those obtained on the 2005 plankton samples with levels of putative palytoxin in the range 0.09–0.40 pg/cell. The presence of putative palytoxin was shown in all the samples by peaks which closely matched those of a reference sample of palytoxin in retention time, fragmentation, and ion ratios.

In order to look for additional palytoxin analogues in the samples, a more detailed and comprehensive MS investigation was carried out by using different MS instrumentation. Initially, full scan mass spectra were recorded on both an ESI triple quadrupole MS (Figure 15A) and an ESI–ion trap-MS (Figure 15B). A different degree of front end fragmentation, likely due to different geometry of ionization sources and ionization parameters used, was observed on the two instruments. However, an accurate comparison between the obtained MS spectra and palytoxin standard's indicated the presence in the sample of a palytoxin-like molecule that did not correspond either to palytoxin itself or to any known palytoxin analogue. We named it ovatoxin–a [17].

The exact mass of ovatoxin–a and its fragments were established by high resolution spectra obtained in LC–MS and LC–product ion MS modes using a linear ion trap hybrid FTMS instrument. The mono–charged ion cluster in the HRMS spectrum of ovatoxin–a presented a mono–isotopic ion peak $[M + H]^+$ at m/z 2647.4868 (Figure 16A) which allowed to infer the molecular formula $C_{129}H_{223}N_3O_{52}$ ($\Delta = -3.918$ ppm) to the molecule. Further confirmation for such elemental composition was provided by the exact masses of bi–charged (mono–isotopic ion peak at m/z 1335.2429 for $C_{129}H_{224}N_3NaO_{52}$, $\Delta = -0.174$ ppm) and tri–charged (mono–isotopic ion peak at m/z 890.4937 for $C_{129}H_{225}N_3NaO_{52}$, $\Delta = -4.657$ ppm) ions. Ovatoxin–a presented two oxygen atoms less than palytoxin ($C_{129}H_{223}N_3O_{54}$). The LC–HR product ion spectrum obtained by selecting the mono–charged ion of ovatoxin–a as precursor ion (Figure 16B) contained abundant peaks due to subsequent losses of two, three, and four water molecules from the $[M + H]^+$ ion and a structurally interesting
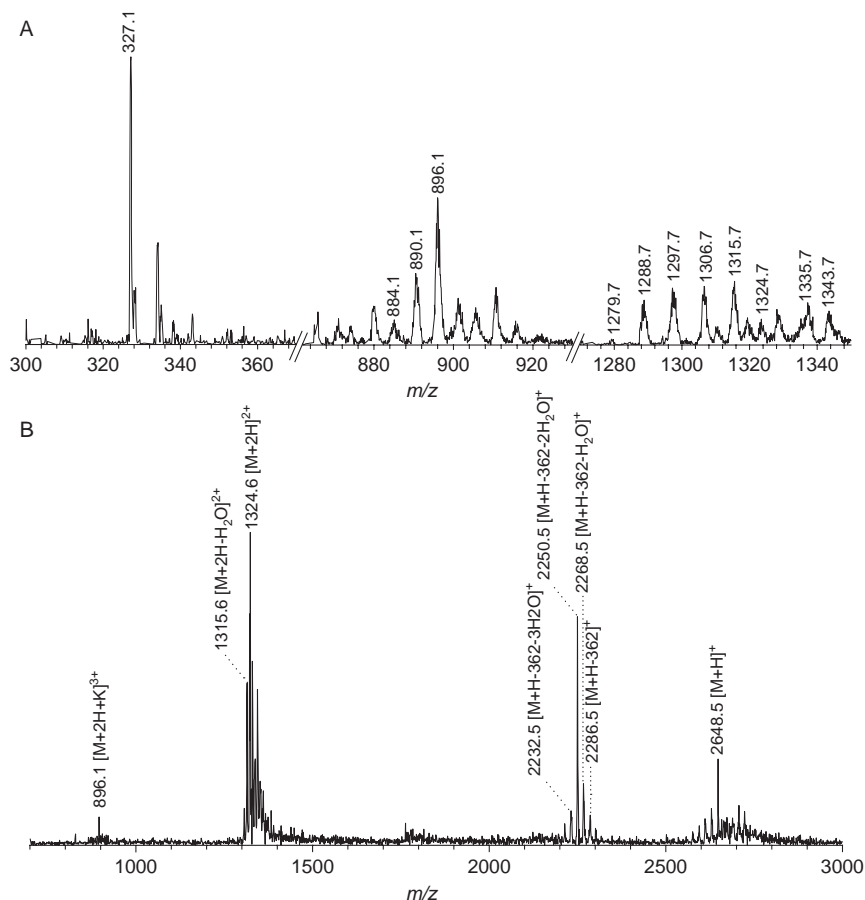
Figure 15 *Full scan* MS spectra of ovatoxin-a acquired on an ESI triple quadrupole MS (A) and an ESI-ion trap-MS (B) instrument, respectively.

fragment ion at m/z 2286.2864 (mono-isotopic ion at m/z 2285.2825) due to loss of 362.2043 amu from the precursor ion, corresponding to a $C_{16}H_{30}N_2O_7$ ($\Delta = -2.765$ ppm) neutral fragment.

In the same experimental conditions, the LC-HR product ion spectrum of palytoxin standard paralleled that of ovatoxin-a in the presence of ions due to multiple water losses and of an ion (m/z 2318.2749) due to neutral loss of 362.2036 amu ($C_{16}H_{30}N_2O_7$). The neutral fragment $C_{16}H_{30}N_2O_7$ originates from cleavage between carbons 8 and 9 and corresponds to A moiety of palytoxin with an additional molecule of water. Thus, structural differences between ovatoxin-a and palytoxin likely lie in the rest of the molecule (part structure B in Figure 17).
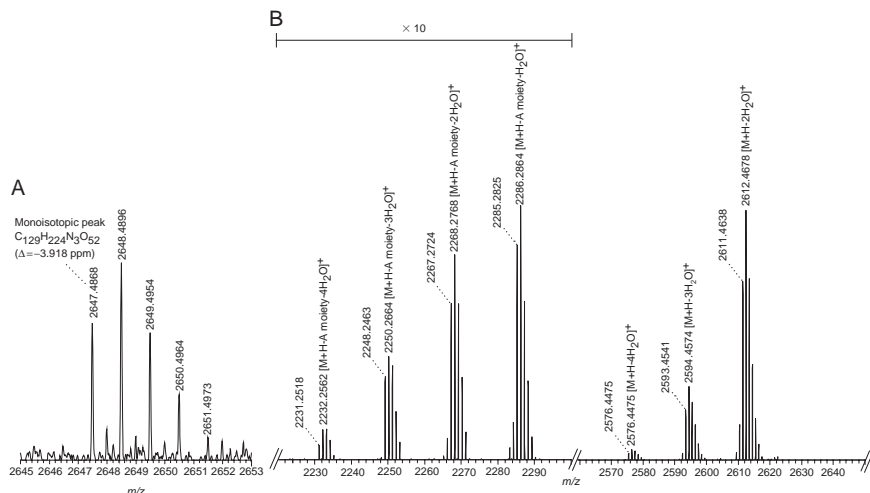
Figure 16 HR *Full scan* MS spectrum (A) and HR product ion MS spectrum (B) of ovatoxin-a acquired on a linear ion trap hybrid FTMS instrument.
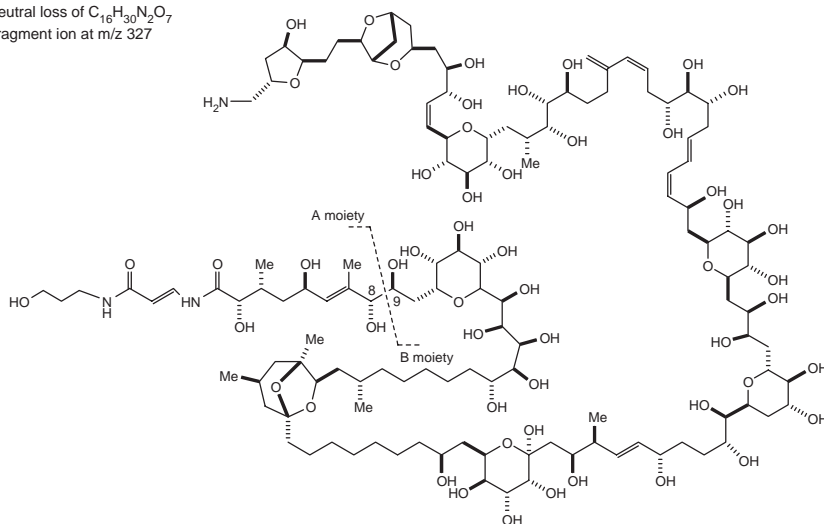

Figure 17 Structure of palytoxin and indication of the structural features common to ovatoxin-a.

On the basis of molecular formula (ovatoxin-a presents two oxygen atoms less than palytoxin), fragmentation pattern, and chromatographic behavior, the structure of ovatoxin-a appeared to be strictly related to palytoxin's.

However, on the account of data reported on bio-activity of palytoxin analogues, even slight structural differences could significantly affect and differentiate the toxicology of the two compounds. By way of example, ostreocin D, whose structure is very similar to palytoxin's, presents a very different citotoxic (2.5 pM for ostreocin D vs. 0.2 pM for palytoxin) and hemolytic activity (39.5 nM for ostreocin D vs. 1.5 nM for palytoxin) from those of palytoxin [80, 142]. Thus, isolation of ovatoxin-a is most necessary both to elucidate its chemical structure and evaluate its toxicology.

Quantitative analyses were carried out by assuming for palytoxin and ovatoxin-a a similar molar response as a consequence of the evident structural similarities between the two compounds. The calculated amount of ovatoxin-a in the analyzed sample were in the range 1.26–3.11 pg/cell, suggesting that ovatoxin-a was by far the predominant palytoxin-like compound in the 2006 plankton. Application of the developed method for detection of palytoxin and ovatoxin-a to the analysis of cultures of *O. ovata* indicated it as the producing organism of both compounds detected in natural plankton. Quantitative analyses afforded a putative palytoxin and an ovatoxin-a contents of 0.55 pg/cell and 3.85 pg/cell, respectively. Interestingly, the two compounds appeared to be produced approximately in the same ratio observed in natural plankton [17].

In summer 2007, *O. ovata* bloomed again in Italy along the whole Tirrenian coasts, from Liguria to Sicily, and in some sites of the Adriatic coasts, in Apulia and Friuli Venezia Giulia (Figure 13). About 80 people reported serious respiratory distress after exposure to toxic marine aerosols along the coasts of Bari (Apulia).

Due to recurring cases of *O. ovata* blooms and palytoxins outbreaks along the Italian coastlines, the Italian Ministry of health has warned local institution about the phenomenon and associated risks for human health [143].

Very recently, an episode of shellfish contamination due to palytoxin-like compounds from *Ostreopsis* species has been reported along the coastal waters of the North Egean Sea (Greece). Studies were carried out by testing toxicity of the samples by mouse bioassay and delayed hemolytic activity [144].

4. Conclusions

Our study carried out over the past 20 years has afforded significant insights into the problem of marine biotoxins infesting the Italian coastline.

Unlike other marine environments across the world, probably due to its geographical and morphological features, the Adriatic Sea shows a pretty unique, complex, and, above all, continuously changing toxin profile. In fact, if from the late 1980s through the mid 1990s OAs have been the main Adriatic toxins, from 1995 onwards, YTXs have dominated the toxic content

of this sea. Successively, around the beginning of the third millennium, desulfoyessotoxins have proven the most abundant toxic compounds detected in Adriatic mollusks; while lately spirolides have been posing health risks to seafood consumers. To make the picture even more complex, also DA has recently entered the Adriatic toxin profile. Even though detected so far at concentrations lying below its regulatory limit, this latter toxin must be attentively monitored as it could any time be rising at alarming levels.

In such a dangerous context, a frequent and in-depth chemical analysis of toxic plankton and contaminated seafood is strongly needed. In fact, routine monitoring based on mouse bioassays alone suffers from at least two main drawbacks.

1. Only already known biotoxins can be individuated, and no information is given on any other new toxic compound possibly occurring in toxic plankton or mollusks.
2. Critical misunderstandings in assessing toxin content of a sample can arise, as demonstrated in the case of OAs and desulfoyessotoxins whose identity cannot be established on the basis of the official mouse bioassay alone.

Besides all of the above hazards, very recently another most dangerous threat has been impending over the Mediterranean Sea: the spreading of the tropical alga *O. ovata*. Our investigation on Mediterranean *O. ovata* has brought to light the presence of a new palytoxin-like compound, named ovatoxin-a, alongside minor amounts of a putative palytoxin. In this field, the next step of our lab will be the isolation and full characterization of ovatoxin-a. This is a prerequisite to evaluate its toxicity and assess whether it represents a serious threat to human beings. The potential of ovatoxin-a of entering the human food chain should be also investigated. In particular, scientific efforts should zero in on singling out edible marine organisms capable of accumulating ovatoxin-a, as well as assessing the extent of the accumulation process.

Another crucial issue entwined with *O. ovata* deals with the release of palytoxins into the marine aerosol, inducing fastidious symptoms—that is, respiratory distress and conjunctivitis-in humans. To this regard it is fundamental studying the environmental factors, such as weather conditions and geographical morphology, favoring the onset of the toxic aerosols, as they cause grave damages to the tourism industry, such an essential component of the Italian economy.

REFERENCES

[1] G.M. Hallegraeff, A review of harmful algal blooms and their apparent global increase, Phycologia 32 (1993) 79–99.
[2] C.P. Soames-Mraci, Shellfish poisoning: public health risks, quality assurance and analytical detection, Chem. Aust. (1995, December) 22–25.

[3] J. Tibbetts, Toxic Tides, Environ. Health Perspect. 106 (1998) A326–A331.

[4] S.E. Shumway, A review of the effects of algal blooms on shellfish and aquaculture, J. World Aquacult. Soc. 21 (1990) 65–104.

[5] F.E. Ahmed, Naturally occurring seafood toxins, J. Toxicol. Toxin Rev. 10 (1991) 263–287.

[6] D.M. Anderson in: T. Okaichi, D.M. Anderson, and T. Nemoto (Eds.). Red Tides: Biology Environmental Science and Toxicology, Elsevier, New York, 1989, pp 11–16.

[7] T. Smayda in: K.L.M.A. Sherman, B.D. Gold (Eds.), Food Chains, Yields, Models, and Management of Large Ecosystems, Westview Press, Boulder.

[8] D.J. Bower, R.J. Hart, P.A. Matthews, M.E.H. Howden, Nonprotein neurotoxins, Clin. Toxicol. 18 (1981) 813–843.

[9] L.M. Botana, M. Rodriguez-Vieytes, A. Alfonso, M.C. Louzao, in: L.M.L. Nollet (Ed.), Handbook of food analysis—residues and other food component analysis, Vol. 2. Marcel Dekker Inc., New York, 1996, pp. 1147–1169.

[10] L.M. Botana, in: L.M. Botana (Ed.), 2nd edn, CRC Press Taylor & Francis Group, Boca Raton, FL, 2008, pp. 149–161.

[11] FAO Food and Nutrition Papers 80, 2004, pp. 1–295, http://www.fao.org/docrep/007/y5486e/y5486e00.htm.

[12] P. Ciminiello and E. Fattorusso, in: G. Cimino, M. Gavagnin (Eds.), Progress in Molecular and Subcellular Biology—Subseries Marine Molecular Biotechnology, 43, Springer-Verlag Berlin, Heidelberg, 2006, 53–82.

[13] P. Ciminiello, C. Dell'Aversano, E. Fattorusso, M. Forino, S. Magno, F. Santelia, M. Tsoukatou, Investigation of the toxin profile of Greek *Mytilus galloprovincialis* by liquid chromatography–mass spectrometry, Toxicon 47 (2006) 174–181.

[14] G. Sansoni, B. Borghini, G. Camici, M. Casotti, P. Righini, C. Rustighi, Fioriture algali di *Ostreopsis ovata* (Gonyaulacales: Dinophyceae): Un problema emergente, Biologia Ambientale 17 (2003) 17–23.

[15] A. Penna, M. Vila, S. Fraga, M.G. Giacobbe, F. Andreoni, P. Riobò, C. Vernesi, Characterization of *Ostreopsis* and *Coolia* (Dinophyceae) isolates in the Western Mediterranean sea based on morphology, toxicity and internal transcribed spacer 5.8S rDNA sequences, J. Phycol. 41 (2005) 212–225.

[16] P. Ciminiello, C. Dell'Aversano, E. Fattorusso, M. Forino, G.S. Magno, L. Tartaglione, C. Grillo, N. Melchiorre, The Genoa 2005 outbreak. Determination of putative palytoxin in Mediterranean *Ostreopsis ovata* by a new liquid chromatography tandem mass spectrometry method, Anal. Chem. 78 (2006) 6153–6159.

[17] P. Ciminiello, C. Dell'Aversano, E. Fattorusso, M. Forino, L. Tartaglione, C. Grillo, N. Melchiorre, Putative palytoxin and its new analogue, ovatoxin-a, in *Ostreopsis ovata* collected along the Ligurian coasts during the 2006 toxic outbreak, J. Am. Soc. Mass Spectrom. 19 (2008) 111–120.

[18] P. Durando, F. Ansaldi, P. Oreste, P. Moscatelli, L. Marensi, C. Grillo, R. Gasparini, G. Icardi, *Ostreopsis ovata* and human health: Epidemiological and clinical features of respiratory syndrome outbreaks from a two-year syndromic surveillance, 2005–06, in north-west Italy, Euro Surveill. 12(6), (2007) 191–193.

[19] Y. Shimizu, Chemistry and mechanism of action, Food Sci. Technol. 103 (2000) 151–172.

[20] S. Hall, G. Strichartz, E. Moczydlowski, A. Ravindran, P.B. Reichardt, in: S. Hall and G. Strichartz (Eds.), Marine toxins: Origin, structure and molecular pharmacology, American Chemical Society, Washington, DC., 1990, pp. 29–65.

[21] T. Yasumoto, M. Murata, Marine Toxins, Chem. Rev. 93 (1993) 1897–1909.

[22] M. Murata, M. Shimatani, H. Sugitani, Y. Oshima, T. Yasumoto, Isolation and structural elucidation of the causative toxin of the diarrhetic shellfish poisoning, Bull. Jpn. Soc. Sci. Fish. 48 (1982) 549–552.

[23] T. Hu, J. Doyle, D. Jackson, J. Mart, E. Nixon, S. Pleasance, M.A. Quilliam, J.A. Walter, J.L.C. Wright, Isolation of a new diarrhetic shellfish poison form Irish mussels, J. Chem. Soc. Chem. Commun. 30 (1992) 39–41.

[24] J.S. Lee, T. Igarashi, S. Fraga, E. Dahl, P. Hovgaard, T. Yasumoto, Determination of diarrhetic shellfish toxins in various dinoflagellate species, J. Appl. Phycol. 1 (1989) 147–152.

[25] G. Eaglesham, S. Brett, B. Davis, N. Holling, Detection of pectenotoxin-2 and pectenotoxin-2 seco acid in phytoplankton and shellfish from the Ballina region of New South Wales, Australia *X International IUPAC Symposium on Mycotoxins and Phycotoxins*, Brazil, 2000, 40.

[26] L.L. Rhodes, M. Syhre, Okadaic acid production by a New Zealand *Prorocentrum lima* isolate, New Zealand J. Mar. Freshwat. Res. 29 (1995) 367–370.

[27] I. Bravo, M.L. Fernandez, I. Ramilo, A. Martinez, Toxin composition of the toxic dinoflagellate *Prorocentrum lima* isolated from different locations along the Galician coast (NW Spain), Toxicon 39 (2001) 1537–1545.

[28] K. Terao, E. Ito, T. Yanagi, T. Yasumoto, Histopathological studies on experimental marine toxin poisoning. 1. Ultrastructural changes in the small-intestine and liver of suckling mice induced by dinophysistoxin-1 and pectenotoxin-1, Toxicon 24 (1986) 1141–1151.

[29] H. Fujiki, M. Suganuma, Tumor promotion by inhibitors of protein phosphatases 1 and 2A: The okadaic acid class of compounds, Adv. Cancer Res. 61 (1993) 143–194.

[30] A. Takai, M. Murata, K. Torigoe, M. Isobe, G. Mieskes, T. Yasumoto, Inhibitory effect of okadaic acid derivatives on protein phosphatases. A study on structure-affinity relationship, Biochem. J. 284 (1992) 539–544.

[31] K. Sasaki, M. Murata, T. Yasumoto, G. Mieskes, A. Takai, Affinity of okadaic acid to type-1 and type-2A protein phosphatases is markedly reduced by oxidation of its 27-hydroxyl group, Biochem. J. 298 (1994) 259–262.

[32] M. Murata, M. Kumagai, J.S. Lee, T. Yasumoto, Isolation and structure of yessotoxin, a novel polyether compound implicated in diarrhetic shellfish poisoning, Tetrahedron Lett. 28 (1987) 5869–5872.

[33] M. Satake, L. MacKenzie, T. Yasumoto, Identification of *Protoceratium reticulatum* as the biogenetic origin of yessotoxin, Nat. Toxins 5 (1997) 164–167.

[34] B. Paz, P. Riobo, M.L. Fernandez, S. Fraga, J.M. Franco, Production and release of yessotoxins by the dinoflagellates *Protoceratium reticulatum* and *Lingulodinium polyedrum* in culture, Toxicon 44 (2004) 251–258.

[35] L. Rhodes, P. McNabb, M. de Salas, L. Briggs, V. Beuzenberg, M. Gladstone, Yessotoxin production by *Gonyaulax spinifera*, Harmful Algae 5 (2006) 148–155.

[36] M. Konishi, X. Yang, B. Li, C.R. Fairchild, Y. Shimizu, Highly cytotoxic metabolites from the culture supernatant of the temperate dinoflagellate *Protoceratium* cf. *reticulatum*, J. Nat. Prod. 67 (2004) 1309–1313.

[37] M. Satake, A. Tubaro, J-S. Lee, T. Yasumoto, Two new analogs of yessotoxin homoyessotoxin, and 45-hydroxyhomoyessotoxin, isolated from mussels of the Adriatic Sea, Nat. Toxins 5 (1997) 107–110.

[38] P. Ciminiello, E. Fattorusso, M. Forino, R. Poletti, R. Viviani, Structure determination of carboxyhomoyessotoxin, a new yessotoxin analog isolated from Adriatic mussels, Chem. Res. Toxicol. 3 (2000) 770–774.

[39] P. Ciminiello, E. Fattorusso, M. Forino, R. Poletti, 42,43,44,45,46,47,55-Heptanor-41-oxohomoyessotoxin, a new biotoxin from mussels of the northern Adriatic Sea, Chem. Res. Toxicol. 14 (2001) 596–599.

[40] J. Aasen, I.A. Samdal, C.O. Miles, E. Dahl, L.R. Briggs, T. Aune, Yessotoxins in Norwegian blue mussels (*Mytilus edulis*): Uptake from *Protoceratium reticulatum,* metabolism and depuration, Toxicon 45 (2005) 265–272.

[41] K. Terao, E. Ito, M. Oarada, M. Murata, T. Yasumoto, Histopathological studies on experimental marine toxin poisoning: 5. The effects in mice of yessotoxin isolated from *Patinopecten yessoensis* and of a desulfated derivative, Toxicon 28 (1990) 1095–1104.

[42] H. Ogino, M. Kumagai, T. Yasumoto, Toxicologic evaluation of yessotoxin, Nat. Toxins 5 (1997) 225–229.

[43] J.M. Huang, C.H. Wu, D.G. Baden, Depolarizing action of a red-tide dinoflagellate brevetoxin on axonal membranes, J. Pharmacol. Exp. Ther. 229 (1984) 615–621.

[44] M. Inoue, M. Dirama, M. Satake, K. Sugiyama, T. Yasumoto, Inhibition of breve-toxins binding to voltage-gated sodium channel by gambierol and gambieric acid-A, Toxicon 41 (2003) 469–474.

[45] L.A. de la Rosa, A. Alfonso, N. Vilarino, M.R. Vieytes, L.M. Botana, Modulation of cytosolic calcium levels of human lymphocytes by yessotoxin, a novel marine phy-cotoxin, Biochem. Pharmacol. 61 (2001) 827–833.

[46] L.A. de la Rosa, A. Alfonso, N. Vilarino, M.R. Vieytes, T. Yasumoto, L.M. Botana, Maitotoxin-induced calcium entry in human lymphocytes: modulation by yesso-toxin, Ca(2+) channel blockers and kinases, Cell. Signal. 13 (2001) 711–716.

[47] A. Alfonso, L.A. de la Rosa, M.R. Vieytes, T. Yasumoto, L.M. Botana, Yessotoxin a novel phycotoxin, activates phosphodiesterases activity. Effect of yessotoxin on cAMP levels in human lymphocytes, Biochem. Pharmacol. 65 (2003) 193–208.

[48] J.L.C. Wright, R.K. Boyd, A.S.W. de Freitas, M. Falk, R.A. Foxall, W.D. Jamieson, M.V. Laycock, A.W. McCulloch, A.G. McInnes, P. Odense, V.P. Pathak, M.A. Quilliam, *et al.* Identification of domoic acid, a neuroexcitatory amino acid, in toxic mussels from eastern Prince Edward Island, Can. J. Chem. 67 (1989) 481–490.

[49] S.S. Bates, C.J. Bird, A.S.W. de Freitas, R. Foxall, M. Gilgan, L.A. Hanic, G.R. Johnson, A.W. McCulloch, P. Odense, R. Pocklington, M.A. Quilliam, P.G. Sim, *et al.* Pennate diatom *Nitzschia pungens* as the primary source of domoic acid a toxin in shellfish from eastern Prince Edward Island, Can. J. Fish. Aq. Sci. 46 (1989) 1203–1215.

[50] D.L. Garrison, S.M. Conrad, P.P. Eilers, E.M. Waldron, Confirmation of domoic acid production by *Pseudo-nitzschia australis* (Bacillariophyceae) cultures, J. Phycol. 28 (1992) 604–607.

[51] J.L. Martin, K. Haya, L.E. Burridge, D.J. Wildish, *Nitzschia pseudodelicatissima*— a source of domoic acid in the Bay of Fundy, eastern Canada, Marine Ecol. Progress Series 67 (1990) 177–182.

[52] F. Cerino, L. Orsini, D. Sarno, C. Dell'Aversano, L. Tartaglione, A. Zingone, The alternation of different morphotypes in the seasonal cycle of the toxic diatom, *Pseudo-nitzschia galaxiae*, Harmful Algae 4 (2005) 33–48.

[53] J. Clayden, B. Read, K.R. Hebditch, Chemistry of domoic acid isodomoic acids and their analogs, Tetrahedron 61 (2005) 5713–5724.

[54] F.W. Bernam, T.F. Murray, Domoic acid neurotoxicity in cultured cerebellar granule neurons is mediated predominantly by NMDA receptors that are activated as a consequence of excitatory amino acid release, J. Neurochem. 69 (1997) 693–703.

[55] M.A. Quilliam, J.L.C. Wright, The amnesic shellfish poisoning mystery, Anal. Chem. 61 (1989) 1053–1060.

[56] T. Suzuki, in: L.M. Botana (Ed.), 2nd Edn,. CRC Press Taylor & Francis Group, Boca Raton, FL, 2008, pp. 343–359.

[57] T. Yasumoto, M. Murata, J.S. Lee, K. Torigoe, in: S. Natori, K. Hashimoto, and Y. Ueno (Eds.), Mycotoxins and Phycotoxins, Elsevier, Amsterdam, 1989, pp. 375–382.

[58] L. Edebo, S. Lange, X.P. Li, S. Allenmark, F. Jennische, in: S. Natori, K. Hashimoto, and Y. Ueno (Eds.), Mycotoxins and Phycotoxins, Elsevier, Amsterdam, 1989, pp. 437–444.

[59] J.C. Gonzalez, F. Leira, O.I. Fontal, M.R. Vieytes, F.F. Arevalo, J.M. Vieites, M. Bermudez-Puente, S. Muniz, C. Salgado, T. Yasumoto, L.M. Botana, Inter-laboratory validation of the fluorescent protein phosphatase inhibition assay to determine diarrhetic shellfish toxins: Intercomparison with liquid chromatography and mouse bioassay, Anal. Chim. Acta 466 (2002) 233–246.

[60] H.A. Lun, D.Z. Chen, J. Magoon, J. Worms, J. Smith, C.F. Holmes, Quantification of Diarrhetic Shellfish Toxins by identification of novel protein phosphatase inhibitors in marine phytoplankton and mussels, Toxicon 31 (1993) 75–83.

[61] J.H. Jung, C.J. Sim, C.O. Lee, Cytotoxic compounds from a two-sponge association, J. Nat. Prod. 58 (1995) 1722–1726.

[62] M. Ishige, N. Satoh, T. Yasumoto, Pathological studies on the mice administered with the causative agent of diarrhetic shellfish poisoning (okadaic acid and pecteno-toxin-2), Bull. Hokkaido Inst. Public Health 38 (1988) 15–19.

[63] A.D. Cembella, M.A. Quilliam, N.I. Lewis, A.G. Bauder, J.L.C. Wright, in: B. Reguera, J. Blanco, M.L. Fernandez, and T. Wyatt (Eds.), Xunta de Galicia and Intergovernmental Oceanographic Commission of UNESCO, 1998, pp. 481–484.

[64] A.D. Cembella, N.I. Lewis, M.A. Quilliam, Spirolide composition of micro-extracted pooled cells isolated from natural plankton assemblages and from cultures of the dinoflagellate Alexandrium ostenfeldii, Nat. Toxins 7 (1999) 197–206.

[65] T. Hu, J.M. Curtis, Y. Oshima, M.A. Quilliam, J.A. Walter, W.M. Watson-Wright, J.L.C. Wright, Spirolides B and D, two novel macrocycles isolated from the digestive glands of shellfish, J. Chem. Soc. Chem. Commun. 20 (1995) 2159–2161.

[66] T. Hu, J.M. Curtis, J.A. Walter, J.L.C. Wright, , Characterization of biologically inactive spirolides E and F: Identification of the spirolide pharmacophore, Tetrahe-dron Lett. 37 (1996) 7671–7674.

[67] T. Hu, I.W. Burton, A.D. Cembella, J.M. Curtis, M.A. Quilliam, J.A. Walter, J.L.C. Wright, Characterization of spirolides A, C and 13-desmethylC, new marine toxins isolated from toxic plankton and contaminated shellfish, J. Nat. Prod. 64 (2001) 308–312.

[68] L. Sleno, M.J. Chalmers, D.A. Volmer, Structural study of spirolide marine toxins by mass spectrometry. Part II. Mass spectrometric characterization of unknown spirolides and related compounds in a cultured phytoplankton extract, Anal. Bioanal. Chem. 378 (2004) 977–986.

[69] J. Aasen, S.L. MacKinnon, P. LeBlanc, J.A. Walter, P. Hovgaard, T. Aune, M.A. Quilliam, Detection and identification of spirolides in Norwegian shellfish and plankton, Chem. Res. Toxicol. 18 (2005) 509–515.

[70] S.L. MacKinnon, J.A. Walter, M.A. Quilliam, A.D. Cembella, P. LeBlanc, I.W. Burton, W.R. Hardstaff, N.I. Lewis, Spirolides isolated from Danish strains of the toxigenic dinoflagellate Alexandrium ostenfeldii, J. Nat. Prod. 69 (2006) 983–987.

[71] D. Richard, E. Arsenault, A. Cembella, M.A. Quilliam, in: G.M. Hallegraeff, S.I. Blackburn, C.J. Bolch, and R.J. Lewis (Eds.), Harmful Algal Blooms 2000, Inter-governmental Oceanographic Commission of UNESCO, Paris, 2001, pp. 383–386.

[72] R.E. Moore, P.J. Scheuer, Palytoxin: A new marine toxin from a coelenterate, Science 172 (1971) 495–498.

[73] R.E. Moore, G. Bartolini, Structure of palytoxin, J. Am. Chem. Soc. 103 (1981) 2491–2494.

[74] D. Uemura, K. Ueda, Y. Hirata, H. Naoki, T. Iwashita, Further studies on palytoxin. II. Structure of palytoxin, Tetrahedron Lett. 22 (1981) 2781–2784.

[75] J.K. Cha, W.J. Christ, J.M. Finan, H. Fujioka, Y. Kishi, L.L. Klein, S.S. Ko, J. Leder, W.W. McWhorter, Jr, K.P. Pfaff, M. Yonaga, D. Uemura, et al. Stereochemistry of palytoxin. Part 4. Complete structure, J. Am. Chem. Soc. 104 (1982) 7369–7371.

[76] R.W. Armstrong, J.M. Beau, S.H. Cheon, W.J. Christ, H. Fujioka, W.H. Ham, L.D. Hawkins, H. Jin, S.H. Kang, Y. Kishi, M.J. Martinelli, W.W. McWhorter, Jr., *et al.* Total synthesis of palytoxin carboxylic acid and palytoxin amide, J. Am. Chem. Soc. 111 (1989) 7530–7533.

[77] M. Usami, M. Satake, S. Ishida, A. Inoue, Y. Kan, T. Yasumoto, Palytoxin analogs from the dinoflagellate *Ostreopsis siamensis*, J. Am. Chem. Soc. 117 (1995) 5389–5390.

[78] S. Taniyama, A. Osamu, T. Masamitsu, N. Sachio, T. Tomohiro, M. Yahia, N. Tamao, *Ostreopsis* sp., a possible origin of palytoxin (PTX) in parrotfish *Scarus ovifrons*, Toxicon 42 (2003) 29–33.

[79] Y. Onuma, M. Satake, T. Ukena, J. Roux, S. Chanteau, N. Rasolofonirina, M. Ratsimaloto, H. Naoki, T. Yasumoto, Identification of putative palytoxin as the cause of clupeotoxism, Toxicon 37 (1999) 55–65.

[80] T. Ukena, M. Satake, M. Usami, Y. Oshima, H. Naoki, T. Fujita, Y. Kan, T. Yasumoto, Structure elucidation of ostreocin D, a palytoxin analog isolated from the dinoflagellate *Ostreopsis siamensis*, Biosci. Biotechnol. Biochem. 65 (2001) 2585–2588.

[81] T. Ukena, M. Satake, M. Usami, Y. Oshima, T. Fujita, H. Naoki, T. Yasumoto, Structural confirmation of ostreocin-D by application of negative-ion fast-atom bombardment collision-induced dissociation tandem mass spectrometric methods, Rapid Commun. Mass Spectrom. 16 (2002) 2387–2393.

[82] S. Lenoir, L. Ten-Hage, J. Turquet, J.P. Quod, C. Bernard, M.C. Hennion, First evidence of palytoxin analogues from an *Ostreopsis mascarenensis* (Dinophyceae) benthic bloom in southwestern Indian Ocean, J. Phycol. 40 (2004) 1042–1051.

[83] D. Uemura, Y. Hirata, T. Iwashita, H. Naoki, Studies on palytoxins, Tetrahedron 41 (1985) 1007–1017.

[84] J.S. Wiles, J.A. Vick, M.K. Christensen, Toxicological evaluation of palytoxin in several animal species, Toxicon 12 (1974) 427–433.

[85] J.A. ick, J.S. Wiles, The mechanism of action and treatment of palytoxin poisoning, Toxicol. Appl. Pharmacol. 34 (1975) 214–223.

[86] T. Yasumoto, D. Yasumura, Y. Ohizumi, M. Takahashi, A.C. Alcala, L.C. Alcala, Palytoxin in two species of xanthid crab from the Philippines, Agric. Biol. Chem. 50 (1986) 163–167.

[87] Y. Hashimoto, N. Fusetani, S. Kimura, Aluterin, a toxin of filefish *Alutera scripta,* probably originating from a zoantharian *Palythoa tuberculosa*, Bull. Jpn. Soc. Scient. Fish. 35 (1969) 1086–1093.

[88] M. Fukui, M. Murata, A. Inoue, M. Gawel, T. Yasumoto, Occurrence of palytoxin in the triggerfish *Melichtys vidua*, Toxicon 25 (1987) 1121–1124.

[89] A.M. Kodama, Y. Hokama, T. Yasumoto, M. Fukui, S.J. Manea, N. Sutherland, Clinical and laboratory findings implicating palytoxin as cause of ciguatera poisoning due to *Decapterus macrosoma* (mackerel), Toxicon 27 (1989) 1051–1053.

[90] A.C. Alcala, L.C. Alcala, J.S. Garth, D. Yasumura, T. Yasumoto, Human fatality due to ingestion of the crab *Demania reynaudii* that contained a palytoxin-like toxin, Toxicon 26 (1988) 105–107.

[91] T. Noguchi, D.F. Hwang, G. Arakawa, K. Daigo, S. Sato, H. Ozaki, N. Kawai, M. Ito, K. Hashimoto, in: P. Gopalakrishnakone and C.K. Tan (Eds.), Progress in Venom and Toxin Research, National University, Singapore, 1987, pp. 325–335.

[92] S. Weidmann, Effects of palytoxin on the electrical activity of dog and rabbit heart, Experientia 33 (1977) 1487–1489.

[93] H. Bottinger, E. Habermann, Palytoxin binds to and inhibits kidney and erythrocyte Na^+, K^+-ATPase, Naunyn Schmiedebergs Arch. Pharmacol. 325 (1984) 85–87.

[94] H. Bottinger, L. Beress, E. Habermann, Involvement of $(Na^+ + K^+)$-ATPase in binding and actions of palytoxin on human erythrocytes, Biochim. Biophys. Acta 861 (1986) 165–176.

[95] C. Li, O. Capendeguy, K. Geering, J-D. Horisberger, A third Na$^+$-binding site in the sodium pump, Proc. Natl. Acad. Sci. USA 102 (2005) 12706–12711.

[96] E.V. Wattemberg, Palytoxin: Exploiting a novel skin tumor promoter to explore signal transduction and carcinogenesis, Am. J. Physiol. Cell Physiol. 292 (2007) C24–C32.

[97] E.V. Wattemberg, D. Uemura, K.L. Byron, M.L. Villereal, H. Fujiki, M.R. Rosner, Structure–activity studies of the norphorbol tumor promoter palytoxin in carcinogenesis, Cancer Res. 49 (1989) 5837–5842.

[98] H. Fujiki, M. Suganuma, M. Nakayasu, H. Hakii, T. Horiuchi, S. Takayama, T. Sugimura, Palytoxin is a non–12–O–tetradecanoylphorbol–13–acetate type tumor promoter in two–stage mouse skin carcinogenesis, Carcinogenesis 7 (1986) 707–710.

[99] Y. Onuma, M. Satake, T. Ukena, J. Roux, S. Chanteau, N. Rasolofonirina, M. Ratsimaloto, H. Naoki, T. Yasumoto, Identification of putative palytoxin as the cause of clupeotoxism, Toxicon 37 (1999) 55–65.

[100] T. Yasumoto, M. Fukui, K. Sasaki, K. Sugiyama, Determinations of marine toxins in foods, J. AOAC Int. 78 (1995) 574–582.

[101] E. Habermann, G. Ahnert-Hilger, G.S. Chatwal, L. Beress, Delayed hemolytic action of palytoxin. General characteristics, Biochim. Biophys. Acta 649 (1981) 481–486.

[102] G.S. Bignami, A rapid and sensitive hemolysis neutralization assay for palytoxin, Toxicon 31 (1993) 817–820.

[103] P. Riobò, B. Paz, J.M. Franco, Analysis of palytoxin-like in *Ostreopsis* cultures by liquid chromatography with precolumn derivatization and fluorescence detection, Anal. Chim. Acta 566 (2006) 217–223.

[104] E. Fattorusso, P. Ciminiello, V. Costantino, S. Magno, A. Mangoni, A. Milandri, R. Poletti, M. Pompei, R. Viviani, Okadaic Acid in Mussels of Adriatic Sea, Mar. Poll. Bull. 24 (1992) 234–237.

[105] L. Boni, L. Mancini, A. Milandri, R. Poletti, M. Pompei, R. Viviani, in: R. A. Vollenweider, R. Marchetti, and R. Viviani (Eds.), Marine coastal eutrophication. Proc. Inter. Conf. Bologna, 21–24 March 1990, Elsevier, Amsterdam, 1992, pp. 419–426.

[106] J. Zhao, G. Lembeye, G. Cenci, B. Wall, T. Yasumoto, in: T.J. Smayda and Y. Shimizu (Eds.), Toxic Phytoplankton Blooms in the Sea, Vol. 3. Elsevier, New York, 1993, pp. 587–592.

[107] J. Zhao, G. Cenci, E. Di Antonio, T. Yasumoto, Analysis of diarrhetic shellfish toxins in mussels from the Adriatic coast of Italy, Fish. Sci. 60 (1994) 687–689.

[108] R. Draisci, L. Lucentini, L. Riannetti, P. Boria, A. Stacchini, Detection of diarrhetic shellfish toxins in mussels from Italy by ionspray liquid chromatography-mass spectrometry, Toxicon 33 (1995) 1591–1603.

[109] P. Ciminiello, E. Fattorusso, M. Forino, S. Magno, R. Poletti, M. Satake, R. Viviani, T. Yasumoto, Yessotoxin in mussels of the northern Adriatic Sea, Toxicon 35 (1997) 177–183.

[110] P. Ciminiello, E. Fattorusso, M. Forino, S. Magno, R. Poletti, R. Viviani, Isolation of 45-hydroxyyessotoxin from mussels of the Adriatic Sea, Toxicon 37 (1999) 689–693.

[111] M. Satake, A. Tubaro, J-S. Lee, T. Yasumoto, Two new analogs of yessotoxin, homoyessotoxin and 45-hydroxyhomoyessotoxin, isolated from mussels of the Adriatic Sea, Nat. Toxins 5 (1997) 107–110.

[112] P. Ciminiello, E. Fattorusso, M. Forino, S. Magno, R. Poletti, R. Viviani, Isolation of adriatoxin, a new analog of yessotoxin from mussels of the Adriatic Sea, Tetrahedron Lett. 39 (1998) 8897–8900.

[113] P. Ciminiello, E. Fattorusso, M. Forino, R. Poletti, R. Viviani, A new analogue of yessotoxin, carboxyyessotoxin, isolated from Adriatic Sea Mussels, Eur. J. Org. Chem. (2000) 291–295.

[114] P. Ciminiello, E. Fattorusso, M. Forino, R. Poletti, R. Viviani, Structure Determination of Carboxyhomoyessotoxin, a New Yessotoxin Analog Isolated from Adriatic Mussels, Chem. Res. Toxicol. 13 (2000) 770–774.

[115] P. Ciminiello, E. Fattorusso, M. Forino, R. Poletti, 42,43,44,45,46,47,55-Heptanor-41-oxohomoyessotoxin, a New Biotoxin from Mussels of the Northern Adriatic Sea, Chem. Res. Toxicol. 14 (2001) 596–599.

[116] A. Tubaro, S. Sosa, M. Carbonatto, G. Altinier, F. Vita, M. Melato, M. Satake, T. Yasumoto, Oral and intraperitoneal toxicity studies of yessotoxin and homoyessotoxins in mice, Toxicon 41 (2003) 783–792.

[117] Directive of the European Commission 2002/225/EC and ''decreto del Ministero della Salute-16/05/2002

[118] T. Yasumoto, Y. Oshima, M. Yamaguchi, Occurrence of a new type of toxic shellfish in Japan and chemical properties of the toxin, Bull. Jpn. Soc. Sci. Fish. 44 (1978) 1249–1255.

[119] M.A. Quilliam, P. Hess, C. Dell'Aversano, in: W.J. deKoe, R.A. Samson, H.P. Van Egmond, J. Gilbert, and M. Sabino (Eds.), Wageningen, The Netherlands, 2001, pp. 383–391.

[120] P. Ciminiello, C. Dell'Aversano, E. Fattorusso, M. Forino, L. Grauso, G.S. Magno, R. Poletti, L. Tartaglione, Desulfoyessotoxins from Adriatic mussels: A new problem for seafood safety control, Chem. Res. Toxicol. 20 (2007) 95–98.

[121] M.A. Quilliam, in: G.M. Hallegraeff, D.M. Anderson, and A.D. Cembella (Eds.), Manual on Harmful Marine Microalgae, IOC/UNESCO, Paris, 2003, pp. 247–266.

[122] J.F. Lawrence, C.F. Charbonneau, C. Menard, M.A. Quilliam, P.G. Sim, Liquid chromatographic determination of domoic acid in shellfish products using the paralytic shellfish poison extraction procedure of the association of official analytical chemists, J. Chromatogr. 462 (1989) 349–356.

[123] R.A.R. Tasker, B.J. Connel, S.M. Strain, Pharmacology of systematically administered domoic acid in mice, Can. J. Physiol. Pharmacol. 69 (1991) 378–382.

[124] M.A. Quilliam, P.G. Sim, A.W. McCulloch, A.G. McInnes, High-performance liquid chromatography of domoic acid, a marine neurotoxin, with application to shellfish and plankton, Int. J. Environ. Anal. Chem. 36 (1989) 139–154.

[125] M.A. Quilliam, M. Xie, W.R. Hardstaff, Rapid extraction and cleanup for liquid chromatographic determination of domoic acid in unsalted seafood, J. AOAC Int. 78 (1995) 543–554.

[126] R. Pocklington, J.E. Milley, S.S. Bates, C.J. Bird, A.S.W. De Freitas, M.A. Quilliam, Trace determination of domoic acid in seawater and phytoplankton by high-performance liquid chromatography of the fluorenylmethoxycarbonyl (FMOC) derivative, Int. J. Environ. Anal. Chem. 38 (1990) 351–368.

[127] A.L. Nguyen, J.H.T. Luong, C. Masson, Capillary electrophoresis for detection and qantitation of domoic acid in mussels, Anal. Lett. 23 (1990) 1621–1634.

[128] J-Y. Zhao, P. Thibault, M.A. Quilliam, Analysis of domoic acid and isomers in seafood by capillary electrophoresis, Electrophoresis 18 (1997) 268–276.

[129] M.A. Quilliam, B.A. Thomson, G.J. Scott, K.W.M. Siu, Ion-spray mass spectrometry of marine neurotoxins, Rapid Commun. Mass Spectrom. 3 (1989) 145–150.

[130] C. Dell'Aversano, G.K. Eaglesham, M.A. Quilliam, Analysis of cyanobacterial toxins by hydrophilic interaction liquid chromatography-mass spectrometry, J. Chromatogr. A. 1028 (2004) 155–164.

[131] C. Dell'Aversano, P. Hess, M.A. Quilliam, Hydrophilic Interaction Liquid Chromatography-Mass Spectrometry for the analysis of Paralytic Shellfish Poisoning Toxins, J. Chromatogr. A. 1081 (2005) 190–201.

[132] P. Ciminiello, C. Dell'Aversano, E. Fattorusso, M. Forino, G.S. Magno, L. Tartaglione, M.A. Quilliam, A. Tubaro, R. Poletti, Hydrophilic interaction liquid

chromatography-mass spectrometry (HILIC-MS) for determination of domoic acid in Adriatic shellfish, Rapid Commun. Mass Spectrom. 19 (2005) 2030–2038.

[133] P. Ciminiello, C. Dell'Aversano, E. Fattorusso, G.S. Magno, L. Tartaglione, M. Cangini, M. Pompei, F. Guerrini, L. Boni, R. Pistocchi, Toxin profile of *Alexandrium ostenfeldii* (Dinophyceae) from the Northern Adriatic Sea revealed by liquid chromatography-mass spectrometry, Toxicon 47 (2006) 597–604.

[134] L. Mackenzie, D. White, Y. Oshima, J. Kapa, The resting cyst and toxicity of *Alexandrium ostenfeldii* (Dinophyceae) in New Zealand, Phycologia 35 (1996) 148–155.

[135] A.D. Cembella, N.I. Lewis, M.A. Quilliam, The marine dinoflagellate *Alexandrium ostenfeldii* (Dinophyceae) as the causative organism of spirolide shellfish toxins, Phycologia 39 (2000) 67–74.

[136] P. Ciminiello, C. Dell'Aversano, E. Fattorusso, M. Forino, L. Grauso, L. Tartaglione, F. Guerrini, R. Pistocchi, Spirolide toxin profile of Adriatic *Alexandrium ostenfeldii* cultures and structure elucidation of 27-hydroxy-13,19-didesmethylspirolide C, J. Nat. Prod. 70 (2007) 1878–1883.

[137] G. Sansoni, B. Borghini, G. Camici, M. Casotti, P. Righini, C. Rustighi, Fioriture algali di *Ostreopsis ovata* (Gonyaulacales: Dinophyceae): Un problema emergente, Biologia Ambientale 17 (2003) 17–23.

[138] A. Penna, M. Vila, S. Fraga, M.G. Giacobbe, F. Andreoni, P. Riobò, C. Vernesi, Characterization of *Ostreopsis* and *Coolia* (Dinophyceae) isolates in the Western Mediterranean sea based on morphology, toxicity and internal transcribed spacer 5.8S rDNA sequences, J. Phycol. 41 (2005) 212–225.

[139] M. Gallitelli, N. Ungaro, L.M. Addante, V. Procacci, N. Gentiloni, C. Sabbà, Respiratory illness as a reaction to tropical algal blooms occurring in a temperate climate, JAMA 293 (2005) 2599–2600.

[140] P. Ciminiello, E. Fattorusso, Shellfish toxins—Chemical studies on Northern Adriatic mussels, Eur. J. Org. Chem. 12 (2004) 2533–2551.

[141] J. Furey, K. Garcia, M. O'Callaghan, M.F. Lehane, K.J. Amandi, James, Brevetoxins: Structures, toxicology, and origin, Phycotoxins (2007) 19–46.

[142] D. Uemura, Bioorganic Studies on Marine Natural Products—Diverse Chemical Structures and Bioactivities, Chem. Rec. 6 (2006) 235–248.

[143] I. Di Girolamo, E. Fattorusso, E. Funari, L. Gramaccioni, C. Grillo, G. Icardi, D. Mattei, R. Poletti, S. Scardala, E. Testai, Linee guida—Gestione del Rischio associato alle fioriture di Ostreopsis ovata nelle coste italiane, Enacted by Consiglio Superiore di Sanità-Ministero della Salute—May 24th 2007.

[144] K. Aligizaki, P. Katikou, G. Nikolaidis, A. Panou, First episode of shellfish contamination by palytoxin -like compounds from *Ostreopsis* species (Aegean Sea, Greece), Toxicon 51 (2008) 418–427.

MECHANISM OF FIBER CARCINOGENESIS: FROM EXTRANUCLEAR TARGET TO TRANSFORMING GROWTH FACTOR SIGNALING PATHWAY

Tom K. Hei*

Contents

* Center for Radiological Research, College of Physicians and Surgeons and Department of Environmental Health Sciences, Mailman School of Public Health, Columbia University, New York, New York 10032
Tel.: +1 212 305 8462; Fax: +1 212 305 3229
E-mail: tkh1@columbia.edul

1. Introduction

The association between exposure to asbestos fibers and the development of lung cancer and mesothelioma has been well-established in both man and experimental animals [1–3]. Furthermore, cigarette smoking can enhance the lung cancer incidence among asbestos workers in a synergistic fashion [4,5]. The fact that asbestos, a known and highly durable carcinogen, which has been used extensively in industry and households for decades, continues to pose an important health concern even though the US Environmental Protection Agency has restricted the industrial use of asbestos since the early 1970s. The danger of developing asbestos related diseases appears to extend beyond that of a simple occupational hazard since it has been documented in family members of asbestos workers [6,7], in individuals living in the neighborhood of industrial sources of asbestos [8], and in some school and public buildings where asbestos is being used as insulation material [9,10]. The attack of the World Trade Center in New York City created an environmental disaster of enormous magnitude and there had been reports that many tons of asbestos-containing dust particles were released into the surrounding neighborhood [11]. The identification in 2000 that approximately one-third of the 4500 residents of Libby, Montana, some as young as 10 years-old, developed asbestos-related diseases from exposure to tremolites-contaminated vermiculites, exemplifies the human toll of environmental asbestos exposure. The continued discovery of routes through which the general public may be exposed to asbestos suggests a long-term, low dosage exposure of a large number of people. A better understanding of the genotoxic/carcinogenic mechanisms of asbestos is critical for the prevention and treatment of asbestos–induced diseases including mesothelioma, an often fatal cancer with an average patient survival of less than 6 months from the time of diagnosis.

The mechanisms by which asbestos produces malignancy are not entirely clear at present. Various *in vitro* and *in vivo* studies, however, have suggested that fiber dimensions, surface properties, and physical durability are important criteria for the carcinogenicity of the fibers [12–14]. The correlation between fiber dimension and carcinogenic potency suggests the importance of fiber–cell interactions [15]. There is evidence to suggest that oxygen free radicals, particular hydroxyl radicals, may play an essential role in fiber toxicology [16–18]. Several studies have shown that iron content in many types of carcinogenic fibers (e.g., crocidolites that contains 21% of iron by weight) provides the necessary catalyst in the formation of reactive oxygen species (ROS) through a series of one electron reduction of molecular oxygen [19–21]. There is evidence that iron from phagocytosized fibers can be mobilized by intracellular chelators, thereby enhancing its redox

activity and allowing cellular damages to occur at sites distant from the fibers [22]. The production of nitric oxide has also been shown in fiber-exposed human lung epithelial cells as well as in rodent alveolar macrophages [23,24].

2. Interaction Between Asbestos and Tobacco Smoke

Earlier studies by Selikoff *et al.*, have shown that tobacco smoking can synergistically enhance the lung cancer incidence among asbestos workers [4]. In addition to various cancer causing chemicals in tobacco smoke, including tobacco specific nitrosamines, phenolic compounds, benzo(*a*) pyrene, tobacco smoke also contains trace amount of polonium–210 radio-nucleotide [25,26]. It is possible that these alpha emitters can interact with asbestos to promote development of lung cancer.

3. Neoplastic Transformation as a Surrogate for *In Vivo* Carcinogenicity

Morphological transformation assays based on rodent cell systems such as C3H 10T1/2, NIH3T3, and Syrian hamster embryo cells occupy a useful intermediate position between the bacterial mutagenesis assays, which are quick and inexpensive, and animal studies, which are cumbersome and inordinately expensive [27]. These assays afford an opportunity to evaluate both the qualitative and quantitative aspects of fiber/particle-induced onco-genic transformation as well as mechanisms involved in the neoplastic process. Upon treatment with mineral fibers, transformed cells, which loss contact inhibition of growth, form multilayered growth and criss–crossing cells at the peripheral over a contact-inhibition background of nontrans-formed cells. The morphology of the foci can be correlated with neoplastic potential with type III foci being the most tumorigenic when injected into either syngeneic animals or immunosuppressed nude mice.

4. Transformation Induction by Asbestos and Radon

Using the mouse C3H 10T1/2 cell system, the oncogenic transform-ing effect of a 1 μg/cm^2 dose of UICC standard reference crocidolite fibers in concert with a 66 cGy dose of alpha particles accelerated with the Radiological Research Accelerator Facility of Columbia University was
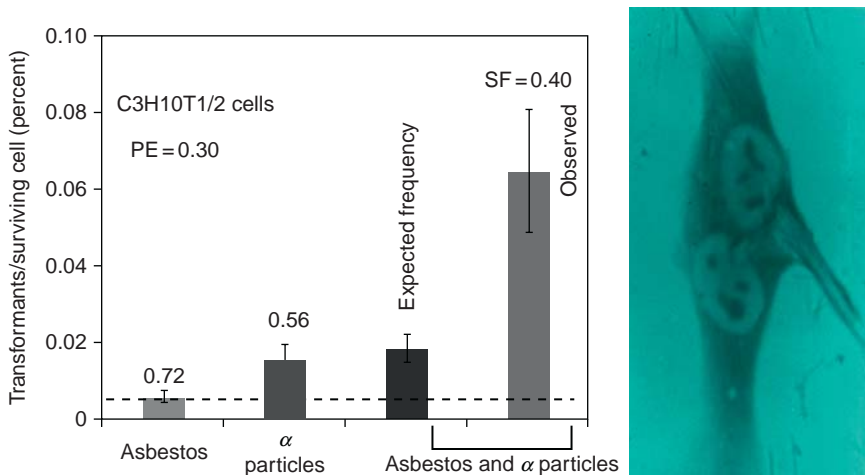
Figure 1   Transformation incidence in C3H 10T1/2 cells treated with crocidolite fibers and alpha particles, either alone or in combination. Expected frequency assuming simple additivity and the actual, observed frequency are shown. Area below dotted line depicts spontaneous frequency. Insert shows a photomicrograph of a binucleated C3H 10T1/2 cells with partially phagocytosed asbestos fibers (400×).

examined, and the results are shown in Figure 1. As shown previously, crocidolite fibers at the dose used which resulted in only moderate cell killing induced an oncogenic transformation incidence which was indistinguishable from the spontaneous rate. However, cells pretreated with the fibers for a period of 24 h and subsequently irradiated with α-particles exhibited a significantly higher transformation yield than those receiving radiation alone ($p < 0.01$, [28]). The combination of asbestos fibers and high LET α-particles produced a transformation incidence which was higher than the sum of the two agents alone. This apparent supra–additivity, in lieu of synergism in the absence of a complete dose response curve, has implications for the possible interaction of radon and asbestos both in the environment as well as in the workplace.

5. Asbestos as a Gene and Chromosomal Mutagen

The physical interaction between asbestos and spindle asters and the presence of binucleated cells in fiber treated mammalian cells suggests that asbestos fibers may interfere with cytokinesis, that is, genotoxic. However, a brief survey of the literature suggests otherwise. Although various types of asbestos fibers have been shown to induce chromosomal aberrations and

sister chromatid exchanges in human mesotheliomas and lung cancers; and in cultured human and mammalian cells [29], mutagenic studies at the hypoxanthine-guanine phosphoribosyl transferase (*hprt*) and ouabain loci in mammalian cells have yielded negative results ([30], for review). Using the human–hamster hybrid (A_L) cells in which mutations are scored at a marker gene (*CD59*) located on human chromosome 11 (11p13) that the A_L cell carries as its only human chromosome, there is evidence that both crocidolite and chrysotile fibers are indeed mutagenic and induce mostly multilocus deletions in mammalian cells (Figure 2, [17,31,32,41]). In contrast, among the same fiber-treated A_L cell population, there were few, if any, mutations scored at the *hprt* locus of the hamster X-chromosome [31,32]. This discrepancy has been attributed to the observation that in assays that are proficient in recovering large deletions, ROS such as those induced by asbestos fibers, have been shown to induce mainly multilocus deletions in mammalian cells [33–35]. Since the *hprt* gene is on the X-chromosome, multilocus deletions in the region of the gene would be lethal and any mutants induced would not be viable [32]. In recent years,
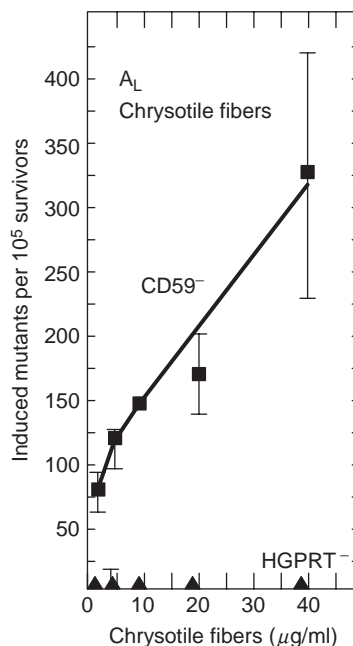
Figure 2 Induced mutation frequencies per 10^5 survivors at either the *S1* (*CD59*) or *HGPRT* loci in A_L cells treated with graded doses of chrysotile asbestos fibers for 24 h. Pooled data from three experiments are shown. Bars represent ±S.E. of means. Induced mutation = total mutant yield minus background, ∼42–100 × 10^{-5} in these experiments for the *S1* locus and between 0.5 and 3 × 10^{-5} for the *HGPRT* locus. Divide the doses by 5 to convert μg/ml to μg/cm^2 growth area.

several other mutagenic assays that are proficient in detecting either large deletions, homologous recombinations, or score mutants located on a nonessential gene have been used successfully to demonstrate the mutagenic potential of various fiber types [36–38]. These findings provide a direct link between chromosomal abnormalities that have frequently been demonstrated in fiber exposed human and rodent cell lines and carcinogenicity *in vivo*. The observation that antioxidant enzymes such as catalase and superoxide dismutase can protect cells against the mutagenic effects of asbestos provides further evidence for the role of oxyradicals in fiber toxicology [39–42].

6. ROLE OF FIBER CELL INTERACTION IN MEDIATING FIBER GENOTOXICITY

The correlation between fiber dimension and carcinogenic potency suggests the importance of fiber-cell interactions. The ability of cells to phagocytose asbestos fibers both *in vitro* and *in vivo* has been well documented [43]. Fibers less than 5 μm in length are usually completely phagocytosed whereas those greater than 25 μm are generally not. This inability to completely engulf long fibers has been termed ''frustrated phagocytosis'' which has been associated with increased membrane permeability and increased oxyradical production [44]. Figure 3 shows the effect of a diminished phagocytic ability on chrysotile-induced mutagenicity in A_L cells. Cytochalasin B at a dose of 1 μg/ml, while being minimally cytotoxic (surviving fraction ~0.82) and largely nonmutagenic, reduced to one third the percentage of A_L
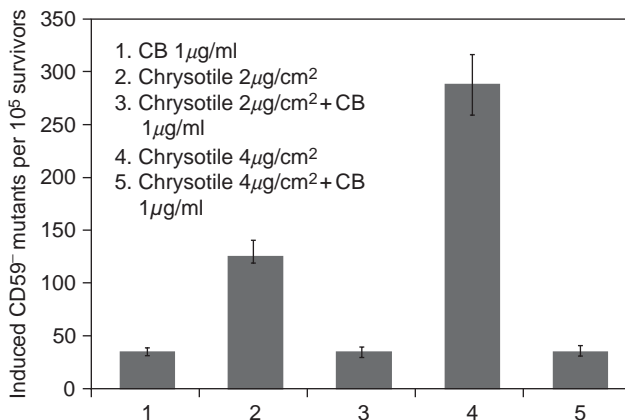

Figure 3   Induced $CD59^-$ mutants in A_L cells treated with UICC chrysotiles with or without concurrent cytochalasin B which inhibits cellular phagocytosis. Data are pooled from 3–5 experiments. Bars, $\pm$ SEM.

cells containing phagocytosed fibers in cells treated with a 2 μg/cm^2 dose of UICC chrysotile fibers as well as the number of internalized fibers per phagocytic cell (data not shown). Concurrent treatment of fiber-exposed cells with cytochalasin B significantly reduced fiber-induced CD59$^-$ mutant yield ($p < 0.05$). In cells exposed to 2 μg/cm^2 dose of fiber, concurrent treatment with cytochalasin B reduced the induced mutant fraction to a level similar to that of cytochalasin B treatment alone (Figure 3). There is evidence that oxyradicals play an essential role in fiber toxicology [45, for review]. Although iron has been shown to be an important source of ROS with the iron-rich crocidolite fibers [22], not all iron containing minerals, for example, iron oxide are toxic. Furthermore, the observation that tremolites and erionites, which contain little or no iron are mutagenic in the A_L cells, suggest that fiber–cell interaction may be an important prerequisite in fiber mutagenesis [46].

7. Asbestos Fibers Induce ROS

If generation of ROS is one of the major mechanisms for asbestos-induced mutagenesis in mammalian cells, then fiber treatment should be expected to induce ROS production in the A_L cells. Using the radical probe, chloromethyl, dichloro–dihydrofluorescein diacetate (CM-H$_2$DCFDA), there is evidence that asbestos fibers induce a dose dependence induction of ROS in mammalian cells [17]. Quantification of relative fluorescence in fiber-treated and control cells indicated that treatment with a 6 μg/cm^2 dose of crocidolite fibers induced a 5-fold increase in the generation of ROS compared with controls ($p < 0.05$). However, there was no further increase in fluorescence induction with fiber concentration >6 μg/cm^2. The oxyradical nature behind the increase in fluorescence intensity was further supported by including the radical scavenger, dimethyl sulfoxide (DMSO) in the reaction mixture. Although DMSO alone had little effect on the formation of ROS among control cells, the relative fluorescence level induced by a 6 μg/cm^2 dose of fibers in A_L cells decreased by 3-fold in the presence of DMSO, which was consistent with the previous observation of a suppressive effect of DMSO on the formation of 8-hydroxyl-deoxyguanosine in crocidolite-treated A_L cells [17].

8. Source of the Reactive Radical Species

Although there is considerable evidence from various *in vivo* and *in vitro* studies supporting the hypothesis that ROS are important in fiber toxicities [30,47], the origin of these ROS in asbestos-treated cells are not clear. Although iron mobilization has been demonstrated to be important in

the induction of ROS among iron containing asbestos, for example, croci-dolites and amosites as stated above, the observation that noniron containing fibers, such as erionites and chrysotiles, are carcinogenic [13,48] suggests that iron mobilization from fibers may not be the only pathway for ROS induction. Since mitochondria produce 80% of the ATP needs of a cell, they are regarded as the energy center of the cell. ROS and other organic free radicals such as ubisemiquinone and flavosemiquinone are generated as byproducts of electron transport in the respiratory chain [49,50]. Normally, these toxic intermediates are disposed of by antioxidants and free radical scavenging enzymes, such as manganese superoxide dismutase, catalase, and glutathione peroxidase inside the mitochondria. However, mitochondria damage induced by chemical exposure results in decreased activity of these antioxidants, as in the case of asbestos exposure [51,52] and a corresponding increase in ROS which may cause further mitochondrial DNA damage and lipid peroxidation of mitochondrial membranes ([53], for review). Mitochondrial membrane damage has been shown to result in leakage of ROS into the cytoplasm and increase the oxidative stress of the cells [54,55]. In the following section, enucleation and cell fusion techniques are applied to show that the nucleus is not the only target in fiber mutagenesis.

9. Extranuclear Target in Fiber Genotoxicity

To clarify whether the nucleus is a necessary and sufficient target for crocidolite fibers-induced genotoxicity in mammalian cells, enucleated cytoplasts were exposed to crocidolite followed by rescue fusion with normal karyoplasts from untreated cells to determine whether gene muta-tions can be induced in the absence of direct nuclear damage by crocidolite fibers. Firstly, the ability of cytoplasts to generate oxyradicals upon crocido-lite treatment was examined using the radical probe, chloromethyl, dichloro-dihydrofluorescein diacetate (CM-H$_2$DCFDA) described above. Cytoplasts were generated from enucleation by treating cells with cytocha-lasin B followed by centrifugation [56,57]. Treatment of cytoplasts with graded doses of crocidolite fibers resulted in a dose dependence increase in fluorescent signaling. A 6 μg/cm^2 dose of crocidolite increased the fluores-cent intensity by more than 4-fold above the control levels. In contrast, concurrent treatment with 0.5% DMSO, a radical quencher, reduced the fluorescence by more than 2-fold, which was consistent with our previous studies indicating that such a dose of DMSO effectively reduced the muta-genicity of crocidolites. Similarly, results of these studies are consistent with the observations that antioxidant enzymes such as superoxide dismutase and catalase effectively reduce the mutagenicity of fibers [41].

10. Mutagenicity of Crocidolite-Treated Cytoplasts

To evaluate whether cytoplasts can initiate signaling pathways resulting in genotoxic damaging upon crocidolite treatment, enucleated cells were exposed to crocidolite at a dose of 4 μg/cm^2 for 3.5 h with or without concurrent DMSO treatment and then immediately fused with karyoplasts at a ratio of 3:1. When cytoplasts were fused with karyoplasts under the conditions used in the experiments, three fusion outcomes are possible: (i) a karyoplast could fuse with another karyoplast to produce an unstable doublet; (ii) a cytoplast could fuse with another cytoplast to produce another nonviable cytoplasmic doublet; and (iii) a cytoplast could fuse with a karyoplast to produce a viable fusion cell. Whereas the fusion efficiency was only 15–20%, the successfully fused cells had a high viability index ($\sim$80%), as determined by colony-forming capacity. Cultures formed by fusion of nontreated cytoplasts with nuclei in a similar manner were used as controls. The mutation yield induced by crocidolite in reconstituted cells was more than 2-fold than that of the control cultures. The average number of spontaneous $CD59^-$ mutants per 10^5 survivors in fused cells used for all the experiments in the present study was 120 ± 58 per 10^5 survivors. This number was about 2-fold higher than normal spontaneous background in A$_L$ cells and was possibly due to enhanced oxidative stress in enucleated cultures. Concurrent treatment with 0.5% of DMSO dramatically reduced the mutation fraction by 5-fold to 43 ± 17 per 10^5 survivors. DMSO alone was nonmutagenic at the dose used in fused cells. These data suggest that extranuclear target(s) play an important role in fiber genotoxicity [57].

The observation that asbestos induces predominately multilocus deletions provides a mechanistic basis for the potential loss of tumor suppressor function. To delineate the step-wise neoplastic transformation of human bronchial epithelial cells by asbestos, an *in vitro* model using human bronchial epithelial cells were used and described below.

11. Transformation Studies with Human Epithelial Cells

One of the main difficulties in studying mechanisms of asbestos carcinogenesis is the lack of a suitable human cell model system whereby the various tumorigenic stages can be dissected and the molecular changes associated with each stage examined. Up to the present moment, no primary human cell model is available for this area of studies because the frequency for human cell transformation has been estimated to be in the

range of 10^{-15}, an incidence too low to be reproduced in any laboratory setting [58]. Treatment of normal human mesothelial cells with amosite asbestos has been shown to extend the proliferative life span of 4 out of 16 independently derived primary cultures [59]. However, the cells eventually all senesced and entered crisis. Using a human papillomavirus immortalized human bronchial epithelial (BEP2D) cells, there is evidence that a single, 7 day-treatment with a $4\,\mu g/cm^2$ dose of chrysotile induced neoplastic transformation of these cells in a step-wise fashion at a frequency of $\sim 10^{-7}$ as shown in Figure 4. The immortalization step, therefore, increases the transformation yield of primary human epithelial cells by more than a million fold. Tumorigenic BEP2D cells show no mutation in any of the *ras* oncogenes [60]. Results of cell fusion studies between asbestos–induced tumorigenic and parental BEP2D cells demonstrated that the tumorigenic phenotype induced by chrysotile treatment could be completely suppressed by fusion with nontumorigenic control cells [61]. These data indicate that nontumorigenic BEP2D cells complement the loss of putative suppressor element among tumorigenic cells and suggest that loss of suppressor gene(s) as an important mechanism of fiber carcinogenesis. Results of these studies are corroborated with frequent chromosomal loss seen in tumorigenic human bronchial epithelial cells induced by asbestos treatment based on karyotype analyses [62] and in human mesotheliomas [63].

Immortalized human bronchial epithelial cells

Weeks

0   UICC chrysotiles $4\,\mu g/cm^2$ for 7 days

2

4   Saturation density
Terminal differentiation altered

6   Growth in soft agar
Chromosomal aberrations

8   Tumorigenicity — Increased

10

12   No mutation in any *Ras* oncogenes
Mutant p53 expressed

14   Cyclin D1 overexpressed
Telomerase activity increased

16   ↓ regulation of *βigH3* and *p21cip1* gene

18

Figure 4 Schematic diagram illustrating the multistep process in the neoplastic transformation of immortalized human bronchial epithelial cells by chrysotile fibers.

12. Causally Linked Genes to Fiber Carcinogenesis

The next question is what kinds of genes are functionally linked to the tumorigenic phenotype in asbestos treated immortalized human bronchial epithelial cells. Using cDNA microarrays to compare differentially expressed genes in asbestos-induced tumorigenic cell lines relative to parental BEP2D cells, there is evidence that the expression of the *βigH3* gene is downregulated by more than 7–8-fold in the tumorigenic cells (Figure 5; [64]). Furthermore, in the fusion cell lines that are no long tumorigenic in nude mice, the expression level of *βigH3* has been found to be restored to control levels. *β*igH3 is a secreted protein induced by transforming growth factor-*β* (TGF-*β*) in human adenocarcinoma cells as well as other human cell types [65]. This protein is highly conserved and has been shown to modulate cell adhesion and tumor formation. Mutations or altered expression of this gene have been linked to the pathogenesis of human corneal dystrophy, osteogenesis [66,67] and in many human cancer cell lines [64].
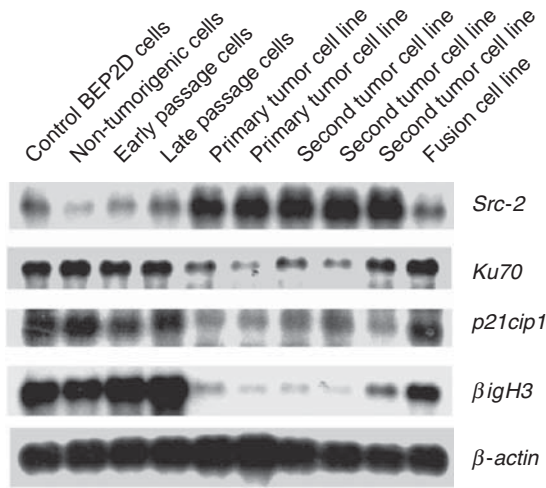
Figure 5 Differentially, expression of *Src2*, *Ku70*, *p21*, and *βigH3* genes in control BEP2D cells, transformed yet nontumorigenic cells, in early and late staged transformed yet nontumorigenic cells, in primary and secondary tumor cell lines and fusion cell between BEP2D cells and secondary tumor cell lines. Expression of *β-actin* levels was used as loading controls.

13. Ectopic Reexpression of *βigH3* Suppresses Tumorigenic Phenotype

To ascertain the tumor suppressive effect of *βigH3* gene, it is necessary to reexpress the lost or down–regulated gene in tumor cells and determines the tumor outcome upon inoculation into nude mice. The approach was to ectopically express the gene in a highly malignant cell line (AsbTB2A) using the pRc/CMV2-*βigH3* expression vector. Two G418 resistant colonies (AsbTB2A–clone 5 and AsbTB2A–clone 11) that expressed different levels of *βigH3* gene were chosen for further studies. From the Northern and Western blotting results, the parental TB2A cells and TB2A-pRc/CMV2 cells expressed a low, detectable, and similar level of *βigH3* gene. After transfection, the expression of *βigH3* gene in TB2A-clone 5 cells was restored to a level similar to that of control BEP2D cells, whereas in TB2A-clone 11 cells it was 2-fold higher than control. Upon inoculation into athymic nude mice, no tumor (0/10 mice) was detected in animals injected with the parental BEP2D cells after more than 20 weeks [64]. However, 10/10 mice that were injected with either TB2A or TB2A-pRc/CMV2 tumorigenic cells developed progressively growing tumors at 4 weeks, with average volumes of 544.9 mm^3 and 495.9 mm^3, respectively. In contrast, only 5/10 mice injected with TB2A-clone 5 and 6/10 mice injected with TB2A–clone 11 cells formed small tumor nodules at 4 weeks, with an average volume of 62.8 mm^3 which was significantly smaller than that of the parental TB2A cells ($p < 0.01$). The results of these studies provide unequivocal evidence of the *βigH3* gene function in fiber carcinogenesis [64].

14. Summary

Asbestos is a well established human carcinogen and, as exemplified by the recent Libby, Montana incidence, the danger of developing asbestos associated disease has extended beyond that of a simple occupational setting. The carcinogenic mechanism of asbestos is complex and no single pathways can account for all of the known effects of asbestos fibers. It is likely that multiple pathways involving physical interaction of asbestos and the target cells and the subsequent inflammatory response are important in the initiation of diseases. A better understanding of the carcinogenic mechanism of asbestos and other mineral fibers will provide important information on interventional and preventive measures in the management of asbestos mediated human diseases.

ACKNOWLEDGMENT

REFERENCES

[1] J.C. Wagner, G. Barry, Mesothelioma in rats following inoculation with asbestos, Brit. J. Cancer 23 (1969) 567–581.

[2] B.T. Mossman, A. Churg, Mechanisms in the pathogenesis of asbestosis and silicosis, Am. J. Respir. Crit. Care Med. 157 (1998) 1666–1680.

[3] C.M. Yarborough, The risk of mesothelioma from exposure to chrysotile asbestos, Curr. Opin. Pulmonary Med. 13 (2007) 334–338.

[4] E.C. Hammond, I.J. Selikoff, H. Seidman, Asbestos exposure, cigarette smoking and death rates, Ann. NY Acad. Sci. 330 (1976) 390–473.

[5] R. Saracci, The interaction of tobacco smoking and other agents in cancer etiology, Epidemiol. Rev. 9 (1987) 175–193.

[6] H.A. Anderson, R. Lilis, S.M. Daum, A.S. Fischbein, I.J. Selikoff, Household contact of asbestos neoplastic risk, Ann. N.Y. Acad. Sci. 271 (1976) 311–317.

[7] B. Risberg, J. Nickels, J. Wagermark, Familial clustering of malignant mesothelioma, Cancer 45 (1980) 2422–2424.

[8] H. Bohlig, E. Hain, Cancer in relation to environmental exposure. in: P. Bogovski (Ed.), Biological Effects of Asbestos, Int. Agency for Res. on Cancer, Lyons, (1973) pp. 217–223

[9] L.C. Oliver, N.L. Sprince, R. Greene, Asbestos-related disease in public school custodians, Am. J. Ind. Med. 19 (1991) 303–316.

[10] J. Whysner, V.T. Covello, M. Kushner, A.B. Rifkind, K.K. Rozman, D. Trichopoulos, G.W. Williams, Asbestos in the air of public building: A public health risk?, Prev. Med. 23 (1994) 119–125.

[11] P.J. Lioy, C.P. Weisel, J.R. Millette, S. Eisenreich, D. Vallero, J. Offenberg, B. Buckley, B. Turpin, M. Zhong, M.D. Cohen, C. Prophete, I. Yang, *et al.* Characterization of the dust/smoke aerosol that settled east of the World Trade Center in Lower Manhattan after the collapse of the WTC 11 September 2001. Environ. Health Perspect. 110 (2002) 703–714.

[12] M.F. Stanton, M. Layard, A. Tegeris, Carcinogenesis of fibrous glass: Pleural response in the rat in relation to the fiber dimension, J.N.C.I. 58 (1977) 587–604.

[13] B.T. Mossman, J. Bignon, M. Corn, A. Seaton, J.B.L. Gee, Asbestos: Scientific development and implications for public policy, Science 247 (1990) 294–306.

[14] R. Schins, T.K. Hei, in: K. Donaldson, P. Borm (Ed.), Particle Toxicology, CRC Press, London, (2006) pp. 287–300.

[15] T.K. Hei, A. Xu, S.X. Huang, Y. Zhao, Mechanism of fiber carcinogenesis: From reactive radical species to silencing of the *βigH3* gene, Inhal. Toxicol. 18 (2006) 985–990.

[16] R.M. Schapira, A.J. Ghio, E.J. Morrisey, C. Dawson, A.D. Hacker, Hydroxyl radicals are formed in the rat lung after asbestos instillation *in vivo*, Am. J. Respir. Cell. Mol. Biol. 10 (1994) 573–579.

[17] A. Xu, L.J. Wu, R. Santella, T.K. Hei, Role of oxyradicals in mutagenicity and DNA damage induced by asbestos in mammalian cells, Cancer Res. 59 (1999) 5615–5624.

[18] A. Shukla, M. Gulumian, T.K. Hei, D. Kamp, Q. Rahman, B.T. Mossman, Multiple role of oxidants in the pathogenesis of asbestos induced diseases, J. Free Radic. Biol. Med. 34 (2003) 1117–1129.

[19] S.A. Weitzman, P. Graceffa, Asbestos catalyzes hydroxyl and superoxide radical generation from hydrogen peroxide, Arch. Biochem. Biophys. 228 (1985) 373–376.

[20] M. Gulumain, J.A. Van Wyke, Hydroxyl radical production in the presence of fibers by a Fenton–type reaction, Chem. Biol. Int. 62 (1987) 89–92.

[21] L.G. Lund, A.E. Aust, Iron catalyzed reactions may be responsible for the biochemical and biological effects of asbestos, Biofactors 3 (1991) 83–89.

[22] A.E. Aust, The role of iron in asbestos induced cancer, In: Cellular and molecular effects of mineral and synthetic dusts and fibres, NATO ASI series H. (1994) 85: 53–61.

[23] D.D. Thomas, M.G. Espey, D.A. Pociask, L.A. Ridnour, S. Donzelli, D.A. Wink, Asbestos reduces nitric oxide signaling through rapid catalytic conversion to nitrite, Cancer Res. 66 (2006) 11600–11604.

[24] C.C. Chao, S.H. Park, A.E. Aust, Participation of nitric oxide and iron in the oxidation of DNA in asbestos treated human lung epithelial cells, Arch. Biochem. Biophys. 326 (1996) 152–157.

[25] E.P. Radford, Jr, V.R. Hunt, Polonium-210: A volatile radioelement in cigarettes, Science 1432 (1964) 247–249.

[26] J.B. Little, R.B. McGandy, Systematic absorption of polonium-210 in cigarette smoke, Arch. Environ. Health 17 (1968) 693–696.

[27] E.J. Hall, T.K. Hei, Modulating factors in expression of radiation induced oncogenic transformation, Environ. Health Perspect. 88 (1991) 149–153.

[28] T.K. Hei, E.J. Hall, R.S. Osmak, Asbestos, radiation and oncogenic transformation, Brit. J. Cancer 50 (1984) 717–720.

[29] M.C. Jaurand, in: A.B. Kane, P. Boffetta, R. Saracci, J.D. Wilbourn (Ed.), Mechanisms of Fibre Carcinogenesis, IARC 140, Lyon, (1996) pp. 55–72.

[30] T.K. Hei, A. Xu, D. Louie, Y.L. Zhao, Genotoxicity versus carcinogenicity: Implications from fiber toxicity studies, Inhal. Toxicol. 12 (2000) 141–147.

[31] T.K. Hei, Z.Y. He, C.Q. Piao, C.A. Waldren, The mutagenicity of mineral fibers, NATO ASI Series 223 (1991) 319–325.

[32] T.K. Hei, C.Q. Piao, Z.Y. He, D. Vannais, C.A. Waldren, Chrysotile fiber is a potent mutagen is mammalian cells, Cancer Res. 52 (1992) 6305–6309.

[33] A.W. Hsie, W. Xu, Y. Yu, M.A. Sognier, P. Hrelia, Molecular analysis of reactive oxygen species induced mammalian gene mutation, Teratog. Carcinog. Mutagen 10 (1990) 115–124.

[34] C. Klein, T.G. Rossman, Transgenic Chinese hamster V79 cell lines, which exhibits variable levels of gpt mutagenesis, Environ. Mol. Mutagen 16 (1990) 1–16.

[35] T.K. Hei, S.X. Liu, C.A. Waldren, Mutagenicity of arsenic in mammalian cells: Role of reactive oxygen species, Proc. Natl. Acad. Sci. USA 95 (1998) 8103–8107.

[36] K. Both, D.W. Henderson, D.R. Turner, Asbestos and erionite fibers can induce mutations in human lymphocytes that resulted in loss of heterozygosity, Int. J. Cancer 59 (1994) 538–542.

[37] K. Lezon-Geyda, C.M. Jaime, J.H. Godbold, E.F. Savransky, A. Hope & 5 others Chrysotile asbestos fibers mediate homologous recombination in Rat2λ fibroblasts: Implications for carcinogenesis, Mutat. Res. 361 (1996) 113–120.

[38] S.H. Park, A.E. Aust, Participation of iron and nitric oxide in the mutagenicity of asbestos in hgprt$^-$, gpt$^+$ Chinese hamster V79 cells, Cancer Res. 58 (1998) 1144–1148.

[39] B.T. Mossman, J.P. Marsh, M.A. Shatos, Alteration of superoxide dismutase activity in tracheal epithelial cells by asbestos and induction of cytotoxicity by antioxidants, Lab. Invest. 54 (1986) 204–209.

[40] L.G. Korkina, A.D. Durmev, T.B. Suslova, Z.P. Cheremisina, N.O. DaugelDauge, I.B. Afanas'ev, Oxygen radical mediated mutagenic effects of asbestos on human lymphocytes: Suppression by oxygen radical scavengers, Mutat. Res. 265 (1992) 245–253.

[41] T.K. Hei, Z.Y. He, K. Suzuki, Effects of antioxidants on fiber mutagenesis, Carcinogenesis 16 (1995) 1573–1578.

[42] K. Suzuki, T.K. Hei, Induction of heme oxygenase in mammalian cells by mineral fibers: Distinctive effect of reactive oxygen species, Carcinogenesis 17 (1996) 661–667.

[43] K. Miller, R. Handfield, E. Kagan, The effect of different mineral dusts on the mechanism of phagocytosis, Environ. Res. 15 (1978) 139–154.

[44] M. Kuschner, G.W. Wright, The effects of intratracheal instillation of glass fiber of varying size in guinea pigs. in: Proceedings of NIOSH conference on Occupational Exposure of Fibrous Glass, College Park, Maryland, (1976) pp. 151–168★.

[45] D.W. Kamp, P. Graceffa, W.A. Prylor, S.A. Weitzman, The role of free radicals in asbestos induced diseases, J. Free Radic. Biol. Med. 12 (1992) 293–315.

[46] R. Okayasu, L. Wu, T.K. Hei, Biological effects of naturally-occurring and man-made fibers: *in vitro* cytotoxicity and mutagenesis in mammalian cells, Br. J. Cancer 79 (1999) 1319–1324.

[47] A. Churg, J. Wright, B. Gilks, J. Dai, Pathogenesis of fibrosis produced by asbestos and man-made mineral fibers, Inhal. Toxicol. 12 (2000) 15–26.

[48] Y.I. Baris, L. Coplu, T.Z. Selcuk, S. Emri, A.A. Sahin, in: M. Sluyser (Ed.), Asbestos Related Cancer, Ellis Horwood, Sussex, UK, (1991) pp. 256–275.

[49] R.S. Sohal, H.H. Ku, S. Agarwal, M.J. Forster, H. Lah, Oxidative damage, mitochondrial oxidant generation, and antioxidant defense during aging and in response to food restriction in the mouse, Mech. Aging Dev. 74 (1994) 121–133.

[50] A. Boveris, E. Cadenas, A. Stoppani, Role of ubiquinone in the mitochondrial generation of hydrogen peroxide, Biochem. J. 156 (1976) 435–444.

[51] Y.M.W. Janssen, J.P. Marsh, K.E. Driscoll, P.J.A. Borm, G. Oberdorster, B.T. Mossman, Increased expression of manganese containing superoxide dismutase in rat lungs after inhalation of inflammatory and fibrogenic minerals, Free. Radic. Biol. Med. 16 (1994) 315–322.

[52] S.A. Golladay, S.H. Park, A.E. Aust, Efflux of reduced glutathione after exposure of human lung epithelial cells to crocidolite fibers, Environ. Health Perspect. 105 (1997) 1273–1278.

[53] Y.H. Wei, Oxidative stress and mitochondrial DNA mutations in human aging, Proc. Soc. Exp. Biol. Med. 217 (1998) 53–63.

[54] S. Agarwal, R.S. Sohal, DNA oxidative damage and life expectancy in houseflies, Proc. Natl. Acad. Sci. USA 91 (1994) 12332–12335.

[55] Y.H. Wei, S.H. Kao, In: C.D. Berdanier (Ed.), Nutrients and Gene Expression-Clinical Aspect, CRC Press, Boca Raton, (1996) pp. 165–188.

[56] S.X. Liu, M.M. Davidson, X.W. Tang, W.F. Walker, M. Athar, V. Ivanov, T.K. Hei, Mitochondrial damage mediates genotoxicity of arsenic in mammalian cells, Cancer Res. 65 (2005) 3236–3242.

[57] A. Xu, S. Huang, Y. Lien, D. Yu, T.K. Hei, Genotoxic mechanisms of asbestos fibers: Role of extranuclear targets, Chem. Res. Toxicol. 20 (2007) 724–733.

[58] T.K. Hei, C.Q. Piao, T. Sutter, J.C. Willey, K. Suzuki, Cellular and molecular alterations in human epithelial cells transformed by high LET radiation, Adv. Space Res. 18 (1996) 137–148.

[59] L. Xu, B.J. Flynn, S. Ungar, H.L. Pass, K. Linnainmaa, K. Mattson, B.I. Gerwin, Asbestos induction of extended lifespan in normal mesothelial cells: Inter-individual susceptibility and SV40 T-antigen, Carcinogenesis 20 (1999) 773–783.

[60] T.K. Hei, L.J. Wu, C.Q. Piao, Malignant transformation of immortalized human bronchial epithelial cells by asbestos fibers, Environ. Health Perspect. 105 (1997) 1085–1088.

[61] Y.L. Zhao, C.Q. Piao, L.J. Wu, M. Suzuki, T.K. Hei, Differentially expressed genes in asbestos-induced tumorigenic human bronchial epithelial cells: Implications for mechanism, Carcinogenesis 21 (2000) 2005–2010.

[62] M. Suzuki, C.Q. Piao, T.K. Hei, Karyotype analysis of tumorigenic human bronchial epithelial cells transformed by chrysotile asbestos using chemically induced premature chromosome condensation technique, Int. J. Mol. Med. 8 (2001) 43–47.

[63] M.C. Jaurand, J. Fluery-Feith, Pathogenesis of malignant pleural mesothelioma, Respirology 10 (2005) 2–8.

[64] Y.L. Zhao, C.Q. Piao, T.K. Hei, Downregulation of *Betaig-h3* gene is causally linked to tumorigenic phenotype in asbestos induced immortalized human bronchial epithelial cells, Oncogene 21 (2002) 7471–7477.

[65] J. Skonier, M. Neubauer, L. Madisen, K. Bennett, G.D. Plowman, A.F. Purchio, cDNA cloning and sequence analysis of beta *Betaig-h3*, a novel gene induced in a human adenocarcinoma cell line after treatment with transforming growth factor-beta, DNA Cell Biol. 11 (1992) 511–522.

[66] A.J. Bron, Genetics of the corneal dystrophies: What we have learned in the past twenty-five years, Cornea 19 (2000) 699–711.

[67] J.E. Kim, E.H. Han, R.W. Park, I.H. Park, S.H. Jun, J.C. Kim, M.F. Young, I.S. Kim, TGF-beta-inducible cell adhesion molecule, *betaig-h3*, is downregulated in melorheostosis and involved in osteogenesis, J. Cell Biochem. 77 (2000) 169–178.

CHAPTER 3

APPLICATIONS OF QUADRUPOLE-LINEAR ION TRAP MASS SPECTROMETRY TO THE ANALYSIS OF REACTIVE METABOLITES IN DRUG DISCOVERY AND DEVELOPMENT

Mingshe Zhu*,[1] *and* Bo Wen[†]

Contents

* Biotransformation, Bristol-Myers Squibb Research and Development, Princeton, New Jersey 08543
† Drug Metabolism and Pharmacokinetics, Roche Palo Alto, Palo Alto, California 94304
1 Corresponding author. Tel.: (609) 252 3324
   E-mail address: mingshe.zhu@bms.com

1. INTRODUCTION

Idiosyncratic drug reactions (IDRs) are a leading cause of patient morbidity and mortality and result in significant attrition in late drug development, restricted drug use, and even drug withdrawal from the market [1]. To date, it has been difficult to predict IDRs, because they have no obvious dose-response relationship, no suitable animal models for evaluation and a very low frequency of occurrence, which are often not clearly observed until clinical trials or use in very large populations. Although mechanisms of IDRs remain to be elucidated, chemically reactive drug metabolites are believed to play a significant role as mediators in drug-induced toxicities including idiosyncratic hepatotoxicity [2,3]. It was reported recently that among 21 drugs which have been either withdrawn from the U.S. market since 1950 or have black box warnings because of hepatotoxcity, 13 formed reactive metabolites via metabolic activation [4]. Because of these safety concerns, a drug candidate that undergoes metabolic activation is less favorable for further development. Therefore, lead compounds or new chemotypes are routinely subjected to *in vitro* evaluation for reactive metabolite formation through covalent protein binding assays [5] or use of chemical trapping agents such as glutathione (GSH) [6,7], since such information is very important to minimize these liabilities and/or prioritize drug candidates in early preclinical stage. As a result, rapid, sensitive, and reliable methods for detecting and characterizing reactive metabolites are highly desired in the drug discovery and development process [2,8].

Significant efforts have been made in the pharmaceutical industry to evaluate and minimize the bioactivation potentials of new chemical entities (NCEs). Reactive metabolites can be detected, structurally characterized, and quantitatively estimated in a variety of *in vitro* "trapping experiments," in which reactive metabolites formed in incubations of liver tissue preparations are trapped by excess amounts of small molecular nucleophiles, such as glutathione (GSH), followed by analysis by liquid chromatography coupled with mass spectrometry (LC/MS) and other analytical methods [6]. Mass spectrometry techniques have been evolved over the years, with the advancing of new mass spectrometric technologies, to improve the sensitivity, selectivity, reliability, as well as higher-throughput capability of these assays. Triple quadrupole, ion trap, and high-resolution mass spectrometers are common LC/MS platforms employed in the analysis of drug metabolites [9], including reactive metabolites [6]. Recently, updated quadrupole-linear ion trap mass spectrometers (API 4000 and API 5500 Q-trap instruments) were introduced [10–13]. Although limited examples are available in the literature, the Q-trap has been demonstrated to be a promising analytical technology for profiling and structural elucidation of drug metabolites [14–21], especially in reactive metabolite screening that often requires

high-throughput and better sensitivity than that in metabolic soft spot determination [22–24]. General instrumentation, scan functions, and utilities of the Q-trap in the identification of stable drug metabolites have been well described in recent review articles [10,25]. The intention of this review is to focus on recent advances in the applications of the Q-trap to the analysis of reactive metabolites. Following brief descriptions of common analytical strategies and LC/MS techniques employed in reactive metabolite screening in the drug discovery and development processes, applications of special scanning capabilities of the Q-trap to the high-sensitivity analysis, high-throughput screening and quantitative estimation of reactive metabolites are discussed. Recent examples of using the Q-trap to investigate bioactivation mechanisms of several drugs, including clozapine, trazodone, amitripthline, and nortriptyline, are presented.

2. REACTIVE METABOLITE ANALYSIS IN DRUG DISCOVERY AND DEVELOPMENT

To evaluate and minimize metabolic activation of drug candidates during the drug discovery process, a variety of experimental approaches have been developed and applied from early optimization of lead compounds to characterization of development candidates [2,3,8,26]. As summarized in Table 1, these studies can be categorized as: (1) rapid screening and characterization of *in vitro* reactive metabolites in ''trapping experiments,'' (2) quantitative analysis of *in vitro* reactive metabolites-trapped by small nucleophiles, (3) evaluation of bioactivation in toxicology animal species, and (4) evaluation of bioactivation in humans. LC/MS techniques play a dominant role in the detection, identification, and quantification of reactive metabolites in these studies. In the early drug discovery, LC/MS is often employed for screening reactive metabolites in a high-throughput fashion, for lead selection and optimization. In this analysis, test compounds are usually incubated with liver microsomes from humans and toxicology species in the presence of trapping agents, such as GSH. GSH-trapped reactive metabolites in the incubations can then be detected and structurally characterized by LC/MS analysis. Results from these *in vitro* screening experiments afford important guidance for the bioactivation potentials of a given compound or chemotype. Further characterization of the trapped adduct by LC–MS/MS may provide an insight into the chemical nature of the reactive species. Such information is invaluable to medicinal chemists who are engaged in the process of structural optimization of lead chemical templates. Consequently, the information of the nature and extent of metabolic activation, as one of parameters in the benefit/risk assessment, contributes to the chemotype or lead selection in the drug design process.

Table 1 Experimental approaches for screening and evaluating bioactivation of drug candidates in drug discovery and development

Study of bioactivation of drug candidates	Study objective	Analytical approach
In vitro reactive Met screening in early discovery	• Chemotype and lead selection	• Screening and characterization of reactive Met *in vitro* using LC/MS

Quantification of *in vitro* reactive Met from early to late discovery	• Lead optimization via SAR analysis and clinical candidate selection	• Quantification of small thiol-adducts
		  – LC/MS/UV
		  – LC/MS [34]
		  – LC/MS/Fluoresce detection [29]
		  – LC/MS/radiodetection [30,32,33]
		• Quantification of protein adducts
		  – Radioactivity analysis [26]

Evaluation of bioactivation in animals at the discovery and preclinical development stages	• Characterization of bioactivation of drug candidates in Tox species
	  – *In vitro* and *in vivo* correlation
	  – Study non-CYP mediated bioactivation
	• Monitoring of reactive Met exposure to Tox species
		• Radiolabeled ADME study
		  – Analysis of small thiol-adducts by LC/MS/radiodetection
		  – Protein covalent binding using radioactivity analysis
		• Use nonlabeled drug candidates
		  – Qualitative analysis of GSH adducts in bile by LC/MS
		  – Screening and quantification of mercapuric acids in urine by LC/MS

Evaluation of bioactivation in humans at the clinical development stage	• Characterization of bioactivation of drug candidates in humans
	• Monitoring of reactive Met exposure to humans
		• Radiolabeled ADME study
		  – Analysis of small thiol-adducts by LC/MS/radiodetection
		• Nonradiolabeled clinical study
		  – Monitoring of mercapuric acids in urine by LC/MS

With advances of modern mass spectrometry and evolved analytical methodology (Table 2), the sensitive detection of *in vitro* reactive metabolites by various types of LC/MS instruments has often been achieved. As a result, multiple novel GSH adducts of model compounds, which are usually present in incubations at very low levels, were discovered by newly developed LC/MS techniques [22,23,27,28]. However, none of these LC/MS methods are applicable to quantification of reactive metabolites due to the lack of GSH adduct standards or the consistency of mass spectrometric responses to different GSH adducts. Quantitative assessment of reactive metabolites formed in *in vitro* screening experiments is crucial for determination of soft spots of bioactivation for structural modifications, optimization of lead compounds by analyzing structure-activity relationship (SAR), and in particular, ranking and selection of drug candidates. Table 2 lists several liquid chromatographic methods that have been employed for quantitative analysis of reactive metabolites. For example, LC/UV analysis of GSH adducts works effectively only for high levels of reactive metabolites, while sensitive quantification of reactive metabolites trapped by dansyl-GSH [29], radiolabeled GSH [30–32], and radiolabeled cyanide [33] can be accomplished by fluorescence or radiochromatographic detection, respectively. In all cases, identities of these thiol-adducts are determined by on-line mass spectrometers. Additionally, a semiquantification method using quaternary ammonium GSH as the trapping agent has been recently reported for estimation of reactive metabolite formation [34]. Compared to the protein covalent binding study which measures the total amount of reactive metabolites formed in human liver microsome (HLM) (Table 1), the major advantage of the LC/UV and LC/fluorescence detection methods is that they can be performed rapidly without using radiolabeled compounds.

LC/MS techniques also play an essential role in the analysis of reactive metabolites formed in *in vivo* animal species in drug discovery and development (Table 1). In general, the first study to assess *in vivo* bioactivation of drug candidates is the detection and structural identification of GSH adducts in bile samples using LC/MS and/or NMR after dosing a non- or radiolabeled compound to rats. Usually, reactive metabolites formed in liver are immediately trapped by endogenous GSH to form GSH adducts. A significant portion of GSH adducts is excreted into bile in rats and other animal species. Many pharmaceutical companies prefer the use of radiolabels in the study because quantitative determination of reactive metabolites can be readily achieved via the radioactivity analyses of GSH adducts in bile and protein covalent binding in liver tissue [26]. When a drug candidate is at the development stage, more comprehensive radiolabeled administration, distribution, metabolism, and excretion (ADME) studies in toxicology species and humans are conducted using various radiodetection techniques combined with LC/MS (Table 1). Results from these ADME studies allow for the confirmation of bioactivation pathways observed in liver microsomal

Table 2 Detection and characterization of GSH-trapped reactive metabolites *in vitro* using various types of mass spectrometers in combination with data acquisition and processing methods

Mass spectrometry	Triple quadrupole	Ion trap and linear ion trap	High resolution MS instrument	Quadrupole-linear ion trap
Method for detecting GSH adducts	• NL scan [39] • PI scan [28] • MRM [40]	• NL filtering of MS/MS data [41,95 and 96]	• Mass defect filtering [46] • MS^E [47]	• NL-EPI [22,23] • PI–EPI [23] • MRM-EPI [22]
Sensitivity and selectivity	MRM > PI scan > NL scan	Good	Good sensitivity; Selectivity is compound- or sample-dependent	As triple quadrupole; EPI acquisition has better sensitivity than product ion scan
MS/MS spectra quality	Rich and small fragments	Fewer and larger fragments	Accurate MH^+ and fragment ions	As those recorded with triple quadrupole
Fast analysis capacity	Poor	Reasonably good with data-dependent MS/MS acquisition	Reasonably good with data-dependent MS/MS or MS^E acquisitions	Excellent with PI-EPI
Comments	Suitable for bioactivation research where high throughput is not critical	Not effective for *in vivo* adducts; MS^2 spectra have limited structural information	Capable of analyzing other metabolites in the same runs; above MS/MS acquisition methods may be not effective for *in vivo* adducts	MRM–EPI provides the highest sensitivity and selectivity. PI–EPI well suited for high-throughput screening

incubations, the identification of reactive metabolites mediated by non-microsomal enzymes or multiple biotransformation reactions, which are usually not detected by *in vitro* screening methods [35], and the contribution of the bioactivation to the total drug clearance in humans and toxicology animal species. At the late stage of drug development, quantitative analysis of mercapturic acids (MA) (*N*-acetyl–systeine conjugates) by LC/MS in urine samples after dosing nonlabeled drug candidates is often required to monitor the exposure of reactive metabolites to humans in special populations and animals in chronic safety studies.

3. Mass Spectrometry in Reactive Metabolite Analysis

3.1. Triple quadrupole mass spectrometry

Neutral loss (NL) scanning using a triple quadrupole mass spectrometer is the first LC/MS method developed for detecting reactive metabolites trapped by GSH or other trapping agents in studies of bioactivation of drugs or other xenobiotics in the late 1980s [36,37]. During the 1990s, this LC/MS approach was employed as a primary tool for screening for *in vitro* reactive metabolites in the pharmaceutical industry [38]. In the NL analysis, GSH adducts formed in HLM incubations with an excess amount of GSH are monitored for a NL of 129 Da, which is a common fragmentation pathway of GSH adducts. The NL experiment can be easily operated following a generic acquisition protocol, and is especially useful in detecting GSH adducts regardless their m/z values. However, the NL scanning method often suffers from relatively poor selectivity, resulting in the appearance of intense false positive peaks in NL ion chromatograms. To improve the selectivity of the NL scanning, a mixture of GSH and stable–isotope labeled GSH (1:1 ratio) was employed as a trapping agent [39]. As a result, false positive peaks displayed in NL ion chromatograms can be readily recognized based on the lack of a unique isotope pattern in their NL MS/MS spectra.

Another major drawback of the NL scan method is the lack of effectiveness in the analysis of certain classes of GSH adducts that do not afford a NL of 129 Da as the primary fragmentation pathway, such as aliphatic/benzylic thioether GSH adducts. Fragmentation patterns of GSH adducts in the positive ion mode are dependent on the linkage structures between the drug moiety and GSH, while in the negative ion mode GSH adducts afford a series of preeminent anions such as m/z 272 corresponding to deprotonated γ-glutamyl–dehydroalanyl–glycine originating from the glutathionyl moiety, regardless of classes of GSH adducts. Based on these observations, a precursor ion (PI) scanning method that monitors the anion at m/z 272 in the negative electrospray ionization mode was developed as a more broadly

useful survey scan for the detection of unknown reactive metabolites using triple quadrupole instruments [28]. Analysis of *in vitro* and *in vivo* GSH adducts have demonstrated that the PI scan method is able to detect various classes of GSH adducts with better selectivity and sensitivity than NL scanning.

In addition to NL and PI scanning modes, a multiple reaction monitoring (MRM) method to monitor six MRM transitions from protonated molecules (MH$^+$) of potential reactive metabolites trapped by glutathione ethyl ester to their product ions [MH $-$ 129]$^+$ was developed for sensitive detection of reactive metabolites [40]. This method was up to 80-fold more sensitive than the NL scanning. However, classical triple quadrupole instruments are incapable of performing more than 10 MRM transitions. Thus, for comprehensive detection of a variety of GSH adducts, multiple LC/MS injections with different MRM transitions are required, each of which targets 4–8 potential GSH adducts. Recently updated triple quadrupole mass spectrometers are capable of performing a large number of MRM transitions (up to 500–10000) in a single run. The new feature can be potentially utilized for improving the throughput of the MRM screening of GSH adducts.

A common major limitation of triple quadrupole instrument-based scanning methods, including NL, PI, and MRM scans, is the lack of high-throughput capability (Table 2). In general, the detection and structural characterization of GSH adducts by these methods are a multiple-step process. For example, in the NL scan analysis, the first step is the detection of GSH conjugates using a NL of 129 Da in the positive ion mode. The second step is the visual inspection of each peak present in a resultant NL ion chromatogram (TIC). Once the detection of a GSH adduct is confirmed, acquisition of the adduct MS/MS spectrum using a compound-dependent product ion scan method can then be carried out in an additional LC/MS injection. The entire process is a truly time-consuming and labor intensive practice.

3.2. Ion trap and linear ion trap mass spectrometry

Ion trap instruments, including linear ion trap mass spectrometers, feature data-dependent MS^n acquisition and high sensitivity in full-scan MS analysis. Because of these advantages, ion traps have been employed as one of the major LC/MS platforms for profiling drug metabolites in the pharmaceutical industry. The data-dependent MS^n acquisition that includes list-, intensity- and isotope-dependent data acquisition enables recording of full-scan MS and MS^n data sets in a single LC/MS run. In the list-dependent MS/MS experiment, full scan MS analysis serves as a survey scan to search for metabolite ions listed in an acquisition method. Once a listed metabolite ion is found in the survey scan, MS/MS acquisition of the metabolite is automatically triggered. As a result, detected metabolites are displayed in

total ion chromatograms of MS/MS data sets. Alternatively, the intensity-dependent MS/MS experiment, in which MS/MS acquisition is carried out for most intense ion(s), in combination with postacquisition data processing, including extracted ion chromatographic analysis of full-scan MS data sets and NL or product ion filtering of MS/MS data sets are employed for rapid drug metabolite detection and structural characterization. Recently, an intensity-dependent scanning method on an LTQ linear ion trap instrument was applied to the data acquisition of reactive metabolites trapped by stable isotope labeled GSH (Table 1) [41]. MS/MS data were further processed with NL filtering of 129 Da. The study demonstrates the feasibility of NL filtering of MS/MS data in detecting GSH adducts and the utility of using stable isotope labeled trapping agents to identify false positive peaks, although the sensitivity and selectivity of this approach in analyzing different classes of GSH adducts were not fully evaluated. MS/MS spectra of GSH adducts also can be acquired with isotope pattern-triggered data-dependent acquisition using stable isotope labeled GSH as a trapping agent. The approach is more effective in selectively recording MS/MS spectra of GSH adducts for postacquisition NL filtering and structural elucidation of GSH adducts (Table 1).

3.3. High-resolution mass spectrometry

High-resolution mass spectrometry provides chemical formulae for metabolites and their fragments, which, in some cases, are required in metabolite structural elucidation [42]. However, in the past, high-resolution mass spectrometry was not employed as a primary or standalone LC/MS platform for drug metabolite profiling due to the lack of the true NL and PI scanning functions. Recently, a mass defect filter (MDF) technique was developed to facilitate the detection of oxidative metabolites by high resolution and accurate mass LC/MS based on predictable and narrow shifts in mass defects of the metabolites [43–45]. The MDF technique was also shown to be applicable to detecting GSH-trapped reactive metabolites *in vitro* and *in vivo* [46]. Table 3 is a summary of common bioactivation reactions leading to GSH adduct formation in HLM. Although the mass shifts of these GSH adducts from the sum of the drug and GSH masses (MH^+ of the drug + GSH − 2H) vary significantly from −34 to + 32 Da, the differences in the mass defects between the GSH adducts and the GSH adduct filter templates (MH^+ of the drug + GSH − 2H) are in a narrow range from −0.024 to + 0.039 Da. Therefore, a mass defect filter (MDF) from −0.025 to + 0.040 Da around the mass defect of the GSH adduct filter template are able to select for all the GSH adducts listed in Table 1. To evaluate the effectiveness of the MDF approach, several model compounds that are known to form reactive metabolites were incubated with

Table 3 Mass and mass defect shifts of GSH-trapped reactive metabolites that are formed via common P450-mediated bioactivation reactions occurred in HLM[a] [22,46]

Mass shift of the drug moiety	GSH adduct composition	Mass defect shift of GSH adduct[b]	Functional group	Common metabolic activation reaction
−34	P + GSH − HCl	+0.0389	β-Cl to a nitrogen or sulfur	Loss of Cl to form aziridinium or episulfonium
−32	P + GSH − S − 2H	+0.0279	Thiourea	R–NH-C(=S)-NH-R$'$→R–NH-C(SG)=N-R$'$
−30	P + GSH − 2N−4H	−0.0157	Hydrazine	R–NH–NH$_2$→R–SG
−18	P + GSH + O − HCl	−0.0109	Aromatic chlorine	Formation of quinone imine or epoxide followed by GSH attack and loss of HCl
−15	P + GSH − NH3		Aromatic amine	Oxidative deamination to formamide
−14	P + GSH − CH$_2$ − 2H	−0.0157	Aromatic ether	Demethylation followed by oxidation to quinone
−12	P + GSH − C − 2H	0	Methylenedioxy	Formation of quinone
−2	P + GSH + O − HF	0.0043	Aromatic fluoride	Epoxidation followed by GSH attack and loss of HF
0	P + GSH − 2H	0	Substituted phenol derivative	Formation of quinone methide
+1	P + GSH + O − NH − 2H	−0.0238	Aromatic amine	Formation of quinone via oxidative deamination
+2	P + GSH	+0.0157	α,β-Unsaturated carbonyl	CH$_2$ = CH-C(=O)-R →GS-CH$_2$-CH-C(=O)-R

+14	P + GSH + O − 4H	−0.0208	Benzylamine	Formation of hydroxylamine followed by oxidation to nitrile oxide
+16	P + GSH + O − 2H	−0.0051	Phenol	Formation of quinone
+18	P + GSH + O	+0.0106	Furan	Formation of epoxide followed by GSH attack
+28	P + GSH + CO − 2H	−0.0051	Benzylamine	Formation of isocyanate
+32	P + GSH + 2O − 2H	−0.0102	Benzene	Formation of quinone

[a] Most listed common bioactivation reactions, example of these reactions and associated references were adapted from a previously published document [22].
[b] The mass defect shifts of GSH adducts are defined as the difference in the mass defects between a detected GSH adduct and the GSH–adduct MDF template (MH$^+$ of the drug + GSH − 2H).

HLM and GSH. Accurate full-scan MS datasets were acquired with the LTQ/Orbitrap or Fourier transform ion cyclotron resonance mass spectrometry (LTQ FTMS) and processed using GSH adduct filter templates [46]. Results from the study demonstrated that the MDF approach has several advantages over the NL scanning method. (1) The MDF approach, in general, is more sensitive in detecting *in vitro* GSH adducts, and far more effective in the analysis of the GSH adducts that do not afford a NL of 129 Da as a significant fragmentation pathway. (2) The MDF approach is more selective in detecting drug–GSH adducts in rat bile, in which there are large amounts of endogenous GSH conjugates that undergo the NL fragmentation pathways similar to those of drug-GSH adducts. (3) The accurate mass spectral data acquired for the GSH adduct detection are also useful in the determination of molecular formulae of GSH adducts and elimination of false positives. (4) In addition to GSH-trapped reactive metabolites, stable oxidative metabolites and other classes of metabolites can be detected via processing the same LC/MS data sets with different MDF templates [44].

Alternatively, an exact mass pseudo NL acquisition method was developed on a Q-Tof instrument for screening GSH adducts [47]. In the analysis, the NL monitoring is achieved via alternating the data acquisition with low- and high-collision energy (MS^E). Once an exact mass difference of 129.0426 Da (within a narrow mass tolerance window) between ions in low- and high-energy full scan mass spectra is detected, product ion acquisition of the potential precursor ion is triggered. High-resolution mass spectrometers have become one of major LC/MS platforms in the analysis of reactive metabolites.

4. Quadrupole-Linear Ion Trap Mass Spectrometry (Q-trap) in Reactive Metabolite Analysis

4.1. Unique scan functions of the Q-trap

The Q-trap retains the MS/MS scan functions of both the triple quadrupole and the ion trap [10]. Therefore, it can be used as a stand alone triple quadrupole instrument to perform NL, PI, and MRM scans or a stand alone ion trap instrument to perform data-dependent MS/MS analysis for metabolite analysis (Table 2). Most importantly, the Q-trap allows for the use of the quadrupole-based NL, PI, or MRM mode as the survey scan to trigger MS/MS acquisition by the ion trap. As a result, the detection and MS/MS acquisition of analytes can be accomplished in a single LC/MS run. In addition to speeding up the data acquisition processes, these information-dependent scan modes take advantages of both the selectivity of precursor

ion, NL and MRM scans by triple quadrupole and the sensitivity of MS/MS spectral acquisition by the ion trap. Furthermore, a survey scan and an information–dependent MS/MS scan can be performed in opposite ion modes using the $+/-$ polarity switching technique. Some of these hybride scanning capabilities are not available in conventional quadrupoles, ions traps, and high resolution mass spectrometers. In the following section, the definitions and workflow of unique Q-trap scan modes applied in the analysis of reactive metabolites are described.

4.1.1. Enhanced resolution scan
The enhanced resolution (ER) scan mode is designed to record increased resolution full-scan spectra by the Q-trap. In the ER experiment, Q1 is typically set to isolate an ion of interest within a mass window of approximately 6 amu wide. The ion is then transmitted through Q2 without fragmentation and stored in the ion trap. The trap operates at the reduced scan speed (250 amu/sec) with a smaller than normal step to generate a full-scan MS spectrum.

4.1.2. Enhanced product ion scan
The enhanced product ion (EPI) scan mode is designed to acquire a high quality product ion spectrum on an ion of interest by the Q-trap. In the EPI experiment, the precursor ion is selected in Q1 with a narrow mass window and fragments in Q2. Resultant fragments are stored and subsequently scanned in the ion trap.

4.1.3. Precursor ion-enhanced product ion scan and neutral loss-enhanced product ion scan
These scan modes combine the triple–quadrupole based precursor ion (PI) or neutral loss (NL) scan with the ion trap based EPI scan by using an information–dependent acquisition (IDA) method. In the PI-EPI or NL-EPI experiment, a PI scan or NL scan is used as a survey scan for selectively detecting any precursor ions that generate a predefined product ion or undergo a predefined NL, respectively. Once a precursor ion or a neutral loss is detected by the survey scan, a subsequent ER scan is carried out to display the ion of interest at an increased resolution full-scan spectrum. Based on the full-scan spectral data, an EPI scan is performed as a dependent scan to acquire an MS/MS spectrum. If the polarity switching function is activated, the m/z value of a precursor ion isolated for MS/MS acquisition in the EPI scan is automatically justified by either $+2$ or -2 Da based on the most intense ion present in the corresponding survey scan.

4.1.4. Multiple reaction monitoring (MRM)-enhanced product ion (EPI) scan

The workflow combines the MRM with the EPI scan using an information–dependent method. In the MRM–EPI experiment, up to 300 pre-defined MRM transitions with the quadrupole are performed as the survey scan [48]. Once a predefined ion is detected by one of the MRM transitions, a dependent EPI scan is performed to acquire its MS/MS spectrum with the ion trap [49]. If the polarity switching is needed in the EPI scan, an ER scan between MRM and EPI scans is performed.

4.2. High-sensitivity analysis using MRM-EPI

One of special applications of the Q-trap mass spectrometry to reactive metabolite screening is the sensitive and selective detection and characterization of GSH-trapped reactive metabolites using the MRM-EPI scan [22]. In this approach, MRM serves as the survey scan to search for potential GSH adduct ions listed in a predefined MRM protocol. Once a GSH adduct ion is detected by MRM, the acquisition of its EPI spectra is triggered (Figure 1A). The MRM scan step is carried out following up to ~110 MRM transitions from protonated molecules of potential GSH adducts to their product ions derived from a NL of 129 or 307 Da since all classes of GSH adducts, including aliphatic, benzylic, and aromatic thioethers, offer the NL of either 129 or 307 Da as a primary or significant fragmentation pathway. In the MRM–EPI analysis, MRM and EPI datasets are recorded for each LC/MS injection and displayed as a total ion chromatogram (TIC) of MRM and a TIC of EPI, respectively. Usually, a TIC
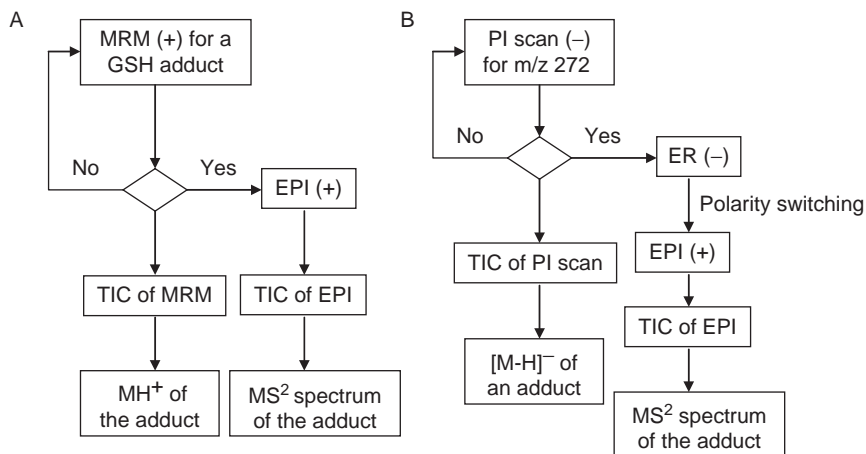
Figure 1   The workflow of MRM-EPI (A) and PI-EPI with polarity switching (B) for the detection and structural elucidation of GSH adducts in HLM.

of MRM of a sample is similar to that of the corresponding EPI scan. EPI spectra of GSH adducts can be directly retrieved from the TIC of EPI for the structural characterization or elimination of false positives (Figure 1A), while the TIC of MRM only reveals m/z values of the GSH adduct molecular ions. MRM transition protocols can be constructed based on predicted common bioactivation reactions in HLM (Table 3) and/or specific bioactivation reactions known for certain types of chemotypes and lead compounds encountered early. To search for the common GSH adducts listed in Table 3, an MRM protocol with a total of 32 MRM transitions is able to detect all of these potential GSH adducts. Alternatively, if a loss of an N atom is not expected in the bioactivation of a test compound, a generic MRM protocol containing all even numbers of mass shifts over a range from $+50$ to -40 Da around the m/z values of the drug–GSH complex (total 90 MRM transitions) can be simply applied for screening potential unknown GSH Conjugates. As indicated in Table 3, the mass shifts of drug moieties of common GSH adducts are usually all odd numbers except for two GSH adducts derived from the bioactivation associated with loss of a nitrogen atom (the mass shift of -15 or $+1$).

The effectiveness of this approach has been demonstrated in the analysis of reactive metabolites of several model compounds formed in HLM incubations, including acetaminophen, diclofenac, carbamazepine, clomipramine, and mefenamic acid [22]. As shown in the TIC of EPI for the carbamazepine HLM incubation (Figure 2A), a number of carbamazepine-GSH adducts, including several minor GSH adducts not observed previously in HLM incubations, are clearly displayed with few false positive peaks. The TIC of EPI can be further processed with extracted ion chromatogram (EIC) analysis to separate coeluting GSH adducts, such as CM2 (Figure 2B) and CM3 (Figure 2D). Additionally, as shown in the example of acetaminophen, the product ion spectrum of the major acetaminophen-GSH adduct recorded with MRM-EPI (Figure 3A) displays much more small fragment ions [22] than that acquired by an LTQ linear ion trap instrument (Figure 3B), which makes the Q-trap more useful in structural elucidation of GSH adducts. Compared to the MRM analysis with a classical triple quadrupole LC/MS, the MRM-EPI scan with the Q-trap has several advantages: (1) MRM-EPI can perform 10-fold more MRM transitions (up to 100 transitions with API 4000 Q-trap) without a significant loss of sensitivity; (2) product ion spectra of detected GSH adducts are recorded in the same LC/MS run; and (3) the sensitivity of EPI acquisition is greatly improved, which is comparable to that of the MRM scan.

Compared to the NL scan with a triple quadrupole instrument or the NL-EPI scan with a Q-trap instrument, the MRM-EPI scan has significantly improved sensitivity and selectivity. As shown in the analysis of clomipramine-GSH adducts [22] (Figure 4), two GSH adducts, LM1 and LM2, were clearly detected by MRM-EPI; the TIC of EPI displayed LM1
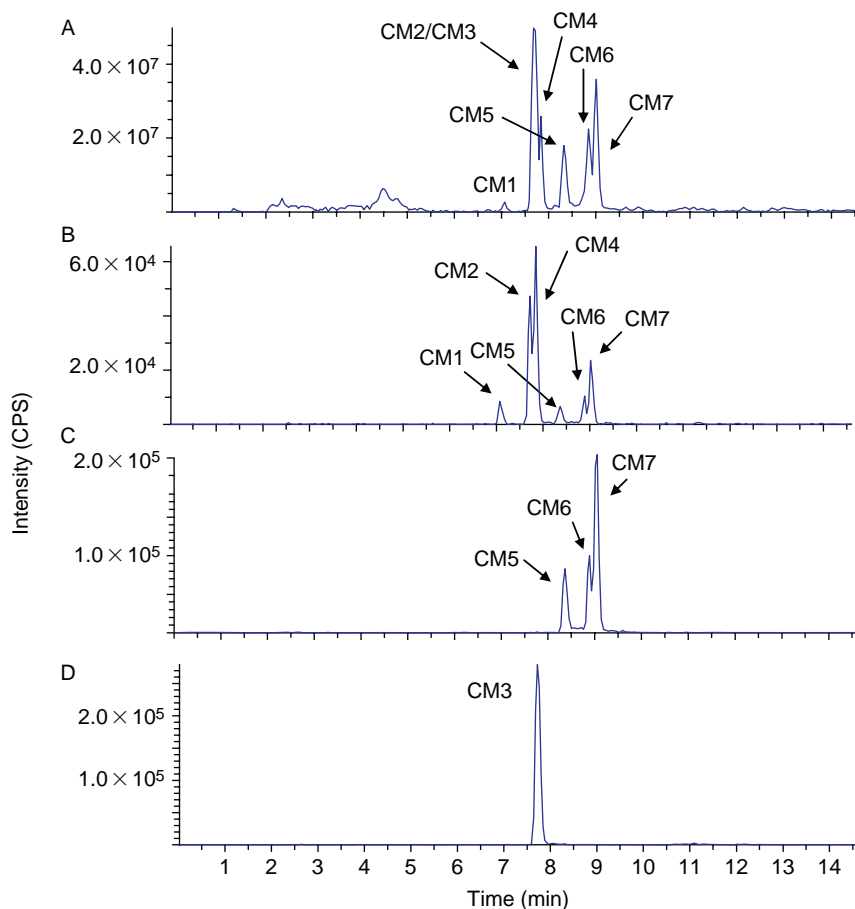
Figure 2 Detection of carbamazepine-GSH adducts formed in the HLM incubations by the MRM analysis with 88 transitions. (A) TIC of EPI, (B) EIC of EPI for m/z 560 (P + GSH + O), (C) EIC of EPI for m/z 558 (P + GSH + O − 2H), and (D) EIC of EPI for m/z 576 (P + GSH + 2O) [22].

and LM2 as predominant chromatographic components with very low background noises (Figure 4C). In contrast, LM1 and LM2 was not detected by the NL-EPI scanning for 129 Da (Figure 4A) and barely detected by the NL-EPI scanning for 307 Da barely detected (Figure 4B). Results from comparative analysis of several *in vitro* incubation samples suggest that MRM-EPI provides higher sensitivity for detection of GSH adducts, up to 179-fold better than the NL-EPI scan and up to 10-fold better than the PI-EPI scan. The major limitation of the MRM-based approach is that it only detects the GSH adducts preset on an MRM transition protocol. Additionally, MRM-EPI is not applicable to high throughput screening of reactive metabolites since the design and
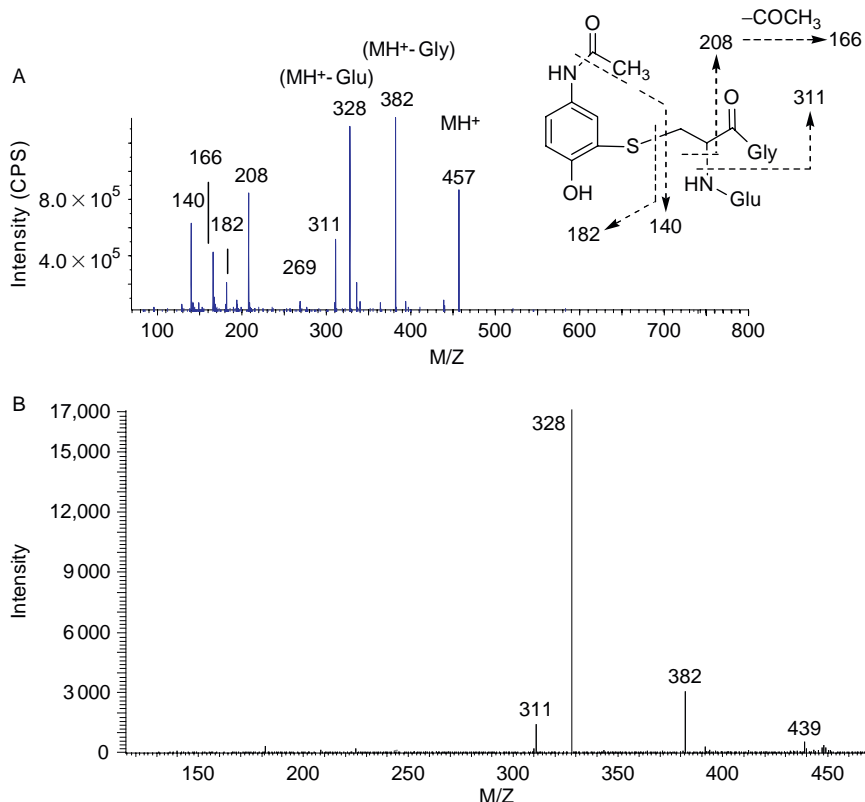
Figure 3 Comparison of MS/MS spectra of the acetaminophen–GSH adduct at m/z 457 (P + GSH − 2H) acquired by MRM-EPI on the Q-trap (A) [22] and data-dependent MS/MS acquisition on an LTQ linear ion trap (B).

preparation of compound-specific MRM transition protocols are required for individual samples before data acquisition.

The superior sensitivity of MRM–EPI is also observed in analyzing MA (N–acetyl-cysteine conjugates) in rat and human urine [50,51]. MA are degradation products of GSH conjugates and formed via peptide hydrolysis and subsequent acetylation. Many of reactive metabolites-trapped by GSH are converted to the corresponding MA and excreted into urine in humans and animals [52]. For example, ~10% of administrated acetaminophen is observed as MA of acetaminophen in human urine [53]. Results from the detection and structural characterization of urinary MA of a test drug candidate provides insight into the chemical mechanism of bioactivation in humans and toxicology species. Additionally, the amount of MA of a drug candidate is an indicator of exposure levels of reactive metabolites of the drug candidate in humans and animals. In many cases, qualitative and quantitative analysis of MA in urine is the only option to assess drug
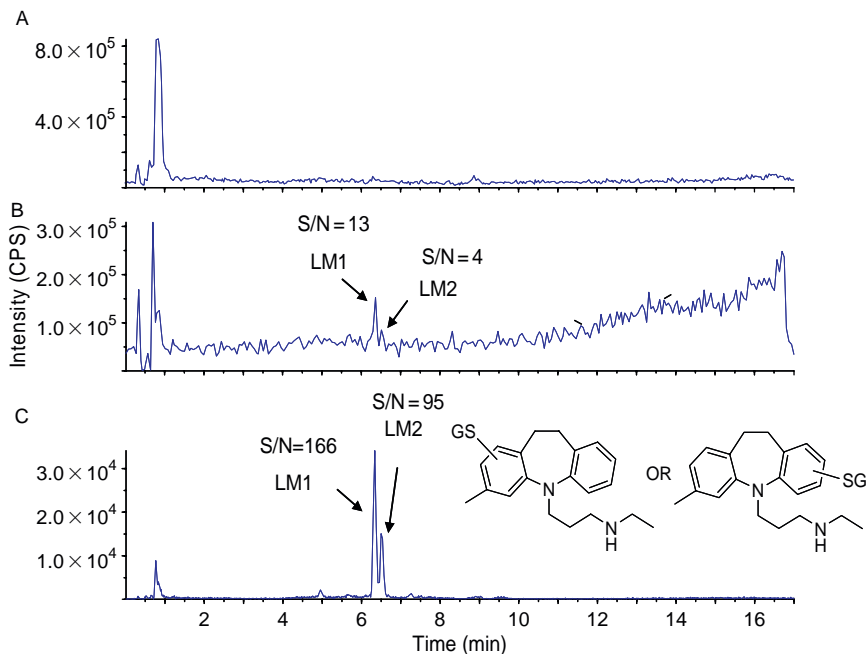
Figure 4 NL and MRM analyses of clomipramine-GSH adducts formed in the HLM [22] incubation. (A) TIC of NL scanning of 129 Da, (B) TIC of NL scanning of 307 Da, (C) TIC of MRM with 14 transitions [22].

bioactivation in clinical and safety studies, such as a clinical trial in a large population or a carcinogenicity study in rats. MA afford the NL of 129 Da as a single major fragmentation pathway in the negative ion electrospray mode [51] (Figure 5, top panel). The unique MS/MS fragmentation has been utilized in screening for MA in urine using the negative ion MRM-EPI scan with a Q-trap instrument. In the analysis, 252 MRM transitions from the [M–H]$^-$ ion of a potential MA to the product ion derived from the NL of 129 Da were monitored. A TIC of the MRM scan (252 transitions) for a control urine sample from a female subject is displayed in Figure 5B, which revealed multiple MA [50]. These MA are metabolites of organic solvents from environment such as benzene and *n*-hexane or food cooking products such as acrylamide-MA, a metabolite of acrylamide that is formed in the processes of French fries or coffee beans. The MRM-based approach can be utilized for sensitive monitoring of potential MA of drugs since their concentrations in urine are usually higher than those from environmental and endogenous compounds. The negative ion NL-EPI scan for the NL of 129 Da was also applied to the analysis of MA in human and rat urine [51,54] (Figure 5A). Although its sensitivity is not as good as MRM, the NL-based approach is well suited for rapid screening of reactive metabolites of lead compounds formed *in vivo* in rats and mice during the lead optimization.
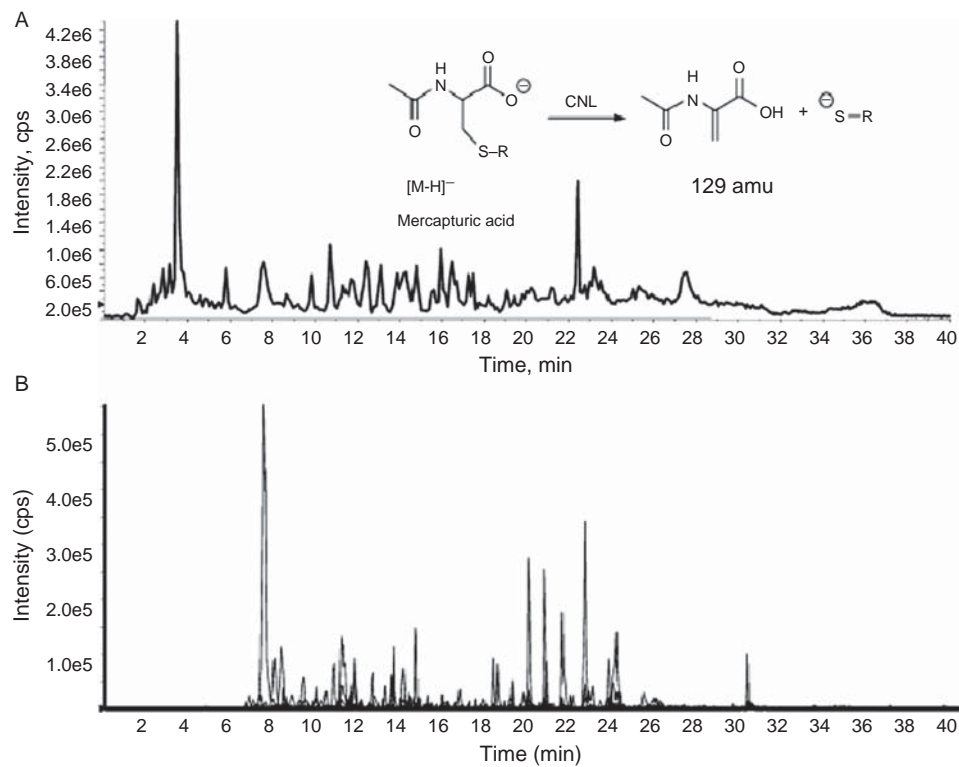
Figure 5 Detection of mercapturic acids in urine using negative ion NL–EPI [51,54] (Top panel) and MRM–EPI scans (Bottom panel) [50,51].

4.3. High-throughput screening using PI-EPI and polarity switching
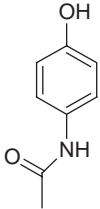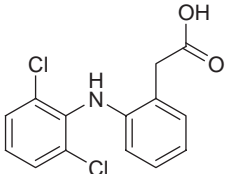
As combinatorial chemical synthesis and high-throughput screens in drug discovery have resulted in large numbers of drug candidates, the need for more efficient methodologies for screening reactive metabolites has become evident. Recently, a high-throughput method was developed for detection and characterization of GSH-trapped reactive metabolites with the Q-trap [23]. This method uses a negative precursor ion (PI) as the survey scan to trigger the acquisition of positive EPI spectra. Polarity switching between MS detection and MS/MS acquisition enables the detection of GSH adducts in the negative ion mode and simultaneous acquisition of MS/MS spectra in the positive ion mode which are much more informative than those acquire in the negative ion mode.

Results from analysis of bioactivation of several model compounds suggest that the PI–EPI approach is a feasible high-throughput method that can be utilized to screen for a large number of diverse compounds with reliable sensitivity and selectivity in a drug discovery setting [23]. As shown in Table 4, a number of new GSH conjugates that have not been detected by traditional NL scanning experiments were identified by this PI–EPI approach. GSH conjugates previously detected by NL scanning experiments are also among the most abundant identified by this approach. Compared to the triple quadrupole-based NL scanning methods, this PI–EPI approach, as a generic method, has displayed several major advantages: (1) high-throughput capability that performs the detection and structural characterization of GSH conjugates in a single LC/MS/MS run, (2) significantly improved sensitivity for detection and MS/MS acquisition of minor GSH conjugates at low levels, (3) superior selectivity for different classes of GSH conjugates with essentially no false positive signals for *in vitro* samples.

4.4. Quantitative determination using MRM
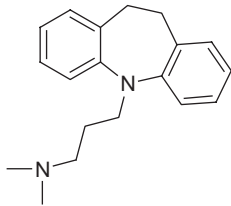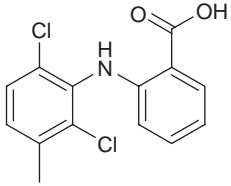
Quantitative determination of reactive metabolites is a crucial step in the assessment of bioactivation for lead optimization and selection of development candidates (Table 1). Reactive metabolites trapped by GSH, dansyl-GSH [29], and radiolabeled GSH [30,32,33] can be quantitatively determined by UV, fluorescence, and radiochromatographic detection, respectively. In these analyses, structural confirmation of chromatographic peaks, including thiol–adducts, is required and often accomplished by an on-line mass spectrometer. Due to the superior sensitivity and selectivity, the MRM–EPI scan with a Q-trap instrument is well suited for this task. In addition, the MRM scanning analysis can be directly applied to determining the relative concentrations of thiol–adducts in incubations without synthetic
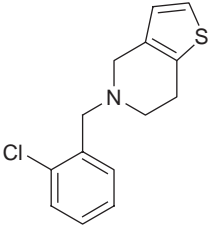
Table 4 Summary of glutathione conjugates identified by the negative precursor ion scanning of *m/z* 272 and positive MS/MS [23]

Compound (MH+)	Structure	GSH conjugate	MH+ and (major fragment) of GSH conjugate[a]	Postulated conjugate composition	GSH conjugate detected previously by NL[b]
Acetaminophen (152)		AM1	473 (**344**, 274, 256, 227, 199, 181, 145)	P + GSH + O − 2H	−
		AM2	473 (398, **344**, 327, 285, 224, 164, 156)	P + GSH + O − 2H	−
		AM3	457 (411, **382**, 336, **328**, 311, 208, 166, 140)	P + GSH − 2H	+
		AM4	457 (411, **382**, 336, **328**, 311, 208, 166, 140)	P + GSH − 2H	−
		AM5	489 (414, **360**, 184, 172, 138)	P + GSH + 2O − 2H	−
Diclofenac (296)		DM1	599 (551, **470**, 452, 307, 290, 262, 199, 181, 145)	P + GSH + 2O − HCl	−
		DM2	583 (**508**, 490, **454**, 436, 419, 334, 315, 290, 230, 199)	P + GSH + O − HCl	−
		DM3	617 (**542**, **488**, 470, 452, 367, 350, 342, 331, 296)	P + GSH + O − 2H	+

(*continued*)

Table 4 (*continued*)

Compound (MH+)	Structure	GSH conjugate	MH+ and (major fragment) of GSH conjugate[a]	Postulated conjugate composition	GSH conjugate detected previously by NL[b]
		DM4	567 (**492**, **438**, 420, 403, 318, 299, 246, 214)	P + GSH − HCl	−
		DM5	583 (**508**, **454**, 316, 308, 262)	P + GSH + O − HCl	+
Imipramine (281)		IM1	574 (**499**, **445**, 301, 159, 117)	P + GSH + O − 2H − 2CH2	−
		IM2	602 (584, **473**, 329, 256, 155)	P + GSH + O − 2H	−
		IM3	517 (499, **442**, **388**, 242, 211)	P + GSH + O − 2H after *N*-dealkylation	
		IM4	586 (568, **457**, 279, 234, 206)	P + GSH − 2H	+
Meclofenamic acid (296)		MM1	583 (**508**, **454**, 334, 282, 260, 256, 177)	P + GSH + O − HCl	−
		MM2	617 (573, **542**, **488**, 470, 444, 331, 298)	P + GSH + O − 2H	−
		MM3	617 (**542**, **488**, 342, 296, 175, 125)	P + GSH + O − 2H	−

	MM4	617 (573, **542**, **488**, 470, 444, 331, 298)	P + GSH + O − 2H	−
Ticlopidine (264)	TM1	569 (525, **494**, **440**, 296, 211, 154, 125)	P + GSH − 2H	+
	TM2	587 (**512**, 494, **458**, 440, 355, 308, 280, 253, 154)	P + GSH + O	−
	TM3	587 (494, **458**, 440, 416, 341, 287, 280, 184, 125)	P + GSH + O	−
	TM4	603 (571, **528**, **474**, 330, 296, 265, 232, 199, 154, 125)	P + GSH + 2O	−
	TM5	585 (**456**, 438, 312, 278, 250, 200, 154, 125)	P + GSH + O − 2H	−

[a] The boldface type denotes characteristic product ions resulting from neutral losses of 75 and 129 Da, respectively.
[b] The + denotes GSH conjugates identified in the NL scanning previously reported in the literature; the − denotes those not detected.
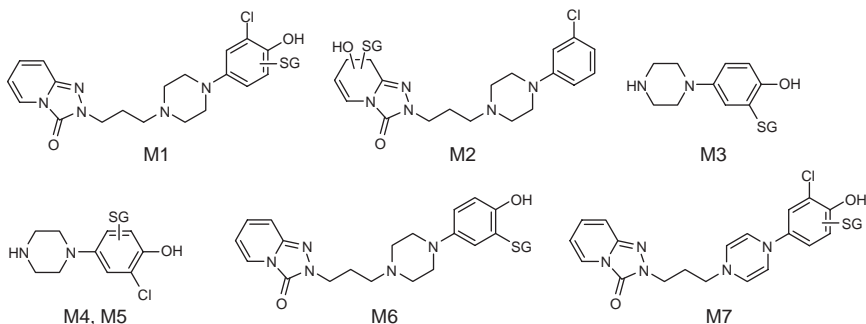
Figure 6 GSH conjugates identified by the PI-EPI analysis in incubations of trazodone with in HLM [24].

standards. The types of experiments are frequently conducted in the CYP reaction phenotyping studies. For example, the Q-trap was employed for rapidly determining major CYP enzymes responsible for bioactivation of antidepressant drugs trazodone [24]. In the experiment, GSH adducts of trazodone formed in HLM were detected and structurally characterized by the PI-EPI scan with the Q-trap (see the Section 5.2) (Figure 6). Trazodone and its N-dealkylated metabolite, 1-(3′-chlorophenyl)piperazine (m-CPP), were then incubated separately with cDNA-expressed recombinant P450 isozymes or with HLM in the presence of specific chemical inhibitors for these individual P450 isozymes. The GSH adducts were quantitatively analyzed by the MRM scan without changing high pressure liquid chromatography (HPLC) conditions. Although absolute amounts of the GSH adducts formed in these incubations could not be determined due to the lack of synthetic GSH adduct standards, relative concentrations of these adducts determined by MRM scans provided sufficient and reliable data for evaluating contributions from individual CYP isozymes [24]. As demonstrated in Figure 7, the results of analyzing relative concentrations of GSH adducts of trazodone and m-CPP formed by the cDNA-expressed recombinant P450 enzymes clearly revealed the significant roles of CYP3A4 and CYP2D6 in the bioactivation of trazodone and m-CPP, respectively.

5. EXAMPLES OF USING THE Q-TRAP TO STUDY DRUG BIOACTIVATION

5.1. Clozapine

Clozapine is a dibenzodiazepine antipsychotic drug whose major advantages include the lack of extrapyramidal adverse effects such as tardive dyskinesia [55] and its effectiveness in otherwise "treatment-resistant" patients [56]. Despite these advantages, the use of clozapine is restricted because of a
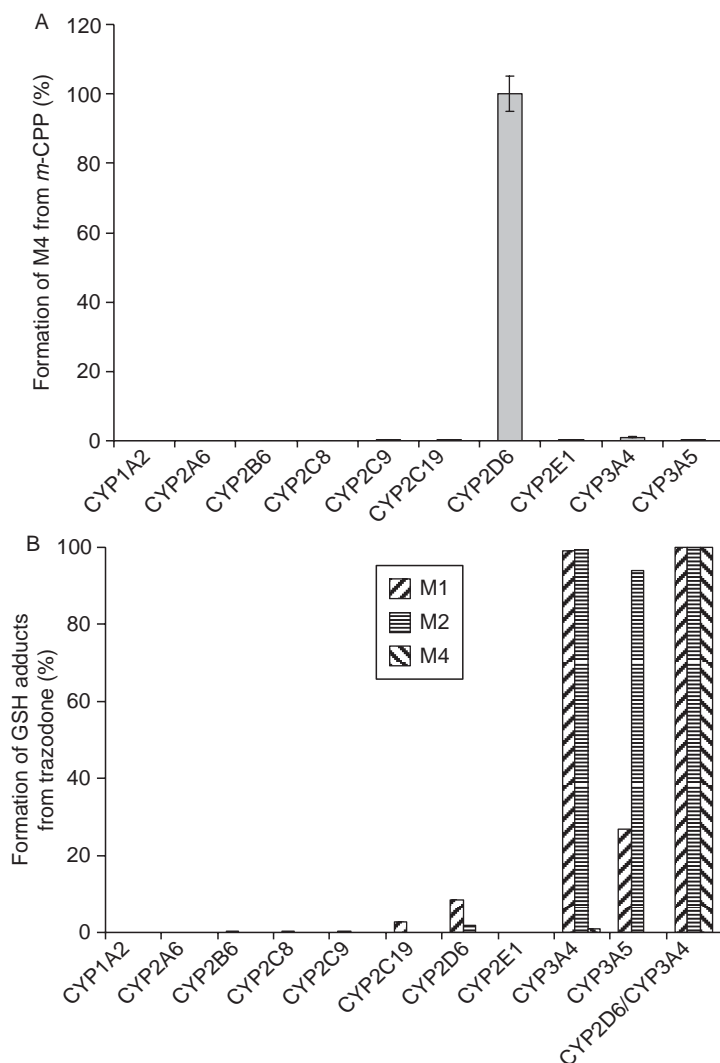
Figure 7 Formation of GSH adducts of trazodone in incubations with cDNA-expressed recombinant P450 isozymes [24]. (A) formation of M4 in incubations of *m*-CPP, (B) formation of M1, M2, and M4 in incubations of trazodone. The enzyme activities were an average of three measurements. Structures and formation pathways of these adducts are displayed in Figures 6 and 12.

relatively high incidence (0.8%) of agranulocytosis, a potentially fatal decrease in circulating neutrophils [57,58]. In defining the chemical entity responsible for clozapine–induced agranulocytosis, evidence centers on drug bioactivation to a chemically reactive intermediate, thought to be a nitrenium ion reactive metabolite [59–62]. It has been postulated that

covalent modifications of neutrophil/bone marrow proteins by this reactive species could be directly toxic to cellular processes causing cell death, or alternatively, lead to hapten formation and immune-mediated toxicity or hypersensitivity [63,64].

To determine the mechanism that may underlie drug-induced agranulo-cytosis, clozapine was incubated with HLM and samples were analyzed by the PI-EPI approach with polarity switching [23]. Within a single LC/MS/MS run, a total of seven GSH conjugates of clozapine were detected (Figure 8) and structures of these detected components were simultaneously verified based on the MS/MS spectra in the positive ion mode. In addition to the major GSH conjugates such as CM6 and CM7 previously reported, at least four conjugates (CM1, CM2, CM4, and CM5) identified by the PI-EPI approach were characterized for the first time (Figure 9). For instance, the MS^2 spectrum of CM1 suggested that monohydroxylation occurred on the dibenzodiazepine ring rather than the piperazine ring of clozapine. CM1 was proposed to be formed via a quinone imine intermediate (Figure 10). Another abundant GSH adduct that has not been reported in the literature was CM5. This adduct has an [M + H]$^+$ ion at m/z 664, corresponding to a GSH adduct of a dioxidation product (P + GSH + 2O − 2H). Product ions at m/z 243, 270, 325 suggest that it was a hydroxylated GSH conjugate of clozapine N-oxide, formed presumably by sequential N-oxidation and a monohydroxylation that leads to quinone imine intermediate (Figure 9D). Based on the mass spectral data, it was
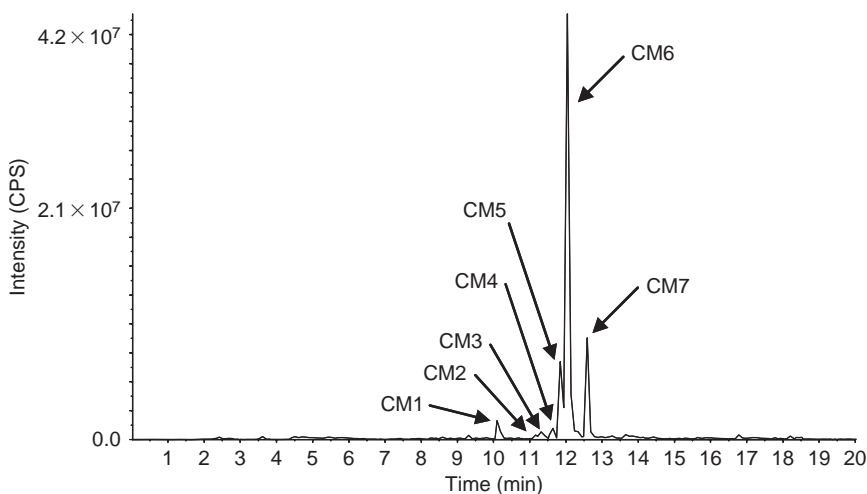
Figure 8   Total ion current chromatogram of negative precursor ion scanning of m/z 272 obtained from the LC/MS/MS analysis of GSH adducts in an HLM incubation of clozapine by the PI-EPI approach [23]. Positive ion MS/MS spectra of selected adducts are presented in Figure 9, and bioactivation pathways of clozapine in HLM is proposed in Figure 10.
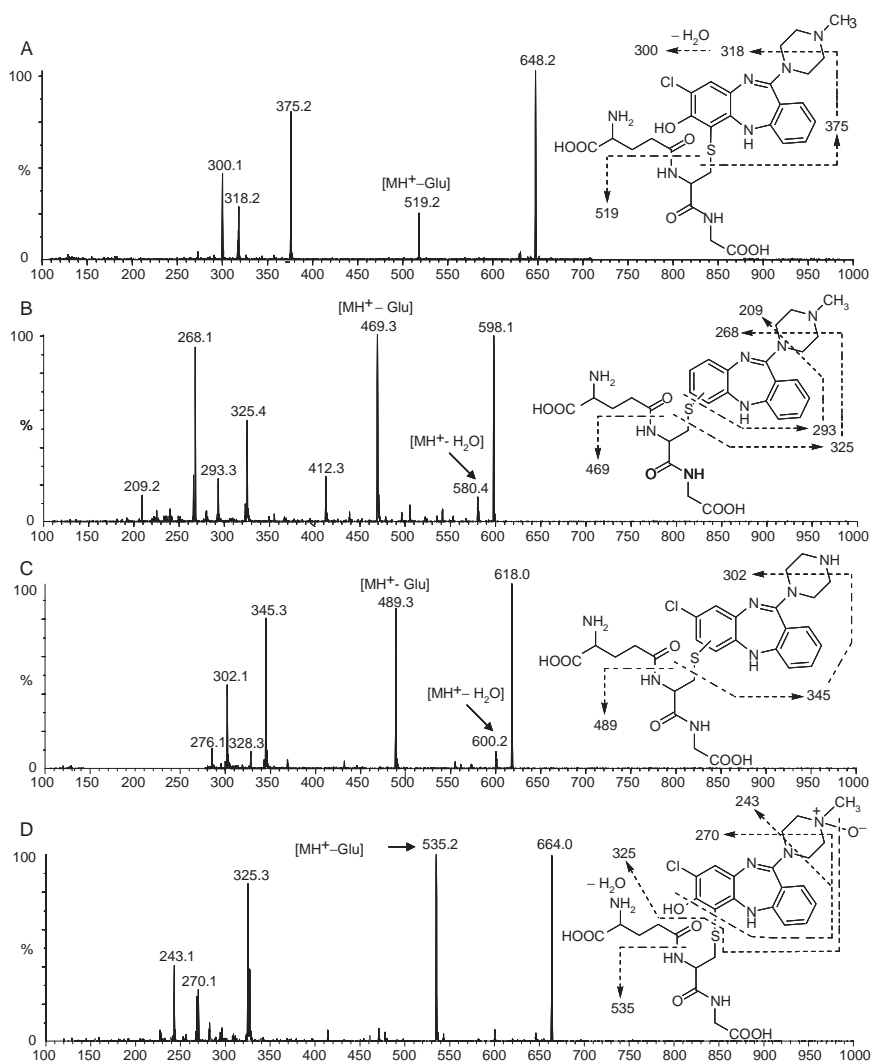
Figure 9 Positive product ion spectra and proposed structures of the newly detected clozapine GSH conjugates acquired by the PI-directed EPI scan with polarity switching [23]. (A) CM1, (B) CM2, (C) CM4, and (D) CM5.

proposed that CM2 was formed via a nitrenium ion reactive intermediate after dechlorination, and CM4 was likely formed from the nitrenium ion of demethylclozapine, which was a major metabolite identified previously from HLM incubations. From the GSH conjugates newly identified by the PI-EPI approach, it has been proposed that clozapine can be bioactivated to electrophlic reactive intermediates via not only nitrenium ions but also quinone imines (Figure 10).
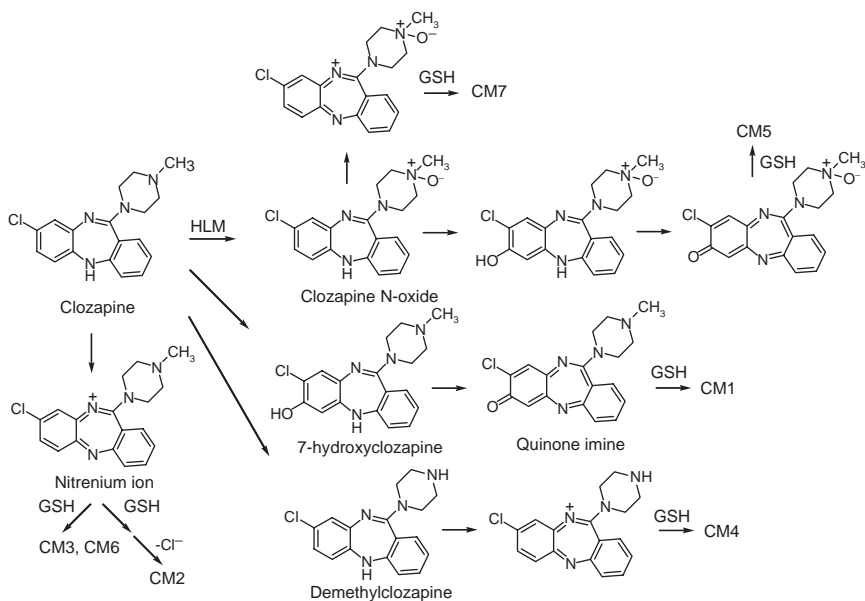
Figure 10 Proposed bioactivation pathways of clozapine in HLM and trapping of reactive metabolites by GSH [23].

5.2. Trazodone

Trazodone is a second-generation triazolopyridinone antidepressant drug (Figure 11), which is structurally distinct from selective serotonin reuptake inhibitors, such as tri- and tetracyclics, and monoamine oxidase inhibitors. It is thought to act through combined 5-HT$_2$ antagonism and 5-HT reuptake blockage [65]. Trazodone is often coprescribed with other antidepressants as a sleep-inducing agent because of its more sedating and less anticholinergic side effects. Despite its therapeutic benefits, treatment with trazodone has been associated with rare, but severe incidence of hepatic injury, which is often described as idiosyncratic toxicity [66–69]. Although the exact mechanism of trazodone hepatotoxicity is not clearly understood, a probable causal link between trazodone use and the onset of hepatic injury has been established [70,71].

As shown in Figure 11, trazodone contains a triazolopyridinone moiety and a 3-chlorophenylpiperazine ring system. In humans, trazodone undergoes extensive hepatic metabolism mainly by hydroxylation, N-dealkylation and N-oxidation [72–74]. Of particular interest in the biotransformation pathways of trazodone in humans is the detection and characterization of a dihydrodiol metabolite and 4′-hydroxytrazodone as major metabolites in urine [72,74,75]. Formation of the dihydrodiol metabolite can presumably occur by nucleophilic addition of water to an electrophilic epoxide
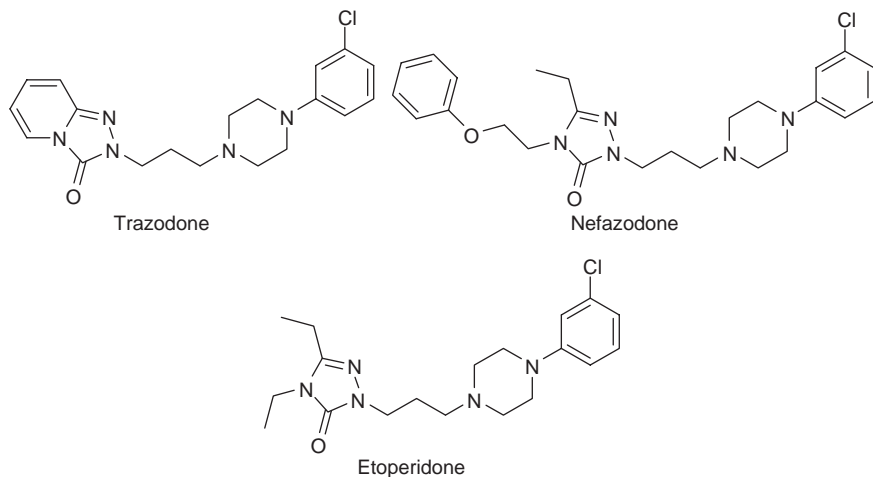
Figure 11 Structures of antidepressant drugs trazodone, nefazodone, and etoperidone.

intermediate. On the other hand, 4′-hydroxytrazodone can undergo a two-electron oxidation leading to formation of an electrophilic quinone imine intermediate, which is capable of reacting with cellular proteins and other nucleophiles such as GSH. In HLM incubations, two glutathione adducts were previously identified arising from quinone imine and epoxide intermediates [76]. The epoxidation of triazolopyridinone, para–hydroxylation of 3-chlorophenylpiperazine and subsequent oxidation to quinone imine were shown to be mediated by cytochrome P450 3A4 [76].

Using the PI-EPI approach of the Q-trap, several new GSH adducts (M3–M7) were detected in the incubations of trazodone with HLM using LC/MS/MS [24]. Bioactivation of m-chlorophenylpiperazine (m-CPP), a major circulating metabolite shared by several antidepressant drugs including trazodone, nefazodone, and etoperidone, was demonstrated by detection of three m-CPP derived GSH conjugates [24]. Formation of the m-CPP derived GSH conjugate M3 was proposed via a quinone imine intermediate after an initial C-4′ hydroxylation and subsequent two-electron oxidations (Figure 12). This mechanism of m-CPP bioactivation was supported by the lack of M3 formation in the incubations of a regioisomer of m-CPP, p-CPP with HLM and recombinant P450 enzymes, which suggested that formation of M3 requires the initial oxidation at the C-4′ position (Figure 12). Moreover, a total blockage of all three m-CPP derived GSH adducts M3–M5 in incubations of p-CPP suggested that they are likely formed via a common reactive quinone imine intermediate by two-electron oxidations, after the initial 4′-hydroxylation on the chlorophenyl ring. An alternate pathway for deschloro adduct formation is P450-mediated epoxidation between the C-3′ and C-4′ or the C-3′ and C-2′
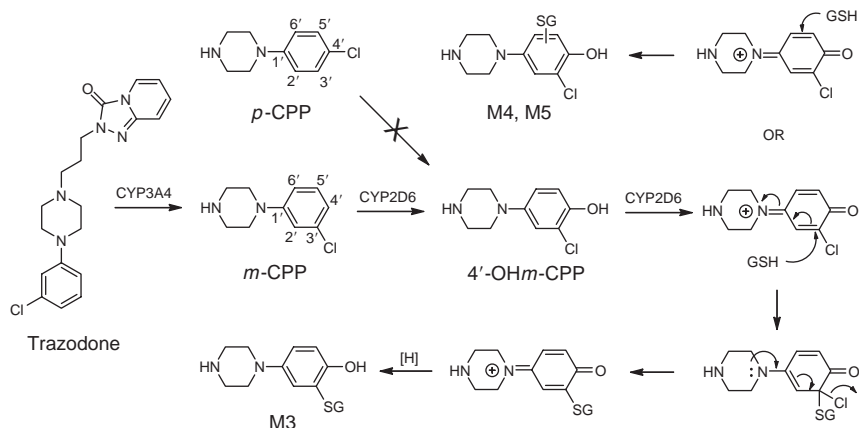
Figure 12 Proposed bioactivation pathways leading to the formation of *m*-CPP derived GSH conjugates M3, M4, and M5 in incubations of trazodone with HLM [24].

positions on the chlorophenyl ring. Loss of chlorine would result from an attack of GSH on the epoxide. This mechanism has been proposed for the formation of the deschloro GSH adduct of diclofenac in HLM incubations [77]. Since such potential epoxides could be formed in incubations of *m*-CPP and the formed epoxides can readily be trapped by GSH to afford corresponding conjugates, this study concluded that *m*-CPP is bioactivated via a quinone imine intermediate instead of an epoxide [24].

In addition, formation of GSH adducts M3, M4, and M5 from *m*-CPP was mediated specifically by CYP2D6 (Figure 7) [24], in contrast to the CYP3A4-catalyzed bioactivation of trazodone (Figure 7) and nefazodone [76]. It was shown that no single P450 isozyme was able to catalyze formation of *m*-CPP derived M4 from the incubations of trazodone [24]. These results further support the conclusion that *N*-dealkylation of trazodone to form the metabolite *m*-CPP is mainly carried by CYP3A enzymes, while bioactivation and/or metabolism of *m*-CPP is specifically mediated CYP2D6 (Figure 12) [24]. These findings are of significance in understanding biochemical mechanisms of idiosyncratic toxicity of several *m*-CPP containing antidepressant drugs and a possible relevance of CYP2D6 polymorphism and/or drug interactions to *m*-CPP toxicokinetics.

5.3. Amitriptyline and Nortriptyline

Amitriptyline, along with other tricyclic antidepressants (TCAs), has been the cornerstone of antidepressive therapy for more than three decades. Current treatment guidelines recommend the use of TCAs only in patients with psychotic features and treatment resistance [78]. Nevertheless, more than 1 million patients received TCAs in the United States in 2000 [79] and

amitriptyline is still used extensively in developing countries because of its favorable cost/benefit ratio. The clinical effects of amitriptyline are characterized by changes in mood, which is thought to be related to its ability to inhibit the neuronal uptake of the biogenic amine, norepinephrine. Despite its therapeutic benefits, treatment with amitriptyline has been associated with very rare, but severe liver toxicity [80–86]. Although the exact mechanism of hepatotoxicity caused by amitriptyline is currently unknown. Similar idiosyncratic hepatotoxicity has also been observed with the antidepressant nortriptyline, which is an N-dealkylated metabolite of amitriptyline [87,88].

The clearance of amitriptyline in humans is heavily dependent on hepatic oxidative metabolism by cytochrome P450s [89–92]. Amitriptyline undergoes extensive metabolism mainly by hydroxylation, N-dealkylation, N-oxidation, and glucuronidation [89]. Of significant interest in many biotransformation pathways of amitriptyline in humans is the detection and characterization of a dihydrodiol metabolite of amitriptyline in urine [91]. Formation of the dihydrodiol metabolite can presumably occur by nucleophilic addition of water to the electrophilic epoxide intermediate as shown in Figure 13. We proposed that the reactive epoxide intermediate, resulting from an initial P450-catalyzed bioactivation on an aromatic ring of amitriptyline, could add water to yield the dihydrodiol M2, react with glutathione to form GSH adduct M1 or react with cellular proteins to trigger a toxicological response (Figure 13). Considering that nortriptyline is similar in structure to the N-dealkylated metabolite of amitriptyline, formation of an epoxide intermediate from nortriptyline could contribute to the observed hepatotoxicity caused by amitriptyline and nortriptyline, respectively (Figure 13).

Direct evidence for bioactivation of amitriptyline comes from the detection of two GSH adducts of this drug using the PI-EPI method on a hybrid Q-trap mass spectrometer (Figure 14). Apart from the literature reports on the involvement of CYP2D6 and CYP3A4 in the hydroxylation of amitriptyline and nortriptyline, these studies demonstrated major roles for these enzymes in the metabolic activation of the two antidepressants. Formation of the glutathione conjugate M1 is consistent with a bioactivation sequence involving initial P450-catalyzed oxidation of the benzene nucleus in amitriptyline to an electrophilic epoxide, which reacts with water and glutathione generating the dihydrodiol metabolite M2 and the sulfydryl conjugate M1, respectively (Figure 13). Formation of the glutathione conjugate M4 is mediated by a similar oxidative pathway after P450-mediated N-demethylation of amitriptyline to afford nortriptyline. Bioactivation of nortriptyline was further confirmed by direct incubations of nortriptyline with HLM and recombinant P450s [94].

Formation of M1 from amitriptyline and formation of M4 from nortriptyline is mainly catalyzed by CYP2D6. In contrast, CYP3A4 and CYP3A5 are

Figure 13   Proposed bioactivation pathways and associated hepatotoxicity of the tricyclic antidepressant amitriptyline and its metabolite nortriptyline [94].
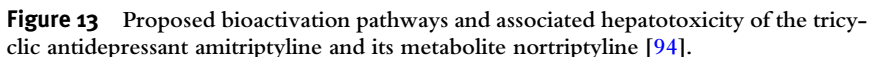
the major enzymes involved in formation of M4 from incubations of amitriptyline [94]. These data are consistent with the previous reports that CYP3A4 and CYP2C19 are the major enzymes catalyzing *N*-demethylation of amitriptyline to nortriptyline, while CYP2D6 has poor *N*-demethylation activity towards amitriptyline [90,93]. In addition, other enzymes such as dihydrodiol dehydrogenase and soluble epoxide hydrolase may also contribute to the bioactivation of amitriptyline. For example, dihydrodiol dehydrogenase may
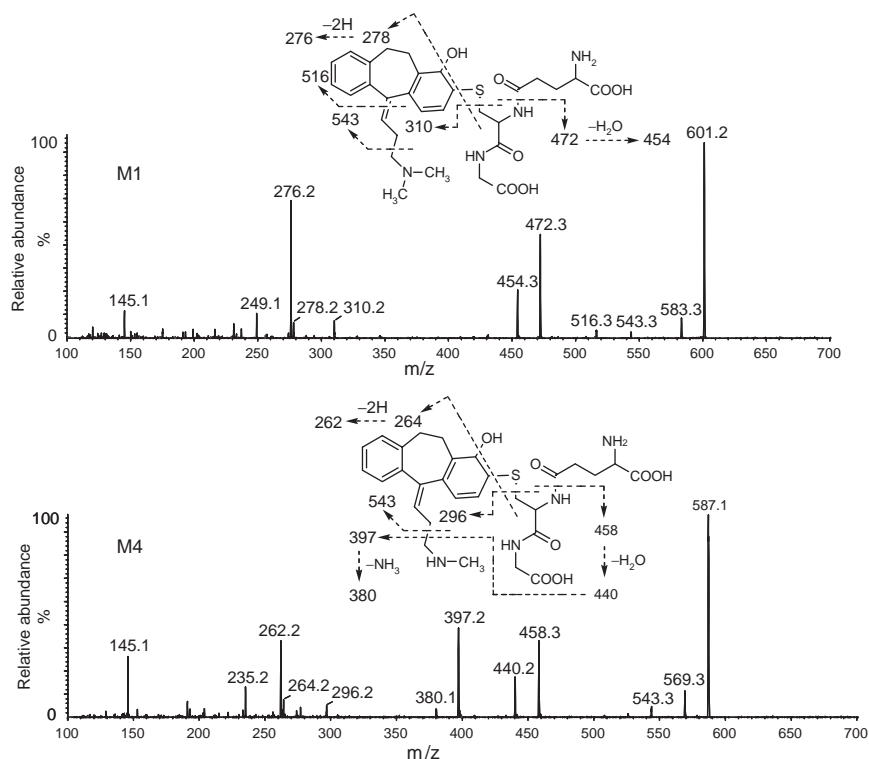
Figure 14 Product ion spectra of GSH conjugates of amitriptyline formed in HLM incubations obtained by the PI-EPI analysis [94].

oxidize the dihydrodiol metabolites M2 and M3 to reactive ortho-quinone intermediates which can contribute to the toxicity of this drug via redox-cycling. The roles of these individual nonmicrosomal enzymes in the bioactivation of amitriptyline and nortriptyline remain to be established [94].

6. Conclusions

Although the updated version of the quadrupole–linear ion trap mass spectrometry (API 4000 Q-trap) has been commercially available only for a few years, it has proved to be a unique, valuable LC/MS platform for profiling and identification of drug metabolite, especially in analysis of reactive metabolites in drug discovery and development. The Q-trap retains all scan functions of classical triple quadrupoles so that it can be used as a stand alone triple quadrupole instrument for quantitative analysis of drugs and metabolites in routine bioanalytical studies. More importantly, the

Q-trap has the information-dependent scan capability that utilizes the selective MS/MS scan modes of quadrupoles, such as NL, PI, and MRM scans, as survey scans to trigger the sensitive MS/MS acquisition (EPI). The unique PI-EPI, NL-EPI, and MRM-EPI scan functions enable the Q-trap to perform a variety of mass spectrometric experiments suitable for the fast, sensitive and selective detection, identification and quantification of chemically reactive drugs metabolites. As demonstrated in the analysis of metabolic activation of a number of model compounds and drugs presented in the review, including clozapine, trazodone, amitripthline, and nortripty-line, the PI-EPI scan with the polarity switching is well suited for the high-throughput screening of reactive metabolites [97,98,99]. This LC/MS approach is able to detect different classes of GSH adducts by scanning for a common product ion such as m/z 272 in the negative ion mode and acquire informative MS/MS spectra of the adducts in the positive ion mode in the same LC/MS injection. The MRM-EPI scan is capable of providing the highest selectivity and sensitivity in the detection of reactive metabolites among common LC/MS methodologies listed in Table 2. This technology has been applied to search for up to 50–300 potential GSH adducts or MA is especially useful in detecting and identifying reactive metabolites at very low levels or present in complex biological matrixes, where endogenous GSH conjugates and mercapturic acids are problematic. Because of these special utilities and the advantages over traditional triple quadrupoles, Q-trap has the potential to become the primary LC/MS platform in some of bioanalytical labs where quantitative analysis of drugs is their primary task and metabolite identification is performed occasionally. In addition, hybrid triple quadrupole-linear ion trap instruments are specially useful in small drug metabolism labs where metabolite profiling and *in vitro* ADME studies, including as metabolic stablity, reactive metabolite screening and CYP inhibtion experiments, are routinely carried out with a limited number of LC/MS instruments.

REFERENCES

[1] J. Uetrecht, Idiosyncratic drug reactions: Past, present, and future, Chem. Res. Toxicol. 21 (2008) 84–92.

[2] K. Park, D.P. Williams, D.J. Naisbitt, N.R. Kitteringham, M. Pirmohamed, Investigation of toxic metabolites during drug development, Toxicol. Appl. Pharmacol. 207 (2005) 425–434.

[3] S.D. Nelson, Structure toxicity relationships – How useful are they in predicting toxicities of new drugs, in: R. S. P. M. Dansette, M. Delaforge, G.G. Gibson, H. Greim, D.J. Jollow, T.J. Monks, and I.G. Sipes (Eds.), Biological Reactive Intermediates, vol. VI. Kluwer Academic/Plenum Publishers, Dordrecht, 2001.

[4] J.L. Walgren, M.D. Mitchell, D.C. Thompson, Role of metabolism in drug-induced idiosyncratic hepatotoxicity, Crit. Rev. Toxicol. 35 (2005) 325–361.

[5] D.C. Evans, T.A. Baillie, Minimizing the potential for metabolic activation as an integral part of drug design, Curr. Opin. Drug Discov. Devel. 8 (2005) 44–50.

[6] S. Ma, R. Subramanian, Detecting and characterizing reactive metabolites by liquid chromatography/tandem mass spectrometry, J. Mass Spectrom. 41 (2006) 1121–1139.

[7] T.A. Baillie, Metabolism and toxicity of drugs. Two decades of progress in industrial drug metabolism, Chem. Res. Toxicol. 21 (2008) 129–137.

[8] J. Uetrecht, Screening for the potential of a drug candidate to cause idiosyncratic drug reactions, Drug Discov. Today 8 (2003) 832–837.

[9] N.J. Clarke, D. Rindgen, W.A. Korfmacher, K.A. Cox, Systematic LC/MS metabolite identification in drug discovery, Anal. Chem. 73 (2001) 430A–439A.

[10] G. Hopfgartner, E. Varesio, V. Tschappat, C. Grivet, E. Bourgogne, L.A. Leuthold, Triple quadrupole linear ion trap mass spectrometer for the analysis of small molecules and macromolecules, J. Mass Spectrom. 39 (2004) 845–855.

[11] J.W. Hager, J.C. Le Blanc, High-performance liquid chromatography-tandem mass spectrometry with a new quadrupole/linear ion trap instrument, J. Chromatogr. A 1020 (2003) 3–9.

[12] J.W. Hager, J.C. Yves Le Blanc, Product ion scanning using a Q-q-Q linear ion trap (Q TRAP) mass spectrometer, Rapid Commun. Mass Spectrom. 17 (2003) 1056–1064.

[13] J.C. Le Blanc, J.W. Hager, A.M. Ilisiu, C. Hunter, F. Zhong, I. Chu, Unique scanning capabilities of a new hybrid linear ion trap mass spectrometer (Q TRAP) used for high sensitivity proteomics applications, Proteomics 3 (2003) 859–869.

[14] Y.Q. Xia, J.D. Miller, R. Bakhtiar, R.B. Franklin, D.Q. Liu, Use of a quadrupole linear ion trap mass spectrometer in metabolite identification and bioanalysis, Rapid Commun. Mass Spectrom. 17 (2003) 1137–1145.

[15] W.Z. Shou, L. Magis, A.C. Li, W. Naidong, M.S. Bryant, A novel approach to perform metabolite screening during the quantitative LC-MS/MS analyses of in vitro metabolic stability samples using a hybrid triple-quadrupole linear ion trap mass spectrometer, J. Mass Spectrom. 40 (2005) 1347–1356.

[16] A.C. Li, D. Alton, M.S. Bryant, W.Z. Shou, Simultaneously quantifying parent drugs and screening for metabolites in plasma pharmacokinetic samples using selected reaction monitoring information-dependent acquisition on a Q-trap instrument, Rapid Commun. Mass Spectrom. 19 (2005) 1943–1950.

[17] A.C. Li, M.A. Gohdes, W.Z. Shou, "N-in-one" strategy for metabolite identification using a liquid chromatography/hybrid triple quadrupole linear ion trap instrument using multiple dependent product ion scans triggered with full mass scan, Rapid Commun. Mass Spectrom. 21 (2007) 1421–1430.

[18] R.C. King, R. Gundersdorf, C.L. Fernandez-Metzler, Collection of selected reaction monitoring and full scan data on a time scale suitable for target compound quantitative analysis by liquid chromatography/tandem mass spectrometry, Rapid Commun. Mass Spectrom. 17 (2003) 2413–2422.

[19] P. Marquet, F. Saint-Marcoux, T.N. Gamble, J.C. Leblanc, Comparison of a preliminary procedure for the general unknown screening of drugs and toxic compounds using a quadrupole-linear ion-trap mass spectrometer with a liquid chromatography–mass spectrometry reference technique, J. Chromatogr. B Anal. Technol. Biomed. Life Sci. 789 (2003) 9–18.

[20] H. Liu, H. Gao, M. Namikoshi, H. Kobayashi, R.E. Mangindaan, N. Wang, X. Yao, Characterization and online detection of aromatic alkaloids in the ascidian Lissoclinum cf. Badium by liquid chromatography/UV detection mass spectrometry, Rapid Commun. Mass Spectrom. 21 (2007) 199–206.

[21] G. Hopfgartner, C. Husser, M. Zell, Rapid screening and characterization of drug metabolites using a new quadrupole-linear ion trap mass spectrometer, J. Mass Spectrom. 38 (2003) 138–150.

[22] J. Zheng, L. Ma, B. Xin, T. Olah, W.G. Humphreys, M. Zhu, Screening and Identification of GSH-Trapped Reactive Metabolites Using Hybrid Triple Quadruple Linear Ion Trap Mass Spectrometry, Chem. Res. Toxicol. 20 (2007) 757–766.

[23] B. Wen, L. Ma, S.D. Nelson, M. Zhu, High-throughput screening and characterization of reactive metabolites using polarity switching of hybrid triple quadrupole linear ion trap mass spectrometry, Anal. Chem. 80 (2008) 1788–1799.

[24] B. Wen, L. Ma, D. Rodrigues, M. Zhu, Detection of novel reactive metabolites of trazodone: Evidence for Cyp2d6-mediated bioactivation of *m*-chlorophenylpiperazine, Drug Metab. Dispos. 36 (2008) 841–850.

[25] R. King, C. Fernandez-Metzler, The use of Q-trap technology in drug metabolism, Curr. Drug Metab. 7 (2006) 541–545.

[26] D.C. Evans, A.P. Watt, D.A. Nicoll-Griffith, T.A. Baillie, Drug-protein adducts: An industry perspective on minimizing the potential for drug bioactivation in drug discovery and development, Chem. Res. Toxicol. 17 (2004) 3–16.

[27] Z. Yan, N. Maher, R. Torres, G.W. Caldwell, N. Huebert, Rapid detection and characterization of minor reactive metabolites using stable-isotope trapping in combination with tandem mass spectrometry, Rapid Commun. Mass Spectrom. 19 (2005) 3322–3330.

[28] C.M. Dieckhaus, C.L. Fernandez-Metzler, R. King, P.H. Krolikowski, T.A. Baillie, Negative ion tandem mass spectrometry for the detection of glutathione conjugates, Chem. Res. Toxicol. 18 (2005) 630–638.

[29] J. Gan, T.W. Harper, M.M. Hsueh, Q. Qu, W.G. Humphreys, Dansyl glutathione as a trapping agent for the quantitative estimation and identification of reactive metabolites, Chem. Res. Toxicol. 18 (2005) 896–903.

[30] D.C. Thompson, K. Perera, R. London, Quinone methide formation from para isomers of methylphenol (cresol), ethylphenol, and isopropylphenol: Relationship to toxicity, Chem. Res. Toxicol. 8 (1995) 55–60.

[31] N. Masubuchi, C. Makino, N. Murayama, Prediction of *in vivo* potential for metabolic activation of drugs into chemically reactive intermediate: Correlation of *in vitro* and *in vivo* generation of reactive intermediates and *in vitro* glutathione conjugate formation in rats and humans, Chem. Res. Toxicol. 20 (2007) 455–464.

[32] M. Zhu, W. Zhao, N. Vazquez, J.G. Mitroka, Analysis of low level radioactive metabolites in biological fluids using high-performance liquid chromatography with microplate scintillation counting: Method validation and application, J. Pharm. Biomed. Anal. 39 (2005) 233–245.

[33] G. Meneses-Lorente, M.Z. Sakatis, T. Schulz-Utermoehl, C. De Nardi, A.P. Watt, A quantitative high-throughput trapping assay as a measurement of potential for bioactivation, Anal. Biochem. 351 (2006) 266–272.

[34] J.R. Soglia, L.G. Contillo, A.S. Kalgutkar, S. Zhao, C.E. Hop, J.G. Boyd, M.J. Cole, A semiquantitative method for the determination of reactive metabolite conjugate levels *in vitro* utilizing liquid chromatography-tandem mass spectrometry and novel quaternary ammonium glutathione analogues, Chem. Res. Toxicol. 19 (2006) 480–490.

[35] S.V. Gopaul, K. Farrell, F.S. Abbott, Identification and characterization of *N*-acetyl-cysteine conjugates of valproic acid in humans and animals, Drug Metab. Dispos. 28 (2000) 823–832.

[36] T.A. Baillie, M.R. Davis, Mass spectrometry in the analysis of glutathione conjugates, Biol. Mass Spectrom. 22 (1993) 319–325.

[37] P.G. Pearson, M.D. Threadgill, W.N. Howald, T.A. Baillie, Applications of tandem mass spectrometry to the characterization of derivatized glutathione conjugates. Studies with *S*-(*N*-methylcarbamoyl)glutathione, a metabolite of the antineoplastic agent *N*-methylformamide, Biomed. Environ. Mass Spectrom. 16 (1988) 51–56.

[38] W.G. Chen, C. Zhang, M.J. Avery, H.G. Fouda, Reactive metabolite screen for reducing candidate attrition in drug discovery, in: R. S. P. M. Dansette, M. Delaforge, G.G. Gibson, H. Greim, D.J. Jollow, T.J. Monks, and I.G. Sipes (Eds.), Biological Reactive Intermediates, vol. VI. Kluwer Academic/Plenum Publishers, New York, 2001, pp. 521–524.

[39] Z. Yan, G.W. Caldwell, Stable-isotope trapping and high-throughput screenings of reactive metabolites using the isotope MS signature, Anal. Chem. 76 (2004) 6835–6847.

[40] J.R. Soglia, S.P. Harriman, S. Zhao, J. Barberia, M.J. Cole, J.G. Boyd, L.G. Contillo, The development of a higher throughput reactive intermediate screening assay incorporating micro-bore liquid chromatography-micro-electrospray ionization-tandem mass spectrometry and glutathione ethyl ester as an *in vitro* conjugating agent, J. Pharm. Biomed. Anal. 36 (2004) 105–116.

[41] A. Mutlib, W. Lam, J. Atherton, H. Chen, P. Galatsis, W. Stolle, Application of stable isotope labeled glutathione and rapid scanning mass spectrometers in detecting and characterizing reactive metabolites, Rapid Commun. Mass Spectrom. 19 (2005) 3482–3492.

[42] C. Prakash, C.L. Shaffer, A. Nedderman, Analytical strategies for identifying drug metabolites, Mass Spectrom. Rev. 26 (2007) 340–369.

[43] H. Zhang, D. Zhang, K. Ray, A software filter to remove interference ions from drug metabolites in accurate mass liquid chromatography/mass spectrometric analyses, J. Mass Spectrom. 38 (2003) 1110–1112.

[44] M. Zhu, L. Ma, D. Zhang, K. Ray, W. Zhao, W.G. Humphreys, G. Skiles, M. Sanders, H. Zhang, Detection and characterization of metabolites in biological matrices using mass defect filtering of liquid chromatography/high resolution mass spectrometry data, Drug Metab. Dispos. 34 (2006) 1722–1733.

[45] Q. Ruan, S. Peterman, M.A. Szewc, L. Ma, D. Cui, W.G. Humphreys, M. Zhu, An integrated method for metabolite detection and identification using a linear ion trap/Orbitrap mass spectrometer and multiple data processing techniques: Application to indinavir metabolite detection, J. Mass Spectrom. 43 (2008) 251–261.

[46] M. Zhu, L. Ma, H. Zhang, W.G. Humphreys, Detection and structural characterization of glutathione-trapped reactive metabolites using liquid chromatography-high-resolution mass spectrometry and mass defect filtering, Anal. Chem. 79 (2007) 8333–8341.

[47] J. Castro-Perez, R. Plumb, L. Liang, E. Yang, A high-throughput liquid chromatography/tandem mass spectrometry method for screening glutathione conjugates using exact mass neutral loss acquisition, Rapid Commun. Mass Spectrom. 19 (2005) 798–804.

[48] C.A. Mueller, W. Weinmann, S. Dresen, A. Schreiber, M. Gergov, Development of a multi-target screening analysis for 301 drugs using a Q-trap liquid chromatography/tandem mass spectrometry system and automated library searching, Rapid Commun. Mass Spectrom. 19 (2005) 1332–1338.

[49] F.L. Sauvage, F. Saint-Marcoux, B. Duretz, D. Deporte, G. Lachatre, P. Marquet, Screening of drugs and toxic compounds with liquid chromatography-linear ion trap tandem mass spectrometry, Clin. Chem. 52 (2006) 1735–1742.

[50] S. Wagner, K. Scholz, M. Sieber, M. Kellert, W. Voelkel, Tools in metabonomics: An integrated validation approach for LC–MS metabolic profiling of mercapturic acids in human urine, Anal. Chem. 79 (2007) 2918–2926.

[51] K. Scholz, W. Dekant, W. Volkel, A. Pahler, Rapid detection and identification of N-acetyl-l-cysteine thioethers using constant neutral loss and theoretical multiple reaction monitoring combined with enhanced product-ion scans on a linear ion trap mass spectrometer, J. Am. Soc. Mass Spectrom. 16 (2005) 1976–1984.

[52] S.V. Gopaul, K. Farrell, F.S. Abbott, Gas chromatography/negative ion chemical ionization mass spectrometry and liquid chromatography/electrospray ionization tandem mass spectrometry quantitative profiling of *N*-acetylcysteine conjugates of valproic acid in urine: Application in drug metabolism studies in humans, J. Mass Spectrom. 35 (2000) 698–704.

[53] P.T. Manyike, E.D. Kharasch, T.F. Kalhorn, J.T. Slattery, Contribution of CYP2E1 and CYP3A to acetaminophen reactive metabolite formation, Clin. Pharmacol. Ther. 67 (2000) 275–282.

[54] S. Wagner, K. Scholz, M. Donegan, L. Burton, J. Wingate, W. Volkel, Metabonomics and biomarker discovery: LC–MS metabolic profiling and constant neutral loss scanning combined with multivariate data analysis for mercapturic acid analysis, Anal. Chem. 78 (2006) 1296–1305.

[55] R.J. Baldessarini, F.R. Frankenburg, Clozapine. A novel antipsychotic agent, N. Engl. J. Med. 324 (1991) 746–754.

[56] J. Kane, G. Honigfeld, J. Singer, H. Meltzer, Clozapine for the treatment-resistant schizophrenic. A double-blind comparison with chlorpromazine, Arch. Gen. Psychiatry 45 (1988) 789–796.

[57] J.A. Lieberman, A.Z. Safferman, Clinical profile of clozapine: Adverse reactions and agranulocytosis, Psychiatr. Q 63 (1992) 51–70.

[58] J.M. Alvir, J.A. Lieberman, A reevaluation of the clinical characteristics of clozapine-induced agranulocytosis in light of the United States experience, J. Clin. Psychopharmacol. 14 (1994) 87–89.

[59] Z.C. Liu, J.P. Uetrecht, Clozapine is oxidized by activated human neutrophils to a reactive nitrenium ion that irreversibly binds to the cells, J. Pharmacol. Exp. Ther. 275 (1995) 1476–1483.

[60] I. Gardner, N. Zahid, D. MacCrimmon, J.P. Uetrecht, A comparison of the oxidation of clozapine and olanzapine to reactive metabolites and the toxicity of these metabolites to human leukocytes, Mol. Pharmacol. 53 (1998) 991–998.

[61] J.L. Maggs, D. Williams, M. Pirmohamed, B.K. Park, The metabolic formation of reactive intermediates from clozapine, a drug associated with agranulocytosis in man, J. Pharmacol. Exp. Ther. 275 (1995) 1463–1475.

[62] M. Pirmohamed, D. Williams, S. Madden, E. Templeton, B.K. Park, Metabolism and bioactivation of clozapine by human liver *in vitro*, J. Pharmacol. Exp. Ther. 272 (1995) 984–990.

[63] D.P. Williams, M. Pirmohamed, D.J. Naisbitt, J.L. Maggs, B.K. Park, Neutrophil cytotoxicity of the chemically reactive metabolite(s) of clozapine: Possible role in agranulocytosis, J. Pharmacol. Exp. Ther. 283 (1997) 1375–1382.

[64] D.P. Williams, M. Pirmohamed, D.J. Naisbitt, J.P. Uetrecht, B.K. Park, Induction of metabolism-dependent and -independent neutrophil apoptosis by clozapine, Mol. Pharmacol. 58 (2000) 207–216.

[65] M. Haria, A. Fitton, D. McTavish, Trazodone. A review of its pharmacology, therapeutic use in depression and therapeutic potential in other disorders, Drugs Aging 4 (1994) 331–355.

[66] A.G. Chu, B.L. Gunsolly, R.W. Summers, B. Alexander, C. McChesney, V.L. Tanna, Trazodone and liver toxicity, Ann. Intern. Med. 99 (1983) 128–129.

[67] G.F. Longstreth, J. Hershman, Trazodone-induced hepatotoxicity and leukonychia, J. Am. Acad. Dermatol. 13 (1985) 149–150.

[68] P.L. Beck, R.J. Bridges, D.J. Demetrick, J.K. Kelly, S.S. Lee, Chronic active hepatitis associated with trazodone therapy, Ann. Intern. Med. 118 (1993) 791–792.

[69] M. Hull, R. Jones, M. Bendall, Fatal hepatic necrosis associated with trazodone and neuroleptic drugs, Br. Med. J. 309 (1994) 378.

[70] N.F. Fernandes, R.R. Martin, S. Schenker, Trazodone-induced hepatotoxicity: A case report with comments on drug-induced hepatotoxicity, Am. J. Gastroenterol. 95 (2000) 532–535.

[71] K.S. Rettman, C. McClintock, Hepatotoxicity after short-term trazodone therapy, Ann. Pharmacother. 35 (2001) 1559–1561.

[72] L. Baiocchi, A. Frigerio, M. Giannangeli, G. Palazzo, Basic metabolites of trazodone in humans, Arzneimittelforschung 24 (1974) 1699–1706.

[73] C. Yamato, T. Takahashi, T. Fujita, Studies on metabolism of trazodone. III Species differences, Xenobiotica 6 (1976) 295–306.

[74] C. Yamato, T. Takahashi, T. Fujita, Studies on metabolism of trazodone. I. Metabolic fate of (14C)trazodone hydrochloride in rats, Xenobiotica 4 (1974) 313–326.

[75] R. Jauch, Z. Kopitar, A. Prox, A. Zimmer, [Pharmacokinetics and metabolism of trazodone in man (author's transl)], Arzneimittelforschung 26 (1976) 2084–2089.

[76] A.S. Kalgutkar, K.R. Henne, M.E. Lame, A.D. Vaz, C. Collin, J.R. Soglia, S.X. Zhao, C.E. Hop, Metabolic activation of the nontricyclic antidepressant trazodone to electrophilic quinone-imine and epoxide intermediates in human liver microsomes and recombinant P4503A4, Chem. Biol. Interact. 155 (2005) 10–20.

[77] Z. Yan, J. Li, N. Huebert, G.W. Caldwell, Y. Du, H. Zhong, Detection of a novel reactive metabolite of diclofenac: Evidence for CYP2C9-mediated bioactivation via arene oxides, Drug Metab. Dispos. 33 (2005) 706–713.

[78] M.L. Crismon, M. Trivedi, T.A. Pigott, A.J. Rush, R.M. Hirschfeld, D.A. Kahn, C. DeBattista, J.C. Nelson, A.A. Nierenberg, H.A. Sackeim, M.E. Thase, The Texas medication algorithm project: Report of the Texas consensus conference panel on medication treatment of major depressive disorder, J. Clin. Psychiatry 60 (1999) 142–156.

[79] G.T. Tucker, Advances in understanding drug metabolism and its contribution to variability in patient response, Ther Drug Monit 22 (2000) 110–113.

[80] R.W. Biagi, B.N. Bapat, Intrahepatic obstructive jaundice from amitriptyline, Br. J. Psychiatry 113 (1967) 1113–1114.

[81] M.L. Cunningham, Acute hepatic necrosis following treatment with amitriptyline and diazepam, Br. J. Psychiatry 111 (1965) 1107–1109.

[82] D.H. Morgan, Jaundice associated with amitriptyline, Br. J. Psychiatry 115 (1969) 105–106.

[83] A.T. Lebre, P.P. Prado, E.S. Yonamine, Z. Rasslan, J.C. Bonadia, C.A. Lima, Severe bradyarrythmia induced by tricyclic antidepressants in an elderly patient, Rev. Assoc. Med. Bras 41 (1995) 271–273.

[84] G. Danan, J. Bernuau, X. Moullot, C. Degott, D. Pessayre, Amitriptyline-induced fulminant hepatitis, Digestion 30 (1984) 179–184.

[85] D. De Craemer, I. Kerckaert, F. Roels, Hepatocellular peroxisomes in human alcoholic and drug-induced hepatitis: A quantitative study, Hepatology 14 (1991) 811–817.

[86] J. Yon, S. Anuras, Hepatitis caused by amitriptyline therapy, J. Am. Med. Assoc. 232 (1975) 833–834.

[87] C. Berkelhammer, N. Kher, C. Berry, A. Largosa, Nortriptyline-induced fulminant hepatic failure, J. Clin. Gastroenterol. 20 (1995) 54–56.

[88] A.M. Pedersen, H.K. Enevoldsen, Nortriptyline-induced hepatic failure, Ther. Drug Monit. 18 (1996) 100–102.

[89] U. Breyer-Pfaff, The metabolic fate of amitriptyline, nortriptyline and amitriptylin-oxide in man, Drug Metab. Rev. 36 (2004) 723–746.

[90] K. Venkatakrishnan, J. Schmider, J.S. Harmatz, B.L. Ehrenberg, L.L. von Moltke, J.A. Graf, P. Mertzanis, K.E. Corbett, M.C. Rodriguez, R.I. Shader, D.J. Greenblatt, Relative contribution of CYP3A to amitriptyline clearance in humans: *in vitro* and *in vivo* studies, J. Clin. Pharmacol. 41 (2001) 1043–1054.

[91] A. Prox, U. Breyer-Pfaff, Amitriptyline metabolites in human urine. Identification of phenols, dihydrodiols, glycols, and ketones, Drug Metab. Dispos. 15 (1987) 890–896.

[92] S.R. Biggs, L.F. Chasseaud, D.R. Hawkins, I. Midgley, Determination of amitriptyline and its major basic metabolites in human urine by high-performance liquid chromatography, Drug Metab. Dispos. 7 (1979) 233–236.

[93] J. Schmider, D.J. Greenblatt, L.L. von Moltke, J.S. Harmatz, R.I. Shader, N-demethylation of amitriptyline in vitro: Role of cytochrome P-450 3A (CYP3A) isoforms and effect of metabolic inhibitors, J. Pharmacol. Exp. Ther. 275 (1995) 592–597.

[94] B. Wen, L. Ma, M. Zhu, Bioactivation of the tricyclic antidepressant amitriptyline and its metabolites nortriptyline to arene oxide intermediates in human liver microsomes and recombinant P450s, Chem. Biol. Interact. 173 (2008) 59-67.

[95] L. Ma, B. Wen, Q. Ruan, M. Zhu, Rapid screening of glutathione-trapped reactive metabolites by linear ion trap mass spectrometry with isotope pattern-dependent scanning and postacquisition data mining, Chem. Res. Toxicol. 7 (2008) 1477-1483.

[96] Z. Yan, N. Maher, R. Torres, N. Huebert, Use of a trapping agent for simultaneous capturing and high-throughput screening of both ''soft'' and ''hard'' reactive metabolites, Anal. Chem. 79 (2007) 4206-4214.

[97] B. Wen, W.L. Fitch, Screening and characterization of reactive metabolites using glutathione ethyl ester in combination with Q-trap mass spectrometry, J. Mass. Spectrom. 44 (2009) 90-100.

[98] J. Gan, Q. Ruan, B. He, M. Zhu, W.C. Shyu, W.G. Humphreys, In vitro screening of 50 highly prescribed drugs for thiol adduct formation comparison of potential for drug-induced toxicity and extent of adduct formation, Chem. Res. Toxicol. (2009) [Epub ahead of print].

[99] B. Wen, K.J. Coe, P. Rademacher, W.L. Fitch, M. Monshouwer, S.D. Nelson, Comparison of in vitro bioactivation of flutamide and its cyano analogue: Evidence for reductive activation by human NADPH: Cytochrome P450 reductase, Chem. Res. Toxicol. 21 (2008) 2393–2406.

Molecular Aspects of Neurotoxins in Dopaminergic Neurons

Juan Segura-Aguilar*

Contents

1. Neurodegeneration of Dopaminergic Neurons

In Parkinson's disease (PD), the dopaminergic neurons containing neuromelanin, which are localized in nigro-striatal system, are lost during the neurodegenerative process. An important feature of this neurodegenerative process of dopaminergic neurons in PD is the fact that this process is very slow, taking years before the symptoms appear when the majority of dopaminergic neurons are lost from the nigro–striatal system. The disease develops very slowly, and patients live with this disease for ~10–25 years. These data contrast with the fact that MPTP is able to induce a pure and severe Parkinsonian syndrome in only a few days, as has been observed in American drug addicts who injected synthetic drugs contaminated with MPTP [1]. The rapid action of MPTP demonstrates that exogenous neurotoxins with high specificity to dopaminergic neurons are able to induce an extensive neurodegenerative process in dopaminergic neurons in a very short time. Therefore, the neurotoxin responsible for the neurodegenerative processes in PD can not be of exogenous origin since

* Molecular and Clinical Pharmacology, ICBM, Faculty of Medicine, Casilla 70000, Santiago-7, Chile;
  Tel.: +56 2 678 6057; Fax: +56 2 737 2783
  Email: jsegura@med.uchile.cl

the neurodegeneration in PD is very slow and takes years. The main question is why does it take years to degenerate dopaminergic neurons in PD when exogenous neurotoxins such as MPTP take only a few days? The neurodegenerative action of MPTP is rapid because a high concentration is injected directly into the blood, which crosses the blood–brain barrier and is taken up into astrocytes where MAO-B converts MPTP to MPP^+ (Figure 1). MPP^+ has a high affinity for the dopamine transporter (DAT), resulting in its accumulation in dopaminergic neurons and the induction of an extensive degeneration of dopaminergic neurons. However, the slow neurodegenerative process in PD probably depends on the action of an endogenous neurotoxin, where the degeneration is localized to one or a few neurons, taking years to induce symptoms.

2. 6-HYDROXYDOPAMINE NEUROTOXIN

6-Hydroxydopamine was the first highly selective neurotoxin for catecholaminergic neurons, and its selectivity of action was dependent on the fact that 6-hydroxydopamine has high affinity for the norepinephrine and DAT [2].
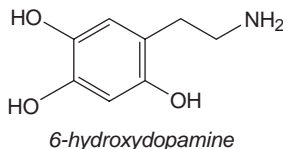
6-hydroxydopamine

Unilateral 6-hydroxydopamine-lesioned rats circle in the direction of the lesion, while dopamine agonists produce contralateral turning—due to the development of D_2 receptor super sensitization on the lessened side [3–7]. The neurotoxin 6-hydroxydopamine has been a valuable tool used to investigate motor and biochemical dysfunctions in PD [8–11]. However, the problem with using 6-hydroxydopamine as a model neurotoxin in preclinical studies to understand the neurodegeneration in PD is that it is an exogenous neurotoxin. Thus, despite its ability to destroy dopaminergic neurons, it is not known whether the same neurotoxic events induced by 6-hydroxydopamine occur in the neurodegenerative process in PD.

It has been suggested that the molecular neurotoxic action of 6-hydroxydopamine involves:

i.   Oxidative stress due to its high reactivity with oxygen since 6-hydroxydopamine oxidizes to 6-hydroxydopamine semiquinone radical, which then autoxidizes to 6-hydroxydopamine quinone(s) by reducing two molecules of dioxygen to superoxide radicals (Figure 2). Superoxide
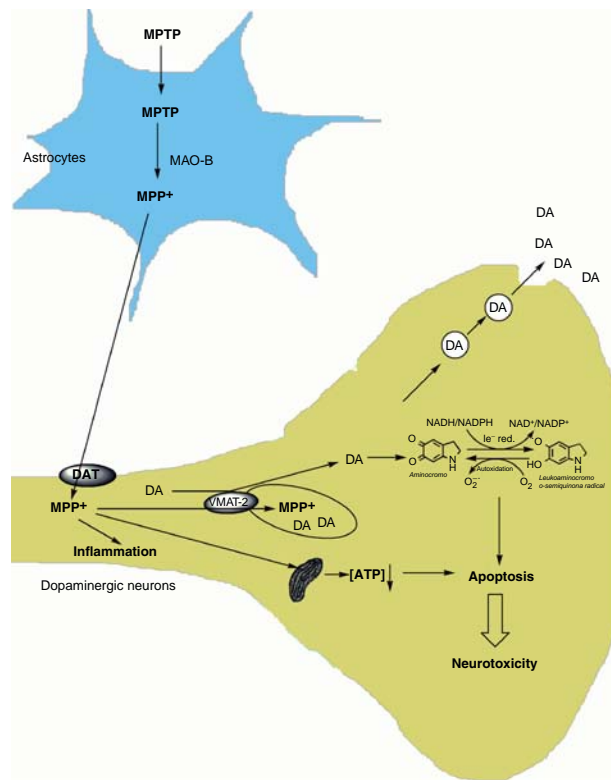
Figure 1 Possible mechanism for MPTP-induced neurotoxicity in dopaminergic neurons. MPTP is metabolized by MAO-B in the astrocytes to MPP^+, which is taken up into dopaminergic neurons and monoaminergic vesicles by dopamine transporter (DAT) and VMAT-2, respectively. MPP^+ induces inflammation and inhibits complex I of mitochondria, resulting in ATP depletion required for cell function. The concentration of cytosolic dopamine increases by competing with dopamine due to the high affinity of MPP^+ for VMAT-2, and in addition, MPP^+ decreases the expression of VMAT-2. Cytosolic dopamine is oxidized to aminochrome which can be one-electron reduced to a leukoaminochrome o-semiquinone radical, which is highly toxic.
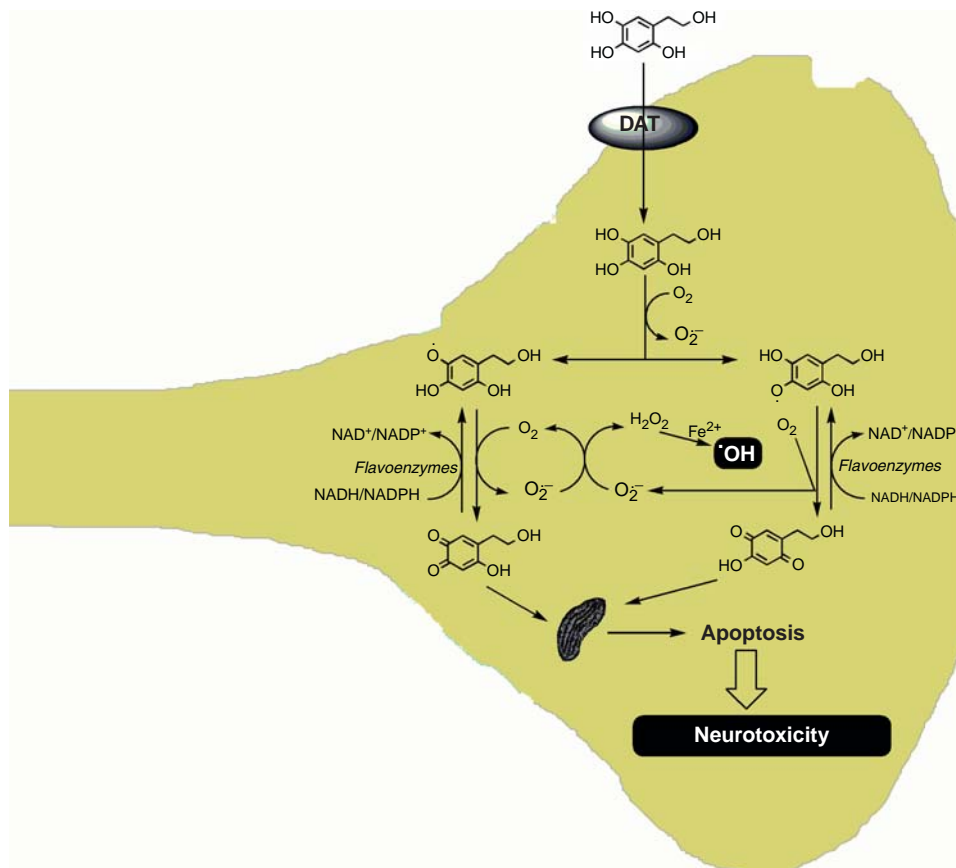
Figure 2 Possible mechanism for 6-hydroxydomaine-induced neurotoxicity in dopaminergic neurons. 6-Hydroxydopamine is taken up by DAT and oxidized by reducing dioxygen to superoxide radicals, generating 6-hydroxydopamine semiquinone radical. A new oxidation of 6-hydroxydopamine semiquinone radical to 6-hydroxydopamine quinone produces a new superoxide molecule, which dismutates to hydrogen

radicals, spontaneously or enzymatically produced by superoxide dismutase, generate hydrogen peroxide, which is the precursor of hydroxyl radicals [12]. However, hydrogen peroxide can also be formed by 6-hydroxydopamine oxidation catalyzed by monoamine oxidase–A [13]. The formation of reactive oxygen species is potentiated by the redox cycling generated between the one-electron reduction of 6-hydroxydopamine quinone to its corresponding semiquinone radical, which directly oxidizes to the 6-hydroxydopamine quinone. This redox cycling will continue until NADH, which is required for energy production, or NADPH, which is required for the biosynthesis and reduction of oxidized glutathione catalyzed by glutathione reductase, is depleted or all oxygen is reduced to superoxide radicals (Figure 2). 6-Hydroxydopamine is oxidized to quinone species, which then attack endocellular nucleophilic groups [14,15]. The increase in the levels of reactive species induced by 6-hydroxydopamine, resulting in the depletion of endocellular antioxidant, potentiates its neurotoxic effects in dopaminergic neurons. Antioxidant agents attenuate 6-hydroxydopamine–induced neurotoxicity [12,16–19], and the overexpression of superoxide dismutase and glutathione peroxidase reduce 6-hydroxydopamine neurotoxicity [20–23]. Compounds related to the nitrone spin trap α-phenyl–N-tert-butylnitrone (PBN) inhibit 6-hydroxydopamine–induced lipid peroxidation and protein carbonylation [24].

ii. Another neurotoxic action of 6-hydroxydopamine is to alter mitochondrial function by inhibiting complex I in isolated brain mitochondria [25]. However, the inhibition of complex I was not dependent on oxidative stress due to the lack of effect of antioxidants [26]. It seems plausible that the lack of effect of antioxidants on 6-hydroxydopamine inhibition on complex I is dependent on the ability of 6-hydroxydopamine quinones to form adducts with mitochondrial proteins. 6-Hydroxydopamine induces profound mitochondrial fragmentation, and silencing of DLP1/Drp1, which is involved in mitochondrial and peroxisomal fission, by siRNA prevented 6-hydroxydopamine–induced fragmentation of mitochondria [27].

iii. The oxidative stress evoked by low concentrations of 6-hydroxydopamine was selective for dopaminergic neurons in culture and fully dependent on COX–2 activity [28]. The EP1 antagonists completely prevented the 40–50% loss of dopaminergic neurons caused by

peroxide. In the presence of reduced iron, hydrogen peroxide is converted to hydroxyl radicals. One-electron reduction of 6-hydroxydopamine to 6-hydroxydopamine semiquinone gererates a redox cycling, which potentiates the formation of superoxide and hydroxyl radicals. Hydroxyl radicals and 6-hydroxydopamine quinones disrupt mitochondrial function, which induces apoptosis and cell death.

exposure to 6-hydroxydopamine [29]. These data suggest that Prosta-glandin E(2) activation of EP1 receptors may be the mediator of 6-hydroxydopamine's neurotoxic action.

iv. 6-Hydroxydopamine activates the apoptosis pathway through the p38 mitogen-activated protein kinase (MAPK)-mediated, p53-independent activation of Bax and p53 upregulated modulator of apoptosis (PUMA) [30]. 6-Hydroxydopamine induces an increase in caspase-3 activity and cytochrome c translocation into the cytosol from mitochondria in three ways: decreasing the Bax/Bcl-2 ratio, activating c-Jun N-terminal kinase, and activating protein kinase C [31]. The toxicity of 6-hydroxydopamine was mediated through the generation of reactive oxygen species and was accompanied by a large increase in phosphorylated ERK1/2 [32]. The rapid activation of ERK1/2 in dopaminergic cells by oxidative stress serves as a self-protective response, reducing the content of reactive oxygen species and caspase-3 activity and increasing downstream ERK1/2 sub-strates [33]. 6-Hydroxydopamine induces caspase 3-dependent PKCδ proteolytic activation in the cell bodies of the substantia nigra pars compact, implicating this kinase in the neurodegenerative process [34]. α-Lipoic acid suppressed 6-hydroxydopamine-induced apoptosis through an increase in cellular glutathione through the stimulation of the glutathione (GSH) synthesis system but not by the expression of heme oxygenase-1 [35].

3. MPTP Neurotoxin

The finding that American drug addicts developed marked parkinson-ism after using an illicit intravenous drug containing MPTP opened a new line of study using this exogenous neurotoxin as a preclinical experimental model [36].
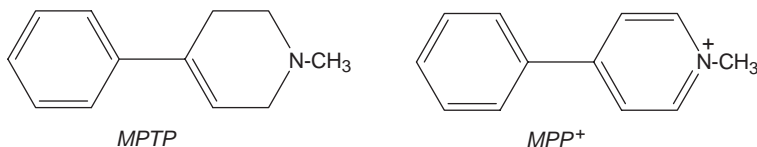
MPTP is a selective dopaminergic proneurotoxin that crosses the blood–brain barrier, and it is converted by monoamine oxidase-B in the astrocytes to MPP$^+$ (1-methyl-4-phenyl-1,2,3,6-tetrahydropyridinium ion), the active neurotoxic metabolite of MPTP (Figure 1). MPP$^+$, with high selec-tive affinity for the DAT, is largely accumulated in DA nerves and inhibits complex I of the mitochondrial respiratory chain [37]. This interferes with energy production, which adversely affects cellular function, leading to a

disruption in Ca^{2+} homeostasis and further adverse effects that lead to neurotoxicity. MPTP produces irreversible parkinsonism in primates, including humans. Additionally, hydroxyl radical is a likely mediator of MPTP/MPP$^+$ since acetyl-L-carnitine attenuates neurotoxicity by reducing hydroxyl radicals as well as xanthine oxidase-generated uric acid [38].

MPP$^+$ has been shown to be taken up into dopaminergic neurons through the plasma membrane DAT as well as into catecholamine storage vesicles through the granule vesicular monoamine transporter (VMAT) [39]. MPP$^+$ is one of the most potent dopamine-releasing agents. MPP$^+$ perfusion into the striatum increases extracellular dopamine levels [39,40]. The sustained elevation of dopamine in the extracellular fluid elicited by MPTP may result in dopamine oxidation with concomitant formation of hydroxyl radicals [41,42]. MPTP significantly decreases VMAT-2 expression, resulting in an increase in cytosolic dopamine and its autoxidation to aminochrome [43,44]. The toxic effect of MPP$^+$ is potentiated by inhibition of the enzyme DT-diaphorase in the presence of dicoumarol, and it appears that dopamine oxidation to aminochrome is a major mechanism by which MPP$^+$ exerts toxicity [45].

Studies done with COX-2-deficient mice revealed that the loss of COX-2 activity reduces MPTP-induced damage to the dopaminergic neurons of the sunstantia nigra but that it does not alter the levels of dopamine and its metabolites in the striatum [46]. The reduction of COX-2 activity mitigates the secondary and progressive loss of dopaminergic neurons, as well as the motor deficits induced by MPTP [47]. Experiments done with insulin-like growth factor-1R(+/−) mice showed a dramatically increased neuroinflammatory response to MPTP. MPTP induced more severe lesions of dopaminergic neurons of the substantia nigra in Insulin-like growth factor-1R(+/−) mice than in wild-type animals [48]. In the MPTP mouse model, MK2-deficient mice show a reduced neuroinflammation and less degeneration of dopaminergic neurons in the substantia nigra after MPTP lesion compared with wild-type mice [49]. Myeloperoxidase, a key oxidant-producing enzyme during inflammation, is upregulated in the ventral midbrain of MPTP mice [50]. Anti-inflammatory drugs such as celecoxib and pioglitazone decreased inflammation and restored mitochondrial function in rats intrastriatally injected with lipopolysaccharide [51].

It has been shown that the Jun-N-terminal kinase (JNK) pathway is a major mediator of MPTP-induced neurotoxicity [52,53]. MPP$^+$ induced not only an activator of c-Jun but also an early and robust stimulator of caspase-9 in the midbrain of rats [54]. MPTP induces caspase-3 and caspase-8 activation in mice cerebellar granule neurons [55]. Compound FLZ, a synthetic derivative of natural squamosamide, inhibited the MPP$^+$-induced release of cytochrome c, apoptosis-inducing factor and the activation of caspase 3 in SH-SY5Y cells [56]. Nucling is a novel type of apoptosis-associated molecule, essential for cytochrome c, apoptosis protease activating factor 1, pro-caspase-9 apoptosome induction, and caspase-9 activation

following proapoptotic stress. Interestingly, Nucling-deficient mice treated with MPTP did not exhibit locomotor dysfunction in an open-field test. The substantia nigra dopaminergic neurons of Nucling-deficient mice were resistant to the damaging effects of the neurotoxin MPTP [57]. MPP^+-induced apoptosis in MES23.5 cells involves DMT1-dependent iron influx and mitochondria dysfunction [58]. MPP^+-induced increases caspase-3 enzymatic activity, DNA fragmentation, and apoptotic cell death, which is inhibited by NADPH oxidase inhibitors [59]. Ultrastructural details of the nucleus under transmission electron microscopy confirmed a distorted nuclear organization with shrunken or condensed nuclei and a disrupted nuclear membrane, which is typical of a nucleus undergoing apoptosis, in rats with unilateral intranigral infusion of MPP^+ [60]. Blockage of glycogen synthase kinase-3β activity by its two specific inhibitors, indirubin-$3'$-oxime and AR-A014418, prevented dopaminergic neurons from undergoing MPTP-induced apoptosis [61]. α-Lipoic acid, a thiol antioxidant, abolished the activation of apoptosis signal regulating kinase (ASK1) and phosphorylation of downstream kinases, MKK4, and JNK, and it also prevented the down-regulation of DJ-1 and translocation of Daxx to the cytosol induced by MPTP [62]. Glial cell line-derived neurotrophic factor protects tyrosine hydroxylase-positive neurons derived from human embryonic stem cells against MPP(+)-induced apoptotic cell death [63]. A possible role for calpain in the mechanism of motorneuron apoptosis induced by MPTP has been suggested [64]. MPTP-induced conversion of the cdk5 activator p35 to a pathogenic p25 form is dependent on calpain activity *in vivo* [65].

4. Aminochrome as Endogenous Neurotoxin

Dopamine in dopaminergic neurons is efficiently incorporated into vesicles by VMAT-2 for neuronal transmission or storage. The low pH inside of the vesicles prevents oxidation of the catechol structure of dopamine to the *o*-quinone aminochrome. However, the protons of dopamine hydroxyl group are dissociated at physiological pH in the cytosol of dopaminergic neurons, and oxygen catalyzes dopamine oxidation to dopamine *o*-quinone, which automatically cyclizes in several steps to aminochrome at this pH.
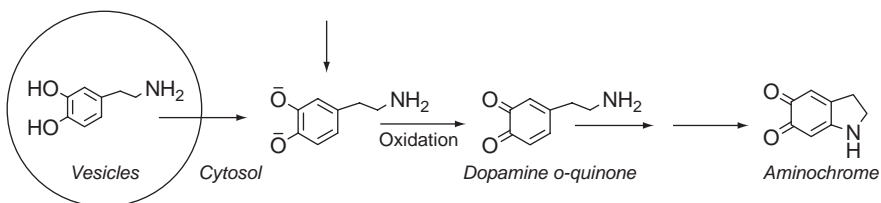
Aminochrome in the cell has the following alternative pathways: (i) Aminochrome can polymerize to neuromelanin, which seems to be a normal process (Figure 3). The evidence that oxidation of dopamine to aminochrome indeed occurs in the brain *in vivo* is the existence of neuromelanin in human substantia nigra, which also accumulates with age [66]. Neuromelanin is able to chelate metals [67,68] and bind proteins. α-Synuclein was detected in neuromelanina of PD patients and controls after cleavage of the melanin backbone under solubilizing conditions [69]. It is important to remember that neuromelanin containing cells are not degenerated in control human substantia nigra, which suggests that neuromelanin formation itself is not a neurotoxic pathway. However, studies *in vitro* with SH–SY5Y cells showed that neuromelanin selectively induced apoptosis by deglutathionylation in mitochondria [70]. (ii) Aminochrome forms adducts with proteins, such as α-synuclein by inhibiting its fibrillization and enhancing and stabilizing its protofibril formation [71,72]. α-Synuclein oligomerization into cytotoxic protofibrils seems to be essential for its neurotoxic effects [71]. Aminochrome is also able to form adducts with proteins, thereby inactivating enzymes (Figure 3, reaction 2). Dopamine *o*–quinone, which binds covalently to nucleophilic sulfhydryl groups on protein cysteinyl residues, has been reported to modify and inactivate tyrosine hydroxylase, human DAT, and parkin [73–75]. It is important to note that the amino chain of dopamine *o*-quinone cyclizes spontaneously at physiological pH generating aminochrome. Aminochrome was also found to inhibit the proteasome [76]. (iii) One–electron-reduction of aminochrome catalyzed by flavoenzymes. Aminochrome can be reduced by one–electron to leukoaminochrome-*o*–semiquinone radical, which is extremely reactive with oxygen, autoxidizing with the generation of a redox cycling between aminochrome and leukoaminochrome *o*-semiquinone radical (Figure 3) [77,78]. This redox cycling is initiated by one–electron reduction of aminochrome and catalyzed by flavoenzymes using NADH or NADPH, and it is extremely rapid and potent, producing acute neurotoxicity. This redox cycling results in (a) the depletion of NADH, which is required for ATP synthesis in the mitochondria; (b) depletion of NADPH required by glutathione reductase to keep GSH in the reduced state necessary to exert its antioxidant action; (c) depletion of oxygen, required for ATP synthesis in the mitochondria; (d) formation of superoxide radicals, which spontaneously or enzymatically generate hydrogen peroxide, the precursor of hydroxyl radicals. Leucoaminochrome *o*-semiquinone radical is highly neurotoxic in cells and rats, and it has been proposed as a endogenous neurotoxin that induces neurodegeneration of dopaminergic neurons in PD [79–85]; and (iv) Aminochrome can be reduced with two-electron to leukoaminochrome catalyzed by DT-diaphorase (Figure 3). This reaction prevents the formation of leucoaminochrome *o*-semiquinone radical during one-electron reduction of aminochrome [77–80,83,86]. DT-diaphorase (EC.1.6.99.2) is the unique flavoenzyme, which catalyzes the two-electron reduction of quinones to
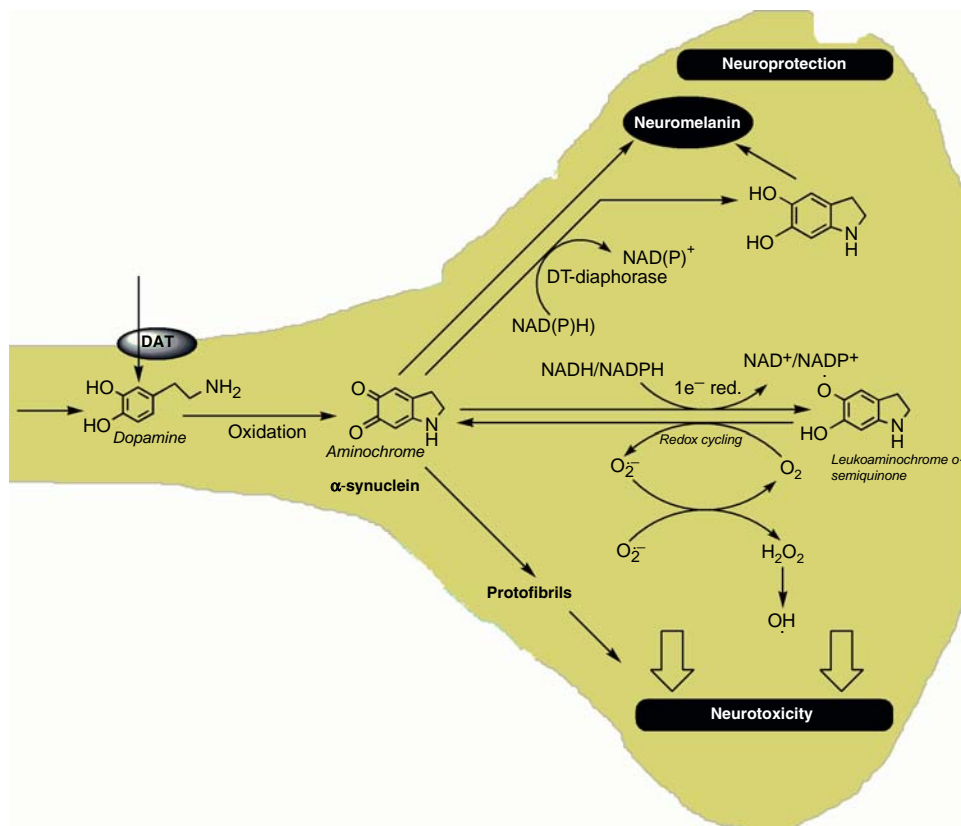
Figure 3 Possible mechanism for aminochrome-induced neurotoxicity in dopaminergic neurons. At physiological pH, dopamine hydroxyl protons are dissociated, and dopamine is oxidized to aminochrome. Aminochrome is able to participate in four different reactions, which can be divided in two neuroprotective reactions (i) and (ii) and two neurotoxic reactions (iii) and (iv). (i) Aminochrome polymerizes to neuromelanin,

hydroquinones and which can use both NADH and NADPH as electron donators. DT–diaphorase immunoreactivity colocalized with tyrosine hydroxylase-like immunoreactivity has been found in neurons of substantia nigra and ventral tegmental area [87]. Interestingly, DT–diaphorase prevents aminochrome neurotoxic actions such as the one–electron reduction of aminochrome [79,80,83,85] and the formation of α–synuclein protofribrils [88].

5. NEUROTOXIN ELECTION TO USE IN PRECLINICAL PARKINSONISM

The lack of success founding elucidating the molecular mechanism(s) in the degenerative process in PD opens the question of whether the preclinical experimental models are suitable for understanding what happens in the degeneration of neuromelanin containing dopaminergic neurons in this disease. The neurodegeneration of neuromelanin containing dopaminergic neurons in PD seems to be a slow progressive process where the symptoms are present only when the majority of dopaminergic neurons are degenerated. This slow degenerative process contrasts with the extremely rapid action of MPTP, which induces parkinsonism in only 3 days [1]. Perhaps the problem with the preclinical experimental models (MPTP or 6-hydroxydopamine) used to investigate the mechanism(s) of the neurodegenerative processes in PD is that they are exogenous neurotoxins, unable to mimic what happens in idiopathic PD. Both neurotoxins have been very useful in understanding cell death mechanisms in dopaminergic neurons where mitochondrial dysfunction seems to be a common feature of both neurotoxins. However, the question is the identity of the neurotoxin that induces mitochondrial dysfunction and where this neurotoxin is acting in the mitochondria. I propose aminochrome as model neurotoxin to study the neurodegenerative processes occurring in neuromelanin containing dopaminergic neurons in PD since (i) Aminochrome is an endogenous metabolite of dopamine oxidation, (ii) Aminochrome is the precursor of

and it is known that healthy people have their melanin-containing dopaminergic neurons intact; (ii) Aminochrome can be two-electron reduced to leukoaminochrome which also forms neuromelanin. This reaction is only catalyzed by DT-diaphorase; (iii) Aminochrome forms adducts with α-synuclein, inhibiting α-synuclein fibrillization and enhancing and stabilizing the formation of neurotoxic protofibrils; and (iv) Aminochrome can be one-electron reduced to leukoaminochrome-*o*-semiquinone radical, which is extremely reactive with oxygen, undergoing autoxidizion with the generation of a redox cycling between aminochrome and leukoaminochrome *o*-semiquinone radical. This redox cycling will continue until NADH, NADPH, or dioxygen are depleted.

neuromelanin, (iii) This model is focused on melanin containing neurons that are lost in the substantia nigra in PD, and (iv) The formation and stabilization of α-synuclein protofibrils in sporadic PD is dependent on aminochrome. Aminochrome induces neurotoxicity under certain aberrant conditions, such as the one-electron reduction of aminochrome catalyzed by flavoenzymes to leukoaminochrome o-semiquinone radical, which is a highly reactive neurotoxin. Aminochrome also induces neurotoxicity through the formation of adducts with α-synuclein, which enhances and stabilizes the formation of neurotoxic protofibrils.

ACKNOWLEDGMENT

REFERENCES

[1] A. Williams, MPTP parkinsonism, Br. Med. J. 289 (1984) 1401–1402.

[2] P. Redman, B.S. Jefferson, C.B. Ziegler, O.V. Mortensen, G.E. Torres, E.S. Levitan, E. Aizenman, A vital role for voltage-dependent potassium channels in dopamine transporter-mediated 6-hydroxydopamine neurotoxicity, Neuroscience 143 (2006) 1–6.

[3] U. Ungerstedt, Post synaptic supersensitivity after 6-hydroxydopamine induced degeneration of the nigrostriatal dopamine system, Acta Physiol. Scand. 367 (1971) 69–93.

[4] J.F. Marshall, U. Ungerstedt, Supersensitivity to apomorphine following destruction of the ascending dopamine neurons: Quantification using the rotational model, Eur. J. Pharmacol. 41 (1977) 361–367.

[5] T. Archer, T. Palomo, R. McArthur, A. Fredriksson, Effects of acute administration of DA agonists on locomotor activity: MPTP versus neonatal intracerebroventricular 6-OHDA treatment, Neurotox. Res. 5 (2003) 95–110.

[6] K. Berger, S. Przedborski, J.L. Cadet, Retrograde degeneration of nigrostriatal neurons induced by intrastriatal 6-hydroxydopamine injection in rats, Brain Res. Bull. 26 (1990) 301–307.

[7] B. Costall, C.D. Marsden, R.J. Naylor, C.J. Pycock, Proceedings: Differences in circling responses following electrolytic and 6-hydroxydopamine lesions of the nigro-striatal pathway, Br. J. Pharmacol. 55 (1975) 289P–290P.

[8] N. Simola, M. Morelli, A.R. Carta, The 6-hydroxydopamine model of Parkinson's disease, Neurotox. Res. 11 (2007) 151–167.

[9] I. Mocchetti, A. Bachis, R.L. Nosheny, G. Tanda, Brain–derived neurotrophic factor expression in the substantia nigra does not change after lesions of dopaminergic neurons, Neurotox. Res. 12 (2007) 135–143.

[10] A.B. Manning-Bog, J.W. Langston, Model fusion, the next phase in developing animal models for Parkinson's disease, Neurotox. Res. 11 (2007) 219–240.

[11] M. Herrera-Marschitz, D. Bustamante, P. Morales, M. Goiny, Exploring neurocircuitries of the basal ganglia by intracerebral administration of selective neurotoxins, Neurotox. Res. 11 (2007) 169–182.

[12] J.L. Cadet, C. Brannock, Free radicals and the pathobiology of brain dopamine systems, Neurochem. Int. 32 (1989) 117–131.

[13] G. Cohen, Oxy-radical toxicity in catecholamine neurons, Neurotoxicology 5 (1984) 77–82.

[14] A. Padiglia, R. Medda, A. Lorrai, G. Biggio, E. Sanna, G. Floris, Modulation of 6-hydroxydopamine oxidation by various proteins, Biochem. Pharmacol. 53 (1997) 1065–1068.

[15] A. Palumbo, Napolitano, P. Barone, M. d'Ischia, Nitrite- and peroxide-dependent oxidation pathways of dopamine: 6-nitrodopamine and 6-hydroxydopamine formation as potential contributory mechanisms of oxidative stress- and nitric oxide-induced neurotoxicity in neuronal degeneration, Chem. Res. Toxicol. 12 (1999) 1213–1222.

[16] R. Soto-Otero, E. Mendez-AAlvarez, A. Hermida-Ameijeiras, A.M. Munoz-Patino, J.L. Labandeira-Garcia, Autoxidation and neurotoxicity of 6-hydroxydopamine in the presence of some antioxidants: Potential implication in relation to the pathogenesis of Parkinson's disease, J. Neurochem. 74 (2000) 1605–1612.

[17] V. Zbarsky, K.P. Datla, S. Parkar, D. Kl Rai, O.I. Aruoma, D.T. Dexter, Neuroprotective properties of the natural phenolic antioxidants curcumin and naringenin but not quercetin and fisetin in a 6-OHDA model of Parkinson's disease, Free Radic. Res. 39 (2005) 1119–1125.

[18] E.C. Stack, J.L. Ferro, J. Kim, S.J. Del Signore, S. Goodrich, S. Matson, B.B. Hunt, K. Cormier, K. Smith, W.R. Matson, H. Ryu, R.J. Ferrante, Therapeutic attenuation of mitochondrial dysfunction and oxidative stress in neurotoxin models of Parkinson's disease, Biochim. Biophys. Acta 1782 (2008) 151–162.

[19] L.L. Tian, Z. Zhou, Q. Zhang, Y.N. Sun, C.R. Li, C.H. Cheng, Z.Y. Zhong, S.Q. Wang, Protective effect of (+/−) isoborneol against 6-OHDA-induced apoptosis in SH–SY5Y cells, Cell Physiol. Biochem. 20 (2007) 1019–1032.

[20] E. Pileblad, T. Magnusson, B. Fornstedt, Reduction of brain glutathione by L-buthionine sulfoximine potentiates the dopamine-depleting action of 6-hydroxydopamine in rat striatum, J. Neurochem. 52 (1989) 978–980.

[21] M. Asanuma, H. Hirata, J.L. Cadet, Attenuation of 6-hydroxydopamine-induced dopaminergic nigros–triatal lesions in superoxide dismutase transgenic mice, Neuroscience 85 (1998) 907–917.

[22] J. Callio, T.D. Oury, C.T. Chu, Manganese superoxide dismutase protects against 6-hydroxydopamine injury in mouse brains, J. Biol. Chem. 280 (2005) 18536–18542.

[23] J.L. Ridet, J.C. Bensadoun, N. Deglon, P. Aebischer, A.D. Zurn, Lentivirus-mediated expression of glutathione peroxidase: Neuroprotection in murine models of Parkinson's disease, Neurobiol. Dis. 21 (2006) 29–34.

[24] R. Soto-Otero, E. Méndez-Alvarez, S. Sánchez-Iglesias, F.I. Zubkov, L.G. Voskressensky, A.V. Varlamov, M. de Candia, C. Altomare, Inhibition of 6-hydroxydopamine-induced inhibition of 6-hydroxydopamine-induced oxidative damage by 4,5-dihydro-3H-2-benzazepine N-oxides, Biochem. Pharmacol. 75 (2008) 1526–1537.

[25] Y. Glinka, M.B. Youdim, Inhibition of mitochondrial complexes I and IV by 6-hydroxydopamine, Eur. J. Pharmacol. 292 (1995) 329–332.

[26] Y. Glinka, K.F. Tipton, M.B. Youdim, Nature of inhibition of mitochondrial respiratory complex I by 6-hydroxydopamine, J. Neurochem. 66 (1996) 2004–2010.

[27] M. Gomez-Lazaro, N.A. Bonekamp, M.F. Galindo, J. Jordán, M. Schrader, 6-Hydroxydopamine (6-OHDA) induces Drp1-dependent mitochondrial fragmentation in SH–SY5Y cells, Free Radic. Biol. Med. (2008) Mar 20 [Epub ahead of print].

[28] E. Carrasco, D. Casper, P. Werner, Dopaminergic neurotoxicity by 6-OHDA and MPP+: Differential requirement for neuronal cyclooxygenase activity, J. Neurosci. Res. 81 (2005) 121–131.

[29] E. Carrasco, D. Casper, P. Werner, PGE(2) receptor EP1 renders dopaminergic neurons selectively vulnerable to low-level oxidative stress and direct PGE(2) neurotoxicity, J. Neurosci. Res. 85 (2007) 3109–3117.

[30] M. Gomez-Lazaro, M.F. Galindo, C.G. Concannon, M.F. Segura, F.J. Fernandez-Gomez, N. Llecha, J.X. Comella, J.H. Prehn, J. Jordan, 6-Hydroxydopamine activates the mitochondrial apoptosis pathway through p38 MAPK-mediated, p53-independent activation of Bax and PUMA, J. Neurochem. 104 (2008) 1599–1612.

[31] L.L. Tian, X.J. Wang, Y.N. Sun, C.R. Li, Y.L. Xing, H.B. Zhao, M. Duan, Z. Zhou, S.Q. Wang, Salvianolic acid B, an antioxidant from *Salvia miltiorrhiza*, prevents 6-hydroxydopamine induced apoptosis in SH–SY5Y cells, Int. J. Biochem. Cell. Biol. 40 (2008) 409–422.

[32] S.M. Kulich, C. Horbinski, M. Patel, C.T. Chu, 6-Hydroxydopamine induces mitochondrial ERK activation, Free Radic. Biol. Med. 43 (2007) 372–383.

[33] E. Lin, J.E. Cavanaugh, R.K. Leak, R.G. Perez, M.J. Zigmond, Rapid activation of ERK by 6-hydroxydopamine promotes survival of dopaminergic cells, J. Neurosci. Res. 86 (2008) 108–117.

[34] K. Hanrott, T.K. Murray, Z. Orfali, M. Ward, C. Finlay, M.J. O'Neill, S. Wonnacott, Differential activation of PKCδ in the substantia nigra of rats following striatal or nigral 6-hydroxydopamine lesions, Eur. J. Neurosci. 27 (2008) 1086–1096.

[35] H. Fujita, M. Shiosaka, T. Ogino, Y. Okimura, T. Utsumi, E.F. Sato, R. Akagi, M. Inoue, K. Utsumi, J. Sasaki, α-Lipoic acid suppresses 6-hydroxydopamine-induced ROS generation and apoptosis through the stimulation of glutathione synthesis but not by the expression of heme oxygenase-1, Brain Res. 1206 (2008) 1–12.

[36] J.W. Langston, P. Ballard, J.W. Tetrud, I. Irwin, Chronic Parkinsonism in humans due to a product of meperidine-analog synthesis, Science 219 (1983) 979–980.

[37] J.R. Richardson, W.M. Caudle, T.S. Guillot, J.L. Watson, E. Nakamaru-Ogiso, B.B. Seo, T.B. Sherer, J.T. Greenamyre, T. Yagi, A. Matsuno-Yagi, G.W. Miller, Obligatory role for complex I inhibition in the dopaminergic neurotoxicity of 1-methyl-4-phenyl-1,2,3,6-tetrahydropyridine (MPTP), Toxicol. Sci. 95 (2007) 196–204.

[38] T. Loots du, L.J. Mienie, J.J. Bergh, C.J. Van der Schyf, Acetyl-L-carnitine prevents total body hydroxyl free radical and uric acid production induced by 1-methyl-4-phenyl-1,2,3,6-tetrahydropyridine (MPTP) in the rat, Life Sci. 75 (2004) 1243–1253.

[39] T. Obata, Dopamine efflux by MPTP and hydroxyl radical generation, J. Neural Transm. 109 (2002) 1159–1180.

[40] T. Obata, Endogenous semicarbazide-sensitive amine oxidase (SSAO) inhibitor increases 1-methyl-4-phenylpyridinium ion (MPP+)-induced dopamine efflux by immobilization stress in rat striatum, Int. J. Dev. Neurosci. 24 (2006) 343–347.

[41] T. Obata, C.C. Chiueh, *In vivo* trapping of hydroxyl free radicals in the striatum utilizing intracranial microdialysis perfusion of salicylate: Effects of MPTP, MPDP+, and MPP+, J. Neural Transm. Gen. Sect. 89 (1992) 139–145.

[42] T. Obata, Y. Yamanaka, H. Kinemuchi, L. Oreland, Release of dopamine by perfusion with 1-methyl-4-phenylpyridinium ion (MPP(+)) into the striatum is associated with hydroxyl free radical generation, Brain Res. 906 (2001) 170–175.

[43] S. Singh, K. Singh, S. Patel, D.K. Patel, C. Singh, C. Nath, M.P. Singh, Nicotine and caffeine-mediated modulation in the expression of toxicant responsive genes and vesicular monoamine transporter-2 in 1-methyl 4-phenyl-1,2,3,6-tetrahydropyridine-induced Parkinson's disease phenotype in mouse, Brain Res. (2008) Feb 21 [Epub ahead of print].

[44] Z. Xu, D. Cawthon, K.A. McCastlain, W. Slikker, S.F. Ali, Selective alterations of gene expression in mice induced by MPTP, Synapse 55 (2005) 45–51.

[45] R. Aguilar Hernandez, M.J. Sanchez De Las Matas, C. Arriagada, C. Barcia, P. Caviedes, M.T. Herrero, J. Segura-Aguilar, MPP(+)-induced degeneration is potentiated by dicoumarol in cultures of the RCSN-3 dopaminergic cell line. Implications of neuromelanin in oxidative metabolism of dopamine neurotoxicity, Neurotox. Res. 5 (2003) 407–410.

[46] T.G. Feng, Wang, D.D. Li, P. Fung, B.C. Wilson, B. Liu, S.F. Ali, R. Langenbach, J.S. Hong, Cyclooxygenase-2-deficient mice are resistant to 1-methyl-4-phenyl1, 2, 3, 6-tetrahydropyridine-induced damage of dopaminergic neurons in the substantia nigra, Neurosci. Lett. 329 (2002) 354–358.

[47] R. Vijitruth, M. Liu, D.Y. Choi, X.V. Nguyen, R.L. Hunter, G. Bing, Cyclooxygenase-2 mediates microglial activation and secondary dopaminergic cell death in the mouse MPTP model of Parkinson's disease, J. Neuroinflammation 27 (2006) 3–6.

[48] A. Nadjar, O. Berton, S. Guo, P. Leneuve, S. Dovero, E. Diguet, F. Tison, B. Zhao, M. Holzenberger, E. Bezard, IGF-1 signaling reduces neuro-inflammatory response and sensitivity of neurons to MPTP, Neurobiol. Aging (2008) Apr 2 [Epub ahead of print].

[49] T. Thomas, M. Timmer, K. Cesnulevicius, E. Hitti, A. Kotlyarov, M. Gaestel, MAP-KAP kinase 2-deficiency prevents neurons from cell death by reducing neuroinflammation—relevance in a mouse model of Parkinson's disease, J. Neurochem. (2008) Mar 19 [Epub ahead of print].

[50] D.K. Choi, S. Pennathur, C. Perier, K. Tieu, P. Teismann, D.C. Wu, V. Jackson-Lewis, M. Vila, J.P. Vonsattel, J.W. Heinecke, S. Przedborski, Ablation of the inflammatory enzyme myeloperoxidase mitigates features of Parkinson's disease in mice, J. Neurosci. 25 (2005) 6594–6600.

[51] R.L. Hunter, N. Dragicevic, K. Seifert, D.Y. Choi, M. Liu, H.C. Kim, W.A. Cass, P.G. Sullivan, G. Bing, Inflammation induces mitochondrial dysfunction and dopaminergic neurodegeneration in the nigrostriatal system, J. Neurochem. 100 (2007) 1375–1386.

[52] W. Wang, L. Shi, Y. Xie, C. Ma, W. Li, X. Su, S. Huang, R. Chen, Z. Zhu, Z. Mao, Y. Han, M. Li, SP600125, a new JNK inhibitor, protects dopaminergic neurons in the MPTP model of Parkinson's disease, Neurosci. Res. 48 (2004) 195–202.

[53] S. Hunot, M. Vila, P. Teismann, R.J. Davis, E.C. Hirsch, S. Przedborski, P. Rakic, R.A. Flavell, JNK-mediated induction of cyclooxygenase 2 is required for neurodegeneration in a mouse model of Parkinson's disease, Proc. Natl. Acad. Sci. USA 101 (2004) 665–670.

[54] S. Pain, L. Barrier, J. Deguil, S. Milin, A. Piriou, B. Fauconneau, G. Page, A cell-permeable peptide inhibitor TAT-JBD reduces the MPP+-induced caspase-9 activation but does not prevent the dopaminergic degeneration in substantia nigra of rats, Toxicology 243 (2008) 124–137.

[55] X. Geng, X. Tian, P. Tu, X. Pu, Neuroprotective effects of echinacoside in the mouse MPTP model of Parkinson's disease, Eur. J. Pharmacol 564 (2007) 66–74.

[56] D. Zhang, J.J. Zhang, G.T. Liu, The novel squamosamide derivative (compound FLZ) attenuated 1-methyl, 4-phenyl-pyridinium ion (MPP+)-induced apoptosis and alternations of related signal transduction in SH-SY5Y cells, Neuropharmacology 52 (2007) 423–429.

[57] X. Teng, T. Sakai, L. Liu, R. Sakai, R. Kaji, K. Fukui, Attenuation of MPTP-induced neurotoxicity and locomotor dysfunction in nucling-deficient mice via suppression of the apoptosome pathway, J. Neurochem 97 (2006) 1126–1135.

[58] S. Zhang, J. Wang, N. Song, J. Xie, H. Jiang, Up-regulation of divalent metal transporter 1 is involved in 1-methyl-4-phenylpyridinium (MPP(+))-induced apoptosis in MES23.5 cells, Neurobiol. Aging (2008) Jan 7 [Epub ahead of print].

[59] V. Anantharam, S. Kaul, C. Song, A. Kanthasamy, A.G. Kanthasamy, Pharmacological inhibition of neuronal NADPH oxidase protects against 1-methyl-4-phenylpyridinium (MPP+)-induced oxidative stress and apoptosis in mesencephalic dopaminergic neuronal cells, Neurotoxicology 28 (2007) 988–997.

[60] R. Banerjee, S. Sreetama, K.S. Saravanan, S.N. Dey, K.P. Mohanakumar, Apoptotic mode of cell death in substantia nigra following intranigral infusion of the parkinsonian neurotoxin, MPP+in Sprague–Dawley rats: Cellular, molecular and ultrastructural evidences, Neurochem. Res. 32 (2007) 1238–1247.

[61] W. Wang, Y. Yang, C. Ying, W. Li, H. Ruan, X. Zhu, Y. You, Y. Han, R. Chen, Y. Wang, M. Li, Inhibition of glycogen synthase kinase-3beta protects dopaminergic neurons from MPTP toxicity, Neuropharmacology 52 (2007) 1678–1684.

[62] S. Karunakaran, L. Diwakar, U. Saeed, V. Agarwal, S. Ramakrishnan, S. Iyengar, V. Ravindranath, Activation of apoptosis signal regulating kinase 1 (ASK1) and translocation of death-associated protein, Daxx, in substantia nigra pars compacta in a mouse model of Parkinson's disease: Protection by α-lipoic acid, FASEB J. 21 (2007) 2226–2236.

[63] X. Zeng, J. Chen, X. Deng, Y. Liu, M.S. Rao, J.L. Cadet, W.J. Freed, An *in vitro* model of human dopaminergic neurons derived from embryonic stem cells: MPP+toxicity and GDNF neuroprotection, Neuropsychopharmacology 31 (2006) 2708–2715.

[64] S. Samantaray, S.K. Ray, S.F. Ali, N.L. Banik, Calpain activation in apoptosis of motoneurons in cell culture models of experimental parkinsonism, Ann. N. Y. Acad. Sci. 1074 (2006) 49–56.

[65] P.D. Smith, M.P. Mount, R. Shree, S. Callaghan, R.S. Slack, H. Anisman, I. Vincent, X. Wang, Z. Mao, D.S. Park, Calpain-regulated p35/cdk5 plays a central role in dopaminergic neuron death through modulation of the transcription factor myocyte enhancer factor 2, J. Neurosci. 26 (2006) 440–447.

[66] L. Zecca, R. Fariello, P. Riederer, D. Sulzer, A. Gatti, D. Tampellini, The absolute concentration of nigral neuromelanin, assayed by a new sensitive method, increases throughout the life and is dramatically decreased in Parkinson's disease, FEBS Lett. 510 (2002) 216–220.

[67] M. Gerlach, K.L. Double, D. Ben-Shachar, L. Zecca, M.B. Youdim, P. Riederer, Neuromelanin and its interaction with iron as a potential risk factor for dopaminergic neurodegeneration underlying Parkinson's disease, Neurotox. Res. 5 (2003) 35–44.

[68] L. Hong, JD. Simon, Current understanding of the binding sites, capacity, affinity, and biological significance of metals in melanin, J. Phys. Chem. B 111 (2007) 7938–7947.

[69] M. Fasano, B. Bergamasco, L. Lopiano, Is neuromelanin changed in Parkinson's disease? Investigations by magnetic spectroscopies, J. Neural Transm. 113 (2006) 769–774.

[70] M. Naoi, W. Maruyama, H. Yi, Y. Yamaoka, M. Shamoto-Nagai, Y. Akao, M. Gerlach, M. Tanaka, P. Riederer, Neuromelanin selectively induces apoptosis in dopaminergic SH-SY5Y cells by deglutathionylation in mitochondria: Involvement of the protein and melanin component, J. Neurochem. (2008) Apr 9 [Epub ahead of print].

[71] K.A. Conway, J.C. Rochet, R.M. Bieganski, P.T. Lansbury, Jr., Kinetic stabilization of the α-synuclein protofibril by a dopamine- α-synuclein adduct, Science 294 (2001) 1346–1349.

[72] E.H. Norris, B.I. Giasson, R. Hodara, S. Xu, J.Q. Trojanowski, H. Ischiropoulos, V.M. Lee, Reversible inhibition of α-synuclein fibrillization by dopaminochrome-mediated conformational alterations, J. Biol. Chem. 280 (2005) 21212–21219.

[73] R.E. Whitehead, J.V. Ferrer, J.A. Javitch, J.B. Justice, Reaction of oxidized dopamine with endogenous cysteine residues in the human dopamine transporter, J. Neurochem. 76 (2001) 1242–1251.

[74] M.J. LaVoie, B.L. Ostaszewski, A. Weihofen, M.G. Schlossmacher, D.J. Selkoe, Dopamine covalently modifies and functionally inactivates parkin, Nat. Med. 11 (2005) 1159–1161.

[75] Y. Xu, A.H. Stokes, R. Roskoski, Jr., K.E. Vrana, Dopamine, in the presence of tyrosinase, covalently modifies and inactivates tyrosine hydroxylase, J. Neurosci. Res. 54 (1998) 691–697.

[76] K.S. Zafar, D. Siegel, D. Ross, A potential role for cyclized quinones derived from dopamine, DOPA, and 3,4-dihydroxyphenylacetic acid in proteasomal inhibition, Mol. Pharmacol. 70 (2006) 1079–1086.

[77] S. Baez, Y. Linderson, J. Segura-Aguilar, Superoxide dismutase and catalase enhance autoxidation during one-electron reduction of aminochrome by NADPH-cytochrome P-450 reductase, Biochem. Mol. Med. 54 (1995) 12–18.

[78] J. Segura-Aguilar, D. Metodiewa, C. Welch, Metabolic activation of dopamine o-quinones to o-semiquinones by NADPH cytochrome P450 reductase may play an important role in oxidative stress and apoptotic effects, Biochim. Biophys. Acta 1381 (1998) 1–6.

[79] I. Paris, A. Dagnino-Subiabre, K. Marcelain, L.B. Bennett, P. Caviedes, R. Caviedes, C. Olea-Azar, J. Segura-Aguilar, Copper neurotoxicity is dependent on dopamine-mediated copper uptake and one-electron reduction of aminochrome in a rat substantia nigra neuronal cell line, J. Neurochem. 77 (2001) 519–529.

[80] C. Arriagada, I. Paris, M.J. Sanchez de las Matas, P. Martinez-Alvarado, S. Cardenas, P. Castañeda, R. Graumann, C. Perez-Pastene, C. Olea-Azar, E. Couve, M.T. Herrero, P. Caviedes,, et al., On the neurotoxicity of leukoaminochrome o-semiquinone radical derived of dopamine oxidation: Mitochondria damage, necrosis and hydroxyl radical formation, Neurobiol. Dis. 16 (2004) 468–477.

[81] G. Diaz-Veliz, S. Mora, P. Gomez, M.T. Dossi, J. Montiel, C. Arriagada, F. Aboitiz, J. Segura-Aguilar, Behavioral effects of manganese injected in the rat substantia nigra are potentiated by dicumarol, a DT-diaphorase inhibitor, Pharmacol. Biochem. Behav. 77 (2004) 245–251.

[82] J. Segura-Aguilar, G. Diaz-Veliz, S. Mora, M. Herrera-Marschitz, Inhibition of DT-diaphorase is a requirement for Mn3+to produce a 6-OH-dopamine like rotational behaviour, Neurotox. Res. 4 (2002) 127–131.

[83] I. Paris, P. Martinez-Alvarado, C. Perez-Pastene, M.N. Vieira, C. Olea-Azar, R. Raisman-Vozari, S. Cardenas, R. Graumann, P. Caviedes, J. Segura-Aguilar, Mono-amine transporter inhibitors and norepinephrine reduce dopamine-dependent iron toxicity in cells derived from the substantia nigra, J. Neurochem. 92 (2005) 1021–1032.

[84] I. Paris, S. Cardenas, J. Lozano, C. Perez-Pastene, R. Graumann, A. Riveros, P. Caviedes, J. Segura-Aguilar, Aminochrome as a preclinical experimental model to study degeneration of dopaminergic neurons in Parkinson's disease, Neurotox. Res. 12 (2007) 125–134.

[85] P. Fuentes, I. Paris, M. Nassif, P. Caviedes, J. Segura-Aguilar, Inhibition of VMAT-2 and DT-diaphorase induce cell death in a substantia nigra–derived cell line-an experimental cell model for dopamine toxicity studies, Chem. Res. Toxicol. 20 (2007) 776–783.

[86] J. Segura-Aguilar, C. Lind, On the mechanism of Mn3+induce neurotoxicity of dopamine: Prevention of quinone derived oxygen toxicity by DT-diaphorase and superoxid dismutase, Chem.Biol. Interact. 72 (1989) 309–324.

[87] M. Schultzberg, J. Segura-Aguilar, C. Lind, Distribution of DT-diaphorase in the rat brain: Biochemical and immunohistochemical studies, Neuroscience 27 (1988) 763–766.

[88] J. Segura-Aguilar, S. Cardenas, A. Riveros, P. Fuentes-Bravo, J. Lozano, R. Graumann, I. Paris, M. Nassif, P. Caviedes, DT-diaphorase prevents the formation of α-synuclein adducts with aminochrome, Soc. Neurosci. Abstr. 824 (2006) 17.

CHAPTER 5

Molecular Mechanisms of 4-(Methylnitrosamino)-1-(3-pyridyl)-1-butanone-Induced Lung Carcinogenesis

Lisa A. Peterson

Contents

Division of Environmental Health Sciences, Cancer Center, University of Minnesota, Mayo Mail Code 806, 420 Delaware St SE, Minneapolis, Minnesota 55455
Tel.: +1 612 626 0164; Fax: +1 612 626 5135
E-mail address: peter431@umn.edu

1. Introduction

Epidemiological studies have linked tobacco use to cancers of the lung, oral cavity, pharynx, larynx, esophagus, pancreas, urinary bladder, liver, and several other tissues [1]. Among these, lung cancer kills more than one million people each year world wide [2]. It is the leading cause of cancer death for both women and men in the United States, with 80–90% of these deaths linked to cigarette smoking [3–5]. Environmental tobacco smoke is also widely accepted as cause of lung cancer, however, the risk is much lower than that associated with smoking [1]. It is important to understand the mechanisms of tobacco–induced cancers so that cancer risk can be decreased, susceptible individuals identified and strategies for early detection can be developed.

Cigarette smoke contains more than 4000 chemicals, of which 55 have been classified as chemical carcinogens in animal models [5]. The tobacco–alkaloid derived nitrosamines are formed during the curing process of tobacco [6]. The focus of this review, 4-(methylnitrosamino)-1-(3-pyridyl)-1-butanone (NNK), is derived from nicotine [7]. Significant levels of NNK are found in tobacco products and tobacco smoke. Levels of NNK in cigarettes range from 55 to 10,745 ng per cigarette [8–12]. They are ~10-fold lower in mainstream smoke (5–1749 ng) [8–13].

2. Carcinogenesis

NNK is carcinogenic in laboratory animals, generating tumors at sites similar to those observed in smokers [14]. NNK is a strong lung specific carcinogen, independent of species and route of administration [15–17].

It also causes liver, nasal, and pancreatic tumors [14]. This compound induces lung adenocarcinomas in rodents at doses that are comparable to those experienced by smokers [14]. This type of cancer is now the most common type of lung cancer observed in humans, having surpassed squamous cell carcinoma. This shift in histology has been attributed not to improvements in diagnoses but rather to the changing cigarette, which increases the exposure of humans to tobacco-specific nitrosamines [18]. Metabolic products of NNK have been detected in urine of smokers and individuals exposed to second hand smoke, indicating that humans are exposed to and metabolize this carcinogen [19–28]. As a result of these studies, NNK is considered to be a human carcinogen [29].

3. METABOLISM

3.1. Overview

NNK is rapidly and extensively metabolized in rodents, primates, and humans [30–35]. The major metabolic pathways, as outlined in Figure 1, consist of carbonyl reduction, *N*-oxidation and α-carbon hydroxylation. Glucuronidation is an important pathway of NNAL metabolism. Each of these four pathways are described below.

3.2. Carbonyl reduction

Carbonyl reduction of NNK by carbonyl reductases generates 4-(methylnitrosamino)-1-(3-pyridyl)-1-butanol (NNAL), a major NNK metabolite (Figure 1). This reduction leads to the formation of enantiomers which have stereoselective differences in tissue distribution and excretion in rats and humans [34,36,37]. At least five different enzymes have been shown to carry out this reduction, microsomal 11β-hydroxysteroid dehydrogenase type 1 [38], cytosolic carbonyl reductases, and three members of the aldo-keto reductase superfamily, AKR1C1, AKR1C2, and AKR1C4 [39]. There may be other reductases that can catalyze the reduction of NNK to NNAL. In a study with human pancreatic tissue, (*S*)-NNAL was the major product when NNK was incubated with cytosolic fractions whereas (*R*)-NNAL was the predominant isomer in microsomal incubations [40]. Significant interindividual differences in the rates of reduction were observed. Therefore, there is likely to be intra-individual variability in the rates and stereoselectivity of carbonyl reduction of NNK in humans. This reaction is not necessarily a detoxification process since NNAL is almost as carcinogenic as NNK in a variety of animal models [14]. Cytochrome P450 is able to oxidize (*S*)-NNAL, but not (*R*)-NNAL to NNK [41,42]. The ability of other enzymes to catalyze this oxidation reaction has not been investigated.
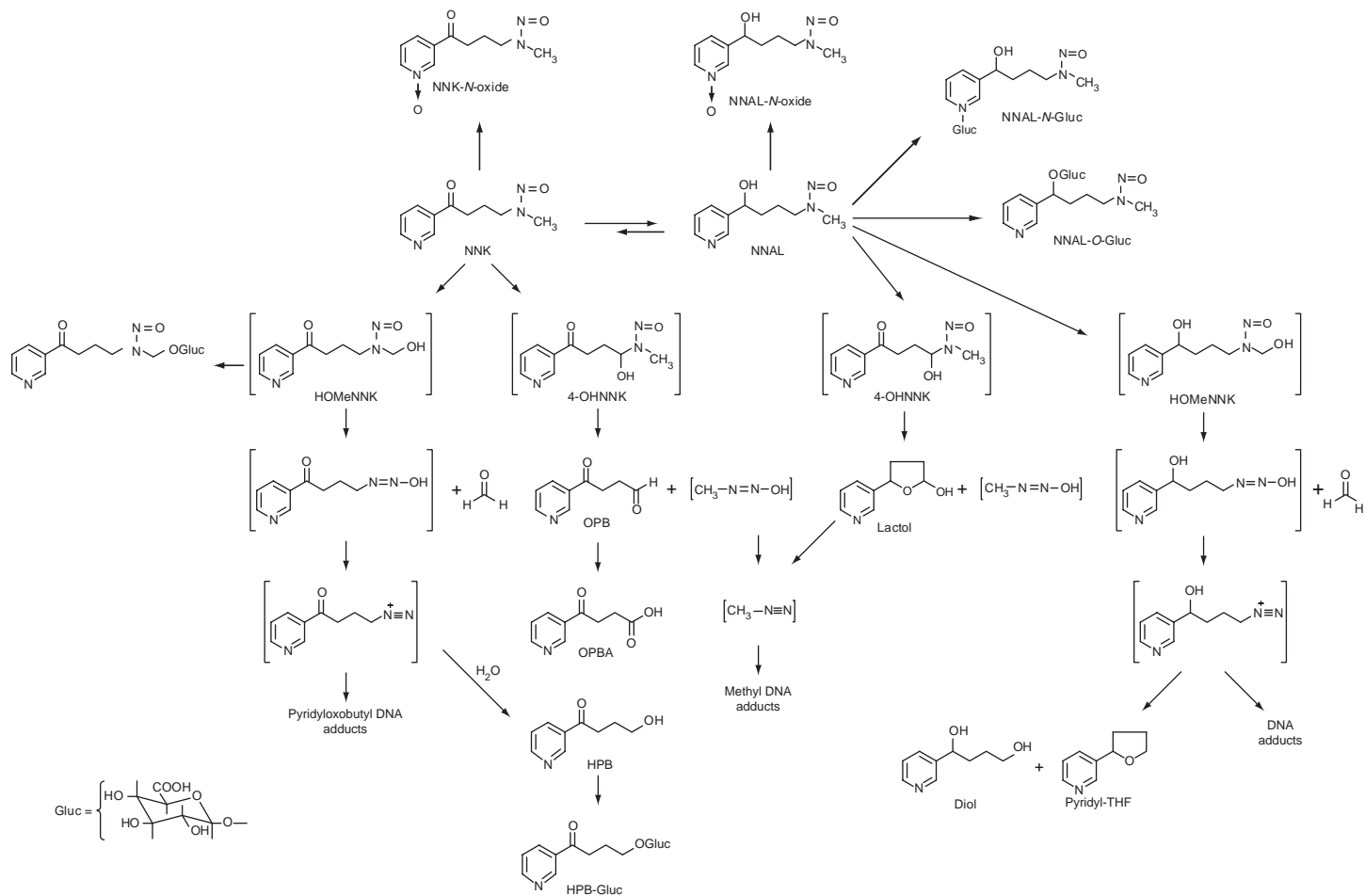
Figure 1 Overview of NNK metabolism.

3.3. *N*-Oxidation

Both NNK and NNAL undergo oxidation to form *N*-oxides (Figure 1). This step is considered a major detoxification pathway in rodents [14]. It is less important pathway in humans where NNK *N*-oxide was not observed and the levels of NNAL *N*-oxide were ~20% the levels of NNAL-glucuronides in smokers' urine [43]. There is wide species and tissue variation in the production of these metabolites in microsomes [14]. Cytochrome P450 2B1 appears to be involved in NNK–*N*-oxide formation in rodents [14,44]. None of the expressed human P450s or FMO have been shown to be effective NNK *N*-oxidases [44,45]. Human P450 2A13, rat P450 2A3, and mouse P450 2A5 catalyze the *N*-oxidation of the (*S*)- but not (*R*)-enantiomer of NNAL [41,42].

3.4. α-Hydroxylation

A major route of metabolism for NNK involves α-carbon hydroxylation leading the formation of two different α-hydroxymetabolites (Figure 1). Methyl hydroxylation leads to the formation of 4-(hydroxymethylnitrosamino)-1-(3-pyridyl)-1-butanone (OHMeNNK). This unstable metabolite spontaneously decomposes to a reactive pyridyloxobutylating agent that reacts with water to generate 4-hydroxy-1-(3-pyridyl)-1-butanone (HPB). Methylene hydroxylation generates 4-hydroxy-4-(methylnitrosamino)-1-(3-pyridyl)-1-butanone (4-OHNNK). This product is also unstable and decomposes to form 4-oxo-1-(3-pyridyl)-1-butanone (OPB) and methanediazohydroxide. OPB is oxidized to 4-oxo-4-(3-pyridyl)-1-butanoic acid (OPBA). Both α-hydroxylation pathways are considered bioactivation routes since they result in the formation of DNA and protein adducts [14].

NNAL is also subjected to α-hydroxylation reactions (Figure 1) [14]. Methyl hydroxylation produces 4-(hydroxymethylnitrosamino)-1-(3-pyridyl)-1-butanol (4-OHMeNNAL) which spontaneously decomposes to a reactive pyridylhydroxybutylating agent that reacts with water to form 4-hydroxy-1-(3-pyridyl)-1-butanol (diol) and 2-(3-pyridyl)-2,3,4,5-tetrahydrofuran (pyridyl–THF). Methylene hydroxylation creates 2-(3-pyridyl)-5-hydroxy-2,3,4,5-tetrahydrofuran (lactol). As with NNK, these oxidation pathways generate reactive metabolites capable of alkylating DNA and protein.

3.4.1. Enzymes involved in NNK α-hydroxylation

Cytochrome P450 is primarily responsible for catalyzing the α-hydroxylation of NNK and NNAL [44]. The recent report indicating the requirement of active cytochrome P450 reductase for NNK-induced tumor formation demonstrates that this pathway is critical for carcinogenesis [46]. The role of various cytochrome P450 enzymes in the α–hydroxylation

of NNK has been recently reviewed [44]. Based on K_m data determined with expressed human P450s, the relative efficiencies of oxidation are (from most efficient to least efficient): 2A13 >> 2B6 > 2A6 > 1A2 $\approx$ 1A1 > 2D6 $\approx$ 2E1 $\approx$ 3A4 [44]. Whether these enzymes are involved in NNK metabolism in humans will depend on numerous factors such as relative expression levels, tissue localization, levels of cytochrome P450 reductase, and the concentration of NNK in human tissues [44]. Studies with human peripheral lung microsomes indicate that NNK α–hydroxylase activity does not correlate well with P450 2A6 and 2A13 levels except in individuals with high levels of P450 2A13 [47,48]. Therefore, it appears that there will be individual differences as to which P450 will be involved in NNK bioactivation in humans. Other P450s that are expressed in human lung include P450 1A1 (in smokers), 1B1, 2B6, 2E1, and 3A5 [49]. The kinetic parameters of P450 1B1 and 3A5 have not been determined for NNK [50].

Another factor complicating the identification of the cytochrome P450 enzymes involved in the α–hydroxylation of NNK is that the lung is a heterogeneous tissue with over 40 different cell types, each of which are likely to have a different distribution of enzymes. Immunohistochemical studies have indicated that cytochrome P450 reductase is expressed in bronchial and bronchiolar epithelium, Clara cells, types I and II alveolar cells, and alveolar macrophages [51]. The localization of a number of P450s in human lung tissue has been investigated with immunohistochemistry with different distribution for each one. P450 1A1 is expressed primarily in bronchiolar, terminal bronchiolar, and alveolar epithelium of smokers [50], P450 1B1 has only been observed in alveolar macrophages [52], and P450 3A5 is distributed in the bronchial, bronchiolar, and alveolar epithelium as well as in alveolar macrophages [53].

Consistently, different lung cell types have different abilities to metabolize NNK. In rat, the relative α–hydroxylation activity of the different lung cell types was Clara cells > alveolar macrophages $\geq$ alveolar type II cells > small cells are the most active in terms of α–hydroxylation of NNK as well as NNAL [54]. The NNK α–hydroxylase activity of human alveolar type II cell and alveolar macrophages were comparable within an individual but varied widely between individuals [55].

3.4.2. Enzymes involved in NNAL α-hydroxylation

The enzymes involved in the α–hydroxylation of NNAL have been less studied. Human P450 2A13, rat P450 2A3, and mouse P450 2A5 all catalyze the α–hydroxylation of NNAL [41,42]. The ratio of methylene (lactol formation) versus methyl hydroxylation (diol plus pyridyl–THF) is dependent on the P450 enzyme catalyzing the reaction. Mouse P450 2A5 preferentially catalyzed methylene hydroxylation [41], rat P450 2A3 preferentially catalyzed methyl hydroxylation [42], and human P450 2A13 had a slight preference for methylene hydroxylation [42]. In general, NNAL

is not as easily oxidized as NNK. The V_{max}/K_m values for NNAL metabolism by P450s 2A3 and 2A13 were 1–2 orders of magnitude lower than those obtained for NNK [42].

3.4.3. Relative amount of NNK methyl versus methylene hydroxylation

The relative amount of methyl versus methylene hydroxylation varies with species and tissue as reviewed by Hecht [14]. For example, the rate of methyl hydroxylation exceeds methylene hydroxylation in lung microsomes from A/J mice, patas monkey, and Sprague–Dawley rats [56–58] whereas methylene hydroxylation is the dominant pathway in A/J mouse liver microsomes [59]. Methylene hydroxylation is similar to methyl hydroxylation in Sprague–Dawley rats and patas monkeys [57,60]. These differences result from the fact that various P450 enzymes differ in the relative amount of methyl versus methylene hydroxylation they produce [44]. For example, human P450 2A13 is 1.5–4 times better at methylene hydroxylation than methyl hydroxylation whereas mouse P450 2A5 is a better methyl hydroxylase [44].

3.5. Glucuronidation

While NNK is not directly glucuronidated, several of its metabolites undergo glucuronidation. NNAL glucuronides are significant *in vivo* metabolites of NNK. The formation of these metabolites is considered to be the primary route of detoxification of NNK in humans [14]. There are several glucuronides formed from this compound, diastereomeric 4-(methylnitrosamino)-1-(3-pyridyl)-1-(O-β-D-glucopyranuronosyl)butane (NNAL-O-Gluc) [33,61,62] and 4-(methylnitrosamino)-1-(3-pyridyl-N-β-D-glucopyranuronosyl)-1-butanolonium inner salt (NNAL-N-Gluc) (Figure 1) [23]. These metabolites have been effectively employed as biomarkers for NNK exposure and absorption from tobacco products [28]. In humans, the glucuronosyl transferases (UGTs) UGT2B7, UGT1A9, and UGT2B17 are important enzymes in the O-glucuronidation of NNAL [63,64] whereas UGT1A4 and UGT2B10 are important catalysts of NNAL-N-Gluc formation [65,66]. The ratio of NNAL-N-Gluc/NNAL-O-Gluc in the urine of smokers is 1 whereas it is 0.5 in snuff-dippers [23].

The O-glucuronides of HPB and OHMeNNK have been observed as minor urinary metabolites of NNK in phenobarbital-treated rats [67]. The latter product is likely a detoxification pathway in NNK metabolism since glucuronidation of this compound would block its decomposition into a DNA alkylating species. Consistent with this hypothesis is that the levels of hemoglobin pyridyloxobutylation is reduced in rats pretreated with phenobarbital despite the fact that the α-hydroxylation pathways are enhanced in

these same animals; glucuronidation of OHMeNNK is also increased in these animals [68]. The presence of this pathway in humans has not been investigated.

3.6. Balance of metabolic pathways *in vivo*

In laboratory animals, α-hydroxylation is the primary pathway [33,61]. When total NNAL metabolites are considered (NNAL plus its glucuronides), they account for 0–50% of mouse urinary metabolites and 0–33% of rat urinary metabolites [61]. NNAL and its glucuronides represented 19–22% of the urinary NNK metabolites in the patas monkey [33]. Pyridine *N*-oxidation was either equal to or less than the levels of NNAL plus NNAL-glucs in these species [33,61]. The rest of the urinary metabolites in these species are products of α-carbon oxidation.

Recent studies in smokeless tobacco users have been designed to determine the relative contribution of each pathway to overall NNK metabolism in humans [35]. NNAL and its glucuronides comprised 14–17% of an NNK dose. Given that pyridine *N*-oxidation was about 7 times less abundant than NNAL and its glucuronides in the urine of smokeless tobacco users [43], it was estimated that α-hydroxylation is the major metabolic pathway in smokeless tobacco users [35].

4. DNA DAMAGE

While the products of this reaction, OHMeNNK and 4-OHNNK, are too unstable for isolation and chemical characterization, these metabolites probably have a significant biological half life. OHMeNNK is stable enough to serve as a substrate for glucuronidation [67]. In addition, several α-hydroxynitrosamines have been prepared and were shown to some limited stability with half-lives greater than 10 s at pH 7 [69]. Therefore, it is likely that α-hydroxymetabolites are sufficiently stable to migrate from the site of formation to other locations within the cell.

α-Hydroxylation generates multiple reactive metabolites of NNK that are capable of damaging DNA. Each α-hydroxymetabolites decomposes to an alkanediazohydroxide and an aldehyde. Both of these decomposition products can damage DNA as outlined below. Given the very short half life of the alkanediazohydroxides, it is likely that the aldehyde product is generated in the vicinity of the reactive diazonium ion. Therefore, when DNA is damaged by the diazonium ion intermediate, an aldehyde is likely generated within the nucleus. The overall contribution of the aldehyde to the toxicological properties of nitrosamines is not well investigated.

In general, the aldehyde decomposition products of α-hydroxynitrosamine metabolites are ignored when considering reactive metabolites of nitrosamines, despite the fact that aldehydes are known toxicants and mutagens [70–75] and are capable of inhibiting DNA repair pathways [71,76]. The types of DNA damage generated by each of the reactive metabolites formed from NNK α-hydroxylation are discussed below.

4.1. Methyl DNA damage

4-OHNNK decomposes to form methanediazohydroxide (Figure 1). The diazohydroxide reaction product further degrades to a methanediazonium ion which reacts with DNA to form well-characterized methyl DNA adducts (Figure 2). As with other methylating nitrosamines, 7-methylguanine (7-mG), O^6-methylguanine (O^6-mG), and O^4-methylthymidine (O^4-mT) have been detected in DNA isolated from tissues of NNK-treated rodents [77–81]. In the absence of DNA repair, the distribution of the various adducts is as expected for a methanediazonium intermediate with 7-mG present in quantities roughly 10 times the levels of O^6-mG which is $\sim$10 times the levels of O^4-mT [82]. The dose and time dependence of NNK-induced methyl DNA adduct formation has been extensively reviewed elsewhere [14,83]. Methyl DNA adducts have been observed as well in NNAL-treated rodents [84]. Methyl adducts have been observed in tobacco smokers but these adducts are also detected in nonsmokers and are likely to be derived from both tobacco and nontobacco sources [83].

4.2. Pyridyloxobutyl DNA damage

OHMeNNK decomposes to 4-(3-pyridyl)-4-oxobutanediazohydroxide and subsequently to 4-(3-pyridyl)-4-oxobutanediazonium ion. Studies investigating the solvolysis of model pyridyloxobutylating agents provide evidence for multiple reactive intermediates generated by the 4-(3-pyridyl)-4-oxobutanediazonium ion (Table 1; Figure 3; [85]). It can react directly with nucleophiles to form 4-oxo-4-(3-pyridyl)-1-butyl adducts (pathway 1). Second, it can cyclize by intramolecular attack of the carbonyl oxygen on the terminal carbon atom to form a reactive cyclic oxonium ion (pathway 2) which reacts with nucleophiles to form cyclic adducts. Finally, it can eliminate a proton and N_2 to generate 4-oxo-4-(3-pyridyl)-but-1-ene which will rearrange to form an α,β-unsaturated ketone, 4-oxo-4-(3-pyridyl)-but-2-ene (pathway 3). This latter compound is reactive with model nucleophiles, such as N-acetylcysteine to generate 4-oxo-4-(3-pyridyl)-2-butyl adducts [86]. An alternative intermediate leading to the α,β-unsaturated ketone involves the formation of a primary carbocation to a secondary carbocation that then loses a hydrogen to become the α,β-unsaturated ketone directly (pathway 4). The absence of 3-hydroxy-1-(3-pyridyl)-1-butanone as a

Methyl adducts
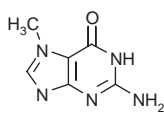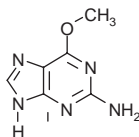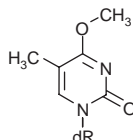
7-mG O^6-mG O^4-mdT

Pyridyloxobutyl adducts
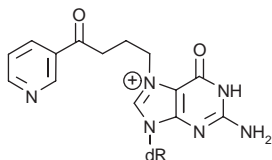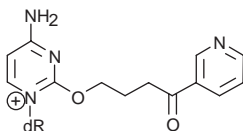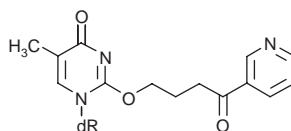
7-pobdG O^2-pobdC O^2-pobdT
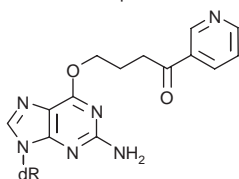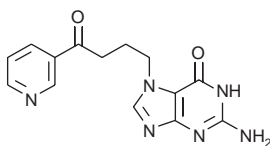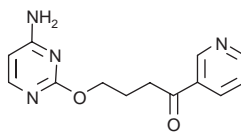
O^6-pobdG   7-pobG O^2-pobC

Formaldehyde adducts
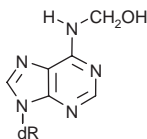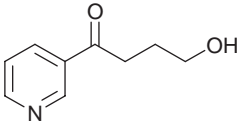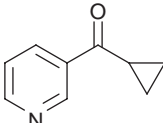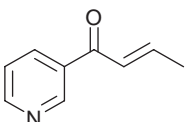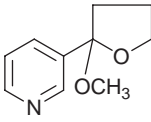

dR = 2'-deoxyribose

N^6-HOCH$_2$-dAdo   dA-CH$_2$-dA
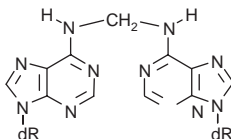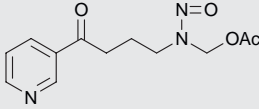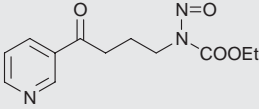
Figure 2   Structure of NNK-derived DNA adducts.

solvolysis product argues against a discrete secondary carbocation as an inter-mediate in this process [85]. The formation of cyclopropyl(pyridin–3–yl)–methanone is explained by the deprotonation of the carbon adjacent to the carbonyl which produces an anion that can intramolecularly react with the electrophilic carbon adjacent to the diazonium ion (pathway 5). While the α,β–unsaturated ketone and the cyclopropyl derivative are observed during the hydrolysis of model pyridyloxobutylating agents, they have not been detected as metabolites of NNK in biological systems [86].

HPB is the major decomposition product formed during the solvolysis of NNKOAc or 4–carbethoxynitrosamino-1-(3-pyridyl)-1-butanone. This product can be formed either via direct reaction with the diazonium ion intermediate or via reaction with the cyclic oxonium ion intermediate to form an unstable hemiacetal that rapidly rearranges to HPB. When the

Table 1 Solvolysis of model pyridlyoxobutylating agents[a] (reproduced from Ref. [85])

Products	3[b,c]		4[b,d]	
	H$_2$O	MeOH^f	H$_2$O	MeOH^e
(structure: 1-(3-pyridyl)-4-hydroxy-1-butanone)	63	48	48	28
(structure: cyclopropyl 3-pyridyl ketone)	4	4	2	3
(structure: 1-(3-pyridyl)-2-buten-1-one)	24	30	17	13
(structure: 2-(3-pyridyl)-2-methoxy-tetrahydrofuran, OCH$_3$)		11		13

[a] Product distribution expressed in percent yield.
[b] Solvolyzed in 10 mM MOPS and 150 mM NaCl, pH 7.4 at 22 °C.
[c] Contained 5.7 μg/ml esterase.
[d] Contained 19 μg/ml esterase.
[e] Contained 4.9 M methanol.

solvolysis is performed in the presence of methanol, only the stable acetal, 2-(3-pyridyl)-2-methoxy-2,3,4,5-tetrahydrofuran is formed, not 4-methoxy-1-(3-pyridyl)-1-butanone. This result suggests that the cyclic oxonium ion represents a significant intermediate in the solvolysis of these compounds. Therefore, it is possible that both 4-(3-pyridyl)-4-oxobutyl and 2-(3-pyridyl)-2,3,4,5-tetrahydrofuran adducts are formed from 4-(3-pyridyl)-4-oxobutanediazonium ion.

Initial attempts to characterize DNA adducts from this pathway were unsuccessful as a result of their instability. When pyridyloxobutylated DNA is subjected to strong acid or neutral hydrolysis conditions, the majority of these adducts decompose to release HPB [14,87]. HPB itself does not react with DNA to form adducts [87], demonstrating that these adducts are
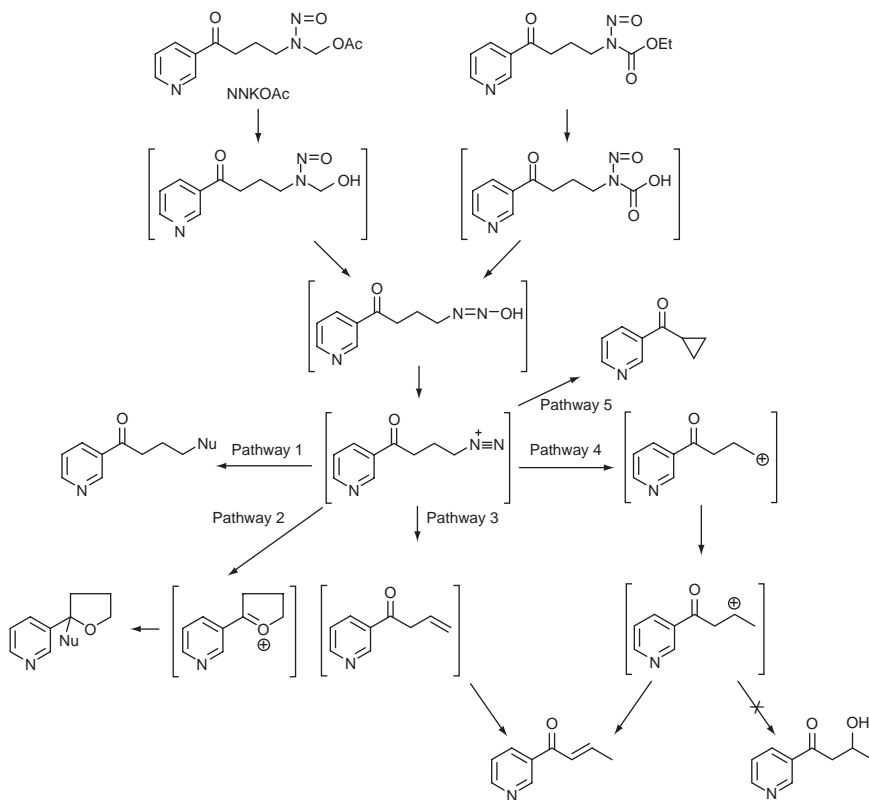
Figure 3 Proposed reactive intermediates in the hydrolysis of NNKOAc.

derived from a reactive intermediate resulting from methyl hydroxylation. The amount of HPB released from DNA (HPB-releasing adducts) has been used as a dosimeter for this pathway [14].

Four pyridyloxobutyl DNA adducts have been recently characterized (Figure 2): 7-[4-3-(pyridyl)-4-oxobut-1-yl]-2′-deoxyguanosine (7-pobdG) [88], O^2-[4-3-(pyridyl)-4-oxobut-1-yl]-2′-deoxycytosine (O^2-pobdC) [89], O^2-[4-3-(pyridyl)-4-oxobut-1-yl]thymidine (O^2-pobdT) [89], and O^6-[4-3-(pyridyl)-4-oxobut-1-yl]-2′-deoxyguanosine (O^6-pobdG) [88–90]. Standards for N^2-[4-3-(pyridyl)-4-oxobut-1-yl]-2′-deoxyguanosine were prepared but this adduct was not observed in pyridyloxobutylated DNA [91]. O^6-pobdG and O^2-pobdT are the most stable of these DNA adducts [89,90]. The other two adducts, 7-pobdG and O^2-pobdC, undergo one of two reactions under neutral thermal hydrolysis conditions: they lose the sugar moiety to generate the nucleobase adducts, 7-[4-3-(pyridyl)-4-oxobut-1-yl] guanine (7-pobG) and O^2-[4-3-(pyridyl)-4-oxobut-1-yl]cytosine or they

dealkylate to release HPB [88,89]. The dealkylation reaction increases in strong acid hydrolysis conditions. Cyclic adducts derived from a cyclic oxonium ion intermediate are expected to dealkylate to generate HPB under neutral thermal, acid or enzymatic degradation of DNA.

Quantitation of these adducts in NNKOAc-treated DNA indicates that HPB–releasing adducts represent about 65% of the total pyridyloxobutyl DNA adducts [92]. The relative amount of adduct formed: 7-pobG $>>$ O^2-pobC $>$ O^2-pobdT $>$ O^6-pobG [92]. When the adduct levels are measured with deuterated standards for each identified adduct, 7-pobG $>$ O^6-pobG $>$ O^2-pobdT $\geq$ O^2-pobC [93].

The presence of phosphate adducts in pyridyloxobutylated DNA is unclear. HPB was not released from pyridyloxobutylated DNA when heated under alkaline conditions [87], suggesting that the HPB–releasing adducts are not derived from adducts attached to the phosphate backbone. However, there is some evidence supporting that there are phosphate adducts in DNA isolated from [5-^{3}H]NNK–treated mice. Indirect evidence for phosphate adducts was obtained when the 3′-termini of NNKOAc–induced strand breaks were resistant to ^{32}P-labeling in the presence of T4 DNA polymerase even after the DNA had been incubated with endonuclease IV [94]. This latter enzyme will remove blocking groups such as 3′-phosphate or 3′-phosphoglycolate. This result suggests that the 3′-position of the NNKOAc–induced strand breaks is blocked with an adduct so that it is not recognized by the endonuclease. However, O^6-pobG blocks 3′-exonuclease degradation of DNA [95], indicating that an investigation into the ability of pyridyloxobutylated nucleobase adducts to inhibit endonuclease IV should be conducted.

Evidence for phosphate adducts was also observed when reaction of enzyme digests of DNA from [5-^{3}H]NNK–treated animals with cob(I)alamin, followed by reduction with sodium borohydride led to the formation of a 4-(3-[5-^{3}H]pyridyl)-4-hydroxy-2-butylcobalam complex [96]. Cob(I)alamin is thought to react selectively with alkyl phosphate adducts [97]. From these studies, it was concluded that phosphate adducts represented up to 22% of the pyridyloxobutyl DNA adducts present in DNA from NNK–treated mice. It is possible that cob(I)alamin reacts with the pyridyloxobutyl nucleobase adducts given the increased reactivity of the pyridyloxobutyl group relative to other simpler alkyl groups. Additional studies are required to explain these discrepant results.

Indirect evidence for the formation of formamidopyrimidine (fapy) adducts in DNA from NNKOAc-treated human cells was obtained using the comet assay [98]. The contribution of these adducts to the overall damage observed in pyridyloxobutyl DNA is unknown since the method of detection assumed that pyridyloxobutyl fapy adducts equally good substrates for formamidopyrimidine glycosylase as methyl fapy adducts.

4.2.1. Formation of specific pyridyloxobutyl DNA adducts in animal studies

The formation and persistence of HPB–releasing adducts has been extensively reviewed [14,83]. More recently, the levels of specific pyridyloxobutyl DNA adducts have been reported in rats treated with NNK. When rats were treated with four daily subcutaneous injections of NNK, all four pyridyloxobutyl DNA adducts were detected (Table 2). The levels of 7-pobG, O^2-pobC, and O^2-pobdT were higher in liver relative to lung DNA. The levels of O^6-pobG were higher in lung relative to liver. This adduct–specific difference likely results from tissue differences in repair as discussed below. The relative adduct levels were O^2-pobdT $\geq$ 7-pobG $>$ O^2-pobC $>>$ O^6-pobG in lung DNA and O^2-pobdT $=$ 7-pobG $\geq$ O^2-pobC $>$ O^6-pobG in liver DNA of the treated animals.

When rats were chronically treated with a lower dose of NNK (10 ppm in drinking water), the levels of the four pyridyloxobutyl adducts were higher in lung versus liver DNA (Figure 4) [99]. A similar dose dependent shift in tissue levels of total pyridyloxobutyl adducts has been previously reported [80]. The relative distribution of pyridyloxobutyl DNA adducts was O^2-pobdT $>$ 7-pobG $>>$ O^2-pobC $>>$ O^6-pobG in lung DNA and O^2-pobdT $>>$ 7-pobG $>$ O^2-pobC in liver DNA; O^6-pobG was not observed in liver DNA from these animals [99].

Interestingly, chronic treatment with (S)–NNAL or (R)–NNAL (10 ppm in the drinking water) led to the formation of these adducts in lung and liver DNA of the exposed animals [99]. The total levels of these adducts in the lung and liver DNA of (S)–NNAL, but not (R)–NNAL, were comparable to those observed with the same dose of NNK: NNK $\geq$ (S)-NNAL $>>$ (R)–NNAL (Figure 5). The distribution of the specific adducts were comparable to that observed with NNK. These results indicate that a significant amount of NNAL is oxidized to NNK *in vivo*.

4.2.2. Pyridyloxobutyl DNA adduct formation in human studies

Levels of HPB–releasing adducts have been measured in human tissue samples. Levels of HPB releasing lung DNA adducts were significantly higher ($p < 0.0001$) in lung cancer cases who were self reported smokers as compared to lung cancer cases who were self-reported nonsmokers (404 $\pm$ 258 vs. 59 $\pm$ 56 fmol HPB/mg, respectively) [100]. In another study, there was no difference in lung HPB–releasing DNA adducts between sudden death victims who were smokers or nonsmokers [101]. These studies suggest that individual smokers who accumulate pyridyloxobutyl DNA adducts may be at increased risk of lung cancer.

Table 2 Adduct levels in NNK-treated rats (reproduced from Ref. [110])

Tissue	Dose of NNK (mmol/kg)[a]	N^6-HOCH$_2$-dA	dA-CH$_2$-dA	7-pobG	O^2-pobdT	O^2-pobC	O^6-pobG
				(fmol/mg DNA)[b]			
Lung	0.025	230 ± 84	2[c]	933 ± 89	1120 ± 66	483 ± 36	251 ± 26
	0.1	615 ± 504	18[c]	1800 ± 478	2020 ± 483	840 ± 169	487 ± 101
	0	84 ± 7	2[d]	N.D.[g]	N.D.	N.D.	N.D.
Liver	0.025	586 ± 191[e]	17 ± 12[e,f]	3550 ± 1600	3530 ± 725	2930 ± 521	28 ± 17
	0.1	3720 ± 2210	303 ± 290	12,200 ± 1600	12,300 ± 1690	7800 ± 1680	140 ± 25
	0	133 ± 126	9[c]	N.D.	N.D.	N.D.	N.D.

[a] Administered by s.c. injection daily for 4 days.
[b] Mean ± S.D., N = 5 except where noted.
[c] dAdo-CH$_2$-dAdo was not detected in 3 samples; number shown is mean of 2.
[d] N = 2.
[e] N = 4.
[f] dAdo-CH$_2$-dAdo was not detected in 1 sample; number shown is mean of 3.
[g] N.D. = not detected (detection limit, 3 fmol/mg DNA).
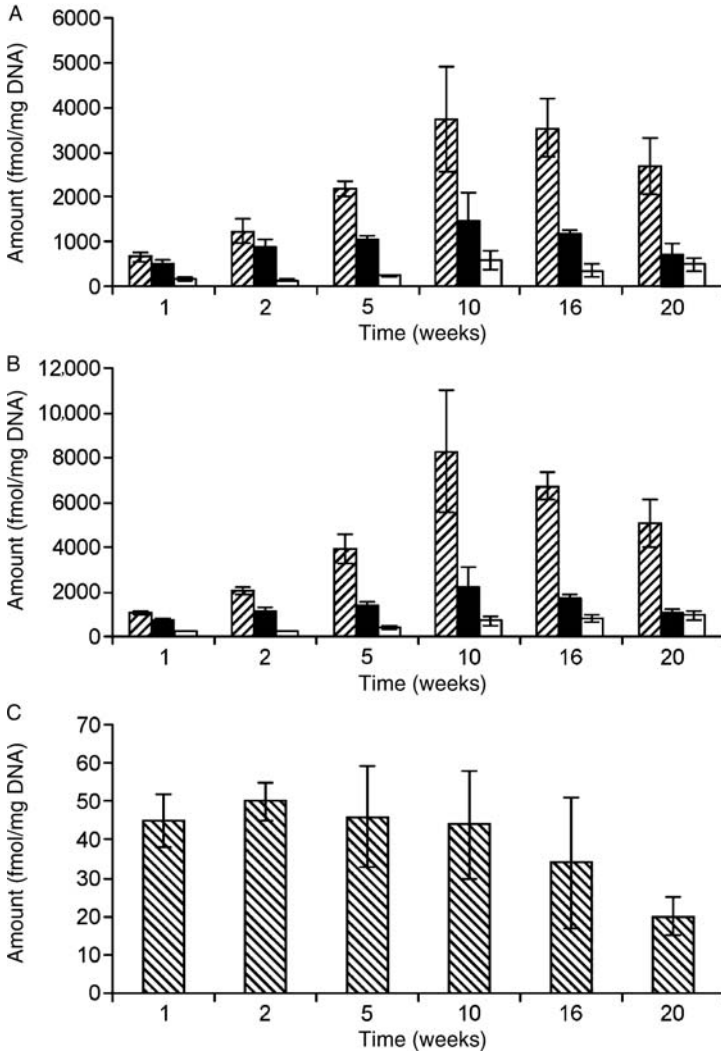
Figure 4 Levels of pyridyloxobutyl DNA adducts in (A) liver and (B) lung DNA of NNK-treated rats; (C) O^6-pobdG in lung DNA of NNK-treated rats on a different scale. Animals were treated with 10 ppm NNK in the drinking water for the time indicated. Symbol designations are: ▨, O^2-pobdT; ■, 7-pobG; ▢, O^2-pobC; ▨, O^6-pobdG. Each value is the mean ± S.D. of single analyses of DNA samples from three rats per group. Reproduced from Ref. [99].
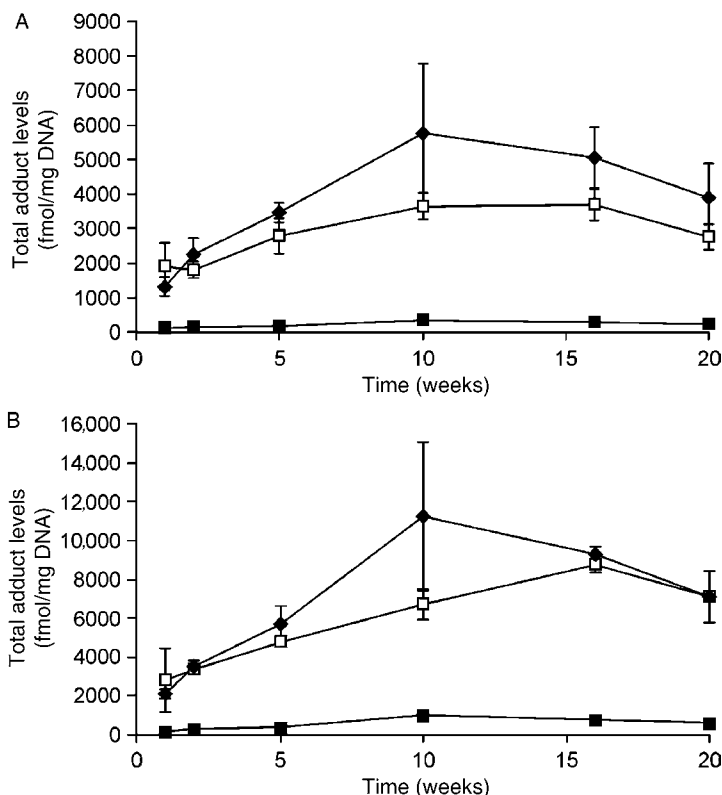
Figure 5   Time course of total levels of pyridyloxobutyl DNA adducts in (A) liver and (B) lung DNA of NNK- and (*R*)- and (*S*)-NNAL-treated rats. Animals receive 10 ppm of each compound in the drinking water for the time indicated. Symbol designations are: ◆, NNK, □, (*S*)-NNAL; ■, (*R*)-NNAL. Values are the sum of amounts of all POB-DNA adducts measured in lung or liver DNA at each time point ± S. D. Reproduced from Ref. [99].

4.3. Pyridylhydroxybutyl DNA damage

α-Methyl hydroxylation of NNAL results in the formation of 4-(3-pyridyl)-4-hydroxybutanediazonium ion which may react with DNA. Reaction of calf thymus DNA with the model pyridylhydroxybutylating agent, 4-(acetoxymethylnitrosamino)-1-(3-pyridyl)-1-butanol led to the detection of 7-[4-3-(pyridyl)-4-hydroxybut-1-yl]-guanine (7-phbG) [102], O^6-[4-3-(pyridyl)-4-hydroxybut-1-yl]-2′-deoxyguanosine (O^6-phbdG) [102], N^2-[4-3-(pyridyl)-4-hydroxybut-1-yl]-2′-deoxyguanosine (N^2-phbdG) [102], O^2-[4-3-(pyridyl)-4-hydroxybut-1-yl]-2′-deoxycytosine (O^2-phbdC) [89], O^2-[4-3-(pyridyl)-4-hydroxybut-1-yl]thymidine (O^2-phbdT) [89] (Figure 6).
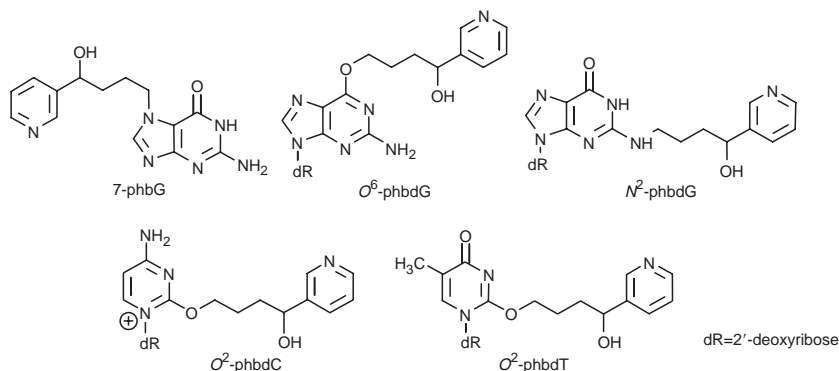
Figure 6 DNA adducts observed when 4-(acetoxymethylnitrosamino)-1-(3-pyridyl)-1-butanol was reacted with calf thymus DNA.

A comprehensive investigation of the presence of these adducts in NNK- or NNAL-treated animals has not been performed.

4.4. OPB-derived DNA damage

OPB is formed along with methanediazohydroxide when 4-OHNNK degrades. OPB induces DNA damage [73] but it is not known if it induces this damage as a result of direct adduct formation or as a result of DNA repair inhibition. The ability of OPB to bind covalently to DNA has not been investigated. It induced sister chromatid exchanges (SCEs) at concentrations from 0.01 to 0.5 mM in V79 cells [73]. DNA single strand breaks (SSB) were observed at concentrations from 0.05 to 1 mM in V79 cells and greater than 0.5 mM in hepatocytes [73–75]. Unlike NNK–induced SSB, this damage was stable to increases in pH. Therefore, it is likely that OPB does not contribute greatly to the SSB observed in NNK-treated tissues.

4.5. Formaldehyde-derived DNA damage

Formaldehyde is formed during the decomposition of 4-OHNNK along with 4-(3-pyridyl)-4-oxobutanediazohydroxide. Formaldehyde damages DNA [71,103], inducing SSB [74] as well as specific adducts [104,105]. It reacts with DNA *in vitro* with the exocyclic amino groups of 2′-deoxyadenosine (dA), 2′-deoxycytidine (dC) and 2′-deoxyguanosine (dG) to form the following adducts in decreasing order: N^6-hydroxymethyl-2′-deoxyadenosine (N^6-HOCH$_2$-dA, Figure 2) $>>$ N^4-hydroxymethyl-2′-deoxycytidine $>$ N^2-hydroxymethyl-2′-deoxyguanosine [104,105]. These initial adducts lead to the formation of crosslinks with exocyclic amino groups of

dA, dC, or dG [105–109]. The major crosslink detected at low concentrations of formaldehyde is a dA–dA crosslink (dA-CH$_2$-dA, Figure 2) [105].

Evidence for the formation of N^6-HOCH$_2$-dA in lung and liver DNA from NNK-treated rats was obtained with a sensitive LC-MS/MS assay [110]. Significant levels of dA-CH$_2$-dA were observed in liver but not lung DNA from these animals [110]. The levels of the formaldehyde derived adducts were comparable to the levels of several pyridyloxobutyl DNA adducts detected in these tissues (Table 2) [110]. Subsequent studies indicated that formaldehyde adducts were also formed in DNA treated with the model pyridyloxobutylating agent, NNKOAc *in vitro* [105]. These data indicate that α–hydroxylation generates two reactive species, the diazonium intermediate as well as an aldehyde. The contribution of the aldehyde to the mutagenic and carcinogenic activity of nitrosamines requires further investigation.

4.6. Other NNK-induced DNA damage

An increase in oxidative damage to lung DNA was observed in rats and mice treated with NNK [111]. How NNK induces oxidative DNA damage is not known.

NNK (0.39 mmol/kg) induced SSB in livers of rats and hamsters [112]. These SSBs persisted up to 4 weeks post injection. Similar results were obtained with dimethylnitrosamine (up to 3 weeks) [112]. NNK induced SSB in hepatocytes. This damage show increased lability with increasing pH [74,75]. *In vitro* studies indicated that both the methylation and the pyridyloxobutylation pathways will generate SSB in DNA [94]. NNKOAc-induced breaks occurred at all four bases in decreasing order guanine > adenine > cytosine > thymine whereas methylation–induced SSB occurred primary at guanine residues [94]. While the methyl derived SSB are likely caused by the depurination of 7-mG, the mechanism by which the pyridyloxobutylation pathway causes SSBs requires further investigation.

5. MUTAGENIC ACTIVITY OF NNK METABOLITES

NNK requires metabolic activation to exert its mutagenic properties [113–116]. α–Deuterium substitution impacts the mutagenic activity of NNK in *Salmonella typhimurium* tester strains TA1535 and TA100 [113]. Deuteration of the methyl group completely blocked the mutagenic activity of NNK whereas [4,4-^{2}H]NNK was equal in activity to unlabeled NNK. Consistently, the model pyridyloxobutylating agent, 4-carbethoxynitrosamino-1-(3-pyridyl)-1-butanone, is a more active mutagen than the model methylating agent, carbethoxynitrosaminomethane [113]. These data suggest that pyridyloxobutyl DNA adducts may be more mutagenic than methyl DNA adducts in bacteria.

In confirmation of the role of cytochrome P-450 in the activation of NNK to a mutagenic metabolite, NNK is active in several strains of *Salmonella typhimurium* YG7108 coexpressing human P450s along with cytochrome P-450 reductase [115]. Since *Salmonella typhimurium* YG7108 lacks both the *ogt* and *ada* O^6-alkylguanine DNA alkyltransferase genes, these strains lack efficient repair of O^6-alkylguanine adducts and will be sensitive to the mutagenic effects of both α-activation pathways of NNK. In this system, the activity of NNK was greatest in the strain expressing CYP1A2. The relative mutagenic activity of NNK was affected by the various P450s in the following order: CYP1A2 > CYP1A1 > CYP1B1 = CYP2A6 > CYP2C19 > CYP3A4. NNK is also mutagenic in human lymphoblastoid cells transfected with cytochrome P450s [116]. The relative order of activation was CYP2A6 = CYP1A2 > CYP2E1 > 2D6.

5.1. Mutation spectrum

The mutational spectrum generated by CYP2A6 catalyzed activation of NNK was determined in the *gpt* gene of AS52 cells, a transgenic Chinese hamster ovary (CHO) cell line. In this cell line, the majority of mutations were GC to AT transitional mutations (84%). Only 5% of the mutations were transversion mutations, with the majority of these being GC to TA mutations.

NNK increases the mutagenic frequency in the *lacZ* and *cII* genes in the lungs and livers of Muta mouse in a dose dependent manner [117]. In this model, NNK induced an increased rate of G–C to A–T transitional mutations at non CpG sites. Transitional mutations were also observed in AT base pairs. In addition, there was a greater than 40-fold increase in A–T to T–A mutations in both lungs and liver. There was also a significant increase in transversion mutations (AT to GC, AT to CG, and GC to CG). There was a 5-fold increase in G–C to T–A transversion mutations in the liver but not lungs of these animals.

Similar trends were observed in the lungs and livers of NNK-treated Big Blue C57BL/6 mice (transgenic for *lacI*) [118]. NNK induced about a 10-fold increase in the mutation frequency in the lungs and livers of these animals. In the lungs, there was a significant shift in the amount of G–C to A–T transitional mutations. Increases in transversion mutations (A–T to T–A, AT to CG, and GC to TA) were also observed.

The complexity of the mutational spectrum induced by NNK contrasts significantly from that generated by compounds that only generate methanediazonium ion. For example, dimethylnitrosamine primarily induces GC to AT mutations at nonCpG sites in the *lacZ*, *cII*, or *lacI* genes from *lacZ* or *lacI* transgenic mice (mutamouse and Big Blue mouse, respectively)

[119–121]. Increases in AT to TA mutations were also observed in DMN treated mice relative to controls [119,121].

NNK-induced mutational spectra also differ substantially from that induced by formaldehyde. Formaldehyde induces predominantly transversion mutations in the *hprt* gene at AT base pairs (AT to CG, AT to TA, or GC to TA) in CHO and human cells [122,123]. Formaldehyde induced DNA–protein crosslinks, SCEs and micronuclei but not point mutations in V79 cells [124] and small scale deletions and chromosomal rearrangements were the major mutations observed in the mouse lymphoma assay [125]. The mutagenic activity of OPB has not been determined.

5.2. Mutagenic activity of NNK-derived DNA adducts

The mutagenic activity of various methyl adducts has been investigated with site-specific substrate. O^6-mG induces primarily GC to AT transition mutations [126,127]. Site specifically incorporated O^4-mT induces primarily TA to CG [126,127]. In addition to TA to CG mutations, a small amount of TA to AT mutations were also induced by this adduct in LoVo cells, a mismatch repair defective human colon tumor cell line [126]. While O^4-mT is more mutagenic than O^6-mG [126,127], the levels of O^6-mG are much higher in NNK-treated rodents [77–81]. Given the dominant mutations observed in *lacZ* or *lacI* transgenic mice treated with methylating agents are GC to AT transitional mutations, O^6-mG is thought to be the dominant mutagenic methyl adduct formed from NNK [119–121].

The only pyridyloxobutyl DNA adduct that has been investigated for its mutagenic activity is O^6-pobG. This adduct induces primarily GC to AT mutations but it also induces a small amount of GC to TA transversions and deletions in human cells [128]. This adduct is almost completely mutagenic in *E. coli* when presented in a gapped vector [128], consistent with the inability of bacterial AGTs to repair this bulky O^6-alkylG adduct [129]. NNKOAc induced G–C to A–T transitions as well as G–C to T–A transversions in the 12th codon of the K-*ras* oncogene of tumors in A/J mice [130]. Therefore, the formation of O^6-pobG is hypothesized to contribute significantly to the mutagenic activity at GC base pairs for the pyridyloxobutylation pathway. Investigation into the mutagenic properties of other pyridyloxobutyl DNA adducts is required to have a more complete understanding of the mechanisms of mutagenesis by pyridyloxobutylating nitrosamines.

6. DNA Adduct Repair

Inadequate removal of DNA damage results in increased rates of mutagenesis and consequently, increased likelihood of cancer development. There are multiple repair pathways that protect a cell against the mutagenic

and carcinogenic activity of NNK metabolites. There are at least three different pathways that are involved in the repair of tobacco-related DNA damage. These include DNA adduct reversal by alkyltransferases or excision of the DNA damage from the DNA in base excision repair or nucleotide excision repair. Mismatch repair also plays an important role in the recognition of mismatched O^6-mG adducts.

6.1. O^6-alkylguanine DNA alkyltransferase

O^6-alkylG adducts are repaired by AGT in a reaction that involves transfer of the alkyl group from the O^6-position of guanine to a cysteinyl residue on the protein ([131] and references therein). This transfer reaction renders the protein inactive. The alkylated protein undergoes a conformational change [132], which leads to its degradation [133]. A consequence of this repair mechanism is that the constitutive levels of AGT determine the initial repair capacity of a cell. Therefore, AGT levels in a cell affect the rate of repair of this class of mutagenic DNA damage.

NNK generates two AGT substrate adducts, O^6-mG and O^6-pobG [90,129,131,134,135]. All AGT orthologs repair O^6-mG efficiently [131]. The ability of these proteins to repair the larger O^6-pobG is highly dependent on protein structure [129]. Rodent AGTs repair O^6-pobG at a rate similar to O^6-mG whereas human AGT repairs O^6-pobG more slowly. This ability of the rodent protein to accommodate such large structural differences likely results from the additional amino acid residue (Gly166) in the binding pocket of the rodent proteins [136]. The inability of bacterial AGTs to repair this damage is related to the much smaller binding pocket in these orthologs [137]. Therefore, the steric constraints of an AGT's active site will determine whether it can repair a bulky O^6-alkylG adduct.

There are two known human AGT variants, G160R and I143V/ K178R, in which the variation occurs in the binding pocket of the protein. G160R is a mutant hAGT predominantly found in Asian populations [138–140]. Another variant, I143V/K178R, was associated with a 2-fold increase in lung cancer risk in a hospital based case–control study [140] as well as an increase risk of lung cancer risk in nonsmokers exposed to second-hand smoke [141]. A recent study provided support for the hypothesis that genetic variations in this protein may affect an individual's response to NNK's genotoxic effects. Increased NNK-induced chromosomal aberrations were observed in lymphocytes from individuals that were homozygous variant as compared to those who had the wild-type genotype [142].

Our laboratory has investigated the ability of expressed human AGT variant proteins to repair O^6-mG relative to O^6-pobG. G160R repaired O^6-pobG very slowly [129] whereas the other human AGTs repaired O^6-mG twice as fast O^6-pobG. More in-depth studies indicated that AGT-mediated repair of O^6-pobG was more profoundly influenced by

sequence context than that of O^6-mG with the I143V/K178R variant less sensitive to the effects of sequence context than the wt or L84F proteins [143]. These studies indicate that the sequence dependence of O^6-pobG repair by human AGT varies with subtle changes in protein structure. Whether this subtle functional difference can influence an individual's susceptibility to the mutagenic and carcinogenic properties requires further investigation.

The mutagenic activity of O^6-mG or O^6-pobG is enhanced when cells are pretreated with the AGT depletor, O^6-benzylguanine [128,144], indicating that this repair pathway is important in protecting against the mutagenic activity of these adducts. Expression of AGT protected against cells against the mutagenic effects of model methylating agents [145,146]. Expression of human AGT protected against the mutagenic effects of NNKOAc in *Salmonella typhimurium* [102,147]. Expression of human AGT did not significantly impact the mutagenic activity of NNKOAc in CHO cells but it altered the mutagenic spectrum of this compound (Li, Pegg, and Peterson, unpublished results). The percentage of GC to AT transitional mutations were reduced in the cells expressing AGT, consistent with the repair of O^6-pobG.

6.1.1. *In vivo* studies

AGT repairs both O^6-mG and O^6-pobG *in vivo*. Levels of O^6-pobG were higher in mice receiving both NNKOAc and the AGT depletor, O^6-benzylguanine [135], indicating that AGT is a significant repair pathway for O^6-pobG *in vivo*. Levels of these adducts were higher in both lung and liver of AGT knockout mice relative to wild-type animals following multiple doses of NNK [118]. In addition, AGT is depleted in tissues from NNK-treated animals, consistent with the hypothesis that this repair pathway is involved in the repair of NNK-induced DNA damage. AGT levels are depleted in Clara cells from NNK-treated rats [148] and lungs and liver of A/J mice [149]. While liver AGT levels recovered to control values by 96 h after exposure, AGT activity remained depressed in the lungs of NNK-treated mice [149]. These results indicate that the lung will be more susceptible to the mutagenic effect of NNK-derived O^6-alkylguanine adducts.

AGT has some protective role in the mutagenic activity of NNK *in vivo*. Knockout of AGT caused a trend towards increased mutation frequency in liver of Big Blue mice treated with NNK [118]. A smaller trend was observed in the lungs of these animals. The absence of this repair protein resulted in a significant increase in the number of GC to AT transitional mutations induced by NNK [118]. Conversely, NNK is a less potent lung carcinogen in transgenic mice containing the human AGT transgene [150]. Together, these data provide support for the hypothesis that AGT is an important protector against the mutagenic properties of NNK.

6.2. Base excision repair

BER is an important pathway for the repair of oxidized DNA bases such as 8-oxoguanine and oxidized pyrimidines, SSBs and small alkyl guanine damage [151,152]. Therefore, it is likely that this pathway is important in the repair of NNK-derived methyl DNA damage. The major methyl adducts repair by this pathway include 7-mG, N^3-methyladenine, O^2-methylcytidine, and O^2-methylthymidine [153].

Little is known about the involvement of BER in the repair of pyridyloxobutyl DNA adducts. Studies in CHO cells lacking an important BER protein, XRCC1, were more sensitive to the cytotoxic and mutagenic properties of NNKOAc (Li and Peterson, unpublished results). This sensitivity is derived from either unrepaired pyridyloxobutylated bases or SSBs induced by this model pyridyloxobutylating agent.

6.3. Nucleotide excision repair

Methyl DNA damage is not significantly repaired by NER. Evidence is accumulating that this is an important repair pathway for some pyridyloxobutyl DNA adducts. Pyridyloxobutyl DNA adducts are repaired by nucleotide excision repair as judged by the ATP-dependent incorporation of $[\alpha^{32}P]dTTP$ in to plasmid DNA upon incubation with extracts from NER competent and deficient human lymphoid cell lines [154]. Cell extracts from XPA and XPC-deficient cell lines were less active in their ability to repair pyridyloxobutylated DNA. The cytotoxicity of NNKOAc (25 μM) was modestly greater in XPA (2.3-fold) or XPC (1.5-fold) deficient cell lines relative to control. The involvement of NER on the repair of specific pyridyloxobutyl DNA adducts was not determined in this study.

Studies in our laboratory indicate that the major adduct repaired by NER in CHO cells is O^2-pobdT (Li and Peterson, unpublished results). Knockout of the NER pathway led to a modest increase in mutagenicity and toxicity induced by NNKOAc, suggesting that O^2-pobdT is a mutagenic adduct (Li and Peterson, unpublished results). O^6-pobG is a weak substrate for the CHO and human NER pathway (Li, Reardon, Sancar, and Peterson, unpublished results). The less stable pyridyloxobutyl adducts, 7-pobG and O^2-pobC, do not appear to be repaired by this pathway in CHO cells (Li and Peterson, unpublished results).

6.4. Mismatch repair

Mismatch repair influences the mutagenic activity of O^6-mG [126,155]. This pathway recognizes O^6-mG-thymidine mismatches and triggers apoptosis in the cases where O^6-mG is not repaired [156]. Therefore, in the absence of mismatch repair, these mismatches proceed through cell division

undetected. Methylating agents are more carcinogenic in the absence of functional mismatch repair [155,157], consistent with the involvement of O^6-mG in the carcinogenic properties of these compounds. It is not known if mismatch repair is involved in the recognition of mispaired pyridyloxobutyl DNA adducts during DNA replication.

6.5. NNK-induced unscheduled DNA synthesis

NNK induces UDS in rabbit Clara cells and rat hepatocytes when incubated *in vitro* [158–160]. The pathway(s) generating the UDS is not clear. Both methylating and pyridyloxobutylating agents can increase UDS in hepatocytes indicating that both pathways of NNK activation can trigger this cellular response [160]. The α, δ, and ε polymerase inhibitors, aphidicolin and arabinocytidine, were capable of completely blocking NNK- and NNKOAc-induced UDS in hepatocytes [160]. The polymerase β inhibitor, dideoxythymidine, was less effective at inhibiting this process [160]. These data are consistent with the involvement of excision repair in the response to NNK-derived DNA damage.

7. RELATIVE ROLE OF α-HYDROXYLATION PATHWAYS IN THE CARCINOGENIC PROPERTIES OF NNK

There is strong evidence that cytochrome P-450 catalyzed α-hydroxylation of NNK is required for tumor formation. Selective knockout of pulmonary cytochrome P450 reductase blocked pulmonary tumor formation in NNK-treated mice [46], indicating that cytochrome P450 catalyzed oxidation of NNK is critical for tumor formation. The relative contribution of each α-hydroxylation pathway to the overall carcinogenic properties of NNK is species dependent. The available experimental data is discussed below.

7.1. A/J mouse studies

In A/J mice, numerous studies indicate that DNA methylation is the critical pathway for NNK-induced lung tumorigenesis [81,161]. Pyridyloxobutylating compounds are only weak lung carcinogens in this model [81]. Deuterium substitution of the methylene but not the methyl protons of NNK significantly reduced the pulmonary carcinogenic effects of NNK in A/J mice [161]. In fact, deuteration of the methyl group resulted in a significant enhancement of the lung tumorigenic activity over the unlabeled compound. Consistently, the levels of pulmonary O^6-mG were substantially lower in [4,4-^{2}H$_2$]NNK-treated A/J mice. More recent studies demonstrated that (4R)-[4-^{2}H$_1$]NNK was 2-fold less carcinogenic than

(4*S*)-[4-^{2}H$_1$]NNK or unlabeled NNK [162]. The (4*R*)-deuterium substitution also led to a 2-fold reduction in pulmonary levels of 7-mG and O^6-mG. Kinetic studies with expressed mouse P450 2A4 and 2A5 demonstrated that these enzymes selectively extracted the 4-pro-(*R*)-hydrogen of NNK [162].

The formation and persistence of O^6-mG is critical for NNK–induced lung tumor formation in A/J mice. While O^6-mG is efficiently repaired in livers of NNK-treated mice, it persists for at least 2 weeks in lung DNA [81,149]. Levels of O^6-mG in lung DNA are highly correlated to pulmonary tumorigenic activity in A/J mice [81,149]. These observations suggest that inefficient repair of O^6-mG, presumably by AGT, is linked to tumorigenic activity of NNK. This conclusion is supported by the observation that high levels of AGT protect against NNK–induced lung tumorigenesis; NNK is a less potent lung carcinogen in transgenic mice expressing the human AGT transgene [150].

K-*ras* mutation and activation is closely associated with pulmonary tumor formation in NNK-treated A/J mice [163,164]. Almost all of the mutations in K-*ras* in tumors from NNK-treated mice were GC to AT transitional mutations in the second base of the 12th codon, consistent with the formation of O^6-mG. NNKOAc induced G–C to T–A transversions as well as G–C to A–T transitions in the twelfth codon of the K-*ras* oncogene of tumors in A/J mice [130]. Together, these data indicates that metabolic activation of NNK to a DNA methylating agent is critical for lung tumor formation in the A/J mouse. As discussed below, the pyridyloxobutylation pathway seems to increase the carcinogenic properties of NNK's methylation pathway in this animal model [81,149].

7.2. Rat studies

In rats, the available experimental evidence is consistent with the hypothesis that both DNA methylation and DNA pyridyloxobutylation are important for tumor formation. Compounds that just generate DNA methyl adducts, such as dimethylnitrosamine, or generate pyridyloxobutyl DNA adducts without forming methyl DNA adducts are not potent lung carcinogens in rats [14,78]. In addition, [4,4-^{2}H$_2$]NNK and [C^{2}H$_3$]NNK were equally active as a pulmonary and liver carcinogen in F344 rats [165]. Higher levels of nasal cavity tumors were observed in [4,4-^{2}H$_2$]NNK-treated animals relative to [C^{2}H$_3$]NNK or NNK treated animals. Consistently, the levels of HPB-releasing adducts but not methyl DNA adducts were elevated in nasal cavity DNA isolated from [4,4-^{2}H$_2$]NNK-treated mice [166]. These results are consistent with the hypothesis that that DNA pyridyloxobutylation may be more important than DNA methylation for nasal cavity tumor formation.

Both methyl and pyridyloxobutyl DNA adducts persist in lung DNA following NNK treatment. O^6-mG persists in F344 rat derived Clara cells

for up to 8 days after NNK treatment (10 mg/kg/day for 4 days) whereas it is efficiently removed from other lung cell types [148]. A strong correlation between tumor formation and levels of O^6-mG in Clara cells, but not type II cells, has been observed in NNK–treated rats [148]. Levels of HPB-releasing adducts in Type II cells are strongly correlated to lung tumor formation in F–344 rats [167]. A correlation was not observed between HPB-releasing adduct levels in Clara cells and tumor formation. Since NNK-induced lung tumors arise from Type II cells [46], these data suggest that there may be signals from initiated Clara cells that influence NNK–triggered carcinogenesis in Type II cells [79]. More recent studies indicate that O^2–pobdT is the major pyridyloxobutyl DNA adduct in lung DNA when rats are chronically treated with NNK in the drinking water. More in–depth studies are required to determine the contribution of each adduct to the overall carcinogenic properties of NNK in rats.

7.3. Role of NNAL in NNK-induced carcinogenesis

The observation of comparable levels of pyridyloxobutyl DNA adducts in the lungs of (S)–NNAL–treated and NNK–treated rats suggests that the oxidation of NNAL back to NNK and the subsequent generation of NNK–derived adducts contributes significantly to the carcinogenic properties of NNAL [99]. There was a shift in time course of pulmonary adduct formation in the (S)–NNAL–treated animals relative to that observed in NNK–treated animals (Figure 5). This delay in adduct formation was proposed to result from tissue-specific retention of (S)–NNAL and its gradual release from a compartment in the lung [99]. The stereoselective retention of (S)–NNAL in rat lung is further supported by pharmacokinetic studies [34,37]. The mechanism of sequestration is unknown but thought to involve selective binding of (S)–NNAL to unknown receptors within the lung [34,37,99]. Together, these data have led to a proposed mechanism for the involvement of NNAL in NNK–induced carcinogenesis as shown in Figure 7. Reduction of NNK to (R)–NNAL is thought to represent
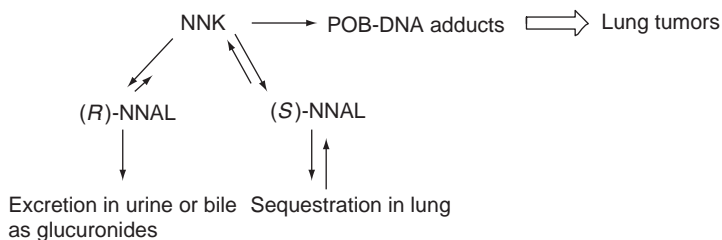
Figure 7 Proposed mechanism for the involvement of NNAL in NNK lung tumor–igenesis in rodents. Reproduced from Ref. [99].

a detoxification pathway as this NNK metabolite is a good substrate for glucuronidation and subsequent excretion. Formation of (S)-NNAL results in tissue selective sequestration followed by slow release. This metabolite can then be reoxidized by cytochrome P-450 to back to NNK for metabolism via α-hydroxylation to generate mutagenic DNA adducts.

8. Co-Carcinogenic Activity of NNK and its Metabolites

Several studies have produced data which suggest that NNK and its metabolites can enhance the genotoxic effects of NNK-derived DNA damage. As discussed below, one mechanism by which this occurs is through the ability of metabolites to influence repair of specific adducts. A second mechanism is derived through tumor promotional activity of the parent molecule.

8.1. Interaction between DNA alkylation pathways

Studies in A/J mice indicate that there is an interaction between the two DNA alkylation pathways derived from NNK [81,149]. The model methylating agent, acetoxymethylmethylnitrosamine (AMMN) was more tumorigenic when given in combination with the model pyridyloxobutylating agent, NNKOAc. The ability of NNKOAc to increase the tumorigenic activity of AMMN was attributed to its ability to enhance the persistence of O^6-mG in lung DNA [81]. While there are multiple mechanisms by which pyridyloxobutylation could lead to increased persistence of O^6-mG, the available evidence supports effects on DNA repair [81,149,168].

Both O^6-pobG and O^6-mG are substrates for AGT as discussed above. Studies with purified proteins indicate that these adduct compete efficiently with one another for repair by AGT variants [129]. Therefore, the presence of both O^6-alkylguanine adducts will lead to their increased persistence in lung DNA. However, the *in vivo* levels of O^6-pobG are not sufficient to explain the persistence of O^6-mG in NNK-treated mouse lung. O^6-pobG was not detected in lung DNA from [5-³H]NNK-treated mice 24 h after exposure; the limits of detection were ~0.5 pmol/μmol guanine [135]. This compares to 14 pmol O^6-mG/μmol guanine at the same dose and time point [81]. In addition, O^6-pobG was also not detected in lung DNA from [5-³H] NNKOAc-treated mice [135]. The low levels of this adduct likely result from efficient repair by AGT since coadministration of the AGT depletor, O^6-benzylguanine with NNKOAc, increased lung DNA adduct levels to 1.5 pmol O^6-pobG/μmol guanine. This dose of NNKOAc (4.2 μmol) doubled O^6-mG levels observed in lungs of 1.0 μmol AMMN-treated

mice (from 20 pmol O^6-mG/μmol guanine to 41 pmol O^6-mG/μmol guanine at 4 h) when the two compounds were coadministered [81]. Such a large increase in O^6-mG levels cannot be fully explained by competition between O^6-mG and O^6-pobG for reaction with AGT given the low levels of O^6-pobG relative to O^6-mG in these animals. Our laboratory is currently exploring other mechanisms by which the pyridyloxobutylating pathway can enhance the carcinogenic activity of the methylating pathway in A/J mice.

8.2. Inhibition of DNA repair by NNK aldehyde metabolites

The aldehyde metabolites formed during NNK metabolism are known inhibitors of AGT activity. Formaldehyde inhibited AGT and increased the mutagenicity of *N*-methylnitrosourea (MNU) in normal human pulmonary fibroblasts [71]. OPB inhibits AGT in rat hepatocytes [76]. Both formaldehyde and OPB synergistically increased the number of SSB induced by MNU [169]. Formaldehyde was more effective in this enhancement than OPB. Studies from our own laboratory suggest that the aldehyde decomposition product can influence the mutagenic activity of methanediazohydroxide (Li, Brown, Cummings, Sungur, Vu and Peterson, unpublished results). The precise mechanism responsible for these effects is not clear but likely involves interference with DNA repair pathways such as AGT. Together, these observations suggest that formaldehyde and OPB interfere with the repair of methyl DNA damage. The effects of the aldehyde metabolites on the repair of pyridyloxobutyl DNA damage have not been investigated.

8.3. Tumor promoting activity of NNK

NNK induces cell survival and proliferation of a number of different cell lines [170–175]. These effects are mediated through two different types of receptors: β-adrenergic receptors and acetyl choline receptors as described below.

NNK is a high affinity agonist for both β_1 and β_2-adrenergic receptors [170,171]. NNK binding to these receptors triggers the release of arachadonic acid, leading to DNA synthesis and cell proliferation [170,171]. These effects were reversed by β-adrenergic antagonists, cyclooxygenase inhibitors or lipoxygenase inhibitors. Consistent with the importance of this pathway to the tumorigenic effects of NNK is the observation that nonsteroidal anti-inflammatory drugs are effective blockers of NNK-induced lung tumorigenesis in mice [176–179]. There are multiple signaling pathways that are activated as a result of NNK binding to the β-adrenergic receptors (Figures 8A and B) [180]. In one pathway, NNK binding to the β-adrenergic receptors activates GTP-binding proteins (G-proteins), triggering the activation of adenylyl cyclase and cyclic AMP (cAMP) leading to the activation of
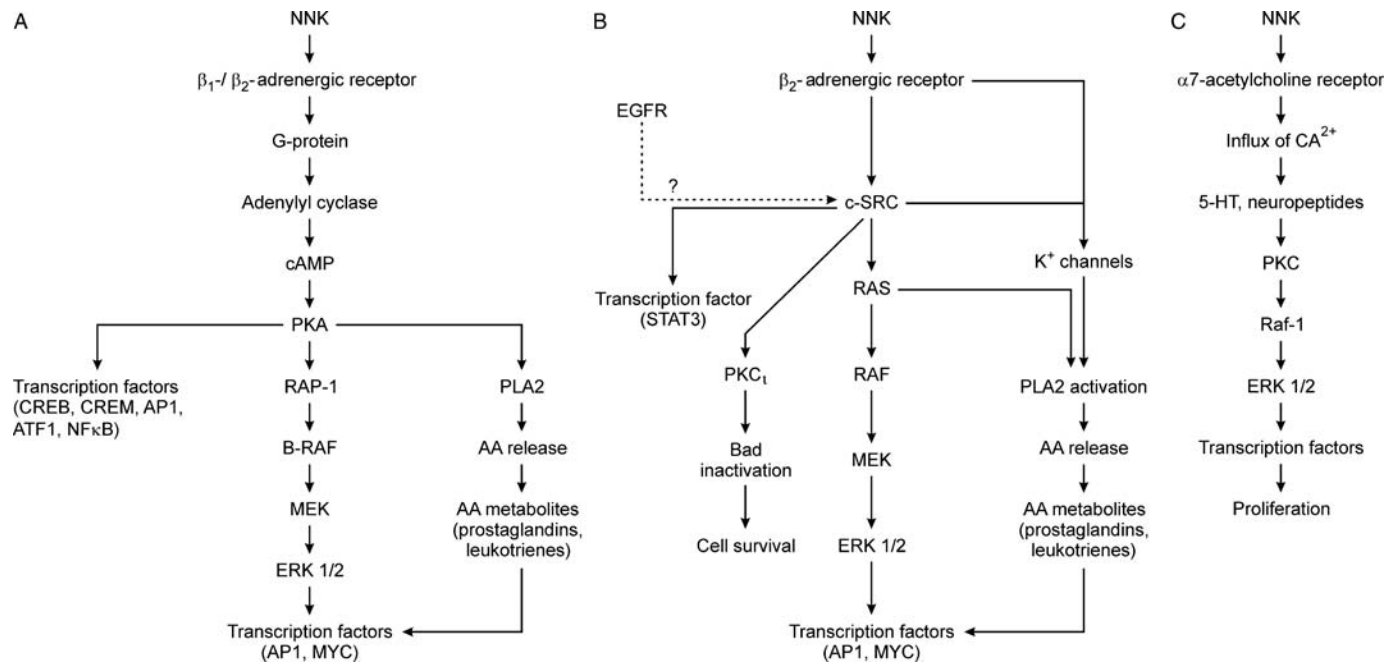
Figure 8 Potential mitogenic signal transduction pathways activated by the binding of NNK to β-adrenergic receptors (A and B) or α7-cholinergic receptors. Adapted from Refs. [180,181,183].

protein kinase A (PKA) (Figure 8A). PKA, then activates various transcription factors that result in increased cell proliferation. PKA activation is also an important trigger for the release of arachidonic acid (AA) from cell–membrane phospholipids which also leads to cell proliferation signals. The precise pathway depends on the cell type [180]. A second major pathway involves the activation of the kinase c-SRC as a result of NNK binding to β–adrenergic receptors (Figure 8B) [180]. This pathway triggers the activation of variety of transcription factors that control cell proliferation and survival. Recently, interaction of NNK with β–adrenergic receptors induced survival of pulmonary adenocarcinoma cells in a mechanism that involves the c-Src/PKCι/Bad signaling pathway (Figure 8B) [181].

NNK is also a site-selective high–affinity agonist for the α7 subunit of the acetylcholine receptor (α7-AChR) [172–174]. Interaction with this receptor increased both cell proliferation and cell survival [172–175] as well as induced a transformed phenotype in several cell lines [174,175]. The signaling mechanisms downstream of α7-AChR likely involved several pathways. NNK binding to α7-AChR led to the activation of the serine/threonine kinase, Akt [174] as well as a Raf-1/MAPK/c-Myc signaling pathway (Figure 8C) [182]. In addition, NNK triggered the phosphorylation of both Bcl2 and c-Myc which promotes functional cooperation of these two proteins resulting in increased cell survival and proliferation in human lung cancer cells [183]. Bcl2 and c-Myc phosphorylation and cell growth were both blocked when a α7-AChR selective inhibitor (α-bungarotoxin) was included.

These receptor mediated activities of NNK indicate that, in addition to generate DNA damage, it likely acts as a tumor promoter. The effects will be mediated via either the β–adrenergic or acetyl choline receptors depending on the cell type. Adenocarcinomas express significant levels of the β–adrenergic receptors whereas small cell carcinomas express acetyl choline receptors [182]. Normal human bronchial epithelial cells (which are the precursors to squamous cell carcinomas) and small airway epithelial cells (which are precursor cells for adenocarcinomas) express acetyl choline receptors and are sensitive to NNK-mediated acetyl choline derived cell proliferation [174]. These cells are capable of activating NNK to DNA reactive metabolites, resulting in mutations. Then, the initiated cells will be subjected to continuous growth stimulation from the promotional effects of NNK as well as those of other tobacco constituents.

9. SUMMARY

Our understanding of the molecular mechanisms of NNK-induced pulmonary carcinogenesis in rodents has increased substantially in the past 5–10 years. NNK requires metabolic activation to elicit its carcinogenic

properties. Both DNA alkylation pathways are important to the carcinogenic properties of this potent lung carcinogen. The DNA methylation pathway is well-characterized and is a critical pathway for the elicitation of NNK-induced pulmonary tumors in A/J mice. The pyridyloxobutylation pathway likely contributes to the mutagenic properties in this animal model by influencing the repair of the mutagenic O^6-mG through several possible mechanisms. The pyridyloxobutylion pathway appears to play an important role in the initiation of lung tumors in rats. Now that specific pyridyloxobutyl DNA adducts have been characterized, more specific details regarding the mutagenic properties of this pathway can be acquired. It is clear that multiple pyridyloxobutyl DNA adducts contribute to the overall mutagenic properties of this compound. Which adduct(s) is (are) more important will likely depend on particular situations. For example, O^6-pobG is likely responsible for the GC to AT transitional mutations triggered by the pyridyloxobutylation pathway. So this adduct may be responsible for GC to AT mutations observed in activated K-*ras* associated with pyridyloxobutylating agents. Other adducts, like O^2-pobdT, are likely responsible for other mutations (i.e., AT to TA transversion). It is important that the mutational specificity of these newly identified adducts be determined. Recent data also indicate the importance of defining the role the aldehyde metabolites of NNK play in the mechanism of tumor induction of this compound. These compounds are likely to enhance as well as contribute to the mutagenic properties of the alkylation pathways. It is also clear from the accumulating data that NNK is an effective promoter of cells which have been initiated by its genotoxic metabolites. Further investigations into the biochemical mechanisms of tumor promotion by this potent carcinogen will provide insights into possible chemoprevention strategies. The identification of all the important steps in the activation, formation, and cellular responses to NNK and its metabolites are critical for our application of the laboratory animal studies to humans for adequate risk assessment. While most lung cancers are attributed to smoking, only 15% of smokers get lung cancer [184]. Genetic variations in the proteins involved in every step in this process likely influence a person's risk. Therefore, genetic susceptibility is likely to be critical in the determination of lung cancer risk in humans. Therefore, it is critical that we establish the biochemical details of NNK-induced carcinogenesis so that we can determine the genetic factors responsible for increased risk in susceptible populations.

ACKNOWLEDGMENTS

REFERENCES

[1] International Agency for Research on Cancer, Tobacco smoke and involuntary smoking monographs.iarc.fr/htdocs/monographs/vol83/(Apr. 16, 2008).

[2] World Cancer Research Fund/American Institute for Cancer Research, Food, nutrition and the prevention of cancer: A global perspective, American Institute for Cancer Research, Washington, DC, (1997).

[3] The Centers for Disease Control Cigarette smoking-related mortality, http://www.cdc.gov/tobacco/data_statistics/Factsheets/tobacco_related_mortality.htm Apr. 20, 2008.

[4] D.R. Shopland, Tobacco use and its contribution to early cancer mortality with a special emphasis on cigarette smoking, Environ. Health Perspect. 103(Suppl. 8), (1995) 131–142.

[5] S.S. Hecht, Tobacco smoke carcinogens and lung cancer, J. Natl. Cancer Instit. 91 (1999) 1194–1210.

[6] S.S. Hecht, D. Hoffmann, Tobacco-specific nitrosamines: An important group of carcinogens in tobacco and tobacco smoke, Carcinogenesis 9 (1988) 875–884.

[7] S.S. Hecht, C.B. Chen, N. Hirota, R.M. Ornaf, T.C. Tso, D. Hoffmann, Tobacco specific nitrosamines: Formation from nicotine *in vitro* and during tobacco curing and carcinogenicity in strain A mice, J. Natl. Cancer Instit. 60 (1978) 819–824.

[8] S. Fischer, B. Spiegelhaler, R. Preussmann, Influence of smoking parameters on the delivery of tobacco-specific nitrosamines in cigarette smoke—a contribution to relative risk evaluation, Carcinogenesis 10 (1989) 1059–1066.

[9] S. Fischer, A. Castonguay, M. Kaiserman, B. Spiegelhalder, R. Preussmann, Tobacco-specific nitrosamines in Canadian cigarettes, J. Cancer Res. Clin. Oncol. 116 (1990) 563–568.

[10] S. Fischer, B. Spiegelhalder, R. Preussmann, Tobacco-specific nitrosamines in European and USA cigarettes, Arch. Geschwulstforsch. 60 (1990) 169–177.

[11] A.R. Tricker, C. Ditrich, R. Preussmann, *N*-nitroso compounds in cigarette tobacco and their occurrence in mainstream tobacco smoke, Carcinogenesis 12 (1991) 257–261.

[12] E.J. Mitacek, K.D. Brunnemann, D. Hoffmann, T. Limsila, M. Suttajit, N. Martin, L.S. Caplan, Volatile nitrosamines and tobacco-specific nitrosamines in the smoke of Thai cigarettes: A risk factor for lung cancer and a suspected risk factor for liver cancer in Thailand, Carcinogenesis 20 (1999) 133–137.

[13] E.J. Mitacek, K.D. Brunnemann, M. Suttajit, N. Martin, T. Limsila, H. Ohshima, L.S. Caplan, Exposure to *N*-nitroso compounds in a population of high liver cancer regions in Thailand: Volatile nitrosamine (VNA) levels in Thai food, Food Chem. Toxicol. 37 (1999) 297–305.

[14] S.S. Hecht, Biochemistry, biology, and carcinogenicity of tobacco-specific *N*-nitrosamines, Chem. Res. Toxicol. 11 (1998) 560–603.

[15] S.S. Hecht, C.B. Chen, T. Ohmori, D. Hoffmann, Comparative carcinogenicity in F344 rats of the tobacco specific nitrosamines, N'-nitrosonornicotine and 4-(*N*-methyl-*N*-nitrosamino)-1-(3-pyridyl)-1-butanone, Cancer Res. 40 (1980) 298–302.

[16] A. Rivenson, D. Hoffmann, B. Prokopczyk, S. Amin, S.S. Hecht, Induction of lung and exocrine pancreas tumors in F344 rats by tobacco-specific and areca-derived *N*-nitrosamines, Cancer Res. 48 (1988) 6912–6917.

[17] S.S. Hecht, M.A. Morse, S.G. Amin, G.D. Stoner, K.G. Jordan, C.I. Choi, F.L. Chung, Rapid single dose model for lung tumor induction in A/J mice by 4-(methylnitrosamino)-1-(3-pyridyl)-1-butanone and the effect of diet, Carcinogenesis 10 (1989) 1901–1904.

[18] M.J. Thun, C.A. Lilly, J.T. Flannery, E.E. Calle, W.D. Flanders, C.W. Heath, Cigarette smoking and changes in the histopathology of lung cancer, J. Natl. Cancer Instit. 89 (1997) 1580–1586.

[19] S.S. Hecht, S.G. Carmella, S.E. Murphy, S. Akerkar, K.D. Brunnemann, D. Hoffmann, A tobacco-specific lung carcinogen in the urine of men exposed to cigarette smoke, N. Engl. J. Med. 329 (1993) 1543–1546.

[20] W.D. Parsons, S.G. Carmella, S. Akerkar, L.E. Bonilla, S.S. Hecht, A metabolite of the tobacco-specific lung carcinogen 4-(methylnitrosamino)-1-(3-pyridyl)-1-buta-none in the urine of hospital workers exposed to environmental tobacco smoke, Cancer Epidemiol. Biomark. Prev. 7 (1998) 257–260.

[21] G.M. Lackmann, U. Salzberger, U. Tollner, M. Chen, S.G. Carmella, S.S. Hecht, Metabolites of a tobacco-specific carcinogen in urine from newborns, J. Natl. Cancer Instit. 91 (1999) 459–465.

[22] S.S. Hecht, Carcinogen biomarkers for lung or oral cancer chemoprevention trials, IARC Sci. Publ. 154 (2001) 245–255.

[23] S.G. Carmella, K.A. Le Ka, P. Upadhyaya, S.S. Hecht, Analysis of N- and O-glucuronides of 4-(methylnitrosamino)-1-(3-pyridyl)-1-butanol (NNAL) in human urine, Chem. Res. Toxicol. 15 (2002) 545–550.

[24] S.S. Hecht, Human urinary carcinogen metabolites: Biomarkers for investigating tobacco and cancer, Carcinogenesis 23 (2002) 907–922.

[25] K.E. Anderson, J. Kliris, L. Murphy, S.G. Carmella, S. Han, C. Link, R.L. Bliss, S. Puumala, S.E. Murphy, S.S. Hecht, Metabolites of a tobacco-specific lung carcinogen in nonsmoking casino patrons, Cancer Epidemiol. Biomarkers Prev. 12 (2003) 1544–1546.

[26] S.S. Hecht, S.E. Murphy, S.G. Carmella, S. Li, J. Jensen, C. Le, A.M. Joseph, D.K. Hatsukami, Similar uptake of lung carcinogens by smokers of regular, light, and ultralight cigarettes, Cancer Epidemiol. Biomarkers Prev. 14 (2005) 693–698.

[27] S.S. Hecht, S.G. Carmella, K.A. Le, S.E. Murphy, A.J. Boettcher, C. Le, J. Koopmeiners, L. An, D.J. Hennrikus, 4-(Methylnitrosamino)-1-(3-pyridyl)-1-butanol and its glucuronides in the urine of infants exposed to environmental tobacco smoke, Cancer Epidemiol. Biomarkers Prev. 15 (2006) 988–992.

[28] S.S. Hecht, Progress and challenges in selected areas of tobacco carcinogenesis, Chem. Res.Toxicol. 21 (2008) 160–171.

[29] International Agency for Research on Cancer Smokeless tobacco and tobacco-specific nitrosamines, IARC Monographs on the Evaluation of Carcinogenic Risks to Humans, v. 89 (2007) IARC, Lyon, FR.

[30] A. Castonguay, H. Tjälve, S.S. Hecht, Tissue distribution of the tobacco-specific carcinogen 4-(methylnitrosamino)-1-(3-pyridyl)-1-butanone, and its metabolites in F344 rats, Cancer Res. 43 (1983) 630–638.

[31] A. Castonguay, H. Tjälve, N. Trushin, S.S. Hecht, Perinatal metabolism of the tobacco-specific carcinogen 4-(methylnitrosamino)-1-(3-pyridyl)-1-butanone in C57B1 mice, J. Natl. Cancer Instit. 72 (1984) 1117–1126.

[32] J.D. Adams, E.J. LaVoie, D. Hoffmann, On the pharmacokinetics of tobacco-specific N-nitrosamines in Fischer rats, Carcinogenesis 6 (1985) 509–511.

[33] S.S. Hecht, N. Trushin, S.G. Carmella, L.M. Anderson, J.M. Rice, C.A. Reid-Quinn, E.S. Burak, A.B. Jones, J.L. Southers, C.T. Gombar, Metabolism of the tobacco specific nitrosamine 4-(methylnitrosamino)-1-(3-pyridyl)-1-butanone in the Patas monkey: Pharmacokinetics and characterization of glucuronide metabolite, Carcinogenesis 14 (1993) 229–236.

[34] Z. Wu, P. Upadhyaya, S.G. Carmella, S.S. Hecht, C.L. Zimmerman, Disposition of 4-(methylnitrosamino)-1-(3-pyridyl)-1-butanone (NNK) and 4-(methylnitrosamino)-1-(3-pyridyl)-1-butanol (NNAL) in bile duct-cannulated rats: Stereoselective metabo-lism and tissue distribution, Carcinogenesis 23 (2002) 171–179.

[35] S.S. Hecht, S.G. Carmella, I. Stepanov, J. Jensen, A. Anderson, D.K. Hatsukami, Metabolism of the tobacco-specific carcinogen 4-(methylnitrosamino)-1-(3-pyridyl)-1-butanone to its biomarker total NNAL in smokeless tobacco users, Cancer Epidemiol. Biomarkers Prev. 17 (2008) 732–735.

[36] S.S. Hecht, S.G. Carmella, M. Ye, K.A. Le, J.A. Jensen, C.L. Zimmerman, D.K. Hatsukami, Quantitation of metabolites of 4-(methylnitrosamino)-1-(3-pyridyl)-1-butanone after cessation of smokeless tobacco use, Cancer Res. 62 (2002) 129–134.

[37] C.L. Zimmerman, Z. Wu, P. Upadhyaya, S.S. Hecht, Stereoselective metabolism and tissue retention in rats of the individual enantiomers of 4-(methylnitrosamino)-1-(3-pyridyl)-1-butanol (NNAL), metabolites of the tobacco-specific nitrosamine, 4-(methylnitrosamino)-1-(3-pyridyl)-1-butanone (NNK), Carcinogenesis 25 (2004) 1237–1242.

[38] E. Maser, E. Richter, J. Friebertshauser, The identification of 11β-hydroxysteroid dehydrogenase as carbonyl reductase of the tobacco-specific nitrosamine (4-methylnitrosamino)-1-(3-pyridyl)-1-butanone, Eur. J. Biochem. 238 (1996) 484–489.

[39] A. Atalla, U. Breyer-Pfaff, E. Maser, Purification and characterization of oxidoreductases-catalyzing carbonyl reduction of the tobacco-specific nitrosamine 4-methylnitrosamino-1-(3-pyridyl)-1-butanone (NNK) in human liver cytosol, Xenobiotica 30 (2000) 755–769.

[40] N. Trushin, G. Leder, K. El Bayoumy, D. Hoffmann, H.G. Beger, D. Henne-Bruns, M. Ramadani, B. Prokopczyk, The tobacco carcinogen NNK is stereoselectively reduced by human pancreatic microsomes and cytosols, Langenbecks Arch. Surg. (2008).

[41] J.R. Jalas, S.S. Hecht, Synthesis of stereospecifically deuterated 4-(methylnitrosamino)-1-(3-pyridyl)-1-butanol (NNAL) diastereomers and metabolism by A/J mouse lung microsomes and cytochrome P450 2A5, Chem. Res. Toxicol. 16 (2003) 782–793.

[42] J.R. Jalas, X. Ding, S.E. Murphy, Comparative metabolism of the tobacco-specific nitrosamines 4-(methylnitrosamino)-1-(3-pyridyl)-1-butanone and 4-(methylnitrosamino)-1-(3-pyridyl)-1-butanol by rat cytochrome P450 2A3 and human cytochrome P450 2A13, Drug Metab. Dispos. 31 (2003) 1199–1202.

[43] S.G. Carmella, A. Borukhova, S.A. Akerkar, S.S. Hecht, Analysis of human urine for pyridine-N-oxide metabolites of 4-(methylnitrosamino)-1-(3-pyridyl)-1-butanone, a tobacco-specific lung carcinogen, Cancer Epidemiol. Biomark. Prev. 6 (1997) 113–120.

[44] J.R. Jalas, S.S. Hecht, S.E. Murphy, Cytochrome P450 enzymes as catalysts of metabolism of 4-(methylnitrosamino)-1-(3-pyridyl)-1-butanone, a tobacco specific carcinogen, Chem. Res. Toxicol. 18 (2005) 95–110.

[45] J. Lamoureux, A. Castonguay, Absence of metabolism of 4-(methylnitrosamino)-1-(3-pyridyl)-1-butanone (NNK) by flavin-containing monooxygenase (FMO), Carcinogenesis 18 (1997) 1979–1984.

[46] Y. Weng, C. Fang, R.J. Turesky, M. Behr, L.S. Kaminsky, X. Ding, Determination of the role of target tissue metabolism in lung carcinogenesis using conditional cytochrome P450 reductase-null mice, Cancer Res. 67 (2007) 7825–7832.

[47] X. Zhang, J. D'Agostino, H. Wu, Q.Y. Zhang, L. von Weymarn, S.E. Murphy, X. Ding, CYP2A13: Variable expression and role in human lung microsomal metabolic activation of the tobacco-specific carcinogen 4-(methylnitrosamino)-1-(3-pyridyl)-1-butanone, J. Pharmacol. Exp. Ther. 323 (2007) 570–578.

[48] P.J. Brown, L.L. Bedard, K.R. Reid, D. Petsikas, T.E. Massey, Analysis of CYP2A contributions to metabolism of 4-(methylnitrosamino)-1-(3-pyridyl)-1-butanone in human peripheral lung microsomes, Drug Metab. Dispos. 35 (2007) 2086–2094.

[49] J. Hukkanen, O. Pelkonen, J. Hakkola, H. Raunio, Expression and regulation of xenobiotic-metabolizing cytochrome P450 (CYP) enzymes in human lung, Crit. Rev. Toxicol. 32 (2002) 391–411.

[50] S. Anttila, E. Hietanen, H. Vainio, A.M. Camus, H.V. Gelboin, S.S. Park, L. Heikkila, A. Karjalainen, H. Bartsch, Smoking and peripheral type of cancer are related to high levels of pulmonary cytochrome P450IA in lung cancer patients, Int. J. Cancer 47 (1991) 681–685.

[51] P.M. Hall, I. Stupans, W. Burgess, D.J. Birkett, M.E. McManus, Immunohisto-chemical localization of NADPH-cytochrome P450 reductase in human tissues, Carcinogenesis 10 (1989) 521–530.

[52] R. Piipari, K. Savela, T. Nurminen, J. Hukkanen, H. Raunio, J. Hakkola, T. Mantyla, P. Beaune, R.J. Edwards, A.R. Boobis, S. Anttila, Expression of CYP1A1, CYP1B1 and CYP3A, and polycyclic aromatic hydrocarbon–DNA adduct formation in bronchoalveolar macrophages of smokers and non-smokers, Int. J. Cancer 86 (2000) 610–616.

[53] S. Anttila, J. Hukkanen, J. Hakkola, T. Stjernvall, P. Beaune, R.J. Edwards, A. R. Boobis, O. Pelkonen, H. Raunio, Expression and localization of CYP3A4 and CYP3A5 in human lung, Am. J. Respir. Cell Mol. Biol. 16 (1997) 242–249.

[54] S.A. Belinsky, C.M. White, N. Trushin, S.S. Hecht, Cell specificity for the pulmo-nary metabolism of tobacco-specific nitrosamines in the Fischer rat, Carcinogenesis 10 (1989) 2269–2274.

[55] G.B. Smith, A. Castonguay, P.J. Donnelly, K.R. Reid, D. Petsikas, T.E. Massey, Biotransformation of the tobacco-specific carcinogen 4-(methylnitrosamino)-1-(3-pyridyl)-1-butanone (NNK) in freshly isolated human lung cells, Carcinogenesis 20 (1999) 1809–1818.

[56] Z.A. Ronai, S. Gradia, L.A. Peterson, S.S. Hecht, G to A transitions and G to T transversions in codon 12 of the Ki-ras oncogene isolated from mouse lung tumors induced by 4-(methylnitrosamino)-l-(3-pyridyl)-l-butanone (NNK) and related DNA methylating and pyridyloxobutylating agents, Carcinogenesis 14 (1993) 2419–2422.

[57] T.J. Smith, A.M. Liao, Y. Liu, A.B. Jones, L.M. Anderson, C.S. Yang, Enzymes involved in the bioactivation of 4-(methylnitrosamino)-1-(3-pyridyl)-1-butanone in patas monkey lung and liver microsomes, Carcinogenesis 18 (1997) 1577–1584.

[58] T.J. Smith, Z. Guo, J.Y. Hong, S.M. Ning, P.E. Thomas, C.S. Yang, Kinetics and enzyme involvement in the metabolism of 4-(methylnitrosamino)-1-(3-pyridyl)-1-butanone (NNK) in microsomes of rat lung and nasal mucosa, Carcinogenesis 13 (1992) 1409–1414.

[59] L.A. Peterson, R. Mathew, S.S. Hecht, Quantitation of microsomal α-hydroxylation of the tobacco-specific nitrosamine, 4-(methylnitrosamino)-1-(3-pyridyl)-1-buta-none, Cancer Res. 51 (1991) 5495–5500.

[60] Z. Guo, T.J. Smith, P.E. Thomas, C.S. Yang, Metabolism of 4-(methylnitrosamino)-1-(3-pyridyl)-1-butanone by inducible and constitutive cytochrome P-450 enzymes in rats, Arch. Biochem. Biophys. 298 (1992) 279–286.

[61] M.A. Morse, K.I. Eklind, M. Toussaint, S.G. Amin, F.L. Chung, Characterization of a glucuronide metabolite of 4-(methyl-nitrosamino)-1-(3-pyridyl)-1-butanone (NNK) and its dose-dependent excretion in the urine of mice and rats, Carcinogenesis 11 (1990) 1819–1823.

[62] J. Schulze, E. Richter, U. Binder, W. Zwickenpflug, Biliary excretion of 4-(methyl-nitrosamino)-1-(3-pyridyl)-1-butanone in the rat, Carcinogenesis 13 (1992) 1961–1965.

[63] Q. Ren, S.E. Murphy, Z. Zheng, P. Lazarus, O-Glucuronidation of the lung carcinogen 4-(methylnitrosamino)-1-(3-pyridyl)-1-butanol (NNAL) by human

UDP-glucuronosyltransferases 2B7 and 1A9, Drug Metab. Dispos. 28 (2000) 1352–1360.

[64] P. Lazarus, Y. Zheng, R.E. Aaron, J.E. Muscat, D. Wiener, Genotype-phenotype correlation between the polymorphic UGT2B17 gene deletion and NNAL glucuronidation activities in human liver microsomes, Pharmacogenet. Genomics 15 (2005) 769–778.

[65] D. Wiener, D.R. Doerge, J.L. Fang, P. Upadhyaya, P. Lazarus, Characterization of N-glucuronidation of the lung carcinogen 4-(methylnitrosamino)-1-(3-pyridyl)-1-butanol (NNAL) in human liver: importance of UDP-glucuronosyltransferase 1A4, Drug Metab. Dispos. 32 (2004) 72–79.

[66] G. Chen, R.W. Dellinger, D. Sun, T.E. Spratt, P. Lazarus, Glucuronidation of tobacco-specific nitrosamines by UGT2B10, Drug Metab. Dispos (2008).

[67] S.E. Murphy, D.A. Spina, M.G. Nunes, D.A. Pullo, Glucuronidation of 4-((hydroxymethyl)nitrosamino)-1-(3-pyridyl)-1-butanone, a metabolically activated form of 4-(methylnitrosamino)-1-(3-pyridyl)-1-butanone, by phenobarbital-treated rats, Chem. Res. Toxicol. 8 (1995) 772–779.

[68] S.E. Murphy, M.G. Nunes, M.A. Hatala, Effects of phenobarbital and 3-methylcholanthrene induction on the formation of three glucuronide metabolites of 4-(methylnitrosamino)-1-(3-pyridyl)-1-butanone, NNK, Chem. Biol. Interact. 103 (1997) 153–166.

[69] M. Mochizuki, T. Anjo, M. Okada, Isolation and characterization of N-alkyl-N-(hydroxymethyl)nitrosamines from N-alkyl-N-(hydroperoxymethyl) nitrosamines by deoxygenation, Tetrahedron Lett. 21 (1980) 3693–3696.

[70] H. Krokan, R.C. Grafström, K. Sundqvist, H. Esterbauer, C.C. Harris, Cytotoxicity, thiol depletion and inhibition of O^6-methylguanine-DNA methyltransferase by various aldehydes in cultured human bronchial fibroblasts, Carcinogenesis 6 (1985) 1755–1759.

[71] R.C. Grafström, R.D. Curren, L.L. Yang, C.C. Harris, Genotoxicity of formaldehyde in cultured human bronchial fibroblasts, Science 228 (1985) 89–91.

[72] R.C. Grafström, J.M. Dypbukt, J.C. Willey, K. Sundqvist, C. Edman, L. Atzori, C.C. Harris, Pathobiological effects of acrolein in cultured human bronchial epithelial cells, Cancer Res. 48 (1988) 1717–1721.

[73] M.A. Alaoui-Jamali, R. Gagnon, N. El Alami and A. Castonguay, Cytotoxicity, sister-chromatid exchanges and DNA single-strand breaks induced by 4-oxo-4-(3-pyridyl)butanal, a metabolite of a tobacco-specific N-nitrosamine, Mutat. Res. 240 (1990) 25–33.

[74] K. Demkowicz-Dobrazanski, A. Castonguay, Comparison of DNA alkali-labile sites induced by 4-(methylnitrosamino)-1-(3-pyridyl)-1-butanone and 4-oxo-4-(3-pyridyl)butanal in rat hepatocytes, Carcinogenesis 12 (1991) 2135–2140.

[75] L. Liu, M.A. Alaoui-Jamali, N.E. Alami, A. Castonguay, Metabolism and DNA single strand breaks induced by 4-(methylnitrosamino)-1-(3-pyridyl)-1-butanone and its analogues in primary culture of rat hepatocytes, Cancer Res. 50 (1990) 1810–1816.

[76] L. Liu, A. Castonguay, S.L. Gerson, Lack of correlation between DNA methylation and hepatocarcinogenesis in rats and hamsters treated with 4-(methylnitrosamino)-1-(3-pyridyl)-1-butatone, Carcinogenesis 13(11), (1992) 2137–2140.

[77] S.A. Belinsky, C.M. White, J.A. Boucheron, F.C. Richardson, J.A. Swenberg, M. Anderson, Accumulation and persistence of DNA adducts in respiratory tissue of rats following multiple administrations of the tobacco specific carcinogen 4-(N-methyl-N-nitrosamino)-1-(3-pyridyl)-1-butanone, Cancer Res. 46 (1986) 1280–1284.

[78] S.S. Hecht, N. Trushin, A. Castonguay, A. Rivenson, Comparative tumorigenicity and DNA methylation in F344 rats by 4-(methylnitrosamino)-1-(3-pyridyl)-1-butanone and N-nitrosodimethylamine, Cancer Res. 46 (1986) 498–502.

[79] S.A. Belinsky, J.A. Foley, C.M. White, M.W. Anderson, R.R. Maronpot, Dose-response relationship between O^6-methylguanine formation in Clara cells and induction of pulmonary neoplasia in the rat by NNK, Cancer Res. 50 (1990) 3772–3780.

[80] S.E. Murphy, A. Palomino, S.S. Hecht, D. Hoffmann, Dose-response study of DNA and hemoglobin adduct formation by 4-(methylnitrosamino)-1-(3-pyridyl)-1-buta-none in F344 rats, Cancer Res. 50 (1990) 5446–5452.

[81] L.A. Peterson, S.S. Hecht, O^6-Methylguanine is a critical determinant of 4-(methyl-nitrosamino)-1-(3-pyridyl)-1-butanone tumorigenesis in A/J mouse lung, Cancer Res. 51 (1991) 5557–5564.

[82] D.T. Beranek, Distribution of methyl and ethyl adducts following alkylation with monofunctional alkylating agents, Mutat. Res. 231 (1990) 11–30.

[83] S.S. Hecht, DNA adduct formation from tobacco-specific N-nitrosamines, Mutat. Res. 424 (1999) 127–142.

[84] S.S. Hecht, N. Trushin, DNA and hemoglobin alkylation by 4-(methylnitrosamino)-1-(3-pyridyl)-1-butanone (NNK) and 4-(methylnitrosamino)-1-(3-pyridyl)-1-buta-nol (NNAL) in F344 rats, Carcinogenesis 9 (1988) 1665–1668.

[85] T.E. Spratt, L.A. Peterson, W.L. Confer, S.S. Hecht, Solvolysis of model compounds for α-hydroxylation of N'-nitrosonornicotine and 4-(methylnitrosamino)-1-(3-pyr-idyl)-1-butanone: Evidence for a cyclic oxonium ion intermediate in the alkylation of nucleophiles, Chem. Res. Toxicol. 3 (1990) 350–356.

[86] S.G. Carmella, S.S. Kagan, T.E. Spratt, S.S. Hecht, Evaluation of cysteine adduct formation in rat hemoglobin by 4-(methylnitrosamino)-1-(3-pyridyl)-1-butanone and related compounds, Cancer Res. 50 (1990) 5453–5459.

[87] S.S. Hecht, T.E. Spratt, N. Trushin, Evidence for 4-(3-pyridyl)-4-oxobutylation of DNA in F344 rats treated with the tobacco specific nitrosamines 4-(methylnitrosa-mino)-1-(3-pyridyl)-1-butanone and N'-nitrosonornicotine, Carcinogenesis 9 (1988) 161–165.

[88] M. Wang, G. Cheng, S.J. Sturla, E.J. McIntee, P.W. Villalta, P. Upadhyaya, S.-S. Hecht, Identification of adducts formed by pyridyloxobutylation of deoxyguano-sine and DNA by 4-(acetoxymethylnitrosamino)-1-(3-pyridyl)-1-butanone, a chemically activated form of tobacco specific carcinogens, Chem. Res. Toxicol. 16 (2003) 616–626.

[89] S.S. Hecht, P.W. Villalta, S.J. Sturla, G. Cheng, N. Yu, P. Upadhyaya, M. Wang, Identification of O^2-substituted pyrimidine adducts formed in reactions of 4-(acet-oxymethylnitrosamino)-1-(3-pyridyl)-1-butanone and 4-(acetoxymethylnitrosa-mino)-1-(3-pyridyl)-1-butanol with DNA, Chem. Res. Toxicol. 17 (2004) 588–597.

[90] L. Wang, T.E. Spratt, X.K. Liu, S.S. Hecht, A.E. Pegg, L.A. Peterson, Pyridylox-obutyl adduct O^6-[4-oxo-4-(3-pyridyl)butyl]guanine is present in 4-(acetoxymethyl-nitrosamino)-1-(3-pyridyl)-1-butanone-treated DNA and is a substrate for O^6-alkylguanine-DNA alkyltransferase, Chem. Res. Toxicol. 10 (1997) 562–567.

[91] T.E. Spratt, N. Trushin, D. Lin, S.S. Hecht, Analysis for N^2-(pyridyloxobutyl) deoxyguanosine adducts in DNA of tissues exposed to tritium labelled 4-(methylni-trosamino)-1-(3-pyridyl)-1-butanone and N'-nitrosonornicotine, Chem. Res. Tox-icol. 2 (1989) 169–173.

[92] S.J. Sturla, J. Scott, Y. Lao, S.S. Hecht, P.W. Villalta, Mass spectrometric analysis of relative levels of pyridyloxobutylation adducts formed in the reaction of DNA with a chemically activated form of the tobacco-specific carcinogen 4-(methylnitrosamino)-1-(3-pyridyl)-1-butanone, Chem. Res. Toxicol. 18 (2005) 1048–1055.

[93] Y. Lao, P.W. Villalta, S.J. Sturla, M. Wang, S.S. Hecht, Quantitation of pyridylox-obutyl DNA adducts of tobacco-specific nitrosamines in rat tissue DNA by

high-performance liquid chromatography-electrospray ionization-tandem mass spectrometry, Chem. Res. Toxicol. 19 (2006) 674–682.

[94] J.F. Cloutier, R. Drouin, M. Weinfeld, T.R. O'Connor, A. Castonguay, Characterization and mapping of DNA damage induced by reactive metabolites of 4-(methylnitrosamino)-1-(3-pyridyl)-1-butanone (NNK) at nucleotide resolution in human genomic DNA, J. Mol. Biol. 313 (2001) 539–557.

[95] S. Park, M. Seetharaman, A. Ogdie, D. Ferguson, N. Tretyakova, 3′-Exonuclease resistance of DNA oligodeoxynucleotides containing O^6-[4-oxo-4-(3-pyridyl)butyl] guanine, Nucleic Acids Res. 31 (2003) 1984–1994.

[96] J. Haglund, A.P. Henderson, B.T. Golding, M. Tornqvist, Evidence for phosphate adducts in DNA from mice treated with 4-(N-methyl-N-nitrosamino)-1-(3-pyridyl)-1-butanone (NNK), Chem. Res. Toxicol. 15 (2002) 773–779.

[97] J. Haglund, A. Rafiq, L. Ehrenberg, B.T. Golding, M. Tornqvist, Transalkylation of phosphotriesters using Cob(I)alamin: Toward specific determination of DNA-phosphate adducts, Chem. Res. Toxicol. 13 (2000) 253–256.

[98] S. Lacoste, A. Castonguay, R. Drouin, Formamidopyrimidine adducts are detected using the comet assay in human cells treated with reactive metabolites of 4-(methylnitrosamino)-1-(3-pyridyl)-1-butanone (NNK), Mutat. Res. 600 (2006) 138–149.

[99] Y. Lao, N. Yu, F. Kassie, P.W. Villalta, S.S. Hecht, Formation and accumulation of pyridyloxobutyl DNA adducts in F344 rats chronically treated with 4-(methylnitrosamino)-1-(3-pyridyl)-1-butanone and enantiomers of its metabolite, 4-(methylnitrosamino)-1-(3-pyridyl)-1-butanol, Chem. Res. Toxicol. 20 (2007) 235–245.

[100] D. Holzle, D. Schlobe, A.R. Tricker, E. Richter, Mass spectrometric analysis of 4-hydroxy-1-(3-pyridyl)-1-butanone-releasing DNA adducts in human lung, Toxicology 232 (2007) 277–285.

[101] D. Schlobe, D. Holzle, D. Hatz, L. Von Meyer, A.R. Tricker, E. Richter, 4-Hydroxy-1-(3-pyridyl)-1-butanone-releasing DNA adducts in lung, lower esophagus and cardia of sudden death victims, Toxicology 245 (2008) 154–161.

[102] P. Upadhyaya, S.J. Sturla, N. Tretyakova, R. Ziegel, P.W. Villalta, M. Wang, S.S. Hecht, Identification of adducts produced by the reaction of 4-(acetoxymethylnitrosamino)-1-(3-pyridyl)-1-butanol with deoxyguanosine and DNA, Chem. Res. Toxicol. 16 (2003) 180–190.

[103] R.C. Grafström, J. Fornace, H. Autrup, J.F. Lechner, C.C. Harris, Formaldehyde damage to DNA and inhibition of DNA repair in human bronchial cells, Science 220 (1983) 216–218.

[104] F.A. Beland, N.F. Fullerton, R.H. Heflich, Rapid isolation hydrolysis and chromatography of formaldehyde-modified DNA, J. Chromatogr. 308 (1984) 121–131.

[105] G. Cheng, M. Wang, P. Upadhyaya, P.W. Villalta, S.S. Hecht, Formation of formaldehyde adducts in the reactions of DNA and deoxyribonucleosides with alpha-acetates of 4-(methylnitrosamino)-1-(3-pyridyl)-1-butanone (NNK), 4-(methylnitrosamino)-1-(3-pyridyl)-1-butanol (NNAL), and N-nitrosodimethylamine (NDMA), Chem. Res. Toxicol. 21 (2008) 746–751.

[106] Y.F.M. Chaw, L.E. Crane, P. Lange, R. Shapiro, Isolation and identification of cross-links from formaldehyde-treated nucleic acids, Biochemistry 19 (1980) 5525–5531.

[107] H. Huang, M.S. Solomon, P.B. Hopkins, Formaldehyde preferentially interstrand cross-links duplex DNA through deoxyadenosine residues at the sequence 5′-d(AT), J. Am. Chem. Soc. 114 (1992) 9240–9241.

[108] H. Huang, P.B. Hopkins, DNA interstrand cross-linking by formaldehyde: Nucleotide sequence preference and covalent structure of the predominant cross-link formed in synthetic oligonucleotides, J. Am. Chem. Soc. 115 (1993) 9402–9408.

[109] G. Cheng, Y. Shi, S.J. Sturla, J.R. Jalas, E.J. McIntee, P.W. Villalta, M. Wang, S.S. Hecht, Reactions of formaldehyde plus acetaldehyde with deoxyguanosine and DNA: Formation of cyclic deoxyguanosine adducts and formaldehyde cross-links, Chem. Res. Toxicol. 16 (2003) 145–152.

[110] M. Wang, G. Cheng, P.W. Villalta, S.S. Hecht, Development of liquid chromatography electrospray ionization tandem mass spectrometry methods for analysis of DNA adducts of formaldehyde and their application to rats treated with N-nitrosodimethylamine or 4-(methylnitrosamino)-1-(3-pyridyl)-1-butanone, Chem. Res. Toxicol. 20 (2007) 1141–1148.

[111] F.L. Chung, Y. Xu, Increased 8-oxodeoxyguanosine levels in lung DNA of A/J mice and F344 rats treated with the tobacco-specific nitrosamine 4-(methylnitrosamino)-1-(3-pyridyl)-1-butanone, Carcinogenesis 13 (1992) 1269–1272.

[112] R. Jorquera, A. Castonguay, H.M. Schuller, DNA single strand breaks and toxicity induced by 4-(methylnitrosamino)-1-(3-pyridyl)-1-butanone or N-nitrosodimethylamine in hamster and rat liver, Carcinogenesis 15(2), (1994) 389–394.

[113] S.S. Hecht, D. Lin, A. Castonguay, Effects of α-deuterium substitution on the mutagenicity of 4-(methylnitrosamino)-1-(3-pyridyl)-1-butanone (NNK), Carcinogenesis 4 (1983) 305–310.

[114] H.F. Tiano, M. Hosokawa, P.C. Chulada, P.B. Smith, R.L. Wang, F.J. Gonzalez, C. L. Crespi, R. Langebach, Retroviral mediated expression of human cytochrome P450 2A6 in C3H/10T1/2 cells confers transformability by 4-(methylnitrosamino)-1-(3-pyridy)1-butanone (NNK, Carcinogenesis 14 (1993) 1421–1427.

[115] K. Fujita, T. Kamataki, Predicting the mutagenicity of tobacco-related N-nitrosamines in humans using 11 strains of Salmonella typhimurium YG7108, each coexpressing a form of human cytochrome P450 along with NADPH-cytochrome P450 reductase, Environ. Mol. Mutagen. 38 (2001) 339–346.

[116] C.L. Crespi, B.W. Penman, H.V. Gelboin, F.J. Gonzalez, A tobacco smoke-derived nitrosamine, 4-(methylnitrosamino)-1-(3-pyridyl)-1-butanone, is activated by multiple human cytochrome P450s including the polymorphic human cytochrome P4502D6, Carcinogenesis 12 (1991) 1197–1201.

[117] K. Hashimoto, K. Ohsawa, M. Kimura, Mutations induced by 4-(methylnitrosamino)-1-(3-pyridyl)-1-butanone (NNK) in the lacZ and cII genes of Muta Mouse, Mutat. Res. 560 (2004) 119–131.

[118] L.E. Sandercock, J.N. Hahn, L. Li, H.A. Luchman, J.L. Giesbrecht, L.A. Peterson, F.R. Jirik, Mgmt deficiency alters the in vivo mutational spectrum of tissues exposed to the tobacco carcinogen 4-(methylnitrosamino)-1-(3-pyridyl)-1-butanone (NNK), Carcinogenesis 29 (2008) 866–874.

[119] V.L. Souliotis, J.H.M. van Delft, M.J.S.T. Steenwinkel, R.A. Baan, S.A. Kyrtopoulos, DNA adducts, mutant frequencies, and mutation spectra in lambdalacZ transgenic mice treated with N-nitrosodimethylamine, Carcinogenesis 19 (1998) 731–739.

[120] B.S. Shane, D.L. Smith-Dunn, J.G. de Boer, B.W. Glickman, M.L. Cunningham, Mutant frequencies and mutation spectra of dimethylnitrosamine (DMN) at the lacI and cII loci in the livers of Big Blue transgenic mice, Mutat. Res. 452 (2000) 197–210.

[121] X. Wang, T. Suzuki, T. Itoh, M. Honma, A. Nishikawa, F. Furukawa, M. Takahashi, M. Hayashi, T. Kato, T. Sofuni, Specific mutational spectrum of dimethylnitrosamine in the lacI transgene of Big Blue C57BL/6 mice, Mutagenesis 13 (1998) 625–630.

[122] R.J. Graves, P. Trueman, S. Jones, T. Green, DNA sequence analysis of methylene chloride-induced HPRT mutations in Chinese hamster ovary cells: Comparison with the mutation spectrum obtained for 1,2-dibromoethane and formaldehyde, Mutagenesis 11 (1996) 229–233.

[123] H.L. Liber, K. Benforado, R.M. Crosby, D. Simpson, T.R. Skopek, Formaldehyde-induced and spontaneous alterations in human *hprt* DNA sequence and mRNA expression, Mutat. Res. 226 (1989) 31–37.

[124] O. Merk, G. Speit, Significance of formaldehyde-induced DNA-protein crosslinks for mutagenesis, Environ. Mol. Mutagen. 32 (1998) 260–268.

[125] G. Speit, O. Merk, Evaluation of mutagenic effects of formaldehyde *in vitro*: Detection of crosslinks and mutations in mouse lymphoma cells, Mutagenesis 17 (2002) 183–187.

[126] G.T. Pauly, R.C. Moschel, Mutagenesis by O^6-methyl-, O^6-ethyl-, and O^6-benzyl-guanine and O^4-methylthymine in human cells: Effects of O^6-alkylguanine-DNA alkyltransferase and mismatch repair, Chem. Res. Toxicol. 14 (2001) 894–900.

[127] K.B. Altshuler, C.S. Hodes, J.M. Essigmann, Intrachromosomal probes for mutagenesis by alkylated DNA bases replicated in mammalian cells: A comparison of the mutagenicities of O^4-methylthymine and O^6-methylguanine in cells with different DNA repair backgrounds, Chem. Res. Toxicol. 9 (1996) 980–987.

[128] G.T. Pauly, L.A. Peterson, R.C. Moschel, Mutagenesis by O^6-[4-oxo-4-(3-pyridyl)butyl]guanine in *Escherichia coli* and human cells, Chem. Res. Toxicol. 15 (2002) 165–169.

[129] R.S. Mijal, N.M. Thomson, N.L. Fleischer, G.T. Pauly, R.C. Moschel, S. Kanugula, Q. Fang, A.E. Pegg, L.A. Peterson, The repair of the tobacco-specific nitrosamine derived adduct O^6-[4-oxo-4-(3-pyridyl)butyl]guanine by O^6-alkylguanine-DNA alkyltransferase variants, Chem. Res. Toxicol. 17 (2004) 424–434.

[130] Z.A. Ronai, S. Gradia, L.A. Peterson, S.S. Hecht, G to A transitions and G to T transversions in codon 12 of the Ki-*ras* oncogene isolated from mouse lung tumors induced by 4-(methylnitrosamino)-1-(3-pyridyl)-1-butanone (NNK) and related DNA methylating and pyridyloxobutylating agents, Carcinogenesis 14 (1993) 2419–2422.

[131] A.E. Pegg, Repair of O^6-alkylguanine by alkyltransferase, Mutat. Res. 462 (2000) 83–100.

[132] D.S. Daniels, C.D. Mol, A.S. Arvai, S. Kanugula, A.E. Pegg, J.A. Tainer, Active and alkylated human AGT structures: A novel zinc site, inhibitor and extrahelical base binding, EMBO J. 19 (2000) 1719–1730.

[133] M. Xu-Welliver, A.E. Pegg, Degradation of the alkylated form of the DNA repair protein O^6-alkylguanine-DNA alkyltransferase, Carcinogenesis 23 (2002) 823–830.

[134] L. Wang, T.E. Spratt, A.E. Pegg, L.A. Peterson, Synthesis of DNA oligonucleotides containing site-specifically incorporated O^6-[4-oxo-4-(3-pyridyl)butyl]guanine and their reaction with O^6-alkylguanine-DNA alkyltransferase, Chem. Res. Toxicol. 12 (1999) 127–131.

[135] N.M. Thomson, P.M. Kenney, L.A. Peterson, The pyridyloxobutyl DNA adduct, O^6-[4-oxo-4-(3-pyridyl)butyl]guanine, is detected in tissues from 4-(methylnitrosamino)-1-(3-pyridyl)-1-butanone-treated A/J mice, Chem. Res. Toxicol. 16 (2003) 1–6.

[136] N.A. Loktionova, A.E. Pegg, Interaction of mammalian O^6-alkylguanine-DNA alkyltransferases with O^6-benzylguanine, Biochem. Pharmacol. 63 (2002) 1431–1442.

[137] K. Goodtzova, S. Kanugula, S. Edara, G.T. Pauly, R.C. Moschel, A.E. Pegg, Repair of O^6-benzylguanine by the *Escherichia coli* Ada and Ogt and the human O^6-alkylguanine-DNA alkyltransferases, J. Biol. Chem. 272 (1997) 8332–8339.

[138] Y. Imai, H. Oda, Y. Nakatsuru, T. Ishikawa, A polymorphism at codon 160 of human O^6-methylguanine-DNA methyltransferase gene in young patients with adult type cancers and functional assay, Carcinogenesis 16 (1995) 2441–2445.

[139] C. Deng, D. Xie, H. Capasso, Y. Zhao, L.D. Wang, J.Y. Hong, Genetic polymorphism of human O^6-alkylguanine-DNA alkyltransferase: identification of a missense variation in the active site region, Pharmacogenetics 9 (1999) 81–87.

[140] T.B. Kaur, J.M. Travaline, J.P. Gaughan, J.P. Richie, Jr., S.D. Stellman, P. Lazarus, Role of polymorphisms in codons 143 and 160 of the O^6-alkylguanine DNA alkyltransferase gene in lung cancer risk, Cancer Epidemiol. Biomark. Prev. 9 (2000) 339–342.

[141] C. Cohet, S. Borel, F. Nyberg, A. Mukeria, I. Bruske-Hohlfeld, V. Constantinescu, S. Benhamou, P. Brennan, J. Hall, P. Boffetta, Exon 5 polymorphisms in the O^6-alkylguanine DNA alkyltransferase gene and lung cancer risk in non-smokers exposed to second-hand smoke, Cancer Epidemiol. Biomarkers Prev. 13 (2004) 320–323.

[142] C.E. Hill, J.K. Wickliffe, K.J. Wolfe, C.J. Kinslow, M.S. Lopez, S.Z. Abdel-Rahman, The L84F and the I143V polymorphisms in the O^6-methylguanine-DNA-methyltransferase (MGMT) gene increase human sensitivity to the genotoxic effects of the tobacco-specific nitrosamine carcinogen NNK, Pharmacogenet. Genomics 15 (2005) 571–578.

[143] R.S. Mijal, S. Kanugula, C.C. Vu, Q. Fang, A.E. Pegg, L.A. Peterson, DNA sequence context affects repair of the tobacco-specific adduct O^6-[4-oxo-4-(3-pyridyl)butyl]guanine by human O^6-alkylguanine-DNA alkyltransferases, Cancer Res. 66 (2006) 4968–4974.

[144] G.T. Pauly, S.H. Hughes, R.C. Moschel, Mutagenesis in *Escherichia coli* by three O^6-substituted guanines in double-stranded or gapped plasmids, Biochemistry 34 (1995) 8924–8930.

[145] M. Sekiguchi, H. Heyakawa, K. Kodama, K. Ishizaki, M. Ikenaga, Acquisition of resistance to alkylating agents by expression of methyltransferase gene in repair-deficient human cells, In: DNA Repair Mechanisms and Their Biological Implications in Mammalian Cells, (M. W.Lambert and JLaval, eds.), (1989) pp. 73–81. Plenum Press, New York.

[146] M. Yamada, K. Matsui, T. Sofuni, T. Nohmi, New tester strains of *Salmonella typhimurium* lacking O^6-methylguanine DNA methyltransferases and highly sensitive to mutagenic alkylating agents, Mutat. Res. 381 (1997) 15–24.

[147] R.S. Mijal, N.A. Loktionova, C.C. Vu, A.E. Pegg, L.A. Peterson, O^6-Pyridyloxobutylguanine adducts contribute to the mutagenic properties of pyridyloxobutylating agents, Chem. Res. Toxicol. 18 (2005) 1619–1625.

[148] S.A. Belinsky, M.E. Dolan, C.M. White, R.R. Maronpot, A.E. Pegg, M.W. Anderson, Cell specific differences in O^6-methylguanine-DNA methyltransferase activity and removal of O^6-methylguanine in rat pulmonary cells, Carcinogenesis 9 (1988) 2053–2058.

[149] L.A. Peterson, N.M. Thomson, D.L. Crankshaw, E.E. Donaldson, P.J. Kenney, Interactions between methylating and pyridyloxobutylating agents in A/J mouse lungs: implications for 4-(methylnitrosamino)-1-(3-pyridyl)-1-butanone-induced lung tumorigenesis, Cancer Res. 61 (2001) 5757–5763.

[150] L. Liu, X. Qin, S.L. Gerson, Reduced lung tumorigenesis in human methylguanine DNA-methyltransferase transgenic mice achieved by expression of transgene within the target cell, Carcinogenesis 20 (1999) 279–284.

[151] J.C. Fromme, A. Banerjee, G.L. Verdine, DNA glycosylase recognition and catalysis, Curr. Opin. Struct. Biol. 14 (2004) 43–49.

[152] P. Fortini, B. Pascucci, E. Parlanti, M. D'Errico, V. Simonelli, E. Dogliotti, The base excision repair: Mechanisms and its relevance for cancer susceptibility, Biochimie 85 (2003) 1053–1071.

[153] M.D. Wyatt, D.L. Pittman, Methylating agents and DNA repair responses: Methylated bases and sources of strand breaks, Chem. Res. Toxicol. 19 (2006) 1580–1594.

[154] P.J. Brown, L.L. Bedard, T.E. Massey, Repair of 4-(methylnitrosamino)-1-(3-pyridyl)-1-butanone-induced DNA pyridyloxobutylation by nucleotide excision repair, Cancer Lett. 260 (2008) 48–55.

[155] H. Kawate, K. Sakumi, T. Tsuzuki, Y. Nakatsuru, T. Ishikawa, S. Takahashi, H. Takano, T. Noda, M. Sekiguchi, Separation of killing and tumorigenic effects of an alkylating agent in mice defective in two of the DNA repair genes, Proc. Natl. Acad. Sci. USA 95 (1998) 5116–5120.

[156] B. Kaina, M. Christmann, S. Naumann, W.P. Roos, MGMT: Key node in the battle against genotoxicity carcinogenicity and apoptosis induced by alkylating agents, DNA Repair (Amst) 6 (2007) 1079–1099.

[157] X. Qin, L. Liu, S.L. Gerson, Mice defective in the DNA mismatch gene PMS2 are hypersensitive to MNU induced thymic lymphoma and are partially protected by transgenic expression of human MGMT, Oncogene 18 (1999) 4394–4400.

[158] J.E. Dahl, R. Becher, M. Lag, H.M. Schuller, E. Dybing, Formation of genotoxic products from N-nitrosoheptamethyleneimine (NHMI), 4-(methylnitrosamino)-1-(3-pyrdyl)-1-butanone (NNK), and N′-nitrosonornicotine (NNN) by isolated rabbit lung cells, Cell Biol. Toxicol. 6 (1990) 399–409.

[159] G.M. Williams, M.F. Laspia, The detection of various nitrosamines in the hepatocyte primary culture/DNA repair test, Cancer Lett. 6 (1979) 199–206.

[160] J.F. Cloutier, A. Castonguay, Modulation of DNA repair by various inhibitors of DNA synthesis following 4-(methylnitrosamino)-1-(3-pyridyl)-1-butanone (NNK) induced DNA damage, Chem. Biol. Interact. 110 (1998) 7–25.

[161] S.S. Hecht, K.G. Jordan, C.I. Choi, N. Trushin, Effects of deuterium substitution on the tumorigenicity of 4-(methylnitrosamino)-1-(3-pyridyl)-1-butanone and 4-(methylnitrosamino)-1-(3-pyridyl)-1-butanol in A/J mice, Carcinogenesis 11 (1990) 1017–1020.

[162] J.R. Jalas, E.J. McIntee, P.M. Kenney, P. Upadhyaya, L.A. Peterson, S.S. Hecht, Stereospecific deuterium substitution attenuates the tumorigenicity and metabolism of the tobacco-specific nitrosamine 4-(methylnitrosamino)-1-(3-pyridyl)-1-butanone, Chem. Res. Toxicol. 16 (2003) 794–806.

[163] S.A. Belinsky, T.R. Devereux, R.R. Maronpot, G.D. Stoner, M.W. Anderson, Relationship between the formation of promutagenic adducts and the activation of the K-ras protooncogene in lung tumors from A/J mice treated with nitrosamines, Cancer Res. 49 (1989) 5305–5311.

[164] R. Kawano, Y. Takeshima, K. Inai, Effects of K-ras gene mutations in the development of lung lesions induced by 4-(N-methyl-N-nitrosamino)-1-(3-pyridyl)-1-butanone in A/J mice, Jpn. J. Cancer Res. 87 (1996) 44–50.

[165] S.S. Hecht, D. Lin, A. Castonguay, A. Rivenson, Effects of α-deuterium substitution on the tumorigenicity of 4-(methylnitrosamino)-1-(3-pyridyl)-1-butanone in F344 rats, Carcinogenesis 8 (1987) 291–294.

[166] N. Trushin, A. Rivenson, S.S. Hecht, Evidence supporting the role of DNA pyridyloxobutylation in rat nasal carcinogenesis by tobacco-specific nitrosamines, Cancer Res. 54 (1994) 1205–1211.

[167] M.E. Staretz, P.G. Foiles, L.M. Miglietta, S.S. Hecht, Evidence for an important role of DNA pyridyloxobutylation in rat lung carcinogenesis by 4-(methylnitrosamino)-1-(3-pyridyl)-1-butanone: Effects of dose and phenethyl isothiocyanate, Cancer Res. 57 (1997) 259–266.

[168] L.A. Peterson, X.K. Liu, S.S. Hecht, Pyridyloxobutyl DNA adducts inhibit the repair of O^6-methylguanine, Cancer Res. 53 (1993) 2780–2785.

[169] K. Demkowicz-Dobrazanski, A. Castonguay, Modulation by glutathione of DNA strand breaks induced by 4-(methylnitrosamino)-1-(3-pyridyl)-1-butanone and its aldehyde metabolites in rat hepatocytes, Carcinogenesis 13 (1992) 1447–1454.

[170] H.M. Schuller, P.K. Tithof, M. Williams, H. Plummer, III, The tobacco-specific carcinogen 4-(methylnitrosamino)-1-(3-pyridyl)-1-butanone is a beta-adrenergic agonist and stimulates DNA synthesis in lung adenocarcinoma via beta-adrenergic receptor-mediated release of arachidonic acid, Cancer Res. 59 (1999) 4510–4515.

[171] H.M. Schuller, B. Porter, A. Riechert, Beta–adrenergic modulation of NNK–induced lung carcinogenesis in hamsters, J. Cancer Res. Clin. Oncol. 126 (2000) 624–630.

[172] H.M. Schuller, M. Orloff, Tobacco-specific carcinogenic nitrosamines. Ligands for nicotinic acetylcholine receptors in human lung cancer cells, Biochem. Pharmacol. 55 (1998) 1377–1384.

[173] H.M. Schuller, B.A. Jull, B.J. Sheppard, H.K. Plummer, Interaction of tobacco-specific toxicants with the neuronal alpha(7) nicotinic acetylcholine receptor and its associated mitogenic signal transduction pathway: Potential role in lung carcinogenesis and pediatric lung disorders, Eur. J. Pharmacol. 393 (2000) 265–277.

[174] K.A. West, J. Brognard, A.S. Clark, I.R. Linnoila, X. Yang, S.M. Swain, C. Harris, S. Belinsky, P.A. Dennis, Rapid Akt activation by nicotine and a tobacco carcinogen modulates the phenotype of normal human airway epithelial cells, J. Clin. Invest. 111 (2003) 81–90.

[175] J. Arredondo, A.I. Chernyavsky, S.A. Grando, Nicotinic receptors mediate tumorigenic action of tobacco-derived nitrosamines on immortalized oral epithelial cells, Cancer Biol. Ther. 5 (2006) 511–517.

[176] C. Duperron, A. Castonguay, Chemopreventive efficacies of aspirin and sulindac against lung tumorigenesis in A/J mice, Carcinogenesis 18 (1997) 1001–1006.

[177] A. Castonguay, N. Rioux, Inhibition of lung tumorigenesis by sulindac: Comparison of two experimental protocols, Carcinogenesis 18 (1997) 491–496.

[178] N. Rioux, A. Castonguay, Recovery from 4-(methylnitrosamino)-1-(3-pyridyl)-1-butanone-induced immunosuppression in A/J mice by treatment with nonsteroidal anti–inflammatory drugs, J. Natl. Cancer Instit. 89 (1997) 874–880.

[179] N. Rioux, A. Castonguay, Prevention of NNK-induced lung tumorigenesis in A/J mice by acetylsalicylic acid and NS-398, Cancer Res. 58 (1998) 5354–5360.

[180] H.M. Schuller, Mechanisms of smoking-related lung and pancreatic adenocarcinoma development, Nat. Rev. Cancer 2 (2002) 455–463.

[181] Z. Jin, M. Xin, X. Deng, Survival function of protein kinase C{iota} as a novel nitrosamine 4-(methylnitrosamino)-1-(3-pyridyl)-1-butanone-activated bad kinase, J. Biol. Chem 280 (2005) 16045–16052.

[182] B.A. Jull, H.K. Plummer, H.M. Schuller, Nicotinic receptor-mediated activation by the tobacco-specific nitrosamine NNK of a Raf-1/MAP kinase pathway, resulting in phosphorylation of c-myc in human small cell lung carcinoma cells and pulmonary neuroendocrine cells, J. Cancer Res. Clin. Oncol. 127 (2001) 707–717.

[183] Z. Jin, F. Gao, T. Flagg, X. Deng, Tobacco-specific nitrosamine 4-(methylnitrosamino)-1-(3-pyridyl)-1-butanone promotes functional cooperation of Bcl2 and c-Myc through phosphorylation in regulating cell survival and proliferation, J. Biol. Chem. 279 (2004) 40209–40219.

[184] M.R. Spitz, Q. Wei, Q. Dong, C.I. Amos, X. Wu, Genetic susceptibility to lung cancer: The role of DNA damage and repair, Cancer Epidemiol. Biomarkers Prev. 12 (2003) 689–698.

CHAPTER 6

Disruption of Heme Synthesis by Polyhalogenated Aromatics

Andrew G. Smith* *and* Tatyana Chernova

Contents

MRC Toxicology Unit, University of Leicester, United Kingdom

* Corresponding author. Tel.: +44 116 252 5617; Fax: +44 116 252 5616
Email address: ags5@le.ac.uk

1. Introduction

Heme is a polycyclic molecule consisting of an atom of iron at its core in a framework of the tetrapyrrole protoporphyrin IX. It is of immense fundamental importance in biology [1]. The redox nature of the iron and its ability to bind oxygen and molecules such as carbon monoxide and nitric oxide are key to the importance of heme in oxidative respiration, transportation, and detection of these gases as well as in the many enzymic oxidation reactions that it catalyzes (Figure 1) [2,3]. In plants, the related molecule chlorophyll, with magnesium at its core and central to photosynthesis, shares much of its route of biosynthesis with heme. Heme operates in mammals not only as the key component of hemoglobin and myoglobin to transport or store oxygen, but is also important in many metabolic and pharmacological processes [4]. Energy production in all organs is dependent on its presence in some mitochondrial cytochromes, while drug, steroid and prostaglandin metabolism are carried out by cytochromes in other cellular regions. Other hemoproteins produce cell messengers, for instance nitric oxide [5]. The diversity of the role of heme in biology depends on its three dimensional environment in the particular protein in which is embedded by co-ordination or covalent binding. For instance, the immense variability in substrate specificity of cytochrome P450 enzymes depends to a great extent on the surrounding protein structures. In some circumstances, for example, cytochrome a3, modifications of the side-chains of heme also influences its precise mode of action.
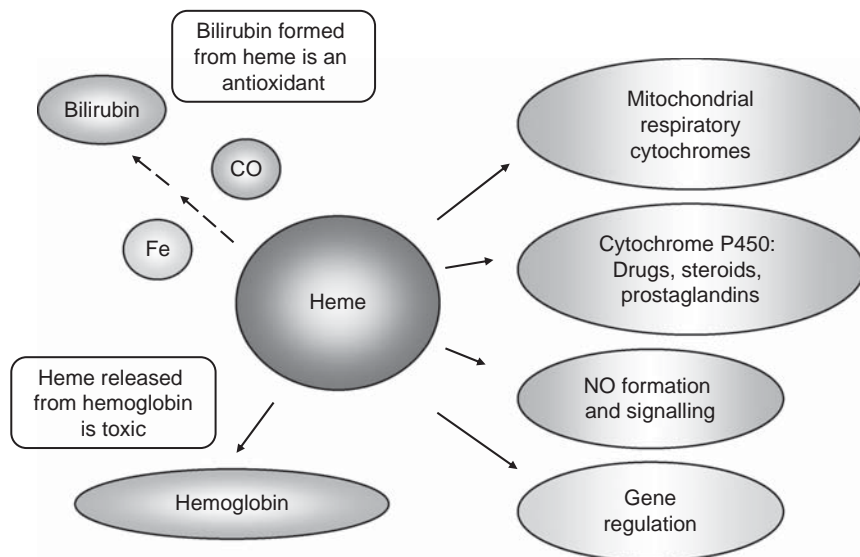
Figure 1   Important roles of heme in mammalian physiological systems.

In contrast to functional levels of heme, high levels of free heme in the body can be toxic by catalyzing uncontrolled free radical oxidations, as occurs as the consequence of the haemolysis of blood in stroke and cerebral malaria [6,7]. The metabolism by heme oxygenase of high levels of extracellular heme in the brain in such circumstances is an active field of research. Degradation of heme by heme oxygenases, as well as being important in erythrocyte turnover, is believed to contribute to the stress response of cells by producing the product biliverdin which is then subsequently reduced to bilirubin that has antioxidant properties [8]. Thus besides an erythroid function, heme as a constituent of hemo-proteins constitutes a vital component of many aspects of the control of gene expression and cellular metabolism in all cell types. Consequently, cellular heme homeostasis is an important consideration of normal metabolism [4].

In nonerythroid cells, including brain and liver, production of the first enzyme of heme synthesis, 5-aminolaevulinic acid synthase (ALAS1) is controlled, at least in part, by levels of a ''free'' regulatory heme pool in the cell [2,9]. However, there is increasing evidence that small pools of unbound heme can also act as an intra- and extracellular messenger with signalling functions for a variety of physiological systems by binding to heme-regulatory motifs of a number of proteins [10,11]. For instance, the operation of the clock transcription factors such as NPAS2, PER, and Rev-erbα and Rev-erb-β modulate metabolic events and coregulate heme biosynthesis and circadian rhythm [12–15]. Heme is also involved in regulating the expression of many genes, by the processing of micro RNAs [16], and by regulating protein degradation [17]. The demonstration of a stable interaction of heme with the Slo-BK channel [18] and its influence on an NMDA receptor-channel [19,20] suggests new roles for heme in modulation of ion channel action.

Heme metabolism can be massively disturbed by both intrinsic and extrinsic factors that may sometimes act synergistically with resulting severe physiological consequences [21]. In this chapter, the broad outline of heme synthesis in mammals will be outlined together with the human inherited diseases that have been described associated with mutations of the eight enzymes catalyzing heme formation [2,3]. A variety of drugs and chemicals are well known to interfere with the action of these enzymes and experimentally have been used as models of the genetic diseases and to explore fundamental aspects of heme metabolism especially in relation to the supply for the drug metabolism cytochrome P450 family [21,22]. Of these, the polychlorinated aromatic chemicals are perhaps the most important and their mechanism is the least understood. The major part of this review will summarize the aspects that we do know about how this particular toxic action of these aryl hydrocarbon receptor (AHR) ligands appears to be associated

with iron metabolism and how this resembles the known human hepatic disorder of heme metabolism, sporadic porphyria cutanea tarda (PCT).

2. Heme Synthesis and Disruption

2.1. Basic heme synthesis

The basic pathway of heme synthesis has been well established for many years. It is a remarkable achievement of nature to produce from simple molecules of intermediary metabolism, complex macrocyclic products in a process of stereospecific polymerizations and modifications; in principle, not unlike that seen in cholesterol and subsequent steroid biosynthesis. Of the eight steps specific to heme synthesis, the initial and last three take place in the mitochondria whereas the intermediate ones occur in the cytosol (Figure 2) [2,3]. In animals, the first precursor, 5-aminolevulinic acid (5-ALA) is formed by the condensation of glycine with succinyl CoA (Figure 2). For hemoglobin synthesis, which accounts for the major part of the body's heme production, regulation of the erythroid specific 5-ALA synthase gene (*ALAS2*) occurs by iron responsive and other elements coupled to requirements of heme demand. Nonerythroid heme synthesis may account for much less heme production but is vital for many cellular systems in all tissues, not the least oxidative respiration (see Section 1). In this case, the expression of the nonerythroid specific enzyme *(ALAS1* gene) is regulated differently. For many years a major influence has been considered to be a pool of "regulatory" heme negatively controlling transcription, mRNA stabilization, and protein processing although the exact mechanisms are not certain [9, 23–27]. More recently, other systems have been identified such as hepatic nutrition, hormones, and induction of particular cytochrome P450 isoforms, that act not only by modulation of transcription, but also on ALAS protein processing and degradation [13,28–31].

Dimerization of 5-ALA by cytosolic ALA dehydratase (*ALAD* gene) leads to the first cyclic product, the pyrrole porphobilinogen, four units of which create a linear tetrapyrrole, 1-hydroxymethylbilane (catalyzed by hydroxymethylbilane synthase, alias porphobilinogen deaminase; *HMBS* gene). At this point, one of two things can happen. Either the semistable bilane can cyclize spontaneously to the symmetrical macrocyclic tetrapyrrole uroporphyrinogen I, or, uroporphyrinogen III synthase cyclizes the bilane but at the same time by *spiro* transformation inverts one pyrrole ring to form the asymmetric isomer uroporphyrinogen III (Figure 2) [2,3]. The reason for this transformation becomes clear at the end of the pathway. Both uroporphyrinogens are highly unstable and *in vitro* will rapidly oxidise by six electron withdrawal to the respective uroporphyrins especially under the presence of light. This is extremely pertinent to the consequences of genetic
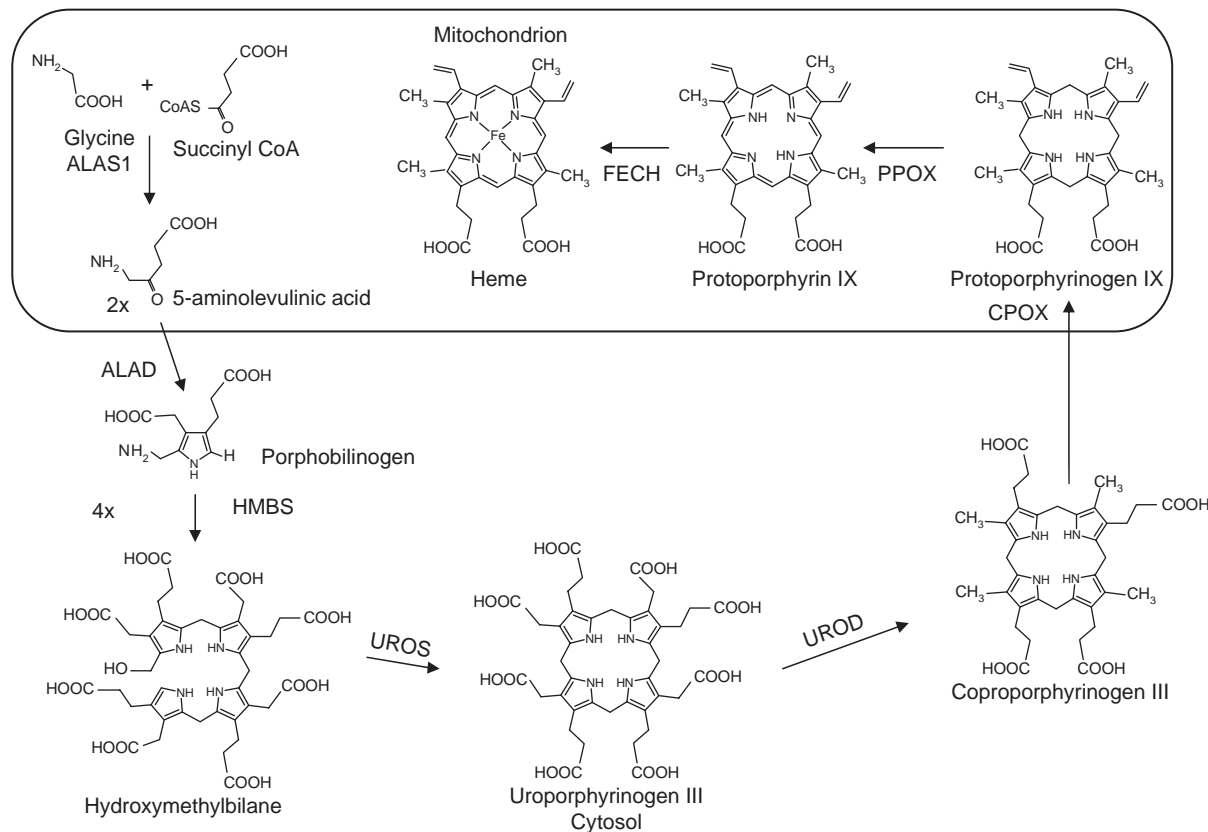
Figure 2 Eight steps of heme synthesis are split between mitochondria and cytosol. ALAS, 5-aminolevulinate synthase; ALAD, aminole-vulinate dehydratase; HMBS, hydroxymethylbilane synthase; UROS, uroporphyrinogen III synthase; UROD, uroporphyrinogen decar-boxylase; CPOX, coproporphyrinogen oxidase; PPOX, protoporphyrinogen oxidase; FECH, ferrochelatase.

and chemical malfunctions of heme metabolism. Uroporphyrinogen I is not a precursor of heme in animals and any formed *in vivo* is excreted. Similarly, any uroporphyrins I and III that may have been formed by endogenous oxidation are not utilized biosynthetically and are excreted. Small amounts are found naturally in urine of humans and animals.

Uroporphyrinogen III undergoes four sequential decarboxylation steps of the acetate side-chains to methyl groups (Figure 2) [32,33]. The enzyme uroporphyrinogen decarboxylase (UROD) exists as a homo dimer [34] and is catholic in its acceptance of substrates, including uroporphyrinogen I, but in a preferred clock-wise sequence of decarboxylation steps uroporphyrinogen III is converted to coproporphyrinogen III [32,35]. Interference in the operation of this enzyme by an unknown mechanism caused by some chemicals is the theme of this review [36]. Intermediate partially decarboxylated porphyrinogens oxidized to their respective porphyrins are found in excreta under normal circumstances, and especially under pathological conditions, in addition to coproporphyrin I. Coproporphyrinogen III is the sole product processed as a precursor of heme. At this point, heme synthesis returns to the mitochondria with two further decarboxylation steps occurring by an oxidative mechanism, this time of adjacent propionic acid side-chains. The resulting divinyl product, protoporphyrinogen IX, will spontaneously oxidize to protoporphyrin IX but *in vivo* this is controlled by protoporphyrinogen IX oxidase (*PPOX* gene) (Figure 2). Finally, Fe^{2+} is inserted into protoporphyrin IX to form heme under the action of a ferrochelatase (*FECH* gene). Thus, the process of heme formation from simple precursors starts and finishes in the mitochondria so that the product is ready to be utilized in respiratory cytochromes. For many other functions, such as in microsomal cytochrome P450s, heme must be exported from the mitochondria. The asymmetric macrocyclic molecule contains two vinyl side-chains on one side and two adjacent carboxy propyl side-chains on the other. In different roles of heme these allow variable covalent or hydrogen bonding to surrounding peptides and together with iron coordination result in highly specific oxidation mechanisms.

Heme released from hemoglobin or in excess of requirements can be toxic due to its ability to catalyze free radical reactions [37]. Reprocessing occurs through the action of microsomal heme oxygenases; enzymes that resemble cytochrome P450 in that they use heme to generate oxidations of the substrate which in this case self cleave the heme molecule itself at a bridge position. This results in the release of the iron atom, CO from a *meso* carbon and the linear pyrrole biliverdin (Figure 2). Biliverdin reductase converts this to bilirubin which is believed to be an important endogenous antioxidant [38] and may be considred an anti-inflammatory response [39]. However, high levels of bilirubin, as produced in liver disease, can be toxic and so the body aids the excretion by coupling to glucuronides to make it more hydrophilic.

2.2. Genetic disorders

Phenotypic consequences of inherited defects in enzymes of the heme pathway in humans (porphyrias) are known for all genes expressed in the liver except for that of ALA synthesis (Table 1) [3,40,41]. Deficiency of ALAS2 in erythroid tissue does not lead to a porphyria but causes X-linked sideroblastic anemia with iron deposition in mitochondria [3]. Some porphyrias are expressed in heterozygotes and in others the phenotype is seen in patients homozygous for the mutation. Although the porphyrias are relatively rare, the frequency varies greatly for each gene. The incidence of a particular mutation can also be much higher in one population than in another. For instance, in variegate porphyria (due to a mutation in PPOX) the incidence in some populations of South Africa is much higher than in other countries probably due its introduction into the Cape region from a Dutch settler over 300 years ago [42]. Over the last decade or so it has become clear that phenotypic manifestation is often considerably less than might be predicted from the genotype. This is probably due to an interaction of "environmental" factors such as nutrition and hormones with genes that modify responses. For each porphyria, one gene mutation dominates but its effect may be very dependent on expression of other genes or factors. Many of the details of these interactions have yet to be fully understood but this is not an unusual scenario. In fact, most diseases are complex interactions between multigenetic actions and physiological and external influences.

The results of enzyme deficiencies of the heme biosynthetic pathway means that intermediates in the pathway, such as 5-ALA and porphyrinogens, may accumulate in tissues and/or are excreted in elevated amounts. In addition, the porphyrinogen intermediates are unstable, especially to light, and form the respective porphyrins. Porphyrias have been classified clinically as either hepatic or erythropoietic, depending on whether the primary gene affected is predominantly expressed in the liver or bone marrow, and as acute or cutaneous depending on symptoms [40]. Broadly, in acute porphyrias there is an over production of simpler precursors such as 5-ALA and porphobilinogen before porphyrinogens are formed (or the oxidative porphyrin products) and this can be manifested clinically by neurological disturbances involving mechanisms that have not yet been resolved. In cutaneous porphyrias, porphyrins are produced in excessive amounts and can be deposited in the skin causing photosensitivity and are probably also toxic to the liver in high quantities. However, the separation between acute and cutaneous porphyrias is not absolute; for instance both types are seen in variegate porphyria (Table 1).

Of particular relevance to this review is the disorder PCT which encompasses a group of diseases characterized by a deficiency of UROD [3,40,43,44]. In familial (or type II) PCT, various mutations in the UROD gene lead to reduced activity in the decarboxylation of uroporphyrinogen III

Table 1 Human genetic diseases associated with heme synthesis

Enzyme	Gene	Condition	Abbreviation	Inheritance
5-Aminolevulinate synthase 1	*ALAS1*	None known		
5-Aminolevulinate synthase 2	*ALAS2*	X-linked sideroblastic anemia	XLSA	X linked R
5-Aminolevulinate dehydratase	*ALAD*	ALA dehydratase deficiency porphyria	ADP	R
Hydroxymethylbilane synthase	*HMBS*	Acute intermittent porphyria	AIP	D
Uroporphyrinogen III synthase	*UROS*	Congenital erythropoietic porphyria	CEP	R
Uroporphyrinogen III decarboxylase	*UROD*	Porphyria cutanea tarda[a]	PCT	V
Uroporphyrinogen III decarboxylase	*UROD*	Hepatoerythropoietic porphyria	HEP	R
Coproporphyrinogen oxidase	*CPOX*	Hereditary coproporphyria	HCP	D
Protoporphyrinogen oxidase	*PPOX*	Variegate porphyria	VP	D
Ferrochelatase	*FECH*	Erythropoietic protoporphyria	EPP	D

[a] PCT is heterozygous; the very rare homozygous form is HEP. R, autosomal recessive; D, autosomal dominant; V, variable.
Many different mutations in these genes have been recorded and affect the phenotypic outcomes.

to coproporphyrinogen III in blood, liver, and other tissues. The result is the accumulation of uroporphyrinogen I and III as well as partial decarboxylation products which become oxidized to the respective porphyrins. These porphyrins not only pile-up in the liver, but are excreted in large quantities in the feces and particularly in the urine (because of their hydrophilic nature). In addition, uroporphyrins are deposited in other tissues especially bone, teeth, and skin. The presence in the skin can cause extreme photosensitivity, especially in sunny climes, for instance causing development of vesicles that progress to crusting, scarring, and pigmentation. Porphyrin-mediated activation of the complement system occurs. Hypertrichosis may develop as a protection mechanism. Liver in PCT patients often shows siderosis but also classic signs of hepatic damage including steatosis, necrosis, and chronic inflammatory responses.

Sporadic (or type I PCT) might be considered more interesting in that it is an acquired disorder characterized by decreased UROD activity in the liver, not in erythrocytes, but otherwise very similar to familial PCT [43,44]. From a toxicological perspective, it has similarities with sporadic adverse reactions to drugs. Precipitating factors include alcohol consumption, estrogen exposure as in contraceptive steroids, various viral infections such as hepatitis C and HIV, and moderately elevated levels of hepatic iron [45]. Some classic toxicological agents, hexachlorobenzene, 2,3,7,8-tetrachlordibenzo-*p*-dioxin and coplanar polychlorinated biphenyls, cause a PCT-like condition in humans and rodents and can be viewed as precipitating factors for a genetic predisposition [44,46]. What the mechanism is that leads to a deficiency of UROD activity in sporadic PCT is not known but it is not apparently accompanied by immunoreactive protein loss [47]. Predisposing genetic factors can include hemochromatosis gene (*HFE*) mutations and there are undoubtedly others not yet identified, perhaps also linked to iron metabolism [48,49]. It is probable that mutations of *UROD* in familial PCT are a predisposing factor for the mechanism of sporadic PCT development.

In treating both sporadic and familial PCT removal of any possible precipitating factor such as alcohol is required. In addition, phlebotomy to reduce iron stores seems to be effective in relieving clinical symptoms [43,44].

2.3. Chemical and drug disruption

It has been known for many years that a range of drugs and chemicals including metals could disrupt heme synthesis, in rodent liver particularly but also other organs, and could be used as models to explore phenotypes of human porphyrias [21,50]. In addition, they were also extremely important in elucidating the fundamentals of the pathway and it interactions with
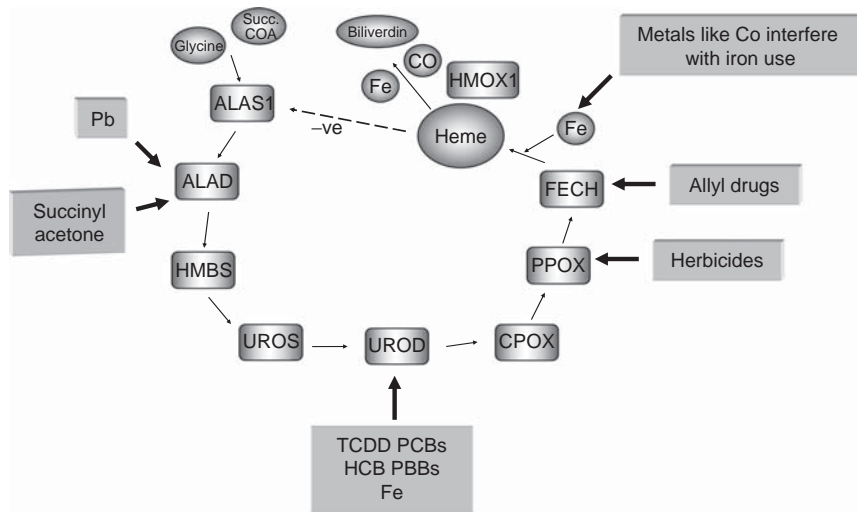
Figure 3 Examples of disruption of heme synthesis by chemicals *in vivo*. Enzyme abbreviations are those shown in legend of Figure 2.

cytochrome P450 in drug metabolism (Figure 3). One of the simplest interactions is the well known inhibition of 5-ALA dehydratase by lead (Pb) which in mice has been shown to be genetically variable [51]. Lead also acts at other stages including 5-ALA formation. Another interesting example is of succinyl acetone that is excreted in human tyrosinemia. This is a powerful inhibitor of ALA dehydratase and has been an extremely useful tool in many studies on the role of heme in biological processes [52]. The demonstration that succinyl acetone is produced in *zeta* glutathione transferase, null mice, identical with maleylacetoacetate isomerase, probably as a consequence of disturbed phenylalanine and tyrosine metabolism, shows the complex interactions that may occur between heme homeostasis and general intermediary metabolism [53].

Although protoporphyrinogen will oxidize naturally to protoporphyrin, both in animals and plants *in vivo*, this is controlled enzymatically by protoporphyrinogen oxidase (PPOX) [2]. Inhibition of this enzyme causes inappropriate oxidation of protoporphyrinogen and accumulation of protoporphyrin that can lead to photosensitivity. This has been exploited by the agrochemical industry to produce herbicides such as acifluoren which inhibit PPOX in weeds making them sensitive to sunlight just as are patients with hepatocutaneous porphyrias. These PPOX inhibitors act similarly in rodents [54]. A number of metals besides lead, including mercury, affect heme synthesis at various steps and these can be tissue and polymorphism

specific [55,56]. One step in heme synthesis sensitive to chemicals that has been particularly studied is the insertion of iron (Fe^{2+}) into protoporphyrin IX by ferrochelatase to form heme. Cobalt ions *in vivo* can substitute for iron in heme production in the liver causing a lack of protoporphyrin for cytochrome P450 [57]. Many of the metals also induce heme oxygenase 1 and modify 5-ALA synthase activity potentially exacerbating heme availability.

Ferrochelatase is also the molecular target for other inhibitors of heme metabolism. Extensive work by De Matteis, Marks, Ortiz de Montellano, and Tephly and their colleagues demonstrated that in the metabolism by cytochrome P450 forms of a range of drugs and chemicals, especially those containing alkene or alkyne functions, the heme moiety of the hemoprotein can be alkylated at one of the pyrrole nitrogens via suicidal inactivation [58]. Once released from the compromised cytochrome P450 the iron atom of the modified heme is lost. If alkylated with a small substituent, especially a methyl or ethyl group, the *N*-alkylated–protoporphyrin IX adducts can be powerful inhibitors of ferrochelatase. In some species and with certain drugs, the consequence is accumulation of protoporphyrin in the liver not unlike that seen with human erythropoietic protoporphyria. Periodically, a drug under development is observed to cause such a response in dogs or other test animals which may be viewed as a toxic effect. Comparisons with erythropoietic protoporphyria can be misleading since the origin of protoporphyrin in the liver in the human disease appears to be mainly of erythropoietic origin, as also occurs in the ferrochelatase mutant mouse, whereas with griseofulvin the porphyrin is mainly of hepatic origin [59].

The most intractable problem of how some chemicals cause dysfunctions of heme metabolism is with the effects of the chlorinated aromatics such as hexachlorobenzene (HCB), chlorinated biphenyls (PCBs), and 2,3,7,8-tetrachlorodibenzo-*p*-dioxin (TCDD) in experimental animals and in humans (Figure 4). The primary site of action is in causing marked inhibition of the action of UROD leading to great accumulation of uroporphyrins in the liver. Excretion of uroporphyrin in the urine can be so great as to color it red (Figure 5). After decades of work the mechanism is still not resolved. It is of considerable interest because of the similarity with sporadic PCT in humans. Both disorders appear to have genetically variable components and seem to involve disturbed iron homeostasis. Experimental studies also implicate a role for the AHR, especially with the polychlorinated aromatic chemicals that binds TCDD as its prototype molecule. The history, including how this was first discovered in humans, details of the biochemical toxicology, genetic investigations, and most the recent pertinent finding are summarized here.
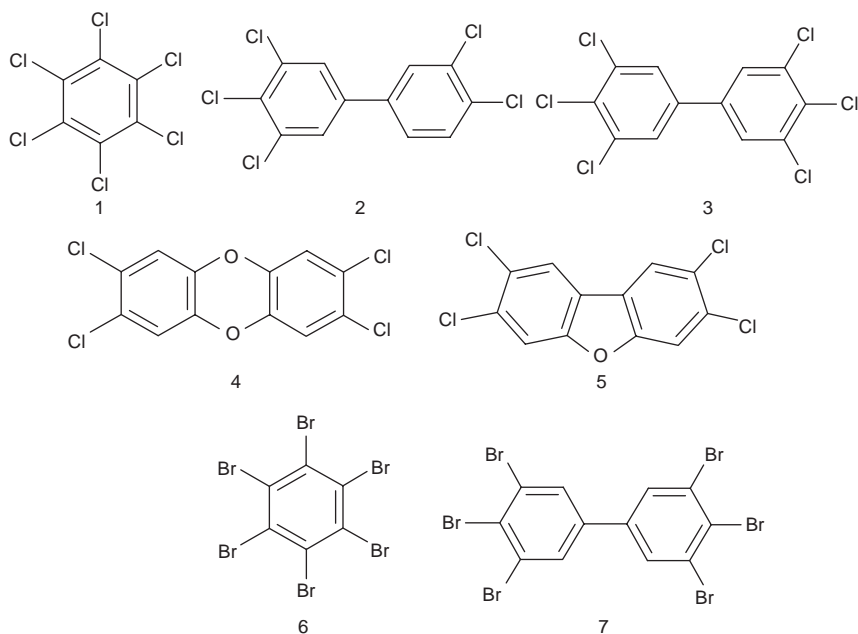
Figure 4 Some polyhalogenated aromatic chemicals that cause porphyria. 1. Hexachlorobenzene; 2. 3,3′,4,4′,5-pentachlorobiphenyl; 3. 3,3′,4,4′,5,5′-hexachlorobiphenyl; 4. 2,3,7,8-tetrachlorodibenzo-*p*-dioxin; 5. 2,3,7,8-tetrachlorodibenzofuran; 6. hexabromobenzene; 7. 3,3′,4,4′,5,5′-hexabromobiphenyl.

3. Porphyria Caused by Polyhalogenated Aromatics

3.1. Incidences in humans

Up until the mid-twentieth century PCT in humans had been reported to occur mainly in middle-age to older men and associated with moderate to heavy drinking of alcohol [3,43–45]. On the whole, some liver damage was usually present but PCT did not seem to occur in patients with severe hepatic problems, as if a moderately healthy liver is required. However, from 1955 until at least 1960, many people were observed in eastern Turkey to be exhibiting PCT-like symptoms unlike the more sporadic occurrences documented in the USA or in Europe [46,60–65]. The usual precipitating factors like alcohol could not be implicated. What is more, most of the cases were young, unlike the majority of sporadic PCT patients. Eventually, and unfortunately, after many more cases, the cause was pin pointed as the fungicide HCB which had been consumed in bread and bulgar prepared from wheat treated with the fungicide and originally destined to be seeds
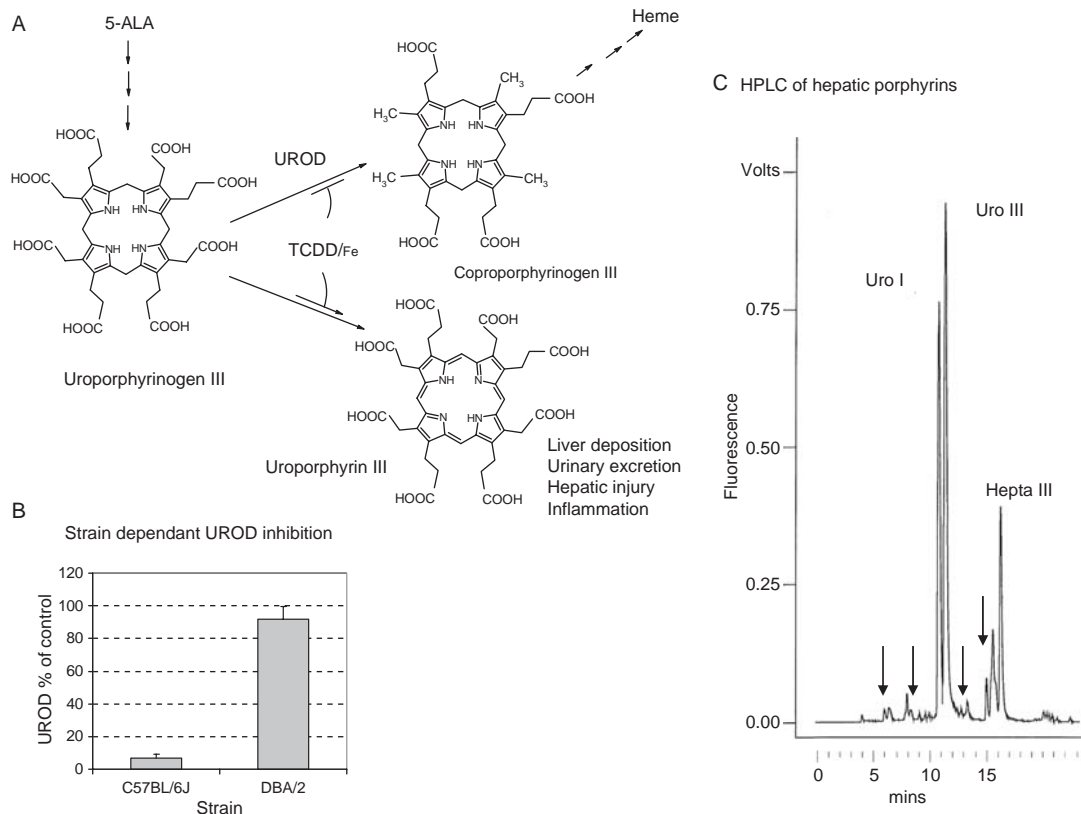
Figure 5 Induction of hepatic porphyria by TCDD in mice by 2,3,7,-tetrachlorodibenzo-*p*-dioxin (TCDD). A. Scheme showing inhibition of UROD by TCDD and oxidation of uroporphyrinogen III to uroporphyrin III leading to porphyria and liver damage. B. Inhibition of UROD in C57BL/6J mice but not in resistant DBA/2. C. Reverse phase HPLC of liver porphyrins showing high levels of uroporphyrins I and III and heptacarboxylic acid porphyrin IIId. Arrows demonstrate presence of oxy porphyrins and chlorins.

for planting. The exact reasons why the HCB-treated wheat was eaten by whole populations, rather than being planted, has never been properly explained. Reasons may included low crop yields coupled with late arrival of seed wheat from abroad so that local seed was planted and imported fungicide-treated wheat was eaten. However, it is difficult to understand why this continued for some years. In addition, local speculators may have bought up cheap seed wheat from the government and sold it on to the local population. Although it was reputed that some thousands of cases of porphyria developed this was still probably less than 10% of those people that had consumed the chemical. In 1959, HCB was withdrawn as a fungicide and cases of ''Turkish porphyria'' declined over the next 2 years. Instead of porphyria, many young patients exhibited a condition known as ''pembe yara'' which was associated with high mortality and has never been reproduced in experimental animals [64,66]. It should be pointed out that the seed wheat also contained mercuric salts although the erythematoid sores reported in babies and toddlers are not symptoms of mercury poisoning.

The majority of those patients in south-east Turkey who developed porphyria were children and male. They developed lesions such as bullae and skin fragility on areas of skin that were frequently exposed to the sun, such as face, arms, and legs [67,68]. These areas were later associated with severe hypertrichosis and hyperpigmenatation and frequently infections and scarring that could lead to partial loss of phalanges and psychiatric problems. In some patients that were examined other symptoms were observed that were probably due to the initial exposure to HCB rather than as a consequence of porphyria. Not surprisingly for a disease of skin sensitization to light, symptoms were much more severe in summer than in winter when days and strength of sunshine were much less [64,67,69].

Although the early literature contains some interesting and suprising studies on the outbreak of the poisoning, opportunities for extensive studies were limited. Fascinating details can be found in full in previous reviews [46,60] and suggest marked individual factors of sex, age, and genetics [70]. Information on liver functions is limited but many patients were reported to have hepatomegaly or were cachectic [64,67,69]. Thyroid enlargement was observed in some individuals. Examination of isolated cases revealed cirrhosis or hydropic and granular degeneration of hepatocytes. Needle biopsy samples of liver fluoresced red under ultraviolet light whereas bone marrow did not, compatible with a hepatic rather than acute type of porphyria [69]. Urine was often dark red-brown, due to the presence of uroporphyrins, similar to that seen with PCT patients. Because of the slow metabolism and persistence of HCB in the body, some patients examined up to 30 years still showed elevated excretion of porphyrins as well as scarring and other symptoms [71,72].

The Turkish HCB–induced porphyria episode still remains one of the most significant mass poisonings in modern history. Other episodes of exposure of humans to such polychlorinated chemicals have been less significant in terms of seeing any reported cases of porphyria [73,74]. Despite significant contamination by HCB of factory workers synthesizing chlorinated chemicals and nearby inhabitants of a village in Spain, very few showed elevated porphyrin levels and no cases of overt PCT were found that could not be explained by alcohol consumption [75]. Only slight irregularities in porphyrin excretion have been reported for other workers exposed to HCB [46,60,76–78]. The marked difference between these cohorts and the Turkish patients in development of porphyria is probably explained by the much greater consumption of HCB by the latter group. In itself this is of importance in assessing the risk from exposure to HCB.

In classic poisonings or contamination of people by polychlorinated biphenyls (PCBs) in Japan, Taiwan, and other countries only mild changes in the excretion of porphyrins have been observed [46,76–84]. Similarly, in contamination of the food chain by polybrominated biphenyls through accidental poisoning of cattle feed in Michigan, only mild changes in patterns of porphyrin excretion by farmers were detected and no overt cases of porphyria [85].

Toxicologically, the most potent polychlorinated aromatic chemicals are the dibenzo-p-dioxins and dibenzofurans. However, again the evidence that TCDD or related chemicals cause porphyria like PCT is weaker than it is for HCB [46,86–88]. In 1964, Bleiberg reported that 11 patients had PCT like symptoms out of 29 workers that had developed chloracne (the most established symptom of TCDD poisoning in humans) while working in a New Jersey factory making the herbicides 2,5-dichloro- and 2,4,5-trichlorophenoxyacetic acids [89]. Most patients probably had uroporphyrinuria (high levels of uroporphyrin in the urine) not the obvious skin lesions seen clinically with PCT. Many cases of uroporphyrinuria or PCT were reported in a similar chemical plant in Czechoslovakia in the 1970s where 55 workers developed chloracne [83,90,91]. Other chemicals were also made at these plants including chlorinated benzenes. A worker exposed to waste oil contaminated with TCDD developed both PCT and chloracne [92]. Other studies of people exposed occupationally or accidentally to TCDD have shown no correlation with chloracne development or their body burdens of TCDD and PCT although disturbances of porphyrin metabolism have detected from analysis of their urine [46]. These studies include the large population poisoned in Seveso, Italy [93] but there may well other groups around the world which have not been investigated.

Clearly, polychlorinated aromatic chemicals can cause disturbance of heme synthesis in man of which HCB is by far the most documented chemical leading to a severe disorder closely resembling PCT. In humans, the action of PCBs and TCDD appear much weaker. However, in

experimental animals TCDD and PCBs, as well as HCB, are powerful disruptors of hepatic heme synthesis.

3.2. Porphyria in animals induced by HCB, PCBs, and TCDD

Following the episode of porphyria in Turkey, feeding HCB to rabbits and rats was found to cause massive hepatic porphyria [94–97]. High levels of the chemical were given to the animals but even so it took several weeks in rats before overt porphyria was manifested as the characteristic fluorescent liver and urine, due to the accumulation and excretion of uroporphyrin isomers I and III as well as 5-ALA and porphobilinogen. Perhaps because of the slow metabolism of HCB the porphyria may take weeks or months to regress. There are also indications that the time to regress may not be entirely related to the body or liver burden of HCB but to additional factors intrinsic in the mechanism of UROD inactivity. Some species, such as the hamster, are very resistant (Smith, unpublished data), whereas quail and cultures of chick embryo liver respond extremely rapidly [98–103]. Mice may succumb to chronic nervous and dermal toxicity before developing porphyria but this can be dramatically altered by manipulation of other physiological systems (see later). Rats will also develop porphyria after exposure to hexabromobenzene although comparisons of potency with HCB are difficult due to the greater insolubility and much higher molecular weight of this chemical [104–106]. The related chemical octachlorostyrene may be porphyrogenic in quail but has little effect in rats or mice [107,108]. Less chlorinated benzenes have been shown to cause disturbances of heme metabolism but nowhere near the severity seen with HCB [46]. Metabolism of HCB is slow but extensive involving hydroxylation to pentachlorophenol and conjugation to glucuronide or direct reaction with glutathione leading to excretion of the mercapturate [109,110]. Overall, there is little evidence that any metabolite causes the inactivation of UROD activity although at one time this was a favored mechanistic hypothesis. HCB-induced porphyria in the rat has been reported to be modulated by a number of endogeneous factors including N-acetylcysteine, S-adenosyl-L-methionine, thyroid and steroid hormones, and various drugs but no particular mechanisms have been identified [46]. Some may involve induction by drugs and chemicals of antioxidant systems. The clearest effect is probably the influence of estrogenic steroids. Male rats are markedly more resistant than females to the porphyria inducing potential of HCB [111–113]. This can be reversed by estrogenic drugs such as diethylstilbestrol [114]. The sexual dimorphism is of interest since with most drugs or chemicals it is the female sex which is usually more resistant to a response due to lower induction of cytochrome P450, etc. In addition, estrogenic drugs have been heavily implicated as precipitating factors in many PCT patients [45].

Higher chlorinated PCB mixtures, such as Aroclor 1254 and 1260, cause porphyria in rats, rabbits, and quail [46,115–119]. Similarly, the polybrominated mixture FireMaster caused chronic induction of porphyria in rats, with symptoms of fluorescent livers and urine, after an initial delay of some weeks, predominantly in female rats, very similar to HCB but with greater potency on a weight for weight basis [120,121]. What is more, unlike HCB, mice are also affected by these chemicals.

The demonstration that TCDD is an extremely powerful inducer of porphyria in mice completed the spectrum of the types of polychlorinated chemicals that could cause this type of disruption of hepatic heme synthesis [122–124]. Rather than continual oral administration of HCB or PCBs, a single small dose of ~2 μg of TCDD per mouse is sufficient to cause both hepatic damage and porphyria (Figure 5) [123]. Interestingly, although porphyria takes a few weeks to manifest, progressive depression of UROD activity in the liver can be detected within a few days but takes some weeks to be reversed. In rats, porphyria takes much longer to develop and with weekly does of TCDD [125,126]. This is partly due to the systemic toxicity observed when larger doses, comparable to that given to the mouse, are administered to the rat and so many small doses have to be given. The extreme potency of TCDD and difference from HCB in structure is further evidence for the lack of association of a specific chemical metabolite with UROD inhibition. The slow metabolism of the polyhalogenated chemicals, with resultant long-term induction of drug metabolism enzymes and other gene expressions including ALAS1, is probably a factor in their ability to induce hepatic toxicity and porphyria.

3.3. Implication of the AHR

The action of TCDD and coplanar PCBs to act as long-term occupancy ligands for the AHR with toxic and carcinogenic consequences has been, and continues to be, a highly researched area which is reviewed frequently. An important aspect is the apparent lack of a similar toxic effect of non-chlorinated high affinity ligands. Here, the focus will be on the evidence that the specific toxicity of polyhalogenated aromatics associated with dysfunction of heme synthesis in the liver is linked to these chemicals acting as AHR ligands.

The early demonstration that TCDD, including a single dose, cause hepatic porphyria in C57BL/6 mice with up-regulation of ALAS1 is an important finding that allowed many further investigations of the mechanism [122]. Using crosses of C57BL/6J and DBA/2 mice with high and low affinity AHRs (b1 and d), respectively for ligands, susceptibility to TCDD for inhibition of UROD and development of porphyria was shown to be inherited with aryl hydrocarbon rsponsiveness [46,127]. This could be complemented by comparisons of the C57BL.D2 congenic strain

expressing the DBA/2 low affinity receptor in the C57BL/6 background [128]. In general, if C57BL and DBA/2 mice are compared this association has stood up not only with TCDD but also with PCBs. Genetic studies of C57BL × DBA/2 F_2 crosses exposed to TCDD have clearly shown the contribution to porphyria of a polymorphic gene consistent with it being *Ahr* [128]. Most recently for porphyria caused by TCDD in mice, the necessity for AHR expression has been demonstrated using *Ahr* null mice. C57BL/6 *Ahr*$^{-/-}$ mice show no susceptibility to porphyria if administered TCDD, and little associated hepatic toxicity, even with a 10-fold increase in dose, in line with previous findings on other aspects of TCDD-induced toxicity [129]. However, it has become clear that the original view that polymorphism in the *Ahr* gene was the only factor for determining susceptibility to TCDD and related chemicals causing porphyria, is an over simplification. Other strains of mice such as BALB/c with a similar AHR to C57BL mice (AHRs) are much less susceptible [130]. On the other hand a number of strains with identical AHR (d type) to DBA/2 respond to TCDD if first given iron, a known factor in human PCT.

In many aspects of its experimental toxicity, HCB causes effects not unlike those of TCDD. Although its shape does not conform to the preferred structure usually accepted for AHR ligands, in its binding properties and enzyme inducing properties HCB does appears to be a weak ligand *in vitro* and *in vivo* [131–133]. Findings of association of porphyria induced by HCB in genetic studies of C57BL × DBA/2 crosses and of the response of C57BL.D2 congenic mice, as well as of other mouse strains, are compatible with a role for the AHR [132,134]. However, despite the fact that the HCB used in most investigations has been of an extremely high grade [135], there have been suggestions over the years that trace levels of TCDD and its congeners might account for its observed toxicity [136]. Recent analyses have shown that even the highly purified preparations do indeed contain trace levels of TCDD but this does not seem to account for its porphyrogenic properties (Smith, unpublished data). It is likely that this is an issue that will rumble on for some time to come. Purifying enough HCB free of all traces of polychlorinated dibenzo-*p*-dioxins and furans to enable unequivocal toxicological investigations on a variety of endpoints will be a challenging task but should be undertaken if there is debate as to whether HCB should be included in the risk assessment of "dioxin" like chemicals [137].

3.4. Evidence for a role of hepatic iron status

A great deal of evidence supports the view that some unknown aspect of hepatic iron homeostasis, with perhaps modest increases in iron levels, is involved in the development of PCT in humans [3,44,45]. Venesection is a well proven treatment for PCT even if patients have no apparent increases in iron stores. Recent evidence shows that inheritance of the hemochromatosis

gene in UK and US populations is associated with increased risk for the disorder although only a few patients develop PCT [48,49]. A variety of studies suggested that iron status may also play a role in the inhibition of UROD and subsequent porphyria in rats administered HCB. Porphyria development is enhanced by injections of iron dextran [138–142] and ameliorated by bleeding or the powerful iron chelator desferrioxamine [143,144]. This suggests that similar mechanisms occur in both human PCT and in the porphyria caused by polyhalogenated chemicals in rodents. Interestingly, in rats hepatic iron levels, and some antioxidant enzymes, are often greater in females than males for reasons that have never been clarified.

As with PCT, lowering hepatic iron by bleeding, an orally active iron chelator, or low iron diets appears to protect mice from the porphyrogenic properties of TCDD or powerful PCBs [124,145–147]. Interpretation of some of these experiments has been queried as it is difficult to do these studies without altering other physiological and nutritional parameters [145]. The influence of a pretreatment of iron dextran on porphyria development in mice has been especially marked and has led to a variety of new models of PCT. Administration of iron dextran to C57BL/10ScSn mice greatly enhances general hepatic toxicity and porphyria induced by TCDD, PCBs, and poly-brominated biphenyls even in $Ahr^{+/-}$ null mice [129,130,135,140,147,148]. Most interestingly, treatment of iron will overcome the resistance of many Ahr^b and Ahr^d mouse strains to the hepatotoxic and porphyrogenic actions of TCDD whereas the DBA/2 strain remains resistant [130,149]. $Ahr^{-/-}$ null mice remain totally resistant [129]. The most significant findings have been with HCB that in mice frequently produces neurotoxicity before hepatic porphyria develops. Pretreatment with iron dextran, often by one subcutaneous injection, sensitises C57BL/10ScSn mice to HCB in the diet to a remarkable degree resulting in hepatic porphyria [135,150]. Although excretory routes of metabolites may be altered, overall metabolism of HCB is not appreciatively affected [151]. Interestingly, after a single oral dose of HCB to iron loaded mice, inhibition of UROD and porphyria is observed after a time lag but continues for the life of the animal despite the fall in the levels of the organochlorine with metabolism [148,152]. Careful estimations showed that inhibition of UROD appeared before major elevation of hepatic porphyrin levels and liver damage [152]. Such effects are also observed with other polyhalogenated aromatic chemicals [123].

The marked potentiation and prolonged effect of iron on porphyra induced by polychlorinated aromatics led to new avenues of thinking about experimental models of PCT. Mechanisms of PCT and experimental porphyria as pathogenic modulations of iron homeostasis were early suggestions in the field but it had been difficult to reconcile PCT and the disorders produced experimentally by TCDD, PCBs, and HCB. As TCDD and other poorly metabolized chemicals of this type are inducers of the cytochrome P450 1A system via activation of the AHR, the hypothesis was proposed

that classic nonchlorinated polycyclic aromatic hydrocarbons might also induce porphyria in iron treated mice. Multiple doses or dietary application of polycyclic aromatic hydrocarbons, such as β–naphthoflavone, 3–methyl–cholanthrene, and dibenz[*ah*]anthracene, do indeed inhibit UROD and caused porphyria [153,154]. In addition, this is extra evidence against the idea that a specific metabolite of the chlorinated chemicals is involved in the inhibition of UROD and demonstrates a novel mode of toxicity of carcinogenic polycyclic aromatic hydrocarbons. That the flux through the heme pathway might be an important factor is supported by the stimulation of porphyria as a consequence of continuous administration of the heme precursor 5–ALA [154].

After more than 15 weeks of chronic iron overload of C57BL/10ScSn mice, iron alone eventually induces porphyria [148,155,156]. Iron also causes porphyria in the related strain C57BL/6J if also administered the heme precursor 5–ALA [157]. This probably accounts for the continued inhibition of UROD after HCB when the level of the chemical has greatly declined. Comparison of other strains show that SWR mice with significantly higher basal hepatic iron levels than C57BL mice also develop porphyria if only given 5–ALA [158]. Null hemochromatosis gene (*Hfe⁻* / *Hfe⁻*) mice with elevated hepatic iron levels and heterozygous null for the *Urod* also exhibited porphyria after a few months [159]as do *Hfe* null mice administered 5–ALA [160].

Although implicated in sporadic PCT, there has been until recently little evidence that alcohol will induce porphyria in experimental animals. Administration of 5% or 10% alcohol in the drinking water iron loaded to C57BL/10ScSn mice for up to 20 weeks failed to induce porphyria to no greater extent or any earlier than iron treatment alone (Smith, unpublished data). In contrast, *Hfe* null mice in the 129S6/SvEvTAC strain, developing elevated tissue iron, given 10% or 15% alcohol for 6.5 months have accumulation of uroporphyrin in the liver whereas *Hfe* null mice on a C57BL/6 background are not susceptible [161,162], although the length of the time and severity are not faster or greater, respectively, than occurs with just iron overload in the wild type C57BL/10ScSn line [155,156]. In rats, ethanol disturbs heme synthesis and seems to be a predisposing factor for HCB [163].

All of these findings demonstrate that the disruption of heme biosynthesis by polyhalogenated aromatic ligands via the AHR, and by other chemicals, can be viewed as potentiating the consequences of an endogenous malfunction of iron metabolism.

3.5. Genetic predispositions

Familial and sporadic PCT were at one time seen as separate disorders [3,164] but it now seems likely that deficiency in UROD in the former acts as a predisposing factor for the latter [44]. Mutations in the

hemochromatosis gene may be a genetic predisposition for some PCT patients. For Turkish patients poisoned by HCB, genetic predispositions also seem likely as even within families some individuals developed the disorder while others did not [70]. Thus it is probable that like other diseases, sporadic PCT and that of the Turkish episode are the result of complex interactions between genetic and so-called "environmental" factors. The experimental findings in rodents are one way to explore these genetic interactions as well as a route to elucidating the mechanisms involved. Two rat strains were originally shown to differ in their response to HCB which could have been associated with differing levels of hepatic iron but this has not been further explored genetically because one was outbred and the other inbred [165]. Analyses of the response of inbred strains of mice to porphyrogenic agents have been much more rewarding.

Extensive studies illustrated that the porphyrias induced by TCDD, with a marked block in UROD activity and high accumulation and excretion of uroporphyrins, varied considerably between mouse strains [127,130,166,167]. Preliminary studies of genetic crosses suggested that this was solely dependent on the inheritance of a responsive allele of the *Ahr* gene [127]. C57BL/6J or C57BL/10ScSn mice with the high affinity AHR (Ahr^{b1} allele) were far more sensitive than DBA/2 mice with the low affinity AHR (Ahr^d allele). In fact, the latter strain appear refractory to the porphyria inducing effects of TCDD. However, with investigations of other strains and crosses the story became more complex illustrating the involvement of genes besides *Ahr*. Strains like BALB/c with the variant responsive Ahr^{b2} allele are less sensitive then Ahr^{b1} mice but become much more susceptible to porphyria if first given iron [130]. In addition, some Ahr^d strains, such as AKR and SWR, also become susceptible with this regimen whereas DBA/2 mice remain resistant.

The conclusion from these studies is that the induction of porphyria in inbred mice is a complex trait. The AHR is usually required and the Ahr^{b1} allele an important susceptibility gene if AHR ligands are administered. However, other susceptibility genes can play a significant role and may implicate polymorphisms of genes of iron homeostasis. Comparison of the susceptibility of 12 inbred strains of mice to porphyria induced by iron treatment showed distinct variability but no correlation with *Ahr* genotype alone [156]. Using quantitative trait locus (QTL) analysis with polymorphic microsatellite DNA markers to associate chromosomal regions (gene positions) with porphyric response [168], susceptibility loci to TCDD and HCB have been identified in iron loaded F_2 crosses between some of these strains and highly resistant DBA/2 mice (Figure 6). A QTL on chromosome 12, corresponding in position to the Ah^{b1} gene, was observed when C57BL/6J or C57BL/10ScSn, respectively, were the sensitive strain [128,134]. As expected in a F_2 cross between the two Ahr^d strains, SWR and DBA/2, given iron and TCDD, a QTL corresponding to the *Ahr* was not detected.
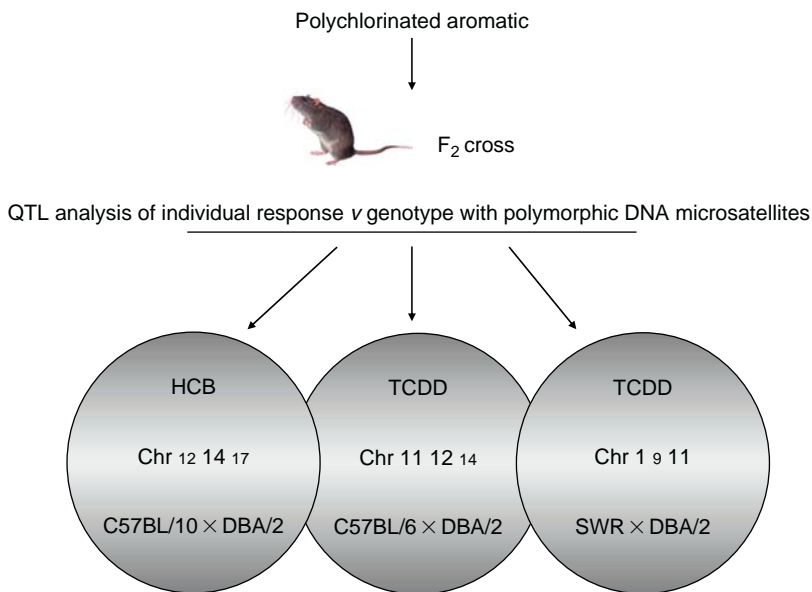
Figure 6 Different susceptibility loci for porphyria induced by TCDD and HCB despite similar quantitative responses. Susceptible C57BL or SWR strains of mice were crossed with highly resistant DBA/2 to give F_1 offspring which were then mated to yield the F_2 generations. Porphyric responses of individual mice after dosing with iron and TCDD or HCB were compared with genotype polymorphism at approximately 10–20 cM positions along each chromosome by quantitative trait analysis (QTL) using polymorphic DNA microsatellite markers.

However, with both C57BL/6J and SWR mice as the susceptible parental lines exposed to TCDD there was at least one susceptibility gene on chromosome 11 (Figure 6) and with porphyria caused by HCB in C57BL/10ScSn mice, loci on chromosomes 14 and 17 were observed. A QTL on chromosome 14 was also detected in the susceptibility of C57BL/6J mice to TCDD but not SWR. In contrast, more than one susceptibility gene on chromosome 1 appeared to contribute to the susceptibility of the SWR strain to TCDD (Figure 6) [128]. Hence, although the endpoint porphyria phenotype is similar in these three models of PCT, polymorphisms in genes affording susceptibility vary in their penetrance and are not identical. Alleles of the *Ahr* may play an important role but expressions of other genes have a marked modulating influence.

It would, of course, be extremely important to identify the susceptibility genes contributing to the QTL as these may have orthologs pertinent to understanding sporadic PCT. So far, QTL studies of the porphyria induced by regimens of iron treatment without polyhalogenated aromatics have not been reported. Studies of this kind would be significant, not only for the

mechanism of porphyria but as an example of iron-induced toxicity rather than iron status that has been mostly studied [169].

3.6. Metabolic responses in porphyria

3.6.1. Modulation of the heme and iron metabolism pathways

Depletion in activity of UROD is the most characteristic enzymic change in the liver that occurs in the porphyria following exposure to TCDD, PCBs, and HCB (Figure 5) [170–172]. This is very similar to PCT [44,173] and although its importance has been debated, it is probable that this is the most significant event leading to the high levels of uroporphyrin isomers in the liver and urine. Assay of the enzyme is not easy because of the instability of the prime substrate uroporphyrinogen III and the number of possible intermediates in coproporphyrinogen formation and their leakage from the enzyme [46]. In most scenarios that have been investigated UROD activity starts to decrease before major rises in porphyrin levels, whatever the causative agent, and correlate with sensitivity of various models [123,152,172]. The reasons for the decreased activity are still not properly elucidated and are discussed later. The few studies that have been conducted show little change in protein or mRNA expression although activity is reduced to less than 50% [129,174,175]. Minor modulations in other enzymes of the heme pathway may occur to contribute to the phenotype. Of these the most important is 5-ALA synthase (ALAS1). In some experimental systems ALAS1 becomes induced, partly as a derepression mechanism following depletion of the end product heme (Figure 3) [46,122,129,141,176–178]. Up-regulation may depend on the degree of porphyria being sufficient to cause a shortage of heme for cytochrome P450 and other cytochromes, perhaps under chronic conditions [9]. This greater supply of heme precursor may also serve to potentiate the block at UROD and thus aggravate the porphyria. This is the rationale, and possibly the reason, why administration of 5-ALA to mice enhances the action of porphyrogenic chemicals [157,158,179]. Iron loaded $Urod^{+/-}$ mice develop porphyria much faster if administered PCBs and 5-ALA than wild type mice [159,180].

Heme oxygenase metabolises heme to biliverdin (which is then reduced to bilirubin), CO and iron. Marked up-regulation of *Hmox1* occurs in most cells under circumstances of stress, including the exposure to chemicals and many drugs, and in current hypotheses might destroy heme destined for hemoproteins (Figures 1 and 3) [1]. Again this could enhance a porphyrogenic mechanism by leading to further up-regulation of 5-ALAS1 activity [181]. Up-regulation of hepatic *Hmox1* following TCDD has been shown recently in mice using gene array but how much this contributes to the porphyria is not entirely clear [129]. Such expression could be due to infiltration by white cells following toxic inflammation in the liver rather than to hepatocytes.

Without prior administration of iron, modest increases in hepatic iron may occur in both PCT and experimental porphyrias [122,123,182–184] although sometimes these may be the consequence of general liver damage, with possible increased intestinal uptake (see [46] for further details). In rats, TCDD aromatics may induce increases in microsomal and mitochondrial iron [185,186]. Microsomal systems that release iron from ferritin have been described but the physiological consequences are obscure [187]. A role for iron release is attractive as it could contribute to oxidation of heme precursors leading to an inhibitor of the UROD. Support for porphyrogenic chemicals mobilizing a ''toxic''pool of iron [22,36] has been found in rats administered HCB in which lysosomal, not mitochondrial, levels are elevated [188]. Ideas of iron homeostasis have become much more sophisticated in recent years with many more genes identified and there are probably more to be found [189]. Gene array analysis and other analyses have shown that hepatic expression of many of these genes is modulated as porphyria develops in C57BL/6J mice caused by TCDD and to a lesser extent in DBA/2 [129,149]. A connection between changes in expression of most of these genes and porphyria development is not clear and does not seem to account for susceptibility loci identified in QTL studies. Future identification of new iron metabolism genes may well do so.

3.6.2. Stimulation of the drug response pathways

Polyhalogenated aromatic chemicals such as TCDD, PCBs (e.g., as constituents of Aroclor 1254), and HCB have been established for many years as inducers of cytochrome P450 species (CYPs) and do not need to be described here in this context. Although the mixtures like Aroclor 1254, individual PCBs and HCB are inducers of a variety of CYPs, it is their ability to up-regulate CYP1A family members in particular that seems to correlate most closely with porphyria induction [36,46,190]. This seemingly would account for the action of the prototype AHR ligand TCDD to inhibit hepatic UROD in rats and mice and cause porphyria. Chronic induction via the transcription factor AHR appears to be required that is a consequence of the slow metabolism of these chemicals. This also accounts for the ability of nonchlorinated, but more quickly metabolized, AHR ligands to produce porphyria if administered for long enough and at high enough doses [153]. Expression of CYP1A2 appears to be much more important than CYP1A1 for porphyria development [179,191,192]. Mice null for the *Cyp1a2* gene are totally resistant to porphyria induced by iron, PCBs, HCB, and TCDD whereas the evidence for the role of *Cyp1a1* gene expression is equivocal [193–198]. It now seems clear that an optimum expression level of CYP1A2 protein is required and that much greater amounts may have no additional effect. This is exemplified by the massive induction of the *Cyp1a2* gene by TCDD in both C57BL/6J and DBA/2 mice yet only the former develop porphyria [128]. It is possible that under

some experimental conditions, for instance with HCB, other CYPs may also contribute to the toxic process [121,176,199–201].

Not only phase I enzymes are induced by polyhalogenated chemicals. Up- or down-regulation of glutathione transferases, transport proteins, genes associated with the antioxidant responses and those of intermediary metabolism can all be associated with a porphyrogenic response [129,149,202]. However, so far, as with iron metabolism, no specific mechanistic explanation has been forthcoming linked specifically to porphyria, and these may be of a general inductive/hepatotoxic nature as seen in a mutant model of porphyria [59].

4. MECHANISTIC HYPOTHESES

For some time it has been hypothesized that the mechanism for the porphyria induced by polyhalogenated chemicals is of an oxidative nature. The fact that these chlorinated chemicals are poorly metabolized and that the most potent chemical, TCDD, is administered in very small amounts, coupled with the establishment that nonchlorinated chemicals will also do this would seem to exclude the possibility of a reactive metabolite. In addition, the clear demonstration that iron itself is a porphyrogenic chemical in mice and as well as enhancing other regimens depending on genetic background, supports the view of an oxidative mechanism [36]. An iron-catalyzed oxidative process would explain not only porphyria caused by these environmental chemicals but also bridge the gap with a mechanism for human PCT.

4.1. Evidence for an oxidative process

Many papers have described hepatic lipid peroxidation and criteria of oxidative stress when rodents are administered HCB, PCBs, and TCDD [185,186,203–209]. In addition, there is evidence for protection from porphyria, induced by HCB or PCBs, by antioxidants [210] and modulation by iron chelators of [143–145,211]. In some of the simplest regimens, up-regulation of antioxidative stress genes has been observed by PCR or gene array [129]. Since lipid peroxidation and changes in antioxidant enzymes are very common in liver injury, one of the many unanswered questions is what selective oxidative stress processes occur which specifically lead to UROD inhibition and porphyria? Any mechanism has to account for the vital role of the AHR and the evidence for essential CYP1A2 expression but to a much lesser extent CYP1A1. The interrelationship between CYP1A2 and AHR seems complex. The role of AHR does not seem to be just as a transcription factor controlling CYP1A2 expression.

High expression of CYP1A2 is not sufficient for a porphyric response [128]. How would these relate to an oxidative mechanism? A sustained oxidative stress response as measured by oxidized GSH levels and 8-hydroxydeoxyguanosine was detected up to eight weeks following exposure of C57BL/6J mice to TCDD [212]. Similar findings have been shown with PCBs [203]. The assumption has been that these could be due to uncoupling of microsomal P450 species. CYP1A2 binds polyhalogenated chemicals of the AHR ligand type and this may perhaps enhance uncoupling [36]. Do such reactions occur *in vivo* with human CYP1A2, as well as with rodent enzyme? On the other hand, increased respiration-dependant generation of reactive oxygen species in mitochondria can be associated with the AHR but is independent of expression of CYP1A forms and leads to H_2O_2 formation and decreased ATP [213–216]. Whether generation of reactive oxygen in mitochondria or microsomes is important in the selective action at the level of UROD inhibition remains to be elucidated.

Many observations suggest that it is not the generation of active oxygen that is the key but the inappropriate release of Fe^{2+} that could catalyze a site-specific oxidative reaction [22,217,218]. Although *in vitro* microsomal systems from TCDD treated animals release iron, the pertinence remains obscure [187]. Even so, a selective mechanism involving some aspect of iron homeostasis could be important in reconciling the diverse experimental regimens that cause porphyria development in rodents and the known association of PCT with iron metabolism.

The inherent instability of uroporphyrinogens and their partially decarboxylated analogs to oxidation would seem to make them prime sensors of an intracellular oxidative environment. Oxidations of porphyrinogens to the porphyrins will lead to their escape from the heme biosynthetic pathway [219]. The conversion of these colorless compounds to products highly fluorescent under UV light is a remarkable natural phenomenon as shown by examination of porphyic animals and tissue as well as urine. Interestingly, in porphyria induced by HCB in rats, only after some time did the liver become really fluorescent as porphyrinogens that accumulated were fully oxidized to the porphyrins [33]. Differential hepatic lobe and lobular distributions were marked in the early stages [220]. In contrast, in mouse experimental systems involving iron overload, the proportion of porphyrins present is far greater (Smith, unpublished data) suggesting some intrinsic factors, differing between species and treatments, may modify intracellular oxidative environments. Similar findings have been reported for mice with PCBs [221] and in PCT [44].

How would CYP1A2 be involved in an oxidation process? Microsomal preparations from rodents and chick liver embryos induced by polychlorinated aromatics, or nonhalogenated CYP1A inducers, oxidise uroporphrinogen to uroporphyrin [222,223]. In rodents, CYP1A2 appears to be the major isoform involved [224,225]. Microsomes from *Cyp1a2* null mice

treated with HCB or 3-methylcholanthrene have a minimal ability to do this and uroporphyria does not result *in vivo* [195]. These findings are persuasive that a process involving CYP1A2 and oxidation of uroporphyrinogen has a role to play in experimental porphyria but there are difficulties that require explanation. A minimal expression seems obligatory [179,192], but levels of CYP1A2 in strains of mice, and in highly responding groups of genetic crosses, do not correlate with differential marked up-regulation of cytochrome P450 [128,134]. It is also curious that CYP1A2 with substrates that are normally highly lipophilic should *in vivo* oxidise the hydrophilic molecule uroporphyrinogen containing eight carboxy1 groups. How would this oxidation process result in greatly depressed activity of hepatic UROD?

4.2. Interrogation of UROD in porphyria

Those studies that have been conducted show no decreased UROD protein by immunoblotting or mRNA following porphyria in animals or in PCT, in contrast to the severe depression of activity [129,173–175]. Although at high concentrations metabolites of HCB have been reported to inhibit the enzyme, evidence with other models of porphyria, described earlier, make a metabolite-derived mechanism of the chemicals *per se* unlikely. Direct inhibition and modification by Fe^{2+} or Hg^{2+} that have been studied *in vitro* are also probably not selective and significant *in vivo*. Efforts to recover enzymic activity from inhibited UROD after HCB or TCDD treatment have not been successful (Smith, unpublished data). Modification of UROD from HCB treated rats seems to protect it from some other chemicals when subsequently exposed *in vitro* [226]. In regenerated liver of two-thirds hepatectomized mice after porphyria induced by HCB or TCDD, enzymic activity does not recover quickly [227]. Unlike many decarboxylases there is no evidence that UROD requires a bound cofactor that becomes destroyed. This suggests that the enzyme is modified in some way at the active site or that a high affinity inhibitor is produced [228]. A number of laboratories have reported that an inhibitor of UROD, more polar than uroporphyrins, can be produced from heat-treated liver cytosols of porphyric rats and mice, whatever the regimen, and which cannot be removed by dialysis and is not produced by or from uroporphyrins present in the samples [121,147,153,229–231]. It can be detected in mouse liver concomitant with decreased UROD activity and before major elevation of porphyrin levels [231]. The relationship between these extracts and inhibition of UROD *in vivo*, however, is not established. The inhibitory fraction from porphyric mice also affects recombinant human UROD [180]. Deproteinisation of cytosol by mild acid treatment gives similar results and the "inhibitor" is unstable following HPLC purification as well as being considerably more polar than uroporphyrin (Smith, unpublished data).

Attention has been given to the possibility that a potential inhibitor may be derived by oxidation of uroporphyrinogens, but not simply to uroporphyrins [232]. This is an attractive hypothesis as oxidation of uroporphyrinogens, catalyzed by Fe^{2+} in some form might be an explanation for the enhancement of porphyria *in vivo* after administering the precursor 5-ALA. Indeed 5-ALA administered to SWR mice is uroporphyrogenic in itself without other treatments [158]. Microsomal oxidation of uroporphyrinogen is associated with concomitant decreased UROD activity which is reversible if the CYP inhibitor ketoconazole is added. One explanation for the UROD decreased activity is that it is due to inhibition by partially oxidized uroporphyrinogens [233]. Most recently using the techniques for isolation of the inhibitory factor, Phillips *et al.* reported isolation of a product from porphyric mice and PCT liver with properties mainly consistent with a uroporphomethene the first step in oxidation of uroporphyrinogens (Figure 7) [234]. Its absolute potency and stoichiometry as an inhibitor of UROD was not ascertained. Some questions have been raised as to the identification [235] and there are difficulties in reconciling considerable historical data with this as the simple explanation for PCT and experimental porphyrias. For instance, it is difficult to explain inhibition of UROD by a partially oxidized porphyrinogen and the severely depressed UROD activity, which is slow to recover in porphyria. However, there may be related processes in which formation of the uroporphomethene is a first step in a sequence that generates a more active inhibitor or a molecule with affinity for UROD that directly modifies the active site. Detailed studies of the oxidation of uroporphyrinogen *in vitro* and *in vivo*, and the consequential end products, are thus important considerations for these hypotheses.

4.3. Oxidation of uroporphyrinogen

Oxidation of uroporphyrinogens to uroporphyrins, under a partial pressure of oxygen and in even dull light, apparently occurs in three steps that lead predominantly to two intermediates [236]. The respective porphomethene and porphodimethene intermediates from uroporphyrinogen III are shown in Figure 7. Similar steps also probably occur rapidly following oxidation
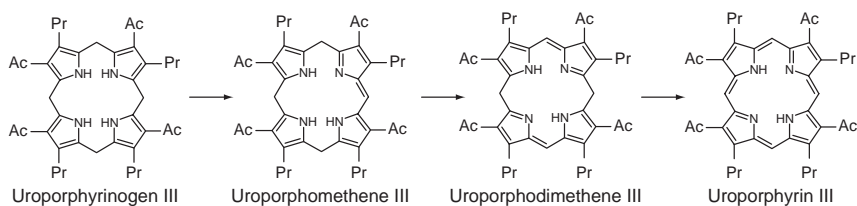
Figure 7 Intermediates in the oxidation of uroporphyrinogen III to uroporphyrin.

with iodine and in the oxidation of other porphyrinogens including hepta-carboxylic acid porphyrinogen III*d*. Uroporphomethene (with an absorbance at 500 nm) and uroporphodimethene are thought to be stable enough for their spectral properties and stability to other reagents to be studied. Experiments show that they are prone to photocatalytic oxidation by uroporphyrin and likely to be more stable after purification although still sensitive to light and air. However, to the authors' knowledge rigorous modern analysis has yet to be performed. The identification of uroporpho-methene in porphyric samples from mice and sporadic PCT liver was based on mass spectral as well as absorption at 500 nm and by comparison with products prepared from biosynthetically-generated uroporphyrinogen exposed to UV light [234], although HPLC properties were not as might be expected [235].

As described above, many investigations have shown the *in vitro* oxidation of uroporphyrinogen as a model of that *in vivo* e.g. [194,224,225]. In contrast to rodent microsomes, the microsomal system from chick embryo liver is stimulated by the presence of 3,3′,4,4′-tetrachlorobiphenyl [223]. The reasons are unclear. The oxidation of the porphyrinogen to uroporphyrin by rodent CYP1A2 *in vitro* does not appear to require bound chlorinated aromatic hydrocarbons or involve free reactive oxygen species such as $O_2^-{}^\cdot$. However, addition of Fe-EDTA to microsomal systems speeds up uroporphyrinogen oxidation and may incorporate another oxidative mechanism as, unlike microsomes alone, catalase, mannitol, and glutathione partially protect [217,223]. This can be interpreted as implicating a reactive oxygen mechanism perhaps the generation of hydroxyl radicals. Curiously, ascorbate protects against uroporphyrin formation in hepatocytes and microsomal incubations apparently by inhibiting porphomethene formation [237]. That this may be pertinent *in vivo* has been demonstrated by the partial protection of dietary ascorbic acid against HCB and 3,3′,4,4′,5-pentachlorophenyl (PCB126) induced porphyria in rat and mouse models under low or modest, but not high, iron contents [210,238].

Fe-EDTA markedly stimulates chemical oxidation of porphyrinogens to porphyrins using H_2O_2 or xanthine oxidase to generate $O_2^-{}^\cdot$ whereas uroporphyrin is only slowly oxidized [217,232]. This illustrates the potential importance of iron–catalyzed oxidation *in vivo* if pools of free iron are released inappropriately. Experiments of this type have shown other important concepts. 1-Hydroxymethylbilane is also oxidized and this may be one reason for the significant proportion of uroporphyrin I that occurs in porphyric tissue (Figure 5) [232]. Careful quantitation of reactions demonstrates the low yield of uroporphyrin, if based on comparisons with mild oxidation by iodine, and the concomitant formation of products that inhibit UROD [232]. Although inhibition is to the degree reported for uropor-phomethene, nonporphyrin products appear to have been formed which are not oxidized back to uroporphyrin if treated with iodine.

Radiochemical experiments with HPLC showed that these are more polar than uroporphyrin. Thus it has become clear that simple conversion of uroporphyrinogen to uroporphyrin is not the only route of oxidation that needs to be considered.

Exposure of uroporphyrinogens to day and UV light produces substituted uroporphyrins hydroxylated at *meso* positions of the porphyrin rings and in the acetate and propionate side-chains [239,260]. These hydroxylated porphyrins have been identified in tissues and excreta from PCT patients and from HCB and TCDD treated animals (Figure 8) [149,240–242]. Of perhaps greater interest is the formation of dihydroxy- and hydroxyspirolactone urochlorins possibly derived by epoxidation of uroporphyrinogen (Figure 8) [239,242]. These chlorins were first observed many years ago but not characterized fully due to lack of appropriate techniques at the time. They could account for the loss of recoverable uroporphyrin observed in systems of chemical oxidation systems of uroporphyrinogen [217,232]. These nonporphyrin products from uroporphyrinogen have recently been found for the first time *in vivo* in porphyric liver of
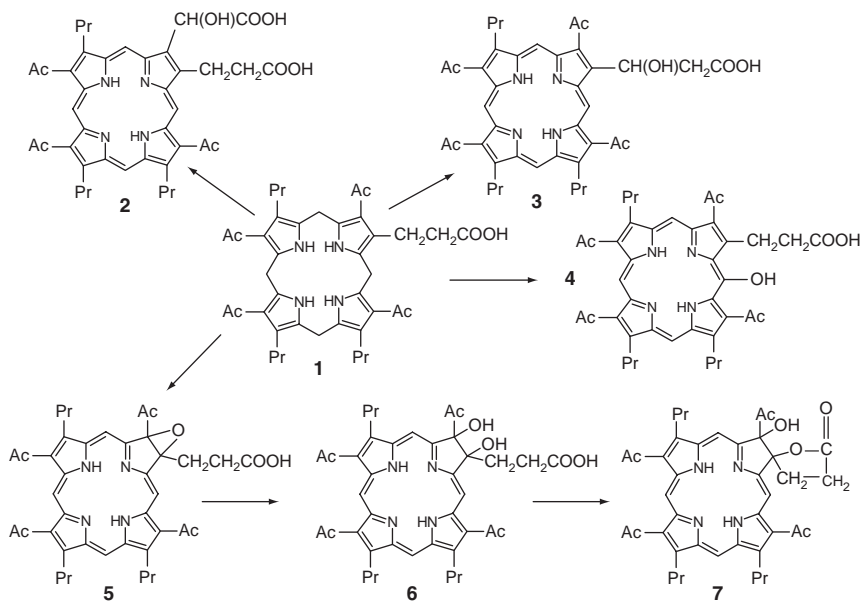
Figure 8 Oxidation reactions of uroporphyrinogen III leading to products incorporating oxy functions. 1. Uroporphyrinogen III; 2. hydroxyacetic acid uroporphyrin III; 3. β-hydroxypropionic acid uroporphyrin III; 4. *meso*-hydroxy uroporphyrin III; 5. possible epoxurochlorin III intermediate; 6. dihydroxyurochlorin III; 7. hydroxyspirolactoneurochlorin III. Isomers of all these are possible depending on positional and stereoisomers as well as the corresponding uroporphyrinogen I [260] products and those from heptacarboxylic acid porphyrinogen III.

TCDD treated mice [242]. It remains to be seen as to whether any of these molecules have significant inhibitory properties towards UROD. Alternatively, such mechanisms of uroporphyrinogen oxidation *in vivo* may be conduits for understanding the inactivation of UROD at the active site. Arguments as to which might come first, oxidation to uroporphyrinogen or to other products causing effects on UROD, are probably misplaced. They may be synchronous processes but vary in degree.

5. Liver Injury, Cancer, and Porphyria

Polyhalogenated aromatic chemicals cause many effects, besides hepatic porphyria, and these are covered elsewhere in many reviews [243]. However, there is evidence that some aspects of the hepatocellular injury and hepatic tumors caused by these agents in rodents may be linked to their property of inducing porphyria [46]. In addition, there are parallels with sporadic PCT patients [3,44]. A lot of this evidence has been reviewed previously but will be summarized here. The topic is of some importance as it may be pertinent to the risk assessment of these chemicals. Unlike the human epidemiology data, the development of liver tumors at relatively high doses is one of the main sites of cancer in rodents [46,244].

5.1. Hepatocellular injury

Exposure of rats and mice to HCB, PCBs, and TCDD generally induce hepatic proliferation of smooth endoplasmic reticulum and hypertrophy with varying degrees of steatosis and necrosis especially in centrilobular regions. Of course other chemicals, including those that are chlorinated like DDT, may also have some of these effects but there seem to be features of injury that are associated with porphyria development. One porphyric patient exposed to HCB in Turkey had chronic inflammation, hepatocyte necrosis, and regenerating lobules, as well as fluorescence under UV light, when a liver biopsy was examined [69]. Porphyric liver from rats treated with HCB shows crystalline inclusions of uroporphyrin in parenchyma as seen in PCT cases [44,46]. In mice with porphyria due to a combination of iron with HCB, uroporphyrin crystals are associated with ferritin within hepatocytes that may indicate involvement in toxic damage [150,245]. Such experiments also show the elevation of plasma transaminases, indicating liver injury as porphyria develops. In rats exposed to PCBs, liver toxicity, as determined by both plasma enzyme levels and histopathology is observed in females before that seen in males and concomitant with porphyria [209,246]. In mice iron overload not only stimulates TCDD induced

porphyria but also plasma enzymes and liver damage although these are not necessarily interdependent [128,130].

5.2. Porphyria and liver cancer

Although not frequently discussed, it is curious that all experimental models in which polyhalogenated aromatic chemicals induce porphyria are also associated with subsequent formation of hepatic adenomas and carcinomas. Like porphyria and liver damage, there is marked sexual dimorphism in rats associated with hepatic tumor response to PCBs, PBBs, and TCDD (Table 2) (see Smith, [46] for a full list of references) and can be exemplified by that of HCB [113]. In contrast, such distinct susceptibility of females is not observed for other genotoxic and nongenotoxic hepatocarcinogenic chemicals such as tamoxifen, diethylnitrosamine, aflatoxin, and phenobarbital. In studies where HCB was used to promote tumors initiated by diethylnitrosamine, tumors were not porphyric (unlike with HCB alone) and a marked sex difference was not observed [247]. Livers from rats fed HCB that have hepatocellular carcinomas and adenomas show accumulation of iron possibly as the result of peliosis followed by regeneration [182].

Table 2 Association of porphyria with hepatocellular tumors

Species	Exposure	Hepatocarcinogenesis response
Human sporadic PCT	Alcohol/estrogen treatment/HCV	Incidence of cancer more significant than due to agents alone or cirrhosis
Rat	HCB, PCBs, PBBs, TCDD	Both porphyria and liver tumors occur predominantly in females (hepatic iron ♀ > ♂)
Rat	Initiation by diethylnitrosamine followed by HCB promotion	No marked sex difference in tumor response
Rat	HCB ± iron	Stimulation of both porphyria and tumor development by iron treatment
Mouse	HCB, PCBs, PBBs ± iron	Massive stimulation of both porphyria and tumor by iron—earlier and to a greater degree
Mouse	PCBs + iron ± CYP1A2 (*Cyp1a2* null)	No porphyria or tumors in absence of CYP1A2

For references see text and [46].

Iron accumulation in hepatocytes and Kupffer cells of females, but not males, is also observed in rats administered coplanar PCBs after developing porphyria and hepatic neoplasms [184]. Iron overload enhances both porphyria and severity of hyperplastic lesions in rats fed HCB [140]. In humans there is good evidence for the association of hepatic cancer with PCT that is not just a consequence of cirrhosis [248–250]. This implies that there is some kind of unique mechanistic link between a toxic process involving iron which not only leads to porphyria but may eventually predispose to hepatocellular tumors. This is not to exclude other mechanisms contributing to the hepatocarcinogenic actions of polyhalogenated aromatics.

Mouse models have been particularly amenable to a comparison of porphyria with subsequent hepatic carcinogenesis. Intriguingly, not only is the porphyria inducing property of HCB and PCBs in C57BL/10ScSn mice massively increased by prior iron treatment but so is the subsequent incidence of liver adenomas and cancer [148,155,205]. In contrast, the DBA/2 strain is highly resistant to both porphyria and hepatocarcinogenesis following iron and PCBs as are, importantly, *Cyp1a2* null mice [193]. The polychlorinated aromatic chemical octachlorostyrene, which does not cause porphyria in iron loaded mice, is very weakly tumorgenic even with additional iron [251]. Tumor developments caused by other nongenotoxic carcinogens phenobarbital and nafenopin are unaffected by iron (Smith, unpublished data). HCB and PCBs tumors in mice do not show increased incidences of Ha-*ras* mutations but do show the emergence of a mononucleated diploid population consistent with precancerous changes [252,253]. In support of an oxidative mechanism for tumorigenesis compatible with that proposed for porphyria, oxidative DNA damage after PCBs has been reported in C57BL/10ScSn mice but not DBA/2 [203]. Point mutations could not be detected, using the $\lambda/LacI$ *in vivo* mutation system suggesting that more complex chromosomal deletions or rearrangement are involved in the oxidative damage or in the mutagenicity of the porphyrins themselves [254]. A scheme illustrating a possible scenario is shown in Figure 9. *Fech (m1/Pas1)* mice that have a mutation in the ferrochelatase gene develop marked hepatic protoporphyrin levels, liver toxicity and, in far less than a year, severe hepatocellular tumors illustrating that porphyria alone can be carcinogenic [59,255]. Protoporphyria may also partially account for the hepatocarcinogenic actions of the drug griseofulvin [256]. That oxidative processes alone can be tumorigenic is illustrated by the mitochondrial disruption, oxidative stress, and subsequent liver tumors that are observed in mice with mutation of the frataxin gene involved in hepatic iron and heme metabolism [257].
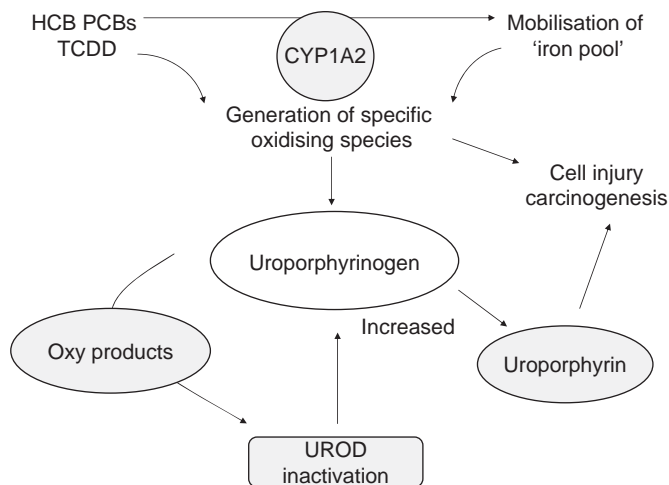
Figure 9   Scheme hypothesizing the association of uroporphyrinogen oxidation with UROD inactivity and hepatic injury and carcinogenesis.

6. SUMMARY

The disruption of heme synthesis by polyhalogenated aromatic chemicals with physiological consequences has been recognized for decades starting with the identification of HCB as the causative factor of the mass porphyria in Turkey. Both chemical-induced porphyria and sporadic PCT are characterized by accumulation and excretion of uroporphyrins and decreased activity of UROD in the liver. However, for a long time, any similarity between the effects of HCB, PCBs, and TCDD in experimental systems (and humans) and sporadic PCT precipitated by other agents and implicating iron metabolism, was difficult to comprehend. The demonstration that not only could manipulation of iron status alter the experimental outcomes but that iron causes porphyria in mice in a genetically variable manner, illustrated that the underlying mechanisms of PCT and that caused by HCB, *etc.* are probably very similar. In fact, uroporphyria in mammals may be viewed as a genetically variable aspect of iron toxicity precipitated or enhanced by a variety of other agents of which the polychlorinated aromatics are the most powerful. The contributions these chemicals make include through binding to the AHR and mediating the expression and action of other gene products. Of these CYP1A2 seems to play an important role, at least in rodents, albeit so far it is not clear how or whether this is true in PCT [258,259]. The key part of iron homeostasis in the molecular pathogenesis of both PCT and chemical porphyria would seem to suggest an oxidative mechanism and this is supported by other experimental

evidence. Since uroporphyrinogen III is a relatively unstable molecule to iron–catalyzed oxidation it is not unreasonable to hypothesise that in such a process products are produced that have an affinity for the active site of UROD and cause long acting inhibition or inactivation. The recent identification of some novel oxidation products of uroporphyrinogen in porphyric tissue (Figures 7 and 8) may be a clue to the generation of such a process (Figure 9). However, it would be unwise to exclude other possible mechanisms that could cause UROD inactivity. There are still many other questions to ask including:

1. Why are polychlorinated aromatics so effective in promoting porphyria? Is it just because of their CYP1A2 inducing effects or do they have additional properties, perhaps physical as well as transcriptional, that contribute to their effectiveness?
2. What are the polymorphic genes in mice that are so influential in the porphyrogenic sequence? What can they tell us about the mechanism and whether such similar polymorphisms explain the sporadic nature of human PCT?
3. If an oxidative mechanism is involved, what is its specific nature in porphyria which is not seen as a consequence of general oxidative stress with other chemicals or agents?
4. What are the specific roles for CYP1A2 and iron?
5. Is a similar specific oxidative process involving iron metabolism operating that predisposes to hepatocarcinogenesis?

Research tools are available to answer these questions.

ACKNOWLEDGMENTS

REFERENCES

[1] K. Furuyama, K. Kaneko, P.D. Vargas, Heme as a magnificent molecule with multiple missions: Heme determines its own fate and governs cellular homeostasis, Tohoku J. Exp. Med. 213 (2007) 1–16.
[2] R.S. Ajioka, J.D. Phillips, J.P. Kushner, Biosynthesis of heme in mammals, Biochim. Biophys. Acta 1763 (2006) 723–736.
[3] K.E. Anderson, S. Sassa, D.F. Bishop, R.J. Desnick, Disorders of heme biosynthesis: X-linked sideroblastic anemia and the porphyrias, in: C.R. Scriver, A.R. Beaudet, W. Sly, D.Valle, B.Vogelstein, B.Childs, (Eds.), The Metabolic and Molecular Basis of Inherited Disease, McGraw-Hill, New York, (2001), pp. 2991–3062.

[4] A.S. Tsiftsoglou, A.I. Tsamadou, L.C. Papadopoulou, Heme as key regulator of major mammalian cellular functions: Molecular, cellular, and pharmacological aspects, Pharmacol. Ther. 111 (2006) 327–345.

[5] D. Boehning, S.H. Snyder, Novel neural modulators, Annu. Rev. Neurosci. 26 (2003) 105–131.

[6] S. Kumar, U. Bandyopadhyay, Free heme toxicity and its detoxification systems in human, Toxicol. Lett. 157 (2005) 175–188.

[7] A. Pamplona, A. Ferreira, J. Balla, V. Jeney, G. Balla, S. Epiphanio, A. Chora, C.D. Rodrigues, I.P. Gregoire, M. Cunha-Rodrigues, S. Portugal, M.P. Soares, et al. Heme oxygenase-1 and carbon monoxide suppress the pathogenesis of experimental cerebral malaria, Nat. Med. 13 (2007) 703–710.

[8] T. Takahashi, H. Shimizu, H. Morimatsu, K. Inoue, R. Akagi, K. Morita, S. Sassa, Heme oxygenase-1: A fundamental guardian against oxidative tissue injuries in acute inflammation, Mini-Rev. Med. Chem. 7 (2007) 745–753.

[9] S. Sassa, T. Nagai, The role of heme in gene expression, Int. J. Hematol. 63 (1996) 167–178.

[10] S. Hou, M.F. Reynolds, F.T. Horrigan, S.H. Heinemann, T. Hoshi, Reversible binding of heme to proteins in cellular signal transduction, Acc. Chem. Res. 39 (2006) 918–924.

[11] M.A. Gilles-Gonzalez, G. Gonzalez, Heme-based sensors: defining characteristics, recent developments, and regulatory hypotheses, J. Inorg. Biochem. 99 (2005) 1–22.

[12] E.M. Dioum, J. Rutter, J.R. Tuckerman, G. Gonzalez, M.A. Gilles-Gonzalez, S.L. McKnight, NPAS2: A gas-responsive transcription factor, Science 298 (2002) 2385–2387.

[13] K. Kaasik, C.C. Lee, Reciprocal regulation of haem biosynthesis and the circadian clock in mammals, Nature 430 (2004) 467–471.

[14] S. Raghuram, K.R. Stayrook, P. Huang, P.M. Rogers, A.K. Nosie, D.B. McClure, L.L. Burris, S. Khorasanizadeh, T.P. Burris, F. Rastinejad, Identification of heme as the ligand for the orphan nuclear receptors REV-erbalpha and REV-erbbeta, Nat. Struct. Mol. Biol. 14 (2007) 1207–1213.

[15] L. Yin, N. Wu, J.C. Curtin, M. Qatanani, N.R. Szwergold, R.A. Reid, G.M. Waitt, D.J. Parks, K.H. Pearce, G.B. Wisely, M.A. Lazar, Rev-erbalpha, a heme sensor that coordinates metabolic and circadian pathways, Science 318 (2007) 1786–1789.

[16] M. Faller, M. Matsunaga, S. Yin, J.A. Loo, F. Guo, Heme is involved in microRNA processing, Nat. Struct. Mol. Biol. 14 (2007) 23–29.

[17] R.G. Hu, H. Wang, Z. Xia, A. Varshavsky, The N-end rule pathway is a sensor of heme, Proc. Natl. Acad. Sci. USA 105 (2008) 76–81.

[18] X.D. Tang, R. Xu, M.F. Reynolds, M.L. Garcia, S.H. Heinemann, T. Hoshi, Haem can bind to and inhibit mammalian calcium-dependent Slo1 BK channels, Nature 425 (2003) 531–535.

[19] T. Chernova, P. Nicotera, A.G. Smith, Heme deficiency is associated with senescence and causes suppression of N-methyl-D-aspartate receptor subunits expression in primary cortical neurons, Mol. Pharmacol. 69 (2006) 697–705.

[20] T. Chernova, J.R. Steinert, C.J. Guerin, P. Nicotera, I.D. Forsythe, A.G. Smith, Neurite degeneration induced by heme deficiency mediated via inhibition of NMDA receptor-dependent extracellular signal-regulated kinase 1/2 activation, J. Neurosci. 27 (2007) 8475–8485.

[21] F. De Matteis, Toxicological aspects of liver heme biosynthesis, Semin. Hematol. 25 (1988) 321–329.

[22] F. De Matteis, M. Stonard, Experimental porphyrias as models for human hepatic porphyrias, Semin. Hematol. 14 (1977) 187–192.

[23] J.W. Hamilton, W.J. Bement, P.R. Sinclair, J.F. Sinclair, J.A. Alcedo, K.E. Wetterhahn, Heme regulates hepatic 5-aminolevulinate synthase mRNA expression by decreasing mrna half-life and not by altering its rate of transcription, Arch. Biochem. Biophys. 289 (1991) 387–392.

[24] S. Kolluri, T.J. Sadlon, B.K. May, H.L. Bonkovsky, Haem repression of the housekeeping 5-aminolaevulinic acid synthase gene in the hepatoma cell line LMH, Biochem. J. 392 (2005) 173–180.

[25] G. Srivastava, I.A. Borthwick, D.J. Maguire, C.J. Elferink, M.J. Bawden, J.F. Mercer, B.K. May, Regulation of 5-aminolevulinate synthase mRNA in different rat tissues, J. Biol. Chem. 263 (1988) 5202–5209.

[26] M. Yamamoto, S. Kure, J.D. Engel, K. Hiraga, Structure, turnover, and heme-mediated suppression of the level of mRNA encoding rat liver delta-aminolevulinate synthase, J. Biol. Chem. 263 (1988) 15973–15979.

[27] T.A. Dailey, J.H. Woodruff, H.A. Dailey, Examination of mitochondrial protein targeting of haem synthetic enzymes: *In vivo* identification of three functional haem-responsive motifs in 5-aminolaevulinate synthase, Biochem. J. 386 (2005) 381–386.

[28] D.J. Fraser, A. Zumsteg, U.A. Meyer, Nuclear receptors constitutive androstane receptor and pregnane X receptor activate a drug-responsive enhancer of the murine 5-aminolevulinic acid synthase gene, J. Biol. Chem. 278 (2003) 39392–39401.

[29] A.S. Guberman, M.E. Scassa, L.E. Giono, C.L. Varone, E.T. Canepa, Inhibitory effect of AP-1 complex on 5-aminolevulinate synthase gene expression through sequestration of camp-response element protein (CRE)-binding protein (CBP) coactivator, J. Biol. Chem. 278 (2003) 2317–2326.

[30] C. Handschin, U.A. Meyer, Induction of drug metabolism: The role of nuclear receptors, Pharmacol. Rev. 55 (2003) 649–673.

[31] M.E. Scassa, A.S. Guberman, C.L. Varone, E.T. Canepa, Phosphatidylinositol 3-kinase and Ras/mitogen-activated protein kinase signaling pathways are required for the regulation of 5-aminolevulinate synthase gene expression by insulin, Exp. Cell Res. 271 (2001) 201–213.

[32] A.H. Jackson, H.A. Sancovich, A.M. Ferramola, N. Evans, D.E. Games, S.A. Matlin, G.H. Elder, S.G. Smith, Macrocyclic intermediates in the biosynthesis of porphyrins, Philos. Trans. R. Soc. Lond. B. Biol. Sci. 273 (1976) 191–206.

[33] A.G. Smith, J.E. Francis, Investigations of rat liver uroporphyrinogen decarboxylase. Comparisons of porphyrinogens I and III as substrates and the inhibition by porphyrins, Biochem. J. 195 (1981) 241–250.

[34] J.D. Phillips, F.G. Whitby, J.P. Kushner, C.P. Hill, Characterization and crystallization of human uroporphyrinogen decarboxylase, Protein Sci. 6 (1997) 1343–1346.

[35] J. Luo, C.K. Lim, Order of uroporphyrinogen III decarboxylation on incubation of porphobilinogen and uroporphyrinogen III with erythrocyte uroporphyrinogen decarboxylase, Biochem. J. 289 (1993) 529–532.

[36] A.G. Smith, F. De Matteis, Oxidative injury mediated by the hepatic cytochrome P-450 system in conjunction with cellular iron. Effects on the pathway of haem biosynthesis, Xenobiotica 20 (1990) 865–877.

[37] V. Jeney, J. Balla, A. Yachie, Z. Varga, G.M. Vercellotti, J.W. Eaton, G. Balla, Pro-oxidant and cytotoxic effects of circulating heme, Blood 100 (2002) 879–887.

[38] S. Sassa, Why heme needs to be degraded to iron, biliverdin IX alpha, and carbon monoxide?, Antioxid. Redox Signal. 6 (2004) 819–824.

[39] F.A. Wagener, H.D. Volk, D. Willis, N.G. Abraham, M.P. Soares, G.J. Adema, C.G. Figdor, Different faces of the heme–heme oxygenase system in inflammation, Pharmacol. Rev. 55 (2003) 551–571.

[40] S. Sassa, A. Kappas, Molecular aspects of the inherited porphyrias, J. Intern. Med. 247 (2000) 169–178.

[41] M.N. Badminton, G.H. Elder, Molecular mechanisms of dominant expression in porphyria, J. Inherit. Metab. Dis. 28 (2005) 277–286.

[42] P.N. Meissner, T.A. Dailey, R.J. Hift, M. Ziman, A.V. Corrigall, A.G. Roberts, D.M. Meissner, R.E. Kirsch, H.A. Dailey, A R59W mutation in human protoporphyrinogen oxidase results in decreased enzyme activity and is prevalent in South Africans with variegate porphyria, Nat. Genet. 13 (1996) 95–97.

[43] G.H. Elder, Porphyria cutanea tarda, Semin. Liver Dis. 18 (1998) 67–75.

[44] G.H. Elder, Porphyria cutanea tarda and related disorders, in: K.M. Kadish, K.M. Smith, R. Guilard (Eds.), Medical Aspects of Porphyrins, Porphyrin Handbook **14**, Academic Press, San Diego, 2003, pp. 67–92.

[45] N.G. Egger, D.E. Goeger, D.A. Payne, E.P. Miskovsky, S.A. Weinman, K.E. Anderson, Porphyria cutanea tarda: Multiplicity of risk factors including HFE mutations, hepatitis C, and inherited uroporphyrinogen decarboxylase deficiency, Dig. Dis. Sci. 47 (2002) 419–426.

[46] A.G. Smith, Porphyria caused by chlorinated AH receptor ligands and associated mechanisms of liver injury and cancer, in: K.M. Kadish, K.M. Smith, R. Guilard (Eds.), Medical Apects of Porphyrins, Porphyrin Handbook **14,** Academic Press, San Diego, 2003, pp. 169–210.

[47] G.H. Elder, A.J. Urquhart, R.E. De Salamanca, J.J. Munoz, H.L. Bonkovsky, Immunoreactive uroporphyrinogen decarboxylase in the liver in porphyria cutanea tarda, Lancet 2 (1985) 229–233.

[48] Z.J. Bulaj, J.D. Phillips, R.S. Ajioka, M.R. Franklin, L.M. Griffen, D.J. Guinee, C.Q. Edwards, J.P. Kushner, Hemochromatosis genes and other factors contributing to the pathogenesis of porphyria cutanea tarda, Blood 95 (2000) 1565–1571.

[49] A.G. Roberts, S.D. Whatley, R.R. Morgan, M. Worwood, G.H. Elder, Increased frequency of the haemochromatosis Cys282Tyr mutation in sporadic porphyria cutanea tarda, Lancet 349 (1997) 321–323.

[50] M.D. Maines, Enzymatic basis of metal ion alterations of cellular heme and glutathione metabolism, Fundam. Appl. Toxicol. 1 (1981) 358–367.

[51] L. Claudio, T. Lee, M.S. Wolff, J.G. Wetmur, A murine model of genetic susceptibility to lead bioaccumulation, Fundam. Appl. Toxicol. 35 (1997) 84–90.

[52] D.P. Tschudy, R.A. Hess, B.C. Frykholm, Inhibition of delta-aminolevulinic acid dehydrase by 4,6-dioxoheptanoic acid, J. Biol. Chem. 256 (1981) 9915–9923.

[53] C.E. Lim, K.I. Matthaei, A.C. Blackburn, R.P. Davis, J.E. Dahlstrom, M.E. Koina, M.W. Anders, P.G. Board, Mice deficient in glutathione transferase zeta/maleylacetoacetate isomerase exhibit a range of pathological changes and elevated expression of alpha, mu, and pi class glutathione transferases, Am. J. Pathol. 165 (2004) 679–693.

[54] P.R. Sinclair, N. Gorman, H.S. Walton, J.F. Sinclair, J.M. Jacobs, N.J. Jacobs, Protoporphyrinogen accumulation in cultured hepatocytes treated with the diphenyl ether herbicide, acifluorfen, Cell. Mol. Biol. (Noisy-le-grand) 40 (1994) 891–897.

[55] B.A. Fowler, E.A. Conner, H. Yamauchi, Metabolomic and proteomic biomarkers for III-V semiconductors: chemical-specific porphyrinurias and proteinurias, Toxicol. Appl. Pharmacol. 206 (2005) 121–130.

[56] J.S. Woods, D. Echeverria, N.J. Heyer, P.L. Simmonds, J. Wilkerson, F.M. Farin, The association between genetic polymorphisms of coproporphyrinogen oxidase and an atypical porphyrinogenic response to mercury exposure in humans, Toxicol. Appl. Pharmacol. 206 (2005) 113–120.

[57] P. Sinclair, A.H. Gibbs, J.F. Sinclair, F. De Matteis, Formation of cobalt protoporphyrin in the liver of rats. A mechanism for the inhibition of liver haem biosynthesis by inorganic cobalt, Biochem. J. 178 (1979) 529–538.

[58] F. De Matteis, G.S. Marks, Cytochrome P450 and its interactions with the heme biosynthetic pathway, Can. J. Physiol. Pharmacol. 74 (1996) 1–8.

[59] R. Davies, A. Schuurman, C.R. Barker, B. Clothier, T. Chernova, F.M. Higginson, D.J. Judah, D. Dinsdale, R.E. Edwards, P. Greaves, T.W. Gant, A.G. Smith, Hepatic gene expression in protoporphyic Fech mice is associated with cholestatic injury but not a marked depletion of the heme regulatory pool, Am. J. Pathol. 166 (2005) 1041–1053.

[60] G.H. Elder, Porphyria caused by hexachlorobenzene and other polyhalogenated aromatic hydrocarbons, in: F. De Matteis, W.N. Aldridge (Eds.), Heme and Hemoproteins, Springer-Verlag, Berlin, 1978, pp. 157–200.

[61] C. Cam, A new epidemic dermatosis of children, Ann. Dermatol. Syphiligr. (Paris) 87 (1960) 393–397.

[62] C. Cam, G. Nigogosyan, Acquired toxic porphyria cutanea tarda due to hexachlorobenzene, J. Am. Med. Ass. 183 (1963) 88–91.

[63] A.I. Cetingil, M.A. Ozen, Toxic porphyria, Blood 16 (1960) 1002–1011.

[64] I. Dogramaci, Porphyrias and porphyrin metabolism, with special reference to porphyria in childhood, Adv. Pediatr. 13 (1964) 11–63.

[65] R. Schmid, Cutaneous porphyria in Turkey, N. Engl. J. Med. 263 (1960) 397–398.

[66] I. Kantemir, C. Cam, O. Kayaalp, Investigations and observations on two diseases: Kara Yara and Pembe Yara which are observed in the South-East part of Turkey, Turk. Bull. Hyg. Exp. Biol. 20 (1960) 79–83.

[67] I. Dogramaci, J.D. Wray, T. Ergene, V. Sezer, Y. Muftu, Porphyria turcica, a survey of 592 cases of cutaneous porphyria seen in southeastern Turkey, Turk. J. Pediatr. 4 (1962) 138–147.

[68] I. Dogramaci, A. Kenanoglu, Y. Muftu, T. Ergene, J.D. Wray, Bone and joint changes in patients with porphyria turcica, Turk. J. Pediatr. 4 (1962) 149–156.

[69] I. Dogramaci, B. Tinaztepe, A. Gunalp, Condition of the liver in patients with toxic cutaneous porphyria, Turk. J. Pediatr. 4 (1962) 103–106.

[70] I. Dogramaci, O. Duzgunes, T. Ergene, A. Gocmen, A possible genetic factor in the etiology of porphyria Turcica, Turk. J. Pediatr. 4 (1962) 193–200.

[71] A. Gocmen, H.A. Peters, D.J. Cripps, G.T. Bryan, C.R. Morris, Hexachlorobenzene episode in Turkey, Biomed. Environ. Sci. 2 (1989) 36–43.

[72] H.A. Peters, A. Gocmen, D.J. Cripps, G.T. Bryan, Epidemiology of hexachlorobenzene-induced porphyria in Turkey-clinical and laboratory, Neurology 31 (1981) 111–111.

[73] A. Morley, D. Geary, F. Harben, Hexachlorobenzene pesticides and porphyria, Med. J. Aust. 1 (1973) 565.

[74] A.I. Selden, L.S. Bodin, H. Westberg, S. Thunell, Porphyrin status in aluminium foundry workers exposed to hexachlorobenzne and octachlorostyrene, Arch. Environ. Health 54 (1999) 248–253.

[75] J. Sunyer, C. Herrero, D. Ozalla, M. Sala, N. Ribas-Fito, J. Grimalt, X. Basagana, Serum organochlorines and urinary porphyrin pattern in a population highly exposed to hexachlorobenzene, Environ. Health 1 (2002) 1.

[76] W.E. Daniell, H.L. Stockbridge, R.F. Labbe, J.S. Woods, K.E. Anderson, D.M. Bissell, J.R. Bloomer, R.D. Ellefson, M.R. Moore, C.A. Pierach, W.E. Schreiber, A. Tefferi, et al. Environmental chemical exposures and disturbances of heme synthesis, Environ. Health Perspect. 105(Suppl. 1), (1997) 37–53.

[77] R. Enriquez de Salamanca, A. Lopez-Miras, J.J. Munoz, J. To-Figueras, C. Conde, Is hexachlorobenzene human overload related to porphyria cutanea tarda? A speculative hypothesis, Med. Hypotheses 33 (1990) 69–71.

[78] J.L. Santos, M. Grandal, A. Fontanellas, M.J. Moran, R. Enriquez de Salamanca, Prevalencia de porfiria cutanea tarda en Madrid y asociacion entre la porfirinuria y el consumo de etanol en un modelo de regresion lineal multiple, Med. Clin. (Barc). 107 (1996) 614–616.

[79] K.J. Chang, F.J. Lu, T.C. Tung, T.P. Lee, Studies on patients with polychlorinated biphenyl poisoning. 2. Determination of urinary coproporphyrin, uroporphyrin, delta-aminolevulinic acid and porphobilinogen, Res. Commun. Chem. Pathol. Pharmacol. 30 (1980) 547–554.

[80] A. Colombi, M. Maroni, A. Ferioli, Increase in urinary porphyrin excretion in workers exposed to polychlorinated biphenyls, J. Appl. Toxicol. 2 (1982) 117–121.

[81] S. Nonaka, T. Shimoyama, T. Honda, H. Yoshida, Analysis of urinary porphyrins in polychlorinated biphenyl poisoning (Yusho) patients, in: J.J.T.W.A. Strik, J.H. Koeman (Eds.), Chemical Porphyria in Man, Elsevier, North Holland, Amsterdam, 1979, pp. 69–73.

[82] J. Osterloh, J. Cone, R. Harrison, R. Wade, C. Becker, Pilot survey of urinary porphyrins from persons transiently exposed to a PCB transformer fire, J. Toxicol. Clin. Toxicol. 24 (1986) 533–544.

[83] J. Pazderova-Vejlupkova, E. Lukas, M. Nemcova, J. Pickova, L. Jirasek, The development and prognosis of chronic intoxication by tetrachlordibenzo-p-dioxin in men, Arch. Environ. Health 36 (1981) 5–11.

[84] Y. Seki, S. Kawanishi, S. Sano, Mechanism of PCB-induced porphyria and Yusho disease, Ann. N. Y. Acad. Sci. 514 (1987) 222–234.

[85] J.J. Strik, Porphyrins in urine as an indication of exposure to chlorinated hydrocarbons, Ann. N. Y. Acad. Sci. 320 (1979) 308–310.

[86] G.M. Calvert, M.H. Sweeney, M.A. Fingerhut, R.W. Hornung, W.E. Halperin, Evaluation of porphyria cutanea tarda in U.S. workers exposed to 2,3,7,8-tetrachlorodibenzo-p-dioxin, Am. J. Ind. Med. 25 (1994) 559–571.

[87] A.S. Boyd, K.H. Neldner, M. Naylor, 2,3,7,8-tetrachlorodibenzo-p-dioxin-induced porphyria cutanea tarda among pediatric patients, J. Am. Acad. Dermatol. 21 (1989) 1320–1321.

[88] R.E. Jones, M. Chelsky, Further discussion concerning porphyria cutanea tarda and TCDD exposure, Arch. Environ. Health 41 (1986) 100–103.

[89] J. Bleiberg, M. Wallen, R. Brodkin, I.L. Applebaum, Industrially-acquired porphyria, Arch. Derm. (Chic.) 89 (1964) 793–797.

[90] L. Jirasek, J. Kalensky, K. Kubec, J. Pazderova, E. Lukas, [Acne chlorina, porphyria cutanea tarda and other manifestations of general poisoning during the manufacture of herbicides. II], Cesk. Dermatol. 49 (1974) 145–157.

[91] L. Jirasek, J. Kalensky, K. Kubec, J. Pazderova, E. Lukas, [Chloracne, porphyria cutanea tarda, and other poisonings due to the herbicides], Hautarzt 27 (1976) 328–333.

[92] R. McConnell, K. Anderson, W. Russell, K.E. Anderson, R. Clapp, E. Silbergeld, P. Landrigan, Angiosarcoma, porphyria cutnea tarda, and probable chloracne in a worker exposed to waste oil contaminated with 2,3,7.,8-tetrachlorodibenzeo-p-dioxin, Br. J. Ind. Med. 50 (2000) 699–703.

[93] R. Caputo, M. Monti, E. Ermacora, G. Carminati, C. Gelmetti, R. Gianotti, E. Gianni, V. Puccinelli, Cutaneous manifestations of tetrachlorodibenzo-p-dioxin in children and adolescents. Follow-up 10 years after the Seveso, Italy, accident, J. Am. Acad. Dermatol. 19 (1988) 812–819.

[94] F. De Matteis, B.E. Prior, C. Rimington, Nervous and biochemical disturbances following hexachlorobenzene intoxication, Nature 191 (1961) 363–366.

[95] A. Gajdos, M. Gajdos-Török, The therapeutic effect of adenosine-5-monophosphoric acid in porphyria, Lancet 2 (1961) 175–177.

[96] I. Kantemir, Porphyrin kimyasi re analiz metodlari, Turk. J. Tecr. Biyol. Derg. 20 (1960) 1.

[97] R.K. Ockner, R. Schmid, Acquired porphyria in man and rat due to hexachlorobenzene intoxication, Nature 189 (1961) 499.

[98] H.M. Carpenter, D.E. Williams, D.R. Buhler, Hexachlorobenzene-induced porphyria in Japanese quail: Changes in microsomal enzymes, J. Toxicol. Environ. Health 15 (1985) 431–444.

[99] H.M. Carpenter, D.E. Williams, M.C. Henderson, R.C. Bender, D.R. Buhler, Hexachlorobenzene-induced porphyria in Japanese quail. Effect of pretreatment with phenobarbital or beta-naphthoflavone, Biochem. Pharmacol. 33 (1984) 3875–3881.

[100] J.J. Strik, Chemical porphyria in Japanese quail (Coturnix c. Japonica), Enzyme 16 (1973) 211–223.

[101] J.J. Strik, Species differences in experimental porphyria caused by polyhalogenated aromatic compounds, Enzyme 16 (1973) 224–230.

[102] J.J.T.W.A. Strik, J.G. Wit, Hepatic porphyria in birds and mammals, TNO-nieuws 27 (1972) 604–610.

[103] J.G. Vos, J.J. Strik, C.W. van Holsteyn, J.H. Pennings, Polychlorinated biphenyls as inducers of hepatic porphyria in Japanese quail, with special reference to -aminolevulinic acid synthetase activity, fluorescence, and residues in the liver, Toxicol. Appl. Pharmacol. 20 (1971) 232–240.

[104] G.P. Carlson, Brominated benzene induction of hepatic porphyria, Experientia 35 (1978) 513–514.

[105] G. Koss, S. Seubert, A. Seubert, J. Seidel, W. Koransky, H. Ippen, Studies on the toxicology of hexachlorobenzene. V. Different phases of porphyria during and after treatment, Arch. Toxicol. 52 (1983) 13–22.

[106] A.G. Smith, J.E. Francis, Relative abilities on a molar basis of hexafluoro-, hexachloro- and hexabromobenzenes to decrease liver uroporphyrinogen decarboxylase activity and cause porphyria in female rats, Res. Commun. Chem. Pathol. Pharmacol. 28 (1980) 377–384.

[107] A.G. Smith, J.E. Francis, I. Bird, Distinction between octachlorostyrene and hexachlorobenzene in their potentials to induce ethoxyphenoxazone deethylase and cause porphyria in rats and mice, J. Biochem. Toxicol. 1 (1986) 105–117.

[108] J.J.T.W.A. Strik, J.G. Wit, Porphyrogenic action of hexachlorbenzene and octachlorostyrene, in: M. Doss (Ed.), Porphyrins in Human Disease, Karker, Basel, 1976, pp. 418–423.

[109] IPCS, Hexachlorobenzene, WHO, Geneva, 1997.

[110] F.P. Stewart, A.G. Smith, Metabolism of the "mixed" cytochrome P-450 inducer hexachlorobenzene by rat liver microsomes, Biochem. Pharmacol. 35 (1986) 2163–2170.

[111] D.L. Grant, J.B. Shields, D.C. Villeneuve, Chemical (HCB) porphyria: Effect of removal of sex organs in the rat, Bull. Environ. Contam. Toxicol. 14 (1975) 422–425.

[112] L.C. San Martin de Viale, A.A. Viale, S. Nacht, M. Grinstein, Experimental porphyria induced in rats by hexachlorobenzene. A study of the porphyrins excreted by urine, Clin. Chim. Acta 28 (1970) 13–23.

[113] A.G. Smith, J.E. Francis, D. Dinsdale, M.M. Manson, J.R. Cabral, Hepatocarcinogenicity of hexachlorobenzene in rats and the sex difference in hepatic iron status and development of porphyria, Carcinogenesis 6 (1985) 631–636.

[114] A.G. Smith, J.E. Francis, Increased inhibition of hepatic uroporphyrinogen decarboxylase by hexachlorobenzene in male rats given the oestrogenic drugs diethylstilboestrol and chlorotrianisene, Biochem. Pharmacol. 30 (1981) 1849–1853.

[115] J.A. Goldstein, P. Hickman, V.W. Burse, H. Bergman, A comparative study of two polychlorinated biphenyl mixtures (Aroclors 1242 and 1016) containing 42% chlorine on induction of hepatic porphyria and drug metabolizing enzymes, Toxicol. Appl. Pharmacol. 32 (1975) 461–473.

[116] R.H. Hill, Effects of polyhalogenated aromatic compounds on porphyria metabolism, Environ. Health Perspect. 60 (1985) 139–145.

[117] T. Honda, S. Nonaka, F. Murayama, T. Ohgami, T. Shimoyama, H. Yoshida, Effects of KC-400 (polychlorinated biphenyls) on porphyrin metabolism—liver and blood porphyrin analyses in rats treated with KC-400, J. Dermatol. 10 (1983) 259–265.

[118] G. Koss, D. Meyer-Rogge, S. Seubert, A. Seubert, M. Losekam, 2,2′,3′,4,4′5,5′-Hepatachlorobiphenyl (PCB 180)—on its toxicokinetics, biotransformation and porphyrinogenic action in female rats, Arch. Toxicol. 67 (1993) 651–654.

[119] S. Sano, S. Kawanishi, Y. Seki, Toxicity of polychlorinated biphenyl with special reference to porphyrin metabolism, Environ. Health Perspect. 59 (1985) 137–143.

[120] B.N. Gupta, E.E. McConnell, J.A. Goldstein, M.W. Harris, J.A. Moore, Effects of a polybrominated biphenyl mixture in the rat and mouse. I. Six-month exposure, Toxicol. Appl. Pharmacol. 68 (1983) 1–18.

[121] A.G. Smith, J.E. Francis, J.A. Green, J.B. Greig, C.R. Wolf, M.M. Manson, Sex-linked hepatic uroporphyria and the induction of cytochromes P450IA in rats caused by hexachlorobenzene and polyhalogenated biphenyls, Biochem. Pharmacol. 40 (1990) 2059–2068.

[122] J.A. Goldstein, P. Hickman, H. Bergman, J.G. Vos, Hepatic porphyria induced by 2,3,7,8-tetrachlorodibenzo-p-dioxin in the mouse, Res. Commun. Chem. Pathol. Pharmacol. 6 (1973) 919–928.

[123] A.G. Smith, J.E. Francis, S.J. Kay, J.B. Greig, Hepatic toxicity and uroporphyrinogen decarboxylase activity following a single dose of 2,3,7,8-tetrachlorodibenzo-p-dioxin to mice, Biochem. Pharmacol. 30 (1981) 2825–2830.

[124] G.D. Sweeney, K.G. Jones, F.M. Cole, D. Basford, F. Krestynski, Iron deficiency prevents liver toxicity of 2,3,7,8-tetrachlorodibenzo-p-dioxin, Science 204 (1979) 332–335.

[125] L. Cantoni, M. Salmona, M. Rizzardini, Porphyrogenic effect of chronic treatment with 2,3,7,8-tetrachlorodibenzo-p-dioxin in female rats. Dose-effect relationship following urinary excretion of porphyrins, Toxicol. Appl. Pharmacol. 57 (1981) 156–163.

[126] J.A. Goldstein, P. Linko, H. Bergman, Induction of porphyria in the rat by chronic versus acute exposure to 2,3,7,8-tetrachlorodibenzo-p-dioxin, Biochem. Pharmacol. 31 (1982) 1607–1613.

[127] K.G. Jones, G.D. Sweeney, Dependence of the porphyrogenic effect of 2,3,7,8-tetrachlorodibenzo(p)dioxin upon inheritance of aryl hydrocarbon hydroxylase responsiveness, Toxicol. Appl. Pharmacol. 53 (1980) 42–49.

[128] S.W. Robinson, B. Clothier, R.A. Akhtar, A.L. Yang, I. Latour, C. Van Ijperen, M.F. Festing, A.G. Smith, Non-Ahr gene susceptibility loci for porphyria and liver injury induced by the interaction of "dioxin" with iron overload in mice, Mol. Pharmacol. 61 (2002) 674–681.

[129] R. Davies, B. Clothier, S.W. Robinson, R.E. Edwards, P. Greaves, J. Luo, T.W. Gant, T. Chernova, A.G. Smith, Essential role of the AH receptor in the dysfunction of heme metabolism induced by 2,3,7,8-tetrachlorodibenzo-p-dioxin, Chem. Res. Toxicol. 21 (2008) 330–340.

[130] J.B. Greig, J.E. Francis, S.J. Kay, D.P. Lovell, A.G. Smith, Incomplete correlation of 2,3,7,8-tetrachlorodibenzo-p-dioxin hepatotoxicity with Ah phenotype in mice, Toxicol. Appl. Pharmacol. 74 (1984) 17–25.

[131] P. Linko, H.N. Yeowell, T.A. Gasiewicz, J.A. Goldstein, Induction of cytochrome P-450 isozymes by hexachlorobenzene in rats and aromatic hydrocarbon (Ah)-responsive mice, J. Biochem. Toxicol. 1 (1986) 95–107.

[132] M.E. Hahn, T.A. Gasiewicz, P. Linko, J.A. Goldstein, The role of the Ah locus in hexachlorobenzene-induced porphyria. Studies in congenic C57BL/6J mice, Biochem. J. 254 (1988) 245–254.

[133] M.E. Hahn, J.A. Goldstein, P. Linko, T.A. Gasiewicz, Interaction of hexachloro-benzene with the receptor for 2,3,7,8-tetrachlorodibenzo-*p*-dioxin *in vitro* and *in vivo*. Evidence that hexachlorobenzene is a weak Ah receptor agonist, Arch. Biochem. Biophys. 270 (1989) 344–355.

[134] R. Akhtar, A.G. Smith, Chromosomal linkage analysis of porphyria in mice induced by hexachlorobenzene–iron synergism: A model of sporadic porphyria cutanea tarda, Pharmacogenetics 8 (1998) 485–494.

[135] A.G. Smith, J.E. Francis, Synergism of iron and hexachlorobenzene inhibits hepatic uroporphyrinogen decarboxylase in inbred mice, Biochem. J. 214 (1983) 909–913.

[136] J.A. Goldstein, M. Friesen, T.M. Scotti, P. Hickman, J.R. Hass, H. Bergman, Assess-ment of the contribution of chlorinated dibenzo-*p*-dioxins and dibenzofurans to hexachlorobenzene-induced toxicity, porphyria, changes in mixed function oxygenases, and histopathological changes, Toxicol. Appl. Pharmacol. 46 (1978) 633–649.

[137] M. Van den Berg, L.S. Birnbaum, M. Denison, M. De Vito, W. Farland, M. Feeley, H. Fiedler, H. Hakansson, A. Hanberg, L. Haws, M. Rose, S. Safe, *et al.* The 2005 World Health Organization reevaluation of human and mammalian toxic equivalency factors for dioxins and dioxin-like compounds, Toxicol. Sci. 93 (2006) 223–241.

[138] M.A. Alleman, J.F. Koster, J.H. Wilson, A. Edixhoven-Bosdijk, R.G. Slee, M.J. Kroos, H.G. von Eijk, The involvement of iron and lipid peroxidation in the pathogenesis of HCB induced porphyria, Biochem. Pharmacol. 34 (1985) 161–166.

[139] P.H. Bach, J.J.F. Taljaard, S.M. Jouubert, B.C. Shanley, The effect of iron overload on the development of hexachlorobenzene (HCB) porphyria, S. Afr. J. Lab. Clin. Med. 17 (1971) 75–76.

[140] A.G. Smith, P. Carthew, J.E. Francis, J.R. Cabral, M.M. Manson, Enhancement by iron of hepatic neoplasia in rats caused by hexachlorobenzene, Carcinogenesis 14 (1993) 1381–1387.

[141] J.J. Taljaard, B.C. Shanley, W.M. Deppe, S.M. Joubert, Porphyrin metabolism in experimental hepatic siderosis in the rat. 2. Combined effect of iron overload and hexachlorobenzene, Br. J. Haemotol. 23 (1972) 513–519.

[142] J.J. Taljaard, B.C. Shanley, W.M. Deppe, S.M. Joubert, Porphyrin metabolism in experimental hepatic siderosis in the rat. 3. Effect of iron overload and hexachlor-obenzene on liver haem biosynthesis, Br. J. Haematol. 23 (1972) 587–593.

[143] G. Blekkenhorst, R.S. Day, L. Eales, The effect of bleeding and iron administration on the development of hexachlorobenzene-induced rat porphyria, Int. J. Biochem. 12 (1980) 1013–1017.

[144] R. Wainstok de Calmanovici, S.C. Billi, C.A. Aldonatti, L.C. San Martin de Viale, Effect of desferrioxamine on the development of hexachlorobenzene induced por-phyria, Biochem. Pharmacol. 35 (1986) 2399–2405.

[145] N. Gorman, A. Zaharia, H.S. Trask, J.G. Szakacs, N.J. Jacobs, J.M. Jacobs, D. Balestra, J.F. Sinclair, P.R. Sinclair, Effect of an oral iron chelator or iron-deficient diets on uroporphyria in a murine model of porphyria cutanea tarda, Hepatology 46 (2007) 1927–1934.

[146] K.G. Jones, F.M. Cole, G.D. Sweeney, The role of iron in the toxicity of 2,3,7,8-tetrachlorodibenzo-(p)-dioxin (TCDD), Toxicol. Appl. Pharmacol. 61 (1981) 74–88.

[147] M.R. Franklin, J.D. Phillips, J.P. Kushner, Attenuation of polychlorinated biphenyl induced uroporphyria by iron deprivation, Environ. Toxicol. Pharmacol. 20 (2005) 417–423.

[148] A. Smith, J.R.P. Cabral, P. Carthew, J. Francis, M.M. Manson, Carcinogenicity of iron in conjunction with a chlorinated environmental chemical, hexachlorobenzene, in C57BL/10scsn mice, Int. J. Cancer 43 (1989) 492–496.

[149] A.G. Smith, B. Clothier, S. Robinson, M.J. Scullion, P. Carthew, R. Edwards, J. Luo, C.K. Lim, M. Toledano, Interaction between iron metabolism and 2,3,7,8-

tetrachlorodibenzo-*p*-dioxin in mice with variants of the Ahr gene: A hepatic oxidative mechanism, Mol. Pharmacol. 53 (1998) 52–61.

[150] P. Siersema, R.P. van Helvoirt, G.M.M. Ketelaars, M.I. Cleton-shoeteman, W.C. Debruin, H. Vanijk, J.H.P. Wilson, Colocalization of iron and uroporphyrin in hepatocytes of mice with hexachlorobenzene-induced porphyria, Hepatology 12 (1990) 446–446.

[151] R.N. Khanna, A.G. Smith, Fate of hexachlorobenzene in C57BL/10 mice with iron overload, Biochem. Pharmacol. 34 (1985) 4157–4162.

[152] A.G. Smith, J.E. Francis, S.J. Kay, J.B. Greig, F.P. Stewart, Mechanistic studies of the inhibition of hepatic uroporphyrinogen decarboxylase in C57BL/10 mice by iron-hexachlorobenzene synergism, Biochem. J. 238 (1986) 871–878.

[153] J.E. Francis, A.G. Smith, Polycyclic aromatic hydrocarbons cause hepatic porphyria in iron-loaded C57BL/10 mice: Comparison of uroporphyrinogen decarboxylase inhibition with induction of alkoxyphenoxazone dealkylations, Biochem. Biophys. Res. Commun. 146 (1987) 13–20.

[154] A.J. Urquhart, G.H. Elder, A.G. Roberts, R.W. Lambrecht, P.R. Sinclair, W.J. Bement, N. Gorman, J.A. Sinclair, Uroporphyria produced in mice by 20-methylcholanthrene and 5-aminolaevulinic acid, Biochem. J. 253 (1988) 357–362.

[155] A.G. Smith, J.E. Francis, P. Carthew, Iron as a synergist for hepatocellular carcinoma induced by polychlorinated biphenyls in Ah-responsive C57BL/10scsn mice, Carcinogenesis 11 (1990) 437–444.

[156] A.G. Smith, J.E. Francis, Genetic variation of iron-induced uroporphyria in mice, Biochem. J. 291 (1993) 29–35.

[157] S. Deam, G.H. Elder, Uroporphyria produced in mice by iron and 5-aminolevulinic acid, Biochem. Pharmacol. 41 (1991) 2019–2022.

[158] D. Constantin, J.E. Francis, R.A. Akhtar, B. Clothier, A.G. Smith, Uroporphyria induced by 5-aminolaevulinic acid alone in Ahrd SWR mice, Biochem. Pharmacol. 52 (1996) 1407–1413.

[159] J.D. Phillips, L.K. Jackson, M. Bunting, M.R. Franklin, K.R. Thomas, J.E. Levy, N.C. Andrews, J.P. Kushner, A mouse model of familial porphyria cutanea tarda, Proc. Natl. Acad. Sci. USA 98 (2001) 259–264.

[160] P.R. Sinclair, N. Gorman, H.S. Walton, W.J. Bement, J.F. Sinclair, G.S. Gerhard, J.G. Szakacs, N.C. Andrews, J.E. Levy, Uroporphyria in Hfe mutant mice given 5-aminolevulinate: a new model of Fe-mediated porphyria cutanea tarda, Hepatology 33 (2001) 406–412.

[161] N. Gorman, H.W. Trask, W.J. Bement, J.G. Szakacs, G.H. Elder, D. Balestra, N.J. Jacobs, J.M. Jacobs, J.F. Sinclair, G.S. Gerhard, P.R. Sinclair, Genetic factors influence ethanol-induced uroporphyria in Hfe$^{(-/-)}$ mice, Hepatology 40 (2004) 942–950.

[162] P.R. Sinclair, N. Gorman, H.W. Trask, W.J. Bement, J.G. Szakacs, G.H. Elder, D. Balestra, J.F. Sinclair, G.S. Gerhard, Uroporphyria caused by ethanol in Hfe$^{(-/-)}$ mice as a model for porphyria cutanea tarda, Hepatology 37 (2003) 351–358.

[163] M.C. Rios De Molina, M.B. Mazzetti, M. Galigniana, C. Aldonatti, J.M. Tomio, L.C. San Martin De Viale, The decrease in uroporphyrinogen decarboxylase activity induced by ethanol predisposes rats to the development of porphyria and accelerates xenobiotic-triggered porphyria, regardless of hepatic damage, Braz. J. Med. Biol. Res. 35 (2002) 1273–1283.

[164] H. de Verneuil, Y. Nordmann, N. Phung, B. Grandchamp, G. Aitken, M. Grelier, J. Noire, Familial and sporadic porphyria cutanea: Two different diseases, Int. J. Biochem. 9 (1978) 927–931.

[165] A.G. Smith, J.R. Cabral, F. De Matteis, A difference between two strains of rats in their liver non-haem iron content and in their response to the porphyrogenic effect of hexachlorobenzene, Chem. Biol. Interact. 27 (1979) 353–363.

[166] J.B. Greig, J.E. Francis, A.G. Smith, Genetic control of the hepatotoxicity of 2,3,7,8-tetrachlorodibenzo-*p*-dioxin in mice, Organohalogen Compd. 1 (1990) 177–180.

[167] J.B. Greig, J.E. Francis, S.J. Kay, T. Lister, D.E. Ray, A.A. Seawright, A.G. Smith, Pleiotropic effect of the gene hairless on hepatotoxicity of 2, 3, 7, 8-tetrachlorodibenzo-*p*-dioxin in mice, Arch. Toxicol. 60 (1987) 350–354.

[168] S. Sen, J.M. Satagopan, K.W. Broman, G.A. Churchill, R/qtldesign: Inbred line cross experimental design, Mamm. Genome 18 (2007) 87–93.

[169] M. Bensaid, S. Fruchon, C. Mazeres, S. Bahram, M.P. Roth, H. Coppin, Multigenic control of hepatic iron loading in a murine model of hemochromatosis, Gastroenterology 126 (2004) 1400–1408.

[170] G.H. Elder, J.O. Evans, S.A. Matlin, The effect of the porphyrogenic compound, hexachlorobenzene, on the activity of hepatic uroporphyrinogen decarboxylase in the rat, Clin. Sci. Mol. Med. 51 (1976) 71–80.

[171] M. Louw, A.C. Neethling, V.A. Percy, M. Carstens, B.C. Shanley, Effects of hexachlorobenzene feeding and iron overload on enzymes of haem biosynthesis and cytochrome P 450 in rat liver, Clin. Sci. Mol. Med. 53 (1977) 111–115.

[172] L.C. San Martin de Viale, M.C. Rios de Molina, R. Wainstok de Calmanovici, J.M. Tomio, Porphyrias and porphyrinogen carboxylase in hexachlorobenzene-induced porphyria, Biochem. J. 168 (1977) 393–400.

[173] G.H. Elder, G.B. Lee, J.A. Tovey, Decreased activity of hepatic uroporphyrinogen decarboxylase in sporadic porphyria cutanea tarda, N. Engl. J. Med. 299 (1978) 274–278.

[174] G.H. Elder, D.M. Sheppard, Immunoreactive uroporphyrinogen decarboxylase is unchanged in porphyria caused by TCDD and hexachlorobenzene, Biochem. Biophys. Res. Commun. 109 (1982) 113–120.

[175] E. Mylchreest, M. Charbonneau, Studies on the mechanism of uroporphyrinogen decarboxylase inhibition in hexachlorobenzene-induced porphyria in the female rat, Toxicol. Appl. Pharmacol. 145 (1997) 23–33.

[176] R. Wainstok de Calmanovici, M.C. Rios de Molina, M.C. Taira de Yamasoto, J.M. Tomio, L.C. San Martin de Viale, Mechanism of hexachlorobenzene-induced porphyria in rats. Effect of phenobarbitone pretreatment, Biochem. J. 218 (1984) 753–763.

[177] J.A. Goldstein, P. Hickman, D.L. Jue, Experimental hepatic porphyria induced by polychlorinated biphenyls, Toxicol. Appl. Pharmacol. 27 (1974) 437–448.

[178] C. Rajamanickam, J. Amrutavalli, M.R. Rao, G. Padmanaban, Effect of hexachlorobenzene on haem synthesis, Biochem. J. 129 (1972) 381–387.

[179] N. Gorman, H.S. Walton, W.J. Bement, C.P. Honsinger, J.G. Szakacs, J.F. Sinclair, P.R. Sinclair, Role of small differences in CYP1A2 in the development of uroporphyria produced by iron and 5-aminolevulinate in C57BL/6 and SWR strains of mice, Biochem. Pharmacol. 58 (1999) 375–382.

[180] M.R. Franklin, J.D. Phillips, J.P. Kushner, Accelerated development of uroporphyria in mice heterozygous for a deletion at the uroporphyrinogen decarboxylase locus, J. Biochem. Mol. Toxicol. 15 (2001) 287–293.

[181] M.D. Stonard, G. Poli, F. De Matteis, Stimulation of liver heme oxygenase in hexachlorobenzene-induced hepatic porphyria, Arch. Toxicol. 72 (1998) 355–361.

[182] P. Carthew, A.G. Smith, Pathological mechanisms of hepatic tumour formation in rats exposed chronically to dietary hexachlorobenzene, J. Appl. Toxicol. 14 (1994) 447–452.

[183] T. Kuiper-Goodman, R.D. Pontefract, D.L. Grant, X-ray(TEM)microanalysis of iron accumulated in liver parenchymal cells of rats with porphyria, Proc. Microsc. Soc. Canada 1 (1974) 14–15.

[184] J. Whysner, C.X. Wang, Hepatocellular iron accumulation and increased cell proliferation in polychlorinated biphenyl-exposed Sprague–Dawley rats and the development of hepatocarcinogenesis, Toxicol. Sci. 62 (2001) 36–45.

[185] Z.Z. Wahba, W.J. Murray, S.J. Stohs, Altered hepatic iron distribution and release in rats after exposure to 2,3,7,8-tetrachlorodibenzo-*p*-dioxin (TCDD), Bull. Environ. Contam. Toxicol. 45 (1990) 436–445.

[186] Z.Z. Wahba, W.J. Murray, S.J. Stohs, Desferrioxamine-induced alterations in hepatic iron distribution, DNA damage and lipid peroxidation in control and 2,3,7,8-tetrachlorodibenzo-*p*-dioxin-treated rats, J. Appl. Toxicol. 10 (1990) 119–124.

[187] B. Rowley, G.D. Sweeney, Release of ferrous iron from ferritin by liver microsomes: A possible role in the toxicity of 2,3,7,8-tetrachlorodibenzo-*p*-dioxin, Can. J. Biochem. Cell Biol. 62 (1984) 1293–1300.

[188] A. Tangeras, Lysosomes, but not mitochondria, accumulate iron and porphyrins in porphyria induced by hexachlorobenzene, Biochem. J. 235 (1986) 671–675.

[189] N.C. Andrews, P.J. Schmidt, Iron homeostasis, Annu. Rev. Physiol. 69 (2007) 69–85.

[190] K.G. Jones, G.D. Sweeney, Association between induction of aryl hydrocarbon hydroxylase and depression of uroporphyrinogen decarboxylase activity, Res. Commun. Chem. Pathol. Pharmacol. 17 (1977) 631–637.

[191] J.M. Jacobs, P.R. Sinclair, J.F. Sinclair, N.J. Jacobs, Role of inducer binding in cytochrome P-450 IA2-mediated uroporphyrinogen oxidation, J. Biochem. Toxicol. 5 (1990) 193–199.

[192] N. Gorman, K.L. Ross, H.S. Walton, W.J. Bement, J.G. Szakacs, G.S. Gerhard, T.P. Dalton, D.W. Nebert, R.S. Eisenstein, J.F. Sinclair, P.R. Sinclair, Uroporphyria in mice: thresholds for hepatic CYP1A2 and iron, Hepatology 35 (2002) 912–921.

[193] P. Greaves, B. Clothier, R. Davies, F.M. Higginson, R.E. Edwards, T.P. Dalton, D.W. Nebert, A.G. Smith, Uroporphyria and hepatic carcinogenesis induced by polychlorinated biphenyls-iron interaction: absence in the Cyp1a2$^{(-/-)}$ knockout mouse, Biochem. Biophys. Res. Commun. 331 (2005) 147–152.

[194] P.R. Sinclair, W.J. Bement, R.W. Lambrecht, N. Gorman, J.F. Sinclair, Chlorinated biphenyls induce cytochrome P450IA2 and uroporphyrin accumulation in cultures of mouse hepatocytes, Arch. Biochem. Biophys. 281 (1990) 225–232.

[195] P.R. Sinclair, N. Gorman, T. Dalton, H.S. Walton, W.J. Bement, J.F. Sinclair, A.G. Smith, D.W. Nebert, Uroporphyria produced in mice by iron and 5-aminolaevulinic acid does not occur in Cyp1a2$^{(-/-)}$ null mutant mice, Biochem. J. 330 (1998) 149–153.

[196] P.R. Sinclair, N. Gorman, H.S. Walton, W.J. Bement, T.P. Dalton, J.F. Sinclair, A.G. Smith, D.W. Nebert, CYP1A2 is essential in murine uroporphyria caused by hexachlorobenzene and iron, Toxicol. Appl. Pharmacol. 162 (2000) 60–67.

[197] A.G. Smith, B. Clothier, P. Carthew, N.L. Childs, P.R. Sinclair, D.W. Nebert, T.P. Dalton, Protection of the Cyp1a2$^{(-/-)}$ null mouse against uroporphyria and hepatic injury following exposure to 2,3,7,8-tetrachlorodibenzo-*p*-dioxin, Toxicol. Appl. Pharmacol. 173 (2001) 89–98.

[198] S. Uno, T.P. Dalton, P.R. Sinclair, N. Gorman, B. Wang, A.G. Smith, M.L. Miller, H.G. Shertzer, D.W. Nebert, Cyp1a1$^{(-/-)}$ male mice: protection against high-dose TCDD-induced lethality and wasting syndrome, and resistance to intrahepatocyte lipid accumulation and uroporphyria, Toxicol. Appl. Pharmacol. 196 (2004) 410–421.

[199] A.P. van Birgelen, M.J. DeVito, J.M. Akins, D.G. Ross, J.J. Diliberto, L.S. Birnbaum, Relative potencies of polychlorinated dibenzo-*p*-dioxins, dibenzofurans, and biphenyls derived from hepatic porphyrin accumulation in mice, Toxicol. Appl. Pharmacol. 138 (1996) 98–109.

[200] M.R. Franklin, J.D. Phillips, J.P. Kushner, CYP3A–inducing agents and the attenuation of uroporphyrin accumulation and excretion in a rat model of porphyria cutanea tarda, Biochem. Pharmacol. 60 (2000) 1325–1331.

[201] H. de Verneuil, S. Sassa, A. Kappas, Effects of polychlorinated biphenyl compounds, 2,3,7,8-tetrachlorodibenzo-*p*-dioxin, phenobarbital and iron on hepatic uroporhyrinogen decarboxylase—implications for the pathogenesis of porphyria, Biochem. J. 214 (1983) 145–151.

[202] S. Madra, F. Mann, J.E. Francis, M.M. Manson, A.G. Smith, Modulation by iron of hepatic microsomal and nuclear cytochrome P450, and cytosolic glutathione S-transferase and peroxidase in C57BL/10scsn mice induced with polychlorinated biphenyls (Aroclor 1254), Toxicol. Appl. Pharmacol. 136 (1996) 79–86.

[203] S.P. Faux, J.E. Francis, A.G. Smith, J.K. Chipman, Induction of 8-hydroxydeoxyguanosine in Ah-responsive mouse liver by iron and Aroclor 1254, Carcinogenesis 13 (1992) 247–250.

[204] E.S. Feldman, B.R. Bacon, Hepatic mitochondrial oxidative metabolism and lipid peroxidation in experimental hexachlorobenzene-induced porphyria with dietary carbonyl iron overload, Hepatology 9 (1989) 686–692.

[205] A.G. Smith, J.E. Francis, J.R.P. Cabral, P. Carthew, M.M. Manson, F.P. Stewart, Iron-enhancement of the hepatic porphyria and cancer induced by polyhalogenated aromatic chemicals, in: G. Poli, K.H. Cheeseman, M.U. Dianzani, T.F. Slater (Eds.), Free Radicals in the Pathogenesis of Liver Injury, Adv. Biosc., 76, Pergamon Press, Oxford, 1989, pp. 205–214.

[206] S.J. Stohs, Oxidative stress induced by 2,3,7,8-tetrachlorodibenzo-*p*-dioxin (TCDD), Free Radic. Biol. Med. 9 (1990) 79–90.

[207] S.J. Stohs, M.A. Shara, N.Z. Alsharif, Z.Z. Wahba, Z.A. al-Bayati, 2,3,7,8-Tetrachlorodibenzo-*p*-dioxin-induced oxidative stress in female rats, Toxicol. Appl. Pharmacol. 106 (1990) 126–135.

[208] B.P. Slezak, G.E. Hatch, M.J. DeVito, J.J. Diliberto, R. Slade, K. Crissman, E. Hassoun, L.S. Birnbaum, Oxidative stress in female B6C3F1 mice following acute and subchronic exposure to 2,3,7,8-tetrachlorodibenzo-*p*-dioxin (TCDD), Toxicol. Sci. 54 (2000) 390–398.

[209] J.F. Brown Jr., K.M. Fish, B.A. Mayes, J.B. Silkworth, S.B. Hamilton, J. Whysner, PCB effects on epigenetic carcinogenic processes, in: L.W. Robertson, L.G. Hansen (Eds.), PCBs. Recent Advances in Environmental Toxicology and Health Effects, University Press of Kentucky, Lexington, Kentucky, 2001, pp. 329–336.

[210] N. Gorman, A. Zaharia, H.S. Trask, J.G. Szakacs, N.J. Jacobs, J.M. Jacobs, D. Balestra, J.F. Sinclair, P.R. Sinclair, Effect of iron and ascorbate on uroporphyria in ascorbate-requiring mice as a model for porphyria cutanea tarda, Hepatology 45 (2007) 187–194.

[211] M.E. Horvath, S.P. Faux, A.G. Smith, A. Blazovics, M. van der Looij, J. Feher, K.H. Cheeseman, Vitamin E protects against iron-hexachlorobenzene induced porphyria and formation of 8-hydroxydeoxyguanosine in the liver of C57BL/10scsn mice, Toxicol. Lett. 122 (2001) 97–102.

[212] H.G. Shertzer, D.W. Nebert, A. Puga, M. Ary, D. Sonntag, K. Dixon, L.J. Robinson, E. Cianciolo, T.P. Dalton, Dioxin causes a sustained oxidative stress response in the mouse, Biochem. Biophys. Res. Commun. 253 (1998) 44–48.

[213] A.P. Senft, T.P. Dalton, D.W. Nebert, M.B. Genter, R.J. Hutchinson, H.G. Shertzer, Dioxin increases reactive oxygen production in mouse liver mitochondria, Toxicol. Appl. Pharmacol. 178 (2002) 15–21.

[214] A.P. Senft, T.P. Dalton, D.W. Nebert, M.B. Genter, A. Puga, R.J. Hutchinson, J.K. Kerzee, S. Uno, H.G. Shertzer, Mitochondrial reactive oxygen production is dependent on the aromatic hydrocarbon receptor, Free Radic. Biol. Med. 33 (2002) 1268–1278.

[215] D. Shen, T.P. Dalton, D.W. Nebert, H.G. Shertzer, Glutathione redox state regulates mitochondrial reactive oxygen production, J. Biol. Chem. 280 (2005) 25305–25312.

[216] H.G. Shertzer, M.B. Genter, D. Shen, D.W. Nebert, Y. Chen, T.P. Dalton, TCDD decreases ATP levels and increases reactive oxygen production through changes in mitochondrial F(0)F(1)-ATP synthase and ubiquinone, Toxicol. Appl. Pharmacol. 217 (2006) 363–374.

[217] F. De Matteis, Role of iron in the hydrogen peroxide-dependent oxidation of hexahydroporphyrins (porphyrinogens): A possible mechanism for the exacerbation by iron of hepatic uroporphyria, Mol. Pharmacol. 33 (1988) 463–469.

[218] F. De Matteis, Porphyria cutanea tarda of the toxic and sporadic varieties, Clin. Dermatol. 16 (1998) 265–275.

[219] T. Heikel, W.H. Lockwood, C. Rimington, Formation of non-enzymic heme, Nature 182 (1958) 313.

[220] A.G. Smith, J.E. Francis, F. De Matteis, Lobes of rat liver respond at different rates to challenge by dietary hexachlorobenzene, Biochem. Pharmacol. 29 (1980) 3127–3131.

[221] Y. Seki, S. Kawanishi, S. Sano, Role of inhibition of uroporphyrinogen decarboxylase in PCB-induced porphyria in mice, Toxicol. Appl. Pharmacol. 90 (1987) 116–125.

[222] P.R. Sinclair, W.J. Bement, H.L. Bonkovsky, R.W. Lambrecht, J.E. Frezza, J.F. Sinclair, A.J. Urquhart, G.H. Elder, Uroporphyrin accumulation produced by halogenated biphenyls in chick-embryo hepatocytes. Reversal of the accumulation by piperonyl butoxide, Biochem. J. 237 (1986) 63–71.

[223] F. De Matteis, C. Harvey, C. Reed, R. Hempenius, Increased oxidation of uroporphyrinogen by an inducible liver microsomal system. Possible relevance to drug-induced uroporphyria, Biochem. J. 250 (1988) 161–169.

[224] J.M. Jacobs, P.R. Sinclair, W.J. Bement, R.W. Lambrecht, J.F. Sinclair, J.A. Goldstein, Oxidation of uroporphyrinogen by methylcholanthrene-induced cytochrome P-450. Essential role of cytochrome P-450d, Biochem. J. 258 (1989) 247–253.

[225] R.W. Lambrecht, P.R. Sinclair, N. Gorman, J.F. Sinclair, Uroporphyrinogen oxidation catalyzed by reconstituted cytochrome P450IA2, Arch. Biochem. Biophys. 294 (1992) 504–510.

[226] G. Chaufan, M.C. Rios de Molina, L.C. San Martin de Viale, How does hexachlorobenzene treatment affect liver uroporphyrinogen decarboxylase?, Int. J. Biochem. Cell Biol. 33 (2001) 621–630.

[227] A.G. Smith, J.E. Francis, J.B. Greig, Continued depression of hepatic uroporphyrinogen decarboxylase activity caused by hexachlorobenzene or 2,3,7,8-tetrachloro-dibenzo-*p*-dioxin despite regeneration after partial hepatectomy, Biochem. Pharmacol. 34 (1985) 1817–1820.

[228] G.H. Elder, A.G. Roberts, A.J. Urquhart, Alterations of uroporphyrinogen decarboxylase by chlorinated organics, Ann. N. Y. Acad. Sci. 514 (1987) 141–147.

[229] L. Cantoni, D. dal Fiume, M. Rizzardini, R. Ruggieri, *In vitro* inhibitory effect on porphyrinogen carboxylyase of liver extracts from TCDD treated mice, Toxicol. Lett. 20 (1984) 211–217.

[230] M.C. Rios de Molina, R. Wainstok de Calmanovici, L.C. San Martin de Viale, Investigations on the presence of porphyrinogen carboxy-lyase inhibitor in the liver of rats intoxicated with hexachlorobenzene, Int. J. Biochem. 12 (1980) 1027–1032.

[231] A.G. Smith, J.E. Francis, Chemically-induced formation of an inhibitor of hepatic uroporphyrinogen decarboxylase in inbred mice with iron overload, Biochem. J. 246 (1987) 221–226.

[232] J.E. Francis, A.G. Smith, Oxidation of uroporphyrinogens by hydroxyl radicals. Evidence for nonporphyrin products as potential inhibitors of uroporphyrinogen decarboxylase, FEBS Lett. 233 (1988) 311–314.

[233] R.W. Lambrecht, J.M. Jacobs, P.R. Sinclair, J.F. Sinclair, Inhibition of uroporphyrinogen decarboxylase activity. The role of cytochrome P-450-mediated uroporphyrinogen oxidation, Biochem. J. 269 (1990) 437–441.

[234] J.D. Phillips, H.A. Bergonia, C.A. Reilly, M.R. Franklin, J.P. Kushner, A porphomethene inhibitor of uroporphyrinogen decarboxylase causes porphyria cutanea tarda, Proc. Natl. Acad. Sci. USA 104 (2007) 5079–5084.

[235] M. Danton, C.K. Lim, Porphomethene inhibitor of uroporphyrinogen decarboxylase: Analysis by high-performance liquid chromatography/electrospray ionization tandem mass spectrometry, Biomed. Chromatogr. 21 (2007) 661–663.

[236] D. Mauzerall, S. Granick, Porphyrin biosynthesis in erythrocytes. 3. Uroporphyrinogen and its decarboxylase, J. Biol. Chem. 232 (1958) 1141–1162.

[237] P.R. Sinclair, N. Gorman, H.S. Walton, W.J. Bement, J.M. Jacobs, J.F. Sinclair, Ascorbic acid inhibition of cytochrome P450-catalyzed uroporphyrin accumulation, Arch. Biochem. Biophys. 304 (1993) 464–470.

[238] P.R. Sinclair, N. Gorman, J.F. Sinclair, H.S. Walton, W.J. Bement, R.W. Lambrecht, Ascorbic acid inhibits chemically induced uroporphyria in ascorbate-requiring rats, Hepatology 22 (1995) 565–572.

[239] W. Lin, R. Timkovich, Oxygenated tetrapyrroles produced from porphyrinogens, Bioorg. Chem. 22 (1994) 72–94.

[240] R. Guo, C.K. Lim, F. De Matteis, Peroxylated and hydroxylated uroporphyrins: a study of their production *in vitro* in enzymic and chemical model systems, Biomed. Chromatogr. 10 (1996) 213–220.

[241] J. Luo, C.K. Lim, Isolation and characterization of new porphyrin metabolites in human porphyria cutanea tarda and in rats treated with hexachlorobenzene by HPTLC, HPLC and liquid secondary ion mass spectrometry, Biomed. Chromatogr. 9 (1995) 113–122.

[242] C.K. Lim, M. Danton, B. Clothier, A.G. Smith, Dihydroxy-, hydroxyspirolactone-, and dihydroxyspirolactone-urochlorins induced by 2,3,7,8-tetrachlorodibenzo-*p*-dioxin in the liver of mice, Chem. Res. Toxicol. 19 (2006) 1660–1667.

[243] A.B. Okey, An aryl hydrocarbon receptor odyssey to the shores of toxicology: the Deichmann Lecture, International Congress of Toxicology-XI, Toxicol. Sci. 98 (2007) 5–38.

[244] R.J. Kociba, D.G. Keyes, J.E. Beyer, R.M. Carreon, C.E. Wade, D.A. Dittenber, R.P. Kalnins, L.E. Frauson, C.N. Park, S.D. Barnard, R.A. Hummel, C.G. Humiston, Results of a two-year chronic toxicity and oncogenicity study of 2,3,7,8-tetrachlorodibenzo-*p*-dioxin in rats, Toxicol. Appl. Pharmacol. 46 (1978) 279–303.

[245] P.D. Siersema, M.I. Cleton-Soeteman, W.C. de Bruijn, F.J. ten Kate, H.G. van Eijk, J.H. Wilson, Ferritin accumulation and uroporphyrin crystal formation in hepatocytes of C57BL/10 mice: A time-course study, Cell Tissue Res. 274 (1993) 405–412.

[246] B.A. Mayes, E.E. McConnell, B.H. Neal, M.J. Brunner, S.B. Hamilton, T.M. Sullivan, A.C. Peters, M.J. Ryan, J.D. Toft, A.W. Singer, J.F. Brown, Jr., R. G. Menton,, *et al.* Comparative carcinogenicity in Sprague–Dawley rats of the polychlorinated biphenyl mixtures Aroclors 1016, 1242, 1254, and 1260, Toxicol. Sci. 41 (1998) 62–76.

[247] F.P. Stewart, M.M. Manson, J.R. Cabral, A.G. Smith, Hexachlorobenzene as a promoter of diethylnitrosamine-initiated hepatocarcinogenesis in rats and comparison with induction of porphyria, Carcinogenesis 10 (1989) 1225–1230.

[248] A.L. Fracanzani, E. Taioli, M. Sampietro, E. Fatta, C. Bertelli, G. Fiorelli, S. Fargion, Liver cancer risk is increased in patients with porphyria cutanea tarda in comparison to matched control patients with chronic liver disease, J. Hepatol. 35 (2001) 498–503.

[249] M. Linet, G. Gridley, O. Nyren, L. Mellemkjaer, J. Olsen, S. Keehn, H. Adami, J. Fraumeni, Primary liver cancer, other malignancies, and mortality risks following porphyria: A cohort study in Denmark and Sweden, Am. J. Epidemiol. 149 (1999) 1010–1015.

[250] H. Salata, J.M. Cortes, R. Enriquez de Salamanca, H. Oliva, A. Castro, E. Kusak, V. Carreno, C. Hernandez Guio, Porphyria cutanea tarda and hepatocellular carcinoma. Frequency of occurrence and related factors, J. Hepatol. 1 (1985) 477–487.

[251] A.G. Smith, P. Carthew, J.E. Francis, K. Ingebrigtsen, Influence of iron on the induction of hepatic tumors and porphyria by octachlorostyrene in C57BL/10scsn mice, Cancer Lett. 81 (1994) 145–150.

[252] S. Madra, J. Styles, A.G. Smith, Perturbation of hepatocyte nuclear populations induced by iron and polychlorinated biphenyls in C57BL/10scsn mice during carcinogenesis, Carcinogenesis 16 (1995) 719–727.

[253] P.C. Rumsby, J.G. Evans, H.E. Phillimore, P. Carthew, A.G. Smith, Search for Ha-ras codon 61 mutations in liver tumours caused by hexachlorobenzene and Aroclor 1254 in C57BL/10scsn mice with iron overload, Carcinogenesis 13 (1992) 1917–1920.

[254] R. Davies, B. Clothier, A.G. Smith, Mutation frequency in the laci gene of liver DNA from lambda/laci transgenic mice following the interaction of PCBs with iron causing hepatic cancer and porphyria, Mutagenesis 15 (2000) 379–383.

[255] L. Libbrecht, L. Meerman, F. Kuipers, T. Roskams, V. Desmet, P. Jansen, Liver pathology and hepatocarcinogenesis in a long-term mouse model of erythropoietic protoporphyria, J. Pathol. 199 (2003) 191–200.

[256] S. Knasmuller, W. Parzefall, C. Helma, F. Kassie, S. Ecker, R. Schulte-Hermann, Toxic effects of griseofulvin: Disease models, mechanisms, and risk assessment, Crit. Rev. Toxicol. 27 (1997) 495–537.

[257] R. Thierbach, T.J. Schulz, F. Isken, A. Voigt, B. Mietzner, G. Drewes, J.C. von Kleist-Retzow, R.J. Wiesner, M.A. Magnuson, H. Puccio, A.F. Pfeiffer, P. Steinberg,, et al. Targeted disruption of hepatic frataxin expression causes impaired mitochondrial function, decreased life span and tumor growth in mice, Hum. Mol. Genet. 14 (2005) 3857–3864.

[258] Z.J. Bulaj, M.R. Franklin, J.D. Phillips, K.L. Miller, H.A. Bergonia, R.S. Ajioka, L.M. Griffen, D.J. Guinee, C.Q. Edwards, J.P. Kushner, Transdermal estrogen replacement therapy in postmenopausal women previously treated for porphyria cutanea tarda, J. Lab. Clin. Med. 136 (2000) 482–488.

[259] P.R. Sinclair, N. Gorman, I.B. Tsyrlov, U. Fuhr, H.S. Walton, J.F. Sinclair, Uroporphyrinogen oxidation catalyzed by human cytochromes P450, Drug Metab. Dispos. 26 (1998) 1019–1025.

[260] M. Danton, C.K. Lim, High-performance liquid chromatography/electrospray ionization tandem mass spectrometry of hydroxylated uroporphyrin and urochlorin derivatives formed by photochemical oxidation of uroporphyrinogen I, Biomed. Chromatogr. 21 (2007) 534–545.

CHAPTER 7

Aristolochic Acid Nephropathy: An Environmental and Iatrogenic Disease

Arthur P. Grollman,* John Scarborough,‡ *and* Bojan Jelaković†

Contents

1. Introduction

The *Aristolochiaceae* family of herbaceous plants, specifically members of the genus *Aristolochia,* has been used for medicinal purposes for more than 2500 years [1]. Remarkably, the extensive *materia medica* describing the therapeutic use of *Aristolochia* rarely mentions its intrinsic toxicity. Recently,

* Laboratory of Chemical Biology, Department of Pharmacological Sciences, Stony Brook University, Stony Brook, New York 11794
† Department of Nephrology and Arterial Hypertension, Zagreb University School of Medicine and University Hospital Center, 10000 Zagreb, Croatia, and Croatian Center for Endemic Nephropathy, 35000 Slavonski Brod, Croatia
‡ School of Pharmacy and Department of History, University of Wisconsin, Madison, Wisconsin, 53705

aristolochic acid (AA), a principal component of all *Aristolochia* sp., was shown to be the toxin responsible for the clinical syndromes known as Chinese herb nephropathy (CHN) and endemic (Balkan) nephropathy (EN). Both disorders are associated with a high incidence of urothelial (transitional cell) cancer and appear to constitute a single disease entity, designated aristolochic acid nephropathy (AAN).

The epidemiology and pathophysiology of CHN and EN have been reviewed extensively [2–7] and the association of these diseases with human cancer is the subject of several comprehensive reports [8,9]. Guided by the hypothesis that AA is the common etiologic agent in CHN and EN [10,11], we review the molecular and clinical toxicology of this potent nephrotoxic chemical carcinogen. Additionally, based on the traditional use of *Aristolochia* in herbal remedies, we posit that AAN represents a long-overlooked iatrogenic disease and an international public health problem of considerable magnitude [12].

2. TOXICITY OF *ARISTOLOCHIA*

Toxicologists have long been aware of the toxic properties of *Aristolochia* sp. In 1825, while investigating the homeopathic principle that "like cures like," Jörg performed experiments on himself and his colleagues, revealing the acute toxic properties of *Aristolochia serpentaria* [13]. Among the effects experienced after ingesting multiple doses of the root (2.5–7.5 gm, each dose estimated to contain ~5 mg AA), were intense gastrointestinal discomfort and polyuria. Later, Orfila, the founder of modern quantitative toxicology, demonstrated the lethal effects of *Aristolochia clematitis* in short-term experiments performed on dogs [14]. More than a century ago, Pohl administered extracts prepared from seeds and roots of *A. clematitis* to rabbits, revealing the nephrotoxic effects of the partially purified phytotoxin [15]. Later, Dumić [16] and Martinčić [17] reported that horses ingesting hay contaminated with *A. clematitis* developed chronic renal failure, recording the histopathology of the diseased kidneys [17]. Subsequently, Mengs documented the acute and chronic toxicities of purified AA in rodents, including its carcinogenicity [18–20]. The molecular and cellular mechanisms underlying AA cytotoxicity have been explored in cultured renal proximal tubule cells and in rodent models of AAN (reviewed in [21]).

3. AA-I AND AA-II

Aristolochia herbs contain a number of structurally related nitrophenanthrene carboxylic acids, principally aristolochic acid I (AA-l) and aristolochic acid II (AA-ll) [22]. Many of the studies discussed here utilize the naturally occurring mixture of AA-l and AA-ll, designated for purposes of this discussion as AA.

4. Chinese Herb Nephropathy

Between 1990 and 1992, ~1800 otherwise healthy Belgian women inadvertently ingested *Aristolochia fangchi* in conjunction with their participation in a weight-loss regimen. Several of these women developed rapidly progressive renal interstitial fibrosis leading to chronic renal failure [23]. Histopathologic examination revealed a corticomedullary gradient of interstitial fibrosis, and marked atrophy of proximal tubules with glomeruli generally being spared. Approximately 5% of women ingesting the herbal supplement developed end-stage renal disease (ESRD), ultimately requiring dialysis or renal transplantation [3]. When the diseased kidneys were removed, urothelial cell atypia and carcinoma were found in the upper urinary tract [24]. Specifically, among 39 patients undergoing prophylactic bilateral nephrectomy, 46% had urothelial cancers located primarily in the renal pelvis and upper ureter [25]. All but two of the remaining patients displayed mild-to-moderate urothelial cell dysplasia.

Definitive evidence that AA was responsible for CHN was obtained when aristolactam (AL)-DNA adducts were detected in renal tissues (reviewed in [26]). Additionally, Cosyns *et al.* reproduced the nephrotoxic and carcinogenic effects observed in humans by treating rabbits with low doses of AA [27]. Based on these reports, the term aristolochic acid nephropathy (AAN) was suggested to reflect the etiologic role of this phytotoxin in CHN [28].

The dramatic revelation that AA is a powerful nephrotoxin and carcinogen for humans drew attention to the worldwide distribution and extensive use of *Aristolochia* sp. as herbal remedies. Unsurprisingly, subsequent reports described almost 200 patients outside of Belgium in whom chronic renal failure followed ingestion of *Aristolochia* herbs (reviewed in [9]).

Undoubtedly, published reports represent only a small fraction of AAN cases. In support of this assertion, we note that in a single year in China, 320,000 kg of *Aristolochia manchuriensis* was harvested for medicinal purposes [29]. And, in 2003, 5000 kg of Qing Mu Xiang and 10,000 kg of Tian Xian Teng, *Aristolochia* herbals listed in the 2005 Chinese Pharmacopeia, were produced in the Shanghai district alone. However, despite heavy and widespread use of Aristolochic herbals, very few cases of AAN were reported in China prior to 1999 [30].

Epidemiologic studies in Taiwan, where the prevalence of chronic kidney disease (CKD) is among the highest in the world, reveal a strong association between CKD and the use of herbal therapies [31]. Furthermore a survey of prescriptions filled between 1997 and 2003 in Taiwan revealed that one-third of the population had been treated with herbal products known to contain, or suspected to be contaminated with *Aristolochia* [32].

CKD also is recognized as a major public health problem in India [33]. Traditional Ayurvedic medicines used in India and elsewhere include several species of *Aristolochia*, predominantly *Aristolochia indica* and *Aristolochia bracteolata*. Vanherweghem [34] suggested that the nephrotoxicity associated with *Aristolochia* herbal remedies may contribute to the high incidence (27.8%) of chronic interstitial nephritis in India [35].

In conclusion, the failure to relate traditional uses of *Aristolochia* sp. to its delayed nephrotoxic and carcinogenic effects has created a global health problem that will require attention from public health authorities for the foreseeable future [12].

5. Endemic (Balkan) Nephropathy

EN is a chronic tubulointerstitial disease occurring in rural villages located near tributaries of the river Danube in Bosnia and Herzogovina, Bulgaria, Croatia, Romania, and Serbia. First described 50 years ago [36–39], EN is estimated to affect at least 25,000 individuals in countries harboring this disease, while another 75,000 men and women residing in endemic regions are believed to be at risk [40]. Significant epidemiologic features of EN include its focal occurrence in certain farming villages; a familial but not inherited pattern of disease, frequently affecting members of the same household; occurrence only in individuals older than 18 years of age; presence in less than 10% of households in endemic villages; and a strong association with upper urinary tract transitional cell (urothelial) cancer (UUC) [4–6,41].

Until quite recently, the etiology of EN remained obscure [42]. A variety of environmental agents, including mycotoxins, heavy metals, viruses, and trace-element deficiencies have been investigated as potential causative agents [42,43], with ochratoxin A (OTA), being a principal focus of EN research in recent years. Residents of villages in endemic areas are exposed to relatively high concentrations of OTA; however, elevated serum levels of OTA have been detected in residents of countries throughout the world [44] while EN is limited to isolated villages in Balkan countries [4–6]. In fact, OTA has never been associated directly with nephrotoxicity in humans [45] and a comprehensive review of the literature concluded that published epidemiologic studies are inadequate to assess a cause-and-effect relationship between OTA and human cancer [46]. Thus, the weight of scientific evidence, including the inability of OTA to form DNA adducts under physiologic conditions [47–49], argues strongly against OTA or other mycotoxins playing a role in the etiology of EN [10,21].

Current experimental evidence supports the view [12,50–51] that chronic dietary poisoning by AA accounts for all of the important characteristics of

EN, including the geographical distribution, characteristic pattern of renal tubulointerstitial fibrosis, and increased risk of developing UUC. Earlier, Kazantzis [52] and Ivić [53] suggested that *A. clematitis* might contain the etiologic agent responsible for EN; however, this insightful observation was not pursued. In fact, our impetus to investigate the role of AA in EN was prompted by the striking clinical and histopathologic similarities between EN and the nephropathy observed in the cluster of Belgian women [54].

6. AAN = BEN = CHN

In the following section, we review critically the toxicology of AA, focusing on renal proximal tubules and urothelial cells, which are targeted by the toxin. In so doing, we integrate observations on the pathophysiology of CHN and EN with research on animal models of AAN and mechanistic studies of the molecular and cellular effects of AA (reviewed in [21]).

7. DOSE–TOXICITY RELATIONSHIP

Estimates have been made of the amount of AA ingested by ∼100 Belgian women who developed end-stage renal failure [3,55] and by many of the ∼200 sporadic cases of CHN reported in the world literature (reviewed in [9]). Our analysis of the dose–toxicity relationship assumes that AA-induced DNA damage in cells is cumulative and largely irreversible. Thus, 1800 Belgian women received a maximum of 0.025 mg/kg of AA over a period averaging 13 months, with 5% of this group developing end-stage renal failure 3–85 months after administration was stopped [3]. Similarly, Chinese patients estimated to have ingested 0.7–1. 5 mg AA per day intermittently over 1–10 years in the form of pills containing *A. manchuriensis* developed chronic renal failure, sometimes within 6 months of initial exposure to the herb [9]. Higher doses of AA, such as those employed in a Phase I clinical study of AA (1 mg/kg intravenously for 3 or more days) [56], and in some Chinese patients (10 mg/day for 10 days) [57] resulted in acute renal toxicity.

In EN, 20 years or more may elapse before renal dysfunction becomes clinically apparent. The slow progression of this endemic disease likely reflects a low level of exposure to AA. However, Croatian farm families who ingest bread contaminated by AA are estimated to accumulate over 8–10 years the same amount of AA as did Belgium women with CHN in a single year [51]. The number of residents in Croatian endemic areas who depend on home-baked bread has decreased substantially in the past 20 years (Jelaković *et al.*, unpublished data). Decreased dietary exposure to AA is

expected to translate into lower incidence of EN and delayed age of onset of nephrotoxicity. The observed shift to the older age group among newly diagnosed EN cases and among EN patients beginning dialysis [5] is in line with this prediction.

8. Renal Histopathology

AAN is marked by progressive tubulointerstitial fibrosis resulting in ESRD. Comparison of patients with CHN and EN revealed a striking histopathologic feature, namely, a corticomedullary gradient of interstitial fibrosis present in both diseases [54]. This gradient, reported only in AAN and cadmium–induced nephropathy [58] is even more pronounced in renal biopsies obtained prior to the development of ESRD.

New Zealand White rabbits treated over a period of 17–21 months with low doses of AA developed impaired renal tubular function displaying and interstitial fibrosis with a corticomedullary gradient [27]. Following treatment with AA, C3H/He mice developed acute tubular necrosis and interstitial fibrosis while C57BL/6 mice are resistant to similar doses of the toxin [59]. AA-I and AA-ll exhibit similar genotoxic potential [60], however, AA-I is solely responsible for the nephrotoxicity observed in C3H mice [59,60]. Histopathologic findings in Wistar rats include necrosis of outer medullary proximal tubules and urothelial dysplasia. As in mice, renal injury in rats is manifested initially by an acute inflammatory/necrotic phase lasting several days, followed by a chronic phase, consisting of interstitial inflammation, tubular atrophy, and interstitial fibrosis [61]. Biochemical markers were consistent with epithelial–mesenchymal transition, although an alternative mechanism involving TGF-β activation of fibroblasts may account for some of the interstitial fibrosis involved [62].

9. Proximal Tubular Function

AAN is characterized by proximal tubule dysfunction, including persistent glycosuria, aminoaciduria, and low–molecular weight (tubular) proteinuria (LMWP) [3,4]. Normally, LMWP are filtered at the glomerulus, reabsorbed by endocytosis in the proximal tubule, and then catabolized. Proximal tubule damage interferes with this process; thus, the urinary LMWP/albumin ratio is strikingly elevated in patients with CHN and EN compared with patients with glomerular disease [63]. This parameter provides a useful biomarker for detecting early proximal tubule dysfunction in AAN [64–66].

Rabbits given AA intraperitoneally 5 days a week for 17–21 months developed impaired proximal tubule function manifested by glycosuria and

tubular proteinuria [27]. In Wistar rats, high doses of AA disrupted proximal tubule function, as reflected by proteinuria, glycosuria, and neutral amino acid enzymuria [67]. Both animal models reproduce the principal features of AAN in humans. The rat was used to investigate early functional impairment of the proximal tubule, revealing that the outer medullary S3 segment of the proximal tubule was the preferential target of AA [67].

10. UROTHELIAL CANCER

The strong association between exposure to AA and the development of urothelial neoplasia was first recognized in Belgian women with CHN [24,68]. Ultimately, 40–45% of this group developed multifocal high-grade transitional cell carcinomas located primarily in the upper urinary tract [25]. Based on this observation, prophylactic bilateral nephroureterectomy is strongly recommended for CHN and EN patients requiring dialysis or renal transplantation.

UUC is prevalent among residents of endemic villages in the Balkan region [69]. In the former Yugoslavia, data from more than 2000 cases of UUC were used to explore the epidemiology of this uncommon cancer [70]. The prevalence of UUC in certain endemic regions can be as much as 100-fold greater than in the country as a whole [71]. More than two-thirds of these cancers are localized in the renal pelvis or ureter [72,73] compared to ∼5% of UUC among patients residing in nonendemic areas [74]. In Serbia, the fraction of urothelial cancers located in the renal pelvis and ureter increased from 18% in the period 1921–1952 to 63% in 1953–1960 [70,72].

Patients undergoing surgery for UUC often exhibit signs of renal dysfunction. Petković *et al.* recorded "renal failure" in 63% (111/187) of patients with UUC [75]. This important observation was confirmed by Nikolić in a review of 710 patients with UUC, 65% of whom had creatinine clearances of less than 80 ml/min [70]. Recently, 9 of 11 residents of endemic villages undergoing nephroureterectomy for UUC were found to have histopathologic changes in the renal cortex compatible with EN [50]. Thus, UUC may precede, accompany, or follow manifestations of nephrotoxicity in patients with EN. The age at which patients in endemic regions develop symptoms associated with UUC has increased steadily over the past 30 years [76], again suggesting that environmental exposure to AA is diminishing over time.

11. AL-DNA ADDUCTS

Both AA–l and AA–ll are subject to enzymatic nitroreduction in mammalian cells, generating active nitrenium intermediates (Figure 1) that react with the exocyclic amino groups of deoxyadenine and deoxyguanine
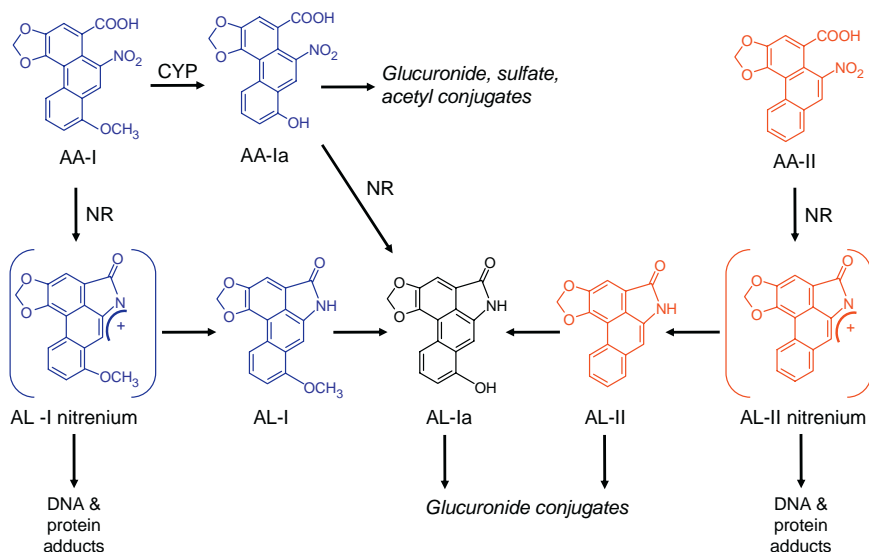
Figure 1　Principal urinary metabolites of aristolochic acids (AA) in rat. Cytochrome P450 (CYP) catalyzed demethylation of AA–I generates AA–Ia, which is subject, in turn, to Phase II biotransformation to form glucuronide, sulfate, and acetyl conjugates. Enzymatic nitroreduction (NR) of AA–I or AA–II yields the biologically inactive aristolactams AL–I and AL–II. Reactive nitrenium intermediates form covalent adducts with DNA and proteins.

bases of DNA (reviewed in [26]). Both AL-l- and AL-ll–derived DNA adducts were detected in the renal cortex of patients with EN and/or UUC [50] and in persons ingesting botanical products containing AA (reviewed in [9]).

The level of AL–DNA adducts in target tissues represents the integration of external exposure with interindividual variability in metabolism, nucleotide excision repair, and other cellular processes, providing a tangible link between exposure to the genotoxin and its cytotoxic and carcinogenic effects [77]. Their usefulness as biomarkers is enhanced by their persistence in target tissues. For example, in humans, AL–DNA adducts were detected 36–89 months following termination of exposure to AA [26,50]. Thus, among Belgian women, AL–DNA adduct levels ranged from 0.1 to 17 adducts per 10^8 deoxynucleotides (dNs), with dA–AL–I being the major adduct found in the renal cortex while dA–AL–II and dG–AL–I were present in significantly lower amounts [26].

In patients with EN, adduct levels ranged from 8 to 59 adducts per 10^8 dNs for dA–AL–l and 2–62 adducts per 10^8 dNs for dG–AL–l [50]. In urothelial tumors, adduct levels were significantly lower, 0.7–1.6 and

0.3–0.5 adducts per 10^8 dNs for dA-AL and dG-AL, respectively [50]. In rodent models of AAN, AL-DNA adducts accumulate in target tissues [26,78]; however, the prominent cytotoxic effects of AA-l in proximal tubule cells appear unrelated to its DNA-damaging effects [60].

12. Mutational Signature of AAN

Mutational analysis of the p53 tumor suppressor gene in UUC tumors from patients residing in endemic villages revealed that the frequency of A:T → T:A mutations was 78% [50]. In contrast, A:T → T:A mutations occur infrequently in transitional cell carcinomas of the renal pelvis (0%), ureter (5%), and bladder (4.8%) in patients from nonendemic regions [79]. Importantly, the p53 mutation pattern in UUC associated with EN is consistent with the mutational spectra induced by AA-I (or by a mixture of AA-I and AA-II) in (i) the H-ras gene of rats [80]; (ii) transgenic rodent models [81]; (iii) the p53 gene in a urothelial cancer from a patient with CHN [82]; (iv) site-specific mutagenesis studies in which a single dA-AL adduct is transfected into nucleotide excision repair (NER)-deficient human cells (Yang and Moriya, unpublished data); and (v) immortalized (Hupki) mouse cell lines carrying the human p53 gene [83]. Indeed, the predominance of A:T → T:A transversions in the p53 mutational spectrum is widely recognized as a mutational signature for human exposure to AA [10,50,83,84].

13. Genetic Considerations

Only 5% of the 1800 Belgian women exposed to similar amounts of AA developed AAN [3] and the reported prevalence of EN is 3–7% [5]. Similarly, various strains of mice exhibit differing susceptibilities to the toxic effects of AA [59,60]. Thus, genetically determined interindividual variability may contribute to the risk of developing AAN and/or its associated UUC [85]. Rarely, however, does a single mutated gene result in a high absolute risk of an associated cancer or other disease. Thus, susceptibility to AA most likely is influenced by the additive or synergistic effects of several genes, none of which individually may result in a large phenotypic effect. Furthermore, the cumulative effect of susceptibility to this environmental mutagen may result from complex interactions among multiple genes and from gene–environment interactions [86]. Molecular epidemiologic studies have been undertaken to potentially capture such interactive effects in EN, and mouse models of AAN have been used to identify genes controlling susceptibility to the nephrotoxic effects of AA [87].

Polymorphisms that affect susceptibility to AA are likely to be found in genes responsible for its absorption, bioactivation, detoxification, excretion, and/or transport. Metabolism of AA, mediated by enzymes known collectively as xenobiotic metabolizing enzymes (XMEs), has been demonstrated in humans and animals treated with AA [88] (Figure 1). *O*-demethylation, mediated by Cytochrome P450s, results in rapid detoxification of AA-1 in rodents [89]. Thus, functional polymorphisms in XMEs may affect the level of critical intermediates produced during biotransformation, some of which bind to DNA and proteins. Similarly, polymorphisms in certain DNA repair enzymes can affect an individual's ability to excise the AL-DNA adducts that initiate UUC [90]. Although individual risks associated with such polymorphisms might be low, they potentially have great public health relevance (i.e., population-attributable risk) because of their high population frequency [91].

14. AAN as an Iatrogenic Disease

The varied uses of *Aristolochia* (birthwort) have been traced from the fourth century BC to the eighteenth century AD, based on excerpts from the original literature [1]. The actual cumulative doses of *Aristolochia* employed in treating illness during the Greco-Roman period were estimated by Scarborough who suggested that this early usage likely resulted in unrecognized iatrogenic disease as a result of the herb's intrinsic toxicity [92].

Extending this novel hypothesis, we have reviewed the use of *Aristolochia* herbal combinations in Ayurvedic and Chinese medicine. Our immediate goal is to document clearly the past and present use, worldwide, of *Aristolochia*, a family of herbs recently shown to be nephrotoxic and carcinogenic to humans.

The first description of *Aristolochia* is found in ''Enquiry into Plants'' by Theophrastus (300 BC) who described the morphology of the plant and its medical uses [93]. At that time, *Aristolochia* was used for snakebites, as a general antidote against poisons, to clean wounds, to alleviate insomnia, cure uterine malfunctions, ease bowel obstruction, and relieve symptoms of dropsy (edema). In the Hippocratic *Diseases of Women,* anonymous writers of that era discuss the use of *Aristolochia* as an oxytocic agent to aid women in childbirth and abortifacient, obstetric and gynecologic practices that continue to this day [94].

Arguably the most influential medical work of classical antiquity, *De Materia Medica,* written ca. 70 AD by Dioscorides, includes almost all herbs then employed in Greco-Roman pharmacology. Individual chapters are devoted to *Aristolochia rotunda, Aristolochia longa, and Aristolochia clematitis* [95]. Interestingly, not one word of caution was expressed regarding the potential toxicity of these herbs [92].

The influence of *De Materia Medica* on Western and Islamic medicine was profound. Dioscorides' descriptions of *Aristolochia* were translated into Arabic and Latin and this information was preserved throughout the Byzantine period and the Middle Ages [96]. With the advent of the printing press, information originating in *De Materia Medica* was incorporated (often verbatim) into the printed herbals of the Renaissance, which enjoyed wide distribution in Europe [97]. Ultimately, an entry for *Aristolochia* appeared in the *Pharmacopeia Londinesis of 1618* and, following that, in other official compendia and textbooks of pharmacology. Literature discussing properties of birthwort continued throughout the twentieth century [98]. Once again, usage of this herb was never associated with nephrotoxicity or cancer.

Ayurveda, one of several codified systems of traditional medicine, enjoys the same legal status in India as does allopathic medicine. The *Carakasamhita*, dating from ca. 400 AD and constituting one of the earliest Ayurvedic medical treatises, contains descriptions of 341 plant products. Scholars have identified in this classic text several species of *Aristolochia* used in Ayurveda today. Undoubtedly, many patients currently treated by Ayurvedic practioners are exposed to the toxic effects of these widely distributed native herbs.

Gandhanakuli, *isvari*, and *nakuli*, identified as *Aristolochia indica* Linn *or A. bracteolata* Lam are mentioned in the *Carakasamhita* as antidotes to snakebite and for intermittent fevers (G.J. Meulenbeld, personal communication). Similar applications of *Aristolochia* sp. appear in more recent Indian pharmacopeia where the herb continues to be used for children with fever as well as an emmenagogue and antiarthritic [99].

In China, the earliest record of herbal medicines is the Shen Nong Ben Cao Jing (Shennong Herbal), compiled sometime between the first century BC and the second century AD [96]. Three hundred sixty-five agents are listed in this text, divided into superior, medium, and inferior based on their relative toxicity. Mou Dou Ling (fruit of *Aristolochcha* debilis) first appears in the Lei Gong Pao Jiu Lun (ca. 421 AD) with no subsequent mention of its potential toxic effects.

The Ben Cao Gang Mu, compiled by Li Shi-Zhen in the latter part of the sixteenth century, was based on the author's experience and on data obtained from earlier herbals. This Chinese herbal classic describes 1892 "drugs" (with 1110 drawings) including many species of *Aristolochia*. For 400 years, the Ben Cao Gang Mu remained the principal source of information in traditional Chinese medicine and the work was translated into numerous languages, reflecting its influence in countries other than China.

In the mid-twentieth century, Ben Cao Gang Mu was replaced by modern *materia medica*, the most comprehensive source being Zhong Hua Ben Cao (Encyclopedia of Chinese Materia Medica), published in 1999 [100]. The Encyclopedia lists 23 species of *Aristolochia*, again with little mention of toxicity. The Chinese government currently lists the following *Aristolochia* herbs: *A. manshuriensis* (stems), *A. fangchi* (root), *A. debilis* (root

and fruit), and A. contorta (*fruit*), two of which (Mou Dou Ling and Quingmuxiang) appear in the 2005 Pharmacopeia.

Thus, for thousands of years, herbs have been used for medicinal purposes and in the twenty-first century 80% of the world's population rely on herbal remedies to treat symptoms of disease. *Aristolochia* herbals play an important role in this tradition. The governments of China and India, countries with populations in excess of one billion, have been slow in implementing measures to reduce human exposure to this toxic herb. Thus, from a global perspective, we conclude that AAN and its associated upper urothelial cancer continues to exist as it has in centuries past as a "silent" but omnipresent iatrogenic disease.

ACKNOWLEDGMENT

REFERENCES

[1] W.R. Dawson, Birthwort: A study of the progress of medical botany through twenty-two centuries, Pharmaceutical J. Pharmacist 396–397 (1927) 427–430.

[2] J.P. Cosyns, Aristolochic acid and "Chinese herb nephropathy": A review of the evidence to date, Drug Safety 26 (2003) 33–48.

[3] J.L. Vanherweghem, F. Debelle, M.C. Muniz-Martinez, J. Nortier, Aristolochic acid nephropathy after Chinese herb remedies, In: M.E. De Broe, G.A. Porter, W.M. Bennett, and G.A. Verpooten (Eds.), Clinical Nephrotoxins 2nd Edition, Kluwer, Dordrecht, 2003, pp. 579–603.

[4] L. Djukanović, Z. Radovanović, Balkan endemic nephropathy, In: M.E. De Broe, G. A. Porter, W.M. Bennett, and G.A. Verpooten (Eds.), Clinical Nephrotoxins, 2nd Edition, Kluwer, Dordrecht, 2003, pp. 588–601.

[5] D. Bukvić, Endemic nephropathy, overview of investigations in the Lazarevac area, Professional Pen Co, Belgrade, 2004.

[6] V. Stefanović, Z. Radovanović, Balkan endemic nephropathy and associated urothelial cancer, Nat. Clin. Pract. Urol. 5 (2008) 105–112.

[7] G. Bamias, J. Boletis, Balkan nephropathy: Evolution of our knowledge, Am. J. Kidney Dis. 52 (2008) 606–616.

[8] Aristolochia species and aristolochic acids, In IARC Monographs on the evaluation of the carcinogenic risk of chemicals to humans: Some traditional herbal medicines, some mycotoxins, napthalene and styrene Vol. 82, pp. 69–128, International Agency for Research on Cancer, Lyon, France, 2002.

[9] Aristolochic acids, In National Toxicology Program Report on Carcinogens 12th Edition, US Dept Health and Human Services, Public Health Service, Research Triangle Park, North Carolina, 2009.

[10] A.P. Grollman, B. Jelaković, Role of environmental toxins in endemic (Balkan) nephropathy, J. Am. Soc. Nephrol. 18 (2007) 2817–2823.

[11] H. de Jonge, Y. Vanrenterghem, Aristolochic acid: The common culprit of Chinese herbs nephropathy and Balkan endemic nephropathy, Nephrol. Dial. Transplant. 23 (2007) 39–41.

[12] F.D. Debelle, J.L. Vanherweghem, J.L. Nortier, Aristolochic acid nephropathy: A worldwide problem, Kidney Int. 74 (2008) 158–169.

[13] J.C.G. Jörg, Materialien zu einer künftigen Heilmittellehre durch Versuche der Arzneyen an gesunden Menschen gewonnen und gesammelt von Dr. Johann Christian Gottfried Jörg, Carl Cnobloch, Leibzig, 1825.

[14] M.J.B. Orfila, de l'Aristoloche (*Aristolochia clematitis*), In Traité des poisons tiré des régnes minéral, vétal et animal; ou, Toxicologie génerale, considére sous les rapports de la physiologie de la pathologie et de la médécine légale, 1851, pp. 296–298.

[15] J. Pohl, Ueber das Aristolochin, einen giftigen Bestandtheil der *Aristochiaarten*, Arch. Exp. Path. u. Pharm. 29 (1892) 282–302.

[16] A. Dumić, Trovanje konja vučjom stopom (*A. clematitis* L), Izdanje vojnotehničkog glasnika, Belgrade, Yugoslavia. 1954, pp. 3–35.

[17] M. Martinčić, Toxische einwirkungen der Aristolochia clematitis auf die Niere des Pferdes, Veterinarski Arhiv. 27 (1958) 51–59.

[18] U. Mengs, W. Lang, J.A. Poch, The carcinogenic action of aristolochic acid in rats, Arch. Toxicol. 51 (1982) 107–119.

[19] U. Mengs, Acute toxicity of aristolochic acid in rodents, Arch. Toxicol. 59 (1987) 328–331.

[20] U. Mengs, C.D. Stotzem, Toxicity of aristolochic acid—a subacute study in male rats, Med. Sci. Res. 20 (1992) 223–224.

[21] K.G. Dickman, A.P. Grollman, Nephrotoxicity of natural products: Aristolochic acid and fungal toxins, In: R.G. Schnellman (Ed.), Comprehensive Toxicology: Renal Toxicology 2nd Edition, Elsevier, New York, 2009.

[22] V. Kumar, A.K. Prasad, V.S. Parmar, Naturally occurring aristolactams, aristolochic acids and diosoaporphines and their biological activities, Nat. Prod. Rep. 20 (2003) 565–583.

[23] J.L. Vanherweghem, M. Depierreux, C. Tielemans, D. Abramowicz, M. Dratwa, M. Jadoul, C. Richard, D. Vandervelde, D. Verbeelen, R. Vanhaelen-Fastre, M. Vanhaelen, Rapidly progressive interstitial renal fibrosis in young women: Association with slimming regimen including chinese herbs, Lancet 341 (1993) 387–391.

[24] J.P. Cosyns, M. Jadoul, J.P. Squifflet, P.J. van Cangh, C. van Ypersele de Strihou, Urothelial malignancy in nephropathy due to Chinese herbs, Lancet 344 (1994) 188.

[25] J.L. Nortier, M.C. Martinez, H.H. Schmeiser, V.M. Arlt, C.A. Bieler, M. Petein, M.F. Depierreux, L. De Pauw, D. Abramowicz, P. Vereerstraeten, J-L. Vanherweghem, Urothelial carcinoma associated with the use of a Chinese herb (Aristolochia fangchi), N. Engl. J. Med 342 (2000) 1686–1692.

[26] V.M. Arlt, M. Stiborová, H.H. Schmeiser, Aristolochic acid as a probable human cancer hazard in herbal remedies: A review, Mutagenesis 17 (2002) 265–277.

[27] J.P. Cosyns, J.P Dehoux, Y. Guiot, *et al.*, Chronic aristolochic acid toxicity in rabbits: A model of Chinese herb nephropathy?, Kidney Int. 5 (2001) 2164–2173.

[28] G. Gillerot, M. Jadoul, V.M Arlt, *et al.*, Aristolochic acid nephropathy in a Chinese patient: Time to abandon the term "Chinese herbs nephropathy"? Am. J. Kidney Dis. 38 (2001) E26.

[29] S.L. Hu, H.Q. Zhang, K. Chan, Q.X. Mei, Studies on the toxicity of *Aristolochia manshuriensis* (Guanmuton), Toxicology 198 (2004) 195–201.

[30] X. Li, H. Wang, Aristolochic acid nephropathy: What we know and what we have to do, Nephrology 9 (2004) 109–111.

[31] J.Y. Guh, H.C. Chen, J.F. Tsai, L.Y. Chuang, Herbal therapy is associated with the risk of CKD in adults not using analgesics in Taiwan, Am. J. Kidney Dis. 49 (2007) 626–633.

[32] S.C. Hsieh, I.H. Lin, W.L. Tseng, C.H. Lee, J.D. Wang, Prescription profile of potentially aristolochic acid-containing Chinese herbal products: An analysis of National Health Insurance data in Taiwan between 1997 and 2003, Chin. Med. 3 (2008) 13.

[33] G.K. Modi, V. Jha, The incidence of end-stage renal disease in India: A population-based study, Kidney Int. 70 (2006) 2131–2133.

[34] J.L. Vanherweghem, *Aristolochia* sp. and chronic interstitial nephropathies in Indians, Lancet 349 (1997) 1399.

[35] M.K. Mani, Chronic renal failure in India, Nephrol. Dial. Transplant. 8 (1993) 684–689.

[36] Y. Tanchev, Z. Evstatiev, D. Dorossiev, J. Pencheva, G. Zvetkov, Studies of the nephritides in the District of Vratza, Savremenna Medicina 7 (1956) 14–29.

[37] V. Danilović, M. Djurišić, M. Mokranjac, B. Stojimirović, J. Živojinović, P. Stojaković, Porodična oboljenia bubrega u selu Šopić izvazvana hroničnom intoksikacijom olovom, Srpski Arh Tcelok Lek 85 (1957) 1115–1125.

[38] N. Foartza, M. Negoescu, Nefrita cronica azotemia endo-epidemica Stud, Cercet Med. 1 (1961) 217–221.

[39] World Health Organization, Memorandum: The endemic nephropathy of South-Eastern Europe, Bull. World Health Organ. 32 (1965) 441–448.

[40] C.A. Tatu, W.H. Orem, R.B. Finkelman, G.L. Feder, The etiology of Balkan endemic nephropathy: Still more questions than answers, Environ. Health Perspect. 106 (1998) 689–700.

[41] S. Čeović, M. Miletić-Medved, Epidemiological features of endemic nephropathy in the focal area of Brodska Posvina, Croatia, In: D. Čvorišćec, S. Čeović, and A. Stavljenić-Rukavina (Eds.), Endemic Nephropathy in Croatia, 1996, pp. 7–21.

[42] V. Batuman, Fifty years of Balkan endemic nephropathy: Daunting questions, elusive answers, Kidney Int. 69 (2006) 644–646.

[43] T.C. Voice, D.T. Long, Z. Radovanović, J.L. Atkins, *et al.*, Critical evaluation of environmental exposure agents suspected in the etiology of Balkan endemic nephropathy, Int. J. Occup. Environ. Health 12 (2006) 369–376.

[44] H.A. Clark, S.M. Snedeker, A. Ochratoxin, Its cancer risk and potential for exposure, J. Toxicol. Environ. Health B Crit. Rev. 3 (2006) 265–296.

[45] M. Godin, J.P. Fillastre, A. Fancois, F. Le Roy, J.P. Morin, Is Ochratoxin A nephrotoxic in human beings? Adv. Nephrol. 26 (1997) 181–206.

[46] J. Fink-Gremmels, A. Ochratoxin, In food: Recent developments and significance, Food Addit. Contam. 22(Suppl. 1), (2005) 1–5.

[47] A. Mally, H. Zepnik, P. Wanek, E. Eder, E.K. Dingley, H. Ihmels, W. Volkel, W. Dekant, Ochratoxin A: Lack of formation of covalent DNA adducts, Chem. Res. Toxicol. 17 (2004) 234–242.

[48] T. Delatour, A. Mally, J. Richoz, S. Özden, W. Dekant, H. Ihmels, D. Otto, D. Gasparutto, M. Marin-Kuan, B. Schilter, C. Cavin, Absence of 2′-deoxyguanosine-carbon-8-bound ochratoxin A adduct in rat kidney DNA monitored by isotope dilution LC–MS/MS, Mol. Nutr. Food Res. 52 (2008) 472–482.

[49] R.J. Turesky, Perspective: Ochratoxin A is not a genotoxic carcinogen. Chem. Res. Toxicol. 18(2005) 1082–1090.

[50] A.P. Grollman, S. Shibutani, M. Moriya, F. Miller, L. Wu, U. Moll, *et al.*, Aristolochic acid and the etiology of endemic (Balkan) nephropathy, Proc. Natl. Acad. Sci. USA 104 (2007) 12129–12134.

[51] T. Hranjec, A. Kovač, J. Kos, W. Mao, J.J. Chen, A.P. Grollman, B. Jelaković, Endemic nephropathy: The case for chronic poisoning by aristolochia, Croat Med J. 46 (2005) 116–125.

[52] G. Kazantzis, Comment in the general discussion of possible nephrotoxic agents, In: G.E. Wolstenholme and J. Knight (Eds.), The Balkan Nephropathy, CIBA Foundation, Boston, MA, 1967, p. 114.

[53] M. Ivić, The problem of etiology of endemic nephropathy, Liječ Vjes 91 (1969) 1273–1281.

[54] J.P. Cosyns, M. Jadoul, J.P Squifflet, J.F. de Plaen, D. Ferluga, C. van Ypersele de Strihou, Chinese herbs nephropathy: A clue to Balkan endemic nephropathy? Kidney Int. 45 (1994) 1680–1688.

[55] M.C.M. Martinez, J.L. Nortier, P. Vereerstraeten, J.L. Vanherweghem, Progression rate of Chinese herb nephropathy: impact of *Aristolochia fangchi* ingested dose, Nephrol. Dial. Transplant. 17 (2002) 408–412.

[56] L. Jackson, S. Kofman, A. Weiss, H. Brodovsky, Aristolochic acid (NSC–50413): phase I clinical study, Cancer Chemother. Rep. 42 (1964) 35–37.

[57] S.H. Lo, K.L Mo, K.S. Wong, S.P Poon, C.K. Chan, C.K. Lai, A. Chan, Aristolochic acid nephropathy complicating a patient with focal segmental glomerulosclerosis, Nephrol. Dial.Transplant. 19 (2004) 1913–1915.

[58] M. Yasuda, A. Miwa, M. Kitagawa, Morphometric studies of renal lesions in Itai–Itai disease: chronic cadmium nephropathy, Nephron 69 (1995) 14–19.

[59] N. Sato, D. Takahashi, S.M. Chen, R. Tsuchiya, T. Mukoyama, S. Yamagata, *et al.*, Acute nephrotoxicity of aristolochic acids in mice, J. Pharm. Pharmacol. 56 (2004) 221–229.

[60] S. Shibutani, H. Dong, N. Suzuki, S. Ueda, F. Miller, A.P. Grollman, Selective toxicity of aristolochic acids I and II, Drug Metab. Dispos. 35 (2007) 1217–1222.

[61] F.D. Debelle, J.L. Nortier, E.G. de Prez, C.H. Garbar, A.R. Vienne, I.J. Salmon, M.M. Deschodt-Lanckman, J.L. Vanherweghem, Aristolochic acids induce chronic renal failure with interstitial fibrosis in salt-depleted rats, J. Am. Soc. Nephrol. 13 (2002) 431–436.

[62] A.A. Pozdzik, I.J. Salmon, F.D. Debelle, C. Decaestecker, C.C. van den Branden, D. Verbeelen, M.M. Deschodt-Lanckman, J.L. Vanherweghem, J.L. Nortier, Aristolochic acid induces proximal tubule apoptosis and epithelial to mesenchymal transformation, Kidney Int. 73 (2008) 595–607.

[63] A. Kabanda, M. Jadoul, R. Lauwerys, A. Bernard, C. van Ypersele de Strihou, Low molecular weight proteinuria in Chinese herbs nephropathy, Kidney Int. 48 (1995) 1571–1576.

[64] P.W. Hall, M. Piscator, M. Vasiljević, N. Popović, Renal function studies in individuals with the tubular proteinuria of endemic Balkan nephropathy, Q. J. Med. 41 (1972) 385–393.

[65] M. Radonić, Beta-2 microglobulin in Balkan endemic nephropathy, Pathol. Biol. 26 (1978) 317–320.

[66] D. Čvorišćec, Early diagnosis of endemic nephroapthy, Clin. Chim. Acta 297 (2000) 85–91.

[67] C. Lebeau, F.D. Debelle, V.M. Arlt, A. Pozdzik, E.G. De Prez, D.H. Phillips, M.M. Deschodt-Lanckman, J.L. Vanherweghem, J.L. Nortier, Early proximal tubule injury in experimental aristolochic acid nephropathy: functional and histological studies, Nephrol. Dial. Transplant. 20 (2005) 2321–2332.

[68] J.P. Cosyns, M. Jadoul, J.P Squifflet, F.X Wese, C. van Ypersele de Strihou, Urothelial lesions in Chinese-herb nephropathy, Am. J. Kidney Dis. 33 (1999) 1011–1017.

[69] V. Stefanović and J.P. Cosyns, Balkan nephropathy, In: A.M. Davison, J.S. Cameron, J-P. Grünfeld, and C. Ponticelli (Eds.), Oxford Textbook of Clinical Nephrology, Newyork, 2005, pp. 1095–1098.

[70] J. Nikolić, Epidemic Nephropathy and Upper Urothelial Tumors, Izdavačko preduzeće, Belgrade, Serbia, 2006.

[71] S. Petković, Epidemiology and treatment of renal pelvic and ureteral tumors, J. Urol. 114 (1975) 858–865.

[72] V. Petronić, Tumors of the upper urothelium and endemic nephropathy, In: Z. Radovanovic, M. Sindic, M. Polenakovic, L. Djukanović, and V. Petronic (Eds.), Endemic Nephropathy, Zavod za udžbenike i nastavna sredstva, Belgrade Serbia, 2000, pp. 350–439.

[73] M. Miletić-Medved, A.M. Domijan, M. Peraica, Recent data on endemic nephropathy and related urothelial tumors in Croatia, Wien Klin. Wochenschr. 117 (2005) 604–609.

[74] E.M. Genega, C.R. Porter, Urothelical neoplasm of the kidney and ureter. An epidemiologic, pathologic, and clinical review, Am. J. Clin. Pathol. 117(Suppl.), (2002) S36–S48.

[75] S. Petković, Correlation of endemic nephropathy and tumors of renal pelvic and ureter, In First Congress of Nephrologists of Yugoslavia, Belgrade, 1981, pp. 177–182.

[76] J. Nikolić, M. Djokić, I. Ignjatović, V. Stefanović, Upper urothelial tumors in emigrants from Balkan endemic nephropathy areas in Serbia, Urol. Int. 77 (2006) 240–244.

[77] G.N. Wogan, S.S. Hecht, J.S. Felton, A.H. Conney, L.A. Loeb, Environmental and chemical carcinogenesis, Sem. Cancer Biol. 473 (2004) 486.

[78] H. Dong, N. Suzuki, M.C. Torres, R.R. Bonala, F. Johnson, A.P. Grollman, S. Shibutani, Quantitative determination of aristolochic acid-derived DNA adducts in rats using ^{32}P-postlabeling/polyacrylamide gel electrophoresis analysis, Drug Metab. Dispos. 34 (2006) 1122–1127.

[79] M. Olivier, R. Eeles, M. Hollstein, M.A. Khan, C.C Harris, P. Hainaut, The IARC TP53 database: new online mutation analysis and recommendations to users, Hum Mutat. 19 (2002) 607–614.

[80] H.H. Schmeiser, J.W. Janssen, J. Lyons, H.R. Scherf, W. Pfau, A. Buchmann, C.R. Bartram, M. Wiessler, Aristolochic acid activates *ras* genes in rat tumors at deoxyadenosine residues, Cancer Res. 50 (1990) 5464–5469.

[81] A. Kohara, T. Suzuki, M. Honma, T. Ohwada, M. Hayashi, Mutagenicity of aristolochic acid in the lambda/lacz transgenic mouse (mutatmmouse), Mutat. Res. 515 (2002) 63–72.

[82] G.M. Lord, T. Cook, V.M. Arlt, H.H. Schmeiser, G. Williams, C.D. Pusey, Urothelial malignant disease and Chinese herbal nephropathy, Lancet 358 (2001) 1515–1516.

[83] T. Nedelko, V.M. Arlt, D.H. Phillips, M. Hollstein, TP53 mutation signature supports involvement of aristolochic acid in the etiology of endemic nephropathy-associated tumors, Int. J. Cancer 124 (2008) 987–990.

[84] V.M. Arlt, M. Stiborová, J. vom Brocke, M.L. Simões, G.M. Lord, J.L. Nortier, M. Hollstein, D.H. Phillips, H.H. Schmeiser, Aristolochic acid mutagenesis: Molecular clues to the aetiology of Balkan endemic nephropathy-associated urothelial cancer, Carcinogenesis 28 (2007) 2253–2261.

[85] R. Their, K. Golka, T. Bruning, *et al.*, Genetic succeptibility to environmental toxicants; the interface between human and experimental studies in the development of new toxicological concepts, Toxicol. Lett. 127 (2002) 321–327.

[86] S.N. Kelada, D.L Eaton, W.W. Wang, N.R. Rothman, M.J. Khoury, The role of genetic polymorphisms in environmental health, Environ. Health Perspect. 111 (2003) 1055–1064.

[87] T.A. Rosenquist, P.A. Strockbine, A. Smith, H. Einolf, A.P. Grollman, Genetics of aristolochic acid nephropathy in mice, Cold Spring Harb. (2008).

[88] G. Krumbiegel, J. Hallensleben, W.H. Mennicke, N. Rittman, H.J. Roth, Studies on the metabolism of aristolochic acids I and II, Xenobiotica 17 (1987) 981–991.

[89] S. Shibutani, R.R Bonala, T. Rosenquist, R. Rieger, N. Suzuki, F. Johnson, F. Miller, A.P. Grollman, Detoxification of aristolochic acid-l by O-demethylation: Less nephrotoxicity and genotoxicity of aristolochic acid la in rodents, Carcinogenesis, (in press).

[90] E.C. Friedberg, G.C Walker, W. Seide, R.D Wood, R.A Schultz, T. Ellenberger, DNA Repair and Mutagenesis, ASM Press, Washington, DC, 2006.

[91] N. Caporaso, A. Goldstein, Cancer genes—single and susceptibility—exposing the difference, Pharmacogenetics 5 (1995) 59–63.

[92] J. Scarborough, Kidney disease among the Romans, Coll. Antropol. 30(Suppl. 1) (2006).

[93] J. Scarborough, Theophrastus on herbals and herbal remedies, J. Hist. Biol. 11 (1978) 353–358.

[94] J. M Riddle, Eve's Herbs, A History of Contraception and Abortion in the West, Harvard University Press, Cambridge, MA, 1997.

[95] Dioscorides, Materia Medica, III, 4, in: M. Wellman (Ed.), Pedanii Dioscuridis Anazarbei De materia medica, 3 vols, Weidmann, Berlin, 1906–1914 (rptd. 1958; Vol. 2, pp. 6–8).

[96] R.H. Major, A History of Medicine, C.C Thomas, Springfield, Ill, 1954.

[97] A. Arber, Herbals: Their Origin and Evolution, A Chapter in the History of Botany 1470–1670 3rd Edition, Cambridge Univ Press, Cambridge.

[98] M. Grieve, A Modern Herbal: The medicinal, culinary, cosmetic and economic properties, cultivation and folk-lore of herbs, grasses, fungi, shrubs and trees with all their modern scientific uses, Dover, New York, 1971, p. 104.

[99] G. Watt, A Dictionary of the Economic Products of India, Vol. 1, 331–336, Superintendent of government printing, Calcutta, 1885.

[100] Zhong Hua Ben Cao, 3–460–509 edited by the Health Department and National Chinese Medicine Management Office, published by Shanghai Science Technology Publication, 1999.

Subject Index